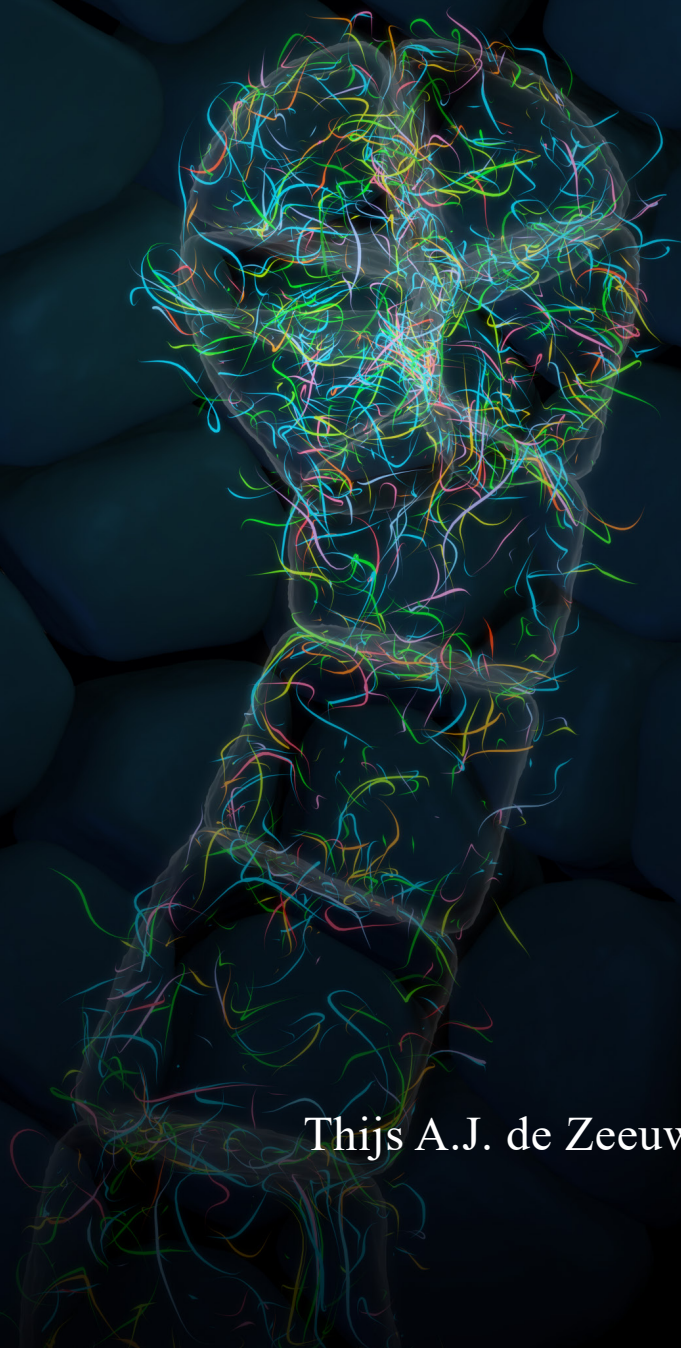


# Dissection of cell division orientation control in *Arabidopsis thaliana*



Thijs A.J. de Zeeuw



# **Dissection of cell division orientation control in *Arabidopsis thaliana***

**Thijs A.J. de Zeeuw**

## **Thesis committee**

### **Promotor**

Prof. Dr D. Weijers

Professor of Biochemistry

Wageningen University & Research

### **Other members**

Prof. Dr G.C. Angenent, Wageningen University & Research

Prof. Dr J. Xu, Radboud University, Nijmegen

Prof. Dr J. Vermeer, University of Neuchâtel, Switzerland

Dr K. Bürstenbinder, Leibniz Institute for Plant Biochemistry, Halle, Germany

This research was conducted under the auspices of the Graduate School of Experimental Plant Sciences

# **Dissection of cell division orientation control in *Arabidopsis thaliana***

**Thijs A.J. de Zeeuw**

## **Thesis**

Submitted in fulfilment of the requirements for the degree of doctor

at Wageningen University

by the authority of the Rector Magnificus

Prof. Dr A.P.J. Mol,

in the presence of the

Thesis Committee appointed by the Academic Board

to be defended in public

on Wednesday 19 Februari 2020

at 1.30 p.m. in the Aula.

Thijs A.J. de Zeeuw

Dissection of cell division orientation control in *Arabidopsis thaliana*.

240 pages

PhD thesis, Wageningen University, Wageningen, the Netherlands (2020)

with references, with summary in English

ISBN: 978-94-6395-224-8

DOI: <https://doi.org/10.18174/507587>

# Table of Contents

## Chapter 1

Introduction and scope of thesis	7
----------------------------------	---

## Chapter 2

Tissue and organ initiation in the plant embryo: A first time for everything	25
--	----

## Chapter 3

A microtubule-based mechanism predicts cell division orientation in plant embryogenesis	79
---	----

## Chapter 4

Cell biology of auxin-regulated control of division orientation in the Arabidopsis embryo	115
---	-----

## Chapter 5

A reference transcriptome of early Arabidopsis embryogenesis	139
--	-----

## Chapter 6

IQD-family proteins connect auxin signalling to microtubule-dependent cell division control	172
---	-----

## Chapter 7

General discussion	213
--------------------	-----

English Summary	228
-----------------	-----

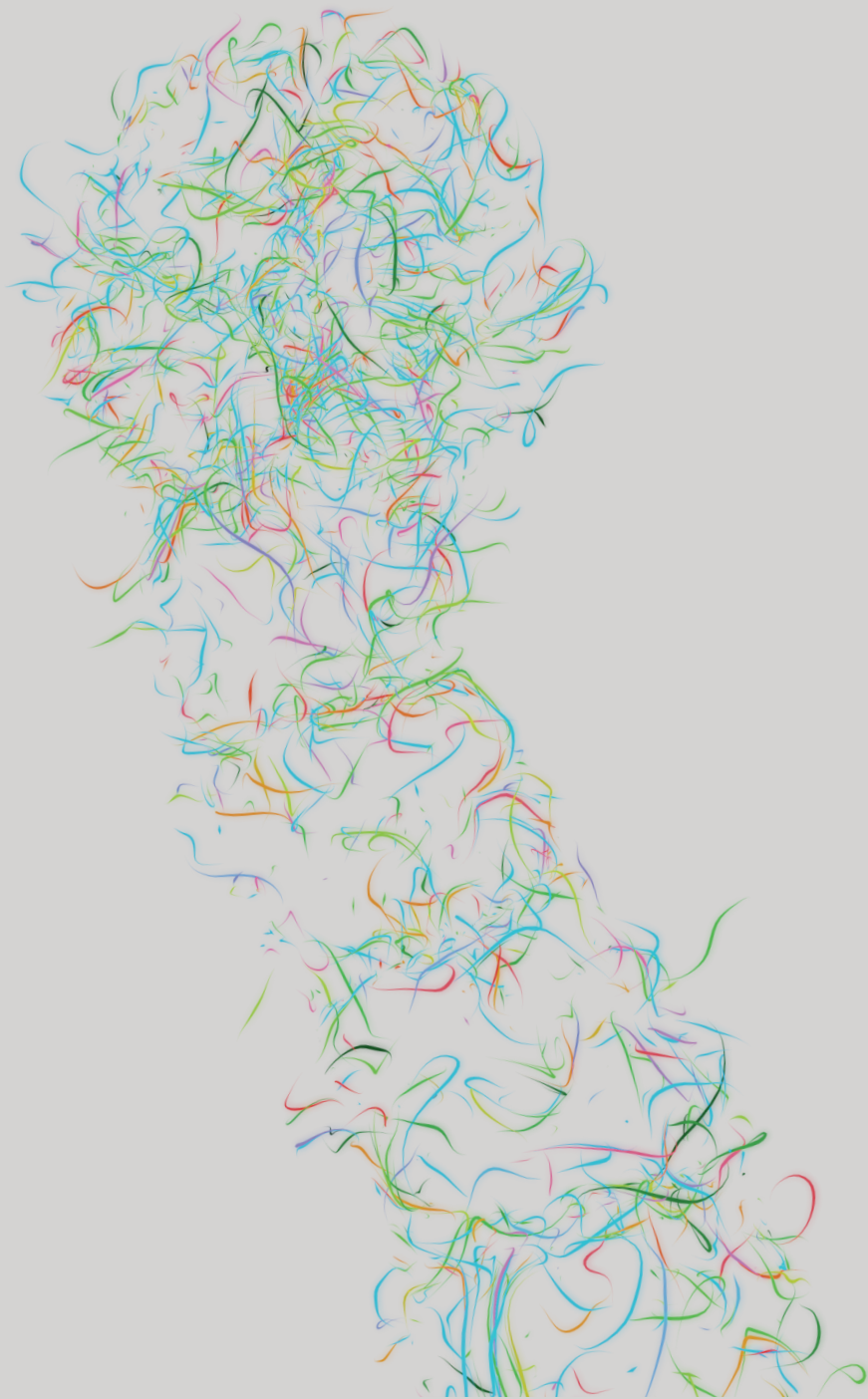
Nederlandse Samenvatting	230
--------------------------	-----

Acknowledgements	232
------------------	-----

Curriculum Vitae	236
------------------	-----

Publications	237
--------------	-----

Education Statement	238
---------------------	-----



# **Chapter 1**

## **Introduction and scope of thesis**



1

## Plant development and generation of plant shapes

In contrast to mammals, plants are fixed in their rooted position for the entity of their life. However, plants have evolved the capacity to adjust to these changes, thus allowing adaptive growth responses under changing environmental conditions. Morphogenesis in plants establishes a basic body plan during embryogenesis that contains all basic tissue types. This body plan is elaborated during postembryonic development through growth of existing organs and the initiation of new ones. Both during embryogenesis and post-embryonically, the body plan is formed through a framework of cell fate decisions and patterning steps that necessitate the coordination of short- and long-range cell-cell communication, cell fate specification, overall- or directed cell expansion and symmetric- or asymmetric oriented cell division (Johnson & Wardlaw, 1956; Johri, 1984; Johri et al., 1992; Vasil, 1979). Plant cells are encapsulated by a rigid pectocellulosic cell wall. Every cell division event generates a new wall with a set position of the daughter cells (Smith, 2001), restricting cell migration and making oriented cell division a key process in plant development and shape determination. As a consequence, orientation of cell division should be under tight regulation, further demonstrated by invariant division patterns in multiple plant organs (Du & Scheres, 2018; Yoshida et al., 2014). Although the analysis of plant development using genetic, molecular and biochemical strategies has generated a large body of data and knowledge (Yruela, 2015), it remains a challenge to uncover the mechanisms underlying plant cell division control. Historically, most progress in plant cell division research was made by plant anatomists and mathematicians working in the 1800's, who established a series of empirical rules emphasizing the importance of cell geometry in plant cell division control (de Wildeman, 1893; Errera, 1888; Thompson & Bonner, 2014). The most prominent geometric rule, formulated by (Errera, 1888) and (de Wildeman, 1893), stated that cells divide along the plane of least area within its fixed cellular space. Experimental data supports this rule (Besson & Dumais, 2011; Yoshida et al., 2014), and it was later termed the “shortest-wall” rule. This type of division is generally considered the default division orientation solely based on geometry. More recent research showed that indeed, by default, cells divide according to the “shortest-wall” rule, but also shows that division plane determination involves a competition between alternative division planes with local area minima, transforming the rule into a probabilistic, rather than a deterministic rule (Besson & Dumais, 2014; Chakraborty et al., 2018b).

## The *Arabidopsis* embryo as a model for plant cell division studies

1 Research focussing on cell division orientation has been hampered by the complexity of plant tissues, the lack of predictability during some developmental processes, and the often-large number of cells involved, complicating tracing of cell division patterns in 3D. Although it comes with its own challenges in terms of accessibility, visualization, and transcriptome analysis, the *Arabidopsis thaliana* embryo is currently one of the most suitable models to study plant cell division regulation and patterning in higher plants, mostly owing to the relative simplicity and the small, predictable number of cells (Jürgens & Mayer, 1994; Sablowski, 2016). The sequence and order of morphogenesis in the *Arabidopsis* embryo is practically invariant, allowing for dissection of complex plant development into individual morphogenetic events. Studies on *Arabidopsis* embryos have led to a vast body of data describing the initiation and maintenance of different cellular lineages (Galinha et al., 2007; Jürgens & Mayer, 1994; Petricka et al., 2009; Scheres et al., 1994). More recently, combining high-resolution imaging of the *Arabidopsis* embryo with computational strategies has led to insight in the cell division orientation machinery (Yoshida et al., 2014). This study showed that the majority of division during embryogenesis divide according the “shortest-wall” division rule, but that formative asymmetric division require additional regulation. Inhibition of auxin response through expression of a nondegradable version of the AUX/IAA protein BODENLOS/IAA12 (BDL) under control of a ubiquitous promoter (RPS5A>>*bdl*; *bdl*-mutant) inhibits all formative divisions during embryogenesis, suggesting that the hormone auxin is involved in regulation of cell division orientation.

### Cellular processes underlying plant cell division control

Generation of cell polarity is a prerequisite for the formation of complex organisms (Nakamura et al., 2012). The three-dimensional structures formed during plant development illustrate the presence and importance of asymmetry during development. Since asymmetry in organs ultimately depends on polarity at the cellular level, considerable efforts have been made to dissect polarity establishment in different developmental contexts (De Smet & Beeckman, 2011; Nakamura et al., 2012; Pietra et al., 2013; Robinson et al., 2011). Well-studied polarity mechanisms identified in yeast and mammalian cells (Chant, 1994; Johnston, 2018) cannot be translated to plants, since yeast- and mammalian polarity regulators seem to be missing from plant genomes. Although mechanisms for polarity are largely unknown in plants, several polarly localized factors are identified (Dong et al.,

2009; Friml et al., 2003, 2002; Gälweiler et al., 1998; Yoshida et al., 2019), and polarity is crucial for correct cell division orientation (Abrash & Bergmann, 2009; Dong et al., 2009; Pillitteri et al., 2016). In yeast and mammalian cells, polarity affects cell division orientation through cytoskeletal rearrangements (Martin & Chang, 2003; Wodarz, 2002). The role of cell polarity in positioning of cytoskeletal structures - and vice versa - in plants cells is not clear, but it is clear that the plant cytoskeleton plays a fundamental role during cell division and cell division orientation regulation (Li et al., 2015; Rasmussen et al., 2011; Takáč et al., 2017).

Microtubule (MT) and actin filaments (AF) cytoskeletal structures are crucial for maintenance of cell morphology and cell expansion (Bashline et al., 2014; Smith & Oppenheimer, 2005). Since cell morphology is a determinant for cell division orientation (Besson & Dumais, 2014; Errera, 1888; Yoshida et al., 2014), cytoskeletal involvement in cell division orientation regulation is likely. Beside interphase orientation of the cortical cytoskeleton, tension on cell walls can alter the cytoskeletal arrangement to form specialized structures known to be essential for correct cell division orientation (Hamant et al., 2008; Louveaux & Hamant, 2013). In addition to the MT-spindle, MTs and AF have evolved a unique set of specialized structure that correspond to the future division plane termed the pre-prophase band (PPB), actin depletion zone (ADZ) and phragmoplast. MTs and AFs reorganize prior to cell division and become spatially restricted to a plane surrounding the nucleus on the membrane, forming the PPB and ADZ. Although some minor variability between PPB and cell plate orientation was observed in specific cases (Oud & Nanninga, 1992), and in some tissues the PPB does not seem to be strictly required for division plane orientation (Schaefer et al., 2017), this arrangement of cytoskeletal structures is observed before every cell division event. In addition to MTs, the PPB contains AFs, which spatially restricts the MT PPB. Actin depolymerization using drugs and mutants leads to widened MT PPBs and affected division plane orientation in higher plants (Hoshino et al., 2003; Yoneda et al., 2005). The PPB is involved in protein- and lipid organisation at the cortical division zone (CDZ) which remain there after PPB disassembly (Mineyuki, 1999; Yabuuchi et al., 2015). These proteins and lipids are thought to guide the phragmoplast to the CDZ, which in turn guides formation of the cell plate. This organisation of cytoskeletal structures during crucial steps in plant cell division make it an obvious candidate for the regulation of cell division orientation.

Additional factors involved in cell division regulation are nuclear position and vacuole distribution. Plant cell divisions are correlated with nuclear position (Lloyd

1 & Chan, 2006), and nuclear position was suggested to be a determinant for division orientation in the *Arabidopsis* embryo (Moukhtar et al., 2019). Whether nuclear position is determined based on cues that define the division plane, or if nuclear position itself is a cue for defining the division plane is not completely clear, but live imaging in the *Arabidopsis* zygote has shown that nuclear position is essential for correct cell division (Kimata et al., 2016). Nuclear position is regulated by cytoskeletal structures and vacuole position (Kimata et al., 2016, 2019; Mineyuki et al., 1991). As plant cell walls expand, the larger cell volume is occupied through enlargement of vacuoles (Sablowski & Carnier Dornelas, 2014). Enlargement of cells has been shown to be controlled by auxin-mediated control of vacuolar morphology (Löffke et al., 2015). This morphological change in cell shape controlled by vacuolar morphology suggests a role for vacuole organisation in plant morphogenesis. In mature *Arabidopsis* zygotes, vacuoles are accumulated at the basal region, which are mostly inherited in the basal cell after the first asymmetric cell division of the zygote (Mansfield & Briarty, 1991; Ueda et al., 2011). The position of the vacuole at this stage is crucial for the position of this first asymmetric divisions, probably through nuclear migration (Kimata et al., 2019). Interestingly, both nuclear position and vacuolar position are dependent on F-actin dynamics (Iwabuchi et al., 2019; Kimata et al., 2019; Scheuring et al., 2016), demonstrating a clear involvement of cytoskeletal structures in the positioning of plant cell division plane.

## Modelling of cortical microtubule array organisation

While molecular- and cell-biological studies can inform us about molecular mechanisms and cellular processes underlying cytoskeleton arrangement, this process is characterised by its large number of stochastic events involving large numbers of MTs (Lindeboom et al., 2013; Mogilner et al., 2012). To study the complex cytoskeletal dynamics and cytoskeleton organisation in relation to cell biological processes, researchers have turned to computational- and mathematical modelling approaches using various strategies (Chakraborty et al., 2018a; Dixit & Cyr, 2004). From this work, focussing on the CMA, predicted mechanisms are formed based on known MT organisation principles. CMT interact through frequent collisions, which together with a homogeneous distribution of MTs and reliable control over array orientation are sufficient for spontaneous MT alignment in models (Tindemans et al., 2014). This led to the formation of a statistically robust hypothesis consistent with observations termed the “survival of the aligned” hypothesis (Tindemans et al., 2010).

This work has been adapted in recent studies to account for realistic three-dimensional plant cell shapes (Chakraborty et al., 2018a) with improved time-efficiency of simulations (Tindemans et al., 2014). These studies reveal that only a minimal set of rules that couple intrinsic MT dynamics to the geometry of the cell are sufficient to predict division patterns that follow symmetric division patterns (Chakraborty et al., 2018a).

## Visualization of subcellular structures in Arabidopsis embryos

To use the Arabidopsis embryo as a model to study cell division and tissue specification pattern, the ability to visualise subcellular structures is crucial. Until recently, few tools were available for subcellular structure visualization in the early embryo, mostly because the position of the embryo within the Arabidopsis ovule makes imaging challenging. To unravel regulation of cell division orientation, we will need to visualize cell biological processes underlying cell division control, including the cytoskeleton, vacuole, nucleus and polarity markers.

A large set of fluorescent subcellular markers that are specifically expressed in the embryo for a variety of subcellular structures, including all structures related to cell division control, has recently been generated (Liao & Weijers, 2018). Imaging of these markers still requires the embryos to be physically removed from the ovule before mounting them in a glucose solution, but allows high resolution imaging of all these structures. This approach has revealed organisation of a variety of subcellular structures during early embryogenesis (Liao, 2018). The downside of this imaging method is that embryos will not survive this treatment over prolonged imaging periods, making temporal imaging of these structures in embryos impossible. To allow temporal imaging of Arabidopsis embryos, several groups have developed *in vitro* ovule culture systems that allow normal ovule growth and embryo development, and tracing of fluorescently marked cell division and tissue specification in real time (Gooh et al., 2015; Kurihara et al., 2017). Visualization of nuclei-, MTs-, AFs-, and vacuoles has been successful using this method, and results have helped understanding developmental processes during the earliest steps of embryogenesis (Gooh et al., 2015; Kimata et al., 2016, 2019). The largest drawback of imaging fluorescent markers through the ovule is the high degree of scattering of the signal due to passing of the signal through several cell layers. This is illustrated by the poor resolution of imaged MTs and AFs in the ovule-culture setup (Kimata et al., 2016, 2019) compared to the MT- and AF imaged outside of the ovule (Liao, 2018). High-resolution temporal imaging will be key to unravel the

function of these highly dynamic subcellular structures in relation to cell division control. It will be interesting to see if future technological improvements can either increase resolution of images obtained through ovule cell layers, or if embryos can be cultured outside the ovule to increase the quality of live-imaging for subcellular structures in the embryo.

## Scope of this thesis

1

Oriented cell division is an essential process in plant development. We use the *Arabidopsis* embryo as a model to study molecular and cell-biological control of oriented cell division. Most cell divisions in the *Arabidopsis* embryo divide according to a geometry-based “shortest-wall” principle, except for formative, asymmetric divisions. We observed that all divisions in the auxin-insensitive *bdl*-mutant switch to “shortest-wall” divisions, suggesting auxin-signalling based control of oriented cell divisions. In this thesis we focus on the identification of mechanisms regulating division plane orientation downstream of auxin in the *Arabidopsis* embryo.

To accomplish the goal of identifying mechanisms underlying regulation of cell division orientation we first describe overall plant morphogenesis and cell fate specification in detail. **Chapter 2** describes the current knowledge regarding regulation and coordination of cell-cell communication, cell fate specification, overall- or directed cell expansion and symmetric- or asymmetric oriented cell division in the *Arabidopsis* embryo. All these processes are initiated in the early embryo to form a basis for the formation of an ordered and adaptive 3D mature plant structure. Asymmetric formative cell divisions at several embryonic stages are essential for correct development, and these divisions are dependent on auxin signalling. Factors mediating this process downstream of auxin are largely unknown.

MT-cytoskeleton dynamics are known to be involved in cell shape- and cell division regulation. In **Chapter 3** we combine high-resolution imaging of cell walls and MTs with a modelling framework for MT organisation using embryonic cell shapes to discover if MT dynamics can explain the division patterns observed in both auxin-insensitive and wild-type *Arabidopsis* embryos. We demonstrate that a simple set of rules coupling intrinsic MT dynamics to the geometry of the cell are sufficient to predict “default” cell division patterns in auxin-insensitive cells. To successfully model wild-type formative divisions we required an additional auxin-dependent face stability factor and an edge-catastrophe reduction

rule. Furthermore, visualization of the MT-cytoskeleton in the *bdl*-mutant confirmed that MT stability is affected in auxin-insensitive cells. These results motivated us to select for factors known to be involved in MT-dynamics regulation when analysing *bdl*-mutant transcriptome datasets in **Chapter 6**.

To explore additional factors involved in regulation of cell division orientation we exploit a previously established high-resolution visualization method for subcellular structures in Arabidopsis embryos. In **Chapter 4** we visualize- and compare AF organisation and nuclear position in wild-type- and *bdl*-mutant embryos. We show that the affected and destabilized AF organisation in the *bdl*-mutant is a possible factor involved in regulation of cell division orientation through cell expansion. The high variability observed for nuclear position in both wild-type and *bdl*-mutant embryonic cells reveals that this is not a determinant for cell division orientation in the embryo.

To identify factors responsible for regulation of cell division orientation downstream of auxin-mediated signalling in early Arabidopsis embryos, in **Chapter 5**, we generate and optimize a transcriptome analysis pipeline. Using this optimized transcriptome analysis pipeline, we generate a reference transcriptome for early Arabidopsis embryogenesis including 2-cell- to early globular embryos, which can be used to explore the genetic a regulatory basis underlying developmental processes during embryogenesis.

**Chapter 6** aims to identify factors transcriptionally regulated downstream of auxin, that are involved in regulation of cell division orientation using the optimized Arabidopsis embryo transcriptome analysis pipeline. The identified factors connect auxin-signalling to Calcium-signalling dependent cytoskeletal control as a mechanism acting in cell division orientation control.

Finally, in **Chapter 7** the findings of this thesis are discussed and are placed in a broader perspective. In this chapter we also discuss approaches to further dissect the mechanisms underlying regulation of cell division orientation in future research.

## References

- Abrash, E. B., & Bergmann, D. C. (2009). Asymmetric Cell Divisions: A View from Plant Development. *Developmental Cell*. <https://doi.org/10.1016/j.devcel.2009.05.014>
- Bashline, L., Lei, L., Li, S., & Gu, Y. (2014). Cell wall, cytoskeleton, and cell expansion in higher plants. *Molecular Plant*. <https://doi.org/10.1093/mp/ssu018>
- Besson, S., & Dumais, J. (2011). Universal rule for the symmetric division of plant cells. *Proceedings of the National Academy of Sciences*. <https://doi.org/10.1073/pnas.1011866108>
- Besson, Sébastien, & Dumais, J. (2014). Stochasticity in the symmetric division of plant cells: When the exceptions are the rule. *Frontiers in Plant Science*. <https://doi.org/10.3389/fpls.2014.00538>
- Chakraborty, B., Blilou, I., Scheres, B., & Mulder, B. M. (2018). A computational framework for cortical microtubule dynamics in realistically shaped plant cells. *PLoS Computational Biology*. <https://doi.org/10.1371/journal.pcbi.1005959>
- Chakraborty, B., Willemsen, V., de Zeeuw, T., Liao, C. Y., Weijers, D., Mulder, B., & Scheres, B. (2018). A Plausible Microtubule-Based Mechanism for Cell Division Orientation in Plant Embryogenesis. *Current Biology*. <https://doi.org/10.1016/j.cub.2018.07.025>
- Chant, J. (1994). Cell polarity in yeast. *Trends in Genetics*. [https://doi.org/10.1016/0168-9525\(94\)90036-1](https://doi.org/10.1016/0168-9525(94)90036-1)
- De Smet, I., & Beeckman, T. (2011). Asymmetric cell division in land plants and algae: the driving force for differentiation. *Nature Reviews. Molecular Cell Biology*, 12(3), 177–188. <https://doi.org/10.1038/nrm3064>
- de Wildeman, E. (1893). Études sur l'attache des cloisons cellulaires. *Mémoires Couronnés et Mémoires Des Savants Étrangers*, 53, 1–84.
- Dixit, R., & Cyr, R. (2004). Encounters between dynamic cortical microtubules promote ordering of the cortical array through angle-dependent modifications of microtubule behavior. *Plant Cell*. <https://doi.org/10.1105/tpc.104.026930>
- Dong, J., MacAlister, C. A., & Bergmann, D. C. (2009). BASL Controls Asymmetric Cell Division in Arabidopsis. *Cell*. <https://doi.org/10.1016/j.cell.2009.04.018>

Du, Y., & Scheres, B. (2018). Lateral root formation and the multiple roles of auxin. *Journal of Experimental Botany*. <https://doi.org/10.1093/jxb/erx223>

Errera, L. (1888). Über Zellformen und Siefenblasen. *Bot. Centralbl.*, 34, 395–399.

Friml, Jiří, Vieten, A., Sauer, M., Weijers, D., Schwarz, H., Hamann, T., ... Jürgens, G. (2003). Efflux-dependent auxin gradients establish the apical-basal axis of Arabidopsis. *Nature*. <https://doi.org/10.1038/nature02085>

Friml, Jiří, Wiśniewska, J., Benková, E., Mendgen, K., & Palme, K. (2002). Lateral relocation of auxin efflux regulator PIN3 mediates tropism in Arabidopsis. *Nature*. <https://doi.org/10.1038/415806a>

Galinha, C., Hofhuis, H., Luijten, M., Willemsen, V., Blilou, I., Heidstra, R., & Scheres, B. (2007). PLETHORA proteins as dose-dependent master regulators of Arabidopsis root development. *Nature*. <https://doi.org/10.1038/nature06206>

Gälweiler, L., Guan, C., Müller, A., Wisman, E., Mendgen, K., Yephremov, A., & Palme, K. (1998). Regulation of polar auxin transport by AtPIN1 in Arabidopsis vascular tissue. *Science*. <https://doi.org/10.1126/science.282.5397.2226>

Gooh, K., Ueda, M., Aruga, K., Park, J., Arata, H., Higashiyama, T., & Kurihara, D. (2015). Live-Cell Imaging and Optical Manipulation of Arabidopsis Early Embryogenesis. *Developmental Cell*. <https://doi.org/10.1016/j.devcel.2015.06.008>

Hamant, O., Heisler, M. G., Jönsson, H., Krupinski, P., Uyttewaal, M., Bokov, P., ... Traas, J. (2008). Developmental patterning by mechanical signals in Arabidopsis. *Science*. <https://doi.org/10.1126/science.1165594>

Hoshino, H., Yoneda, A., Kumagai, F., & Hasezawa, S. (2003). Roles of actin-depleted zone and preprophase band in determining the division site of higher-plant cells, a tobacco BY-2 cell line expressing GFP-tubulin. *Protoplasma*. <https://doi.org/10.1007/s00709-003-0012-8>

Iwabuchi, K., Ohnishi, H., Tamura, K., Fukao, Y., Furuya, T., Hattori, K., ... Hara-Nishimura, I. (2019). ANGUSTIFOLIA Regulates Actin Filament Alignment for Nuclear Positioning in Leaves. *Plant Physiology*. <https://doi.org/10.1104/pp.18.01150>

Johnson, M. A., & Wardlaw, C. W. (1956). Embryogenesis in Plants. *Bulletin of the Torrey*

*Botanical Club*. <https://doi.org/10.2307/2482745>

Johnston, D. S. (2018). Establishing and transducing cell polarity: common themes and variations. *Current Opinion in Cell Biology*. <https://doi.org/10.1016/j.ceb.2017.10.007>

Johri, B.M. (1984). Embryology of Angiosperms. *Springer-Verlag Berlin Heidelberg*.

Johri, Brij M., Ambegaokar, K. B., & Srivastava, P. S. (1992). Comparative Embryology of Angiosperms. In *Comparative Embryology of Angiosperms*. <https://doi.org/10.1007/978-3-642-76395-3>

Jürgens, G., & Mayer, U. (1994). “Arabidopsis,” in A colour Atlas of Developing Embryos. *Harcourt Health Sciences*.

Kimata, Y., Higaki, T., Kawashima, T., Kurihara, D., Sato, Y., Yamada, T., ... Ueda, M. (2016). Cytoskeleton dynamics control the first asymmetric cell division in Arabidopsis zygote. *Proceedings of the National Academy of Sciences*. <https://doi.org/10.1073/pnas.1613979113>

Kimata, Y., Kato, T., Higaki, T., Kurihara, D., Yamada, T., Segami, S., ... Ueda, M. (2019). Polar vacuolar distribution is essential for accurate asymmetric division of Arabidopsis zygotes. *Proceedings of the National Academy of Sciences of the United States of America*. <https://doi.org/10.1073/pnas.1814160116>

Kurihara, D., Kimata, Y., Higashiyama, T., & Ueda, M. (2017). In vitro ovule cultivation for live-cell imaging of zygote polarization and embryo patterning in Arabidopsis thaliana. *Journal of Visualized Experiments*. <https://doi.org/10.3791/55975>

Li, S., Sun, T., & Ren, H. (2015). The functions of the cytoskeleton and associated proteins during mitosis and cytokinesis in plant cells. *Frontiers in Plant Science*, 6, 282. <https://doi.org/10.3389/fpls.2015.00282>

Liao, C. Y., & Weijers, D. (2018). A toolkit for studying cellular reorganization during early embryogenesis in Arabidopsis thaliana. *Plant Journal*. <https://doi.org/10.1111/tpj.13841>

Lindeboom, J. J., Lioutas, A., Deinum, E. E., Tindemans, S. H., Ehrhardt, D. W., Mie, A. C. E., ... Mulder, B. M. (2013). Cortical microtubule arrays are initiated from a nonrandom prepattern driven by atypical microtubule initiation. *Plant Physiology*. <https://doi.org/10.1104/pp.112.204057>

- Lloyd, C., & Chan, J. (2006). Not so divided: the common basis of plant and animal cell division. *Nature Reviews Molecular Cell Biology*, 7(2), 147–152. <https://doi.org/10.1038/nrm1831>
- Löfke, C., Dünser, K., Scheming, D., & Kleine-Vehn, J. (2015). Auxin regulates SNARE-dependent vacuolar morphology restricting cell size. *ELife*. <https://doi.org/10.7554/eLife.05868>
- Louveaux, M., & Hamant, O. (2013). The mechanics behind cell division. *Current Opinion in Plant Biology*. <https://doi.org/10.1016/j.pbi.2013.10.011>
- Mansfield, S. G., & Briarty, L. G. (1991). Early embryogenesis in *Arabidopsis thaliana* . II. The developing embryo . *Canadian Journal of Botany*. <https://doi.org/10.1139/b91-063>
- Martin, S. G., & Chang, F. (2003). Cell polarity: A new mod(e) of anchoring. *Current Biology*. <https://doi.org/10.1016/j.cub.2003.08.046>
- Mineyuki, Y. (1999). The preprophase band of microtubules: Its function as a cytokinetic apparatus in higher plants. *International Review of Cytology*.
- Mineyuki, Y., Marc, J., & Palevitz, B. A. (1991). Relationship Between the Preprophase Band, Nucleus and Spindle in Dividing *Allium* Cotyledon Cells. *Journal of Plant Physiology*. [https://doi.org/10.1016/S0176-1617\(11\)81309-X](https://doi.org/10.1016/S0176-1617(11)81309-X)
- Mogilner, A., Allard, J., & Wollman, R. (2012). Cell polarity: Quantitative modeling as a tool in cell biology. *Science*. <https://doi.org/10.1126/science.1216380>
- Moukhtar, J., Trubuil, A., Belcram, K., Legland, D., Khadir, Z., Urbain, A., ... Andrey, P. (2019). Cell geometry determines symmetric and asymmetric division plane selection in *arabidopsis* early embryos. *PLoS Computational Biology*. <https://doi.org/10.1371/journal.pcbi.1006771>
- Nakamura, M., Kiefer, C. S., & Grebe, M. (2012). Planar polarity, tissue polarity and planar morphogenesis in plants. *Current Opinion in Plant Biology*. <https://doi.org/10.1016/j.pbi.2012.07.006>
- Oud, J. L., & Nanninga, N. (1992). Cell shape, chromosome orientation and the position of the plane of division in *Vicia faba* root cortex cells. *Journal of Cell Science*.
- Petricka, J. J., Van Norman, J. M., & Benfey, P. N. (2009). Symmetry breaking in plants:

molecular mechanisms regulating asymmetric cell divisions in Arabidopsis. *Cold Spring Harbor Perspectives in Biology*.

Pietra, S., Gustavsson, A., Kiefer, C., Kalmbach, L., Hörstedt, P., Ikeda, Y., ... Grebe, M. (2013). Arabidopsis SABRE and CLASP interact to stabilize cell division plane orientation and planar polarity. *Nature Communications*, 4. <https://doi.org/10.1038/ncomms3779>

Pillitteri, L. J., Guo, X., & Dong, J. (2016). Asymmetric cell division in plants: mechanisms of symmetry breaking and cell fate determination. *Cellular and Molecular Life Sciences*. <https://doi.org/10.1007/s00018-016-2290-2>

Rasmussen, C. G., Humphries, J. A., & Smith, L. G. (2011). Determination of symmetric and asymmetric division planes in plant cells. *Annual Review of Plant Biology*, 62, 387–409. <https://doi.org/10.1146/annurev-arplant-042110-103802>

Robinson, S., De Reuille, P. B., Chan, J., Bergmann, D., Prusinkiewicz, P., & Coen, E. (2011). Generation of spatial patterns through cell polarity switching. *Science*. <https://doi.org/10.1126/science.1202185>

Sablowski, R. (2016). Coordination of plant cell growth and division: collective control or mutual agreement? *Current Opinion in Plant Biology*. <https://doi.org/10.1016/j.pbi.2016.09.004>

Sablowski, R., & Carnier Dornelas, M. (2014). Interplay between cell growth and cell cycle in plants. *Journal of Experimental Botany*. <https://doi.org/10.1093/jxb/ert354>

Schaefer, E., Belcram, K., Uyttewaal, M., Duroc, Y., Goussot, M., Legland, D., ... Bouchez, D. (2017). The preprophase band of microtubules controls the robustness of division orientation in plants. *Science*. <https://doi.org/10.1126/science.aal3016>

Scheres, B., Wolkenfelt, H., Willemsen, V., Terlouw, M., Lawson, E., Dean, C., & Weisbeek, P. (1994). Embryonic origin of the Arabidopsis primary root and root meristem initials. *Development*.

Scheuring, D., Löffke, C., Krüger, F., Kittelmann, M., Eisa, A., Hughes, L., ... Kleine-Vehn, J. (2016). Actin-dependent vacuolar occupancy of the cell determines auxin-induced growth repression. *Proceedings of the National Academy of Sciences of the United States of America*. <https://doi.org/10.1073/pnas.1517445113>

Smith, L. G. (2001). Plant cell division: Building walls in the right places. *Nature Reviews Molecular Cell Biology*. <https://doi.org/10.1038/35048050>

Smith, L. G., & Oppenheimer, D. G. (2005). Spatial control of cell expansion by the plant cytoskeleton. *Annual Review of Cell and Developmental Biology*. <https://doi.org/10.1146/annurev.cellbio.21.122303.114901>

Takáč, T., Šamajová, O., Pechan, T., Luptovčiak, I., & Šamaj, J. (2017). Feedback Microtubule Control and Microtubule-Actin Cross-talk in Arabidopsis Revealed by Integrative Proteomic and Cell Biology Analysis of KATANIN 1 Mutants . *Molecular & Cellular Proteomics*. <https://doi.org/10.1074/mcp.m117.068015>

Thompson, D. W., & Bonner, J. T. (2014). On growth and form. In *On Growth and Form*. <https://doi.org/10.1017/CBO9781107589070>

Tindemans, S. H., Deinum, E. E., Lindeboom, J. J., & Mulder, B. M. (2014). Efficient event-driven simulations shed new light on microtubule organization in the plant cortical array. *Frontiers in Physics*. <https://doi.org/10.3389/fphy.2014.00019>

Tindemans, S. H., Hawkins, R. J., & Mulder, B. M. (2010). Survival of the aligned: Ordering of the plant cortical microtubule array. *Physical Review Letters*. <https://doi.org/10.1103/PhysRevLett.104.058103>

Ueda, M., Zhang, Z., & Laux, T. (2011). Transcriptional Activation of Arabidopsis Axis Patterning Genes WOX8/9 Links Zygote Polarity to Embryo Development. *Developmental Cell*. <https://doi.org/10.1016/j.devcel.2011.01.009>

Vasil, V. (1979). Embryology of Gymnosperms. *Encyclopedia of Plant Anatomy, Volume X, Part 2*. Hardev Singh . *The Quarterly Review of Biology*. <https://doi.org/10.1086/411361>

Wodarz, A. (2002). Establishing cell polarity in development. *Nature Cell Biology*. <https://doi.org/10.1038/ncb0202-e39>

Yabuuchi, T., Nakai, T., Sonobe, S., Yamauchi, D., & Mineyuki, Y. (2015). Preprophase band formation and cortical division zone establishment: RanGAP behaves differently from microtubules during their band formation. *Plant Signaling and Behavior*. <https://doi.org/10.1080/15592324.2015.1060385>

Yoneda, A., Akatsuka, M., Hoshino, H., Kumagai, F., & Hasezawa, S. (2005). Decision of

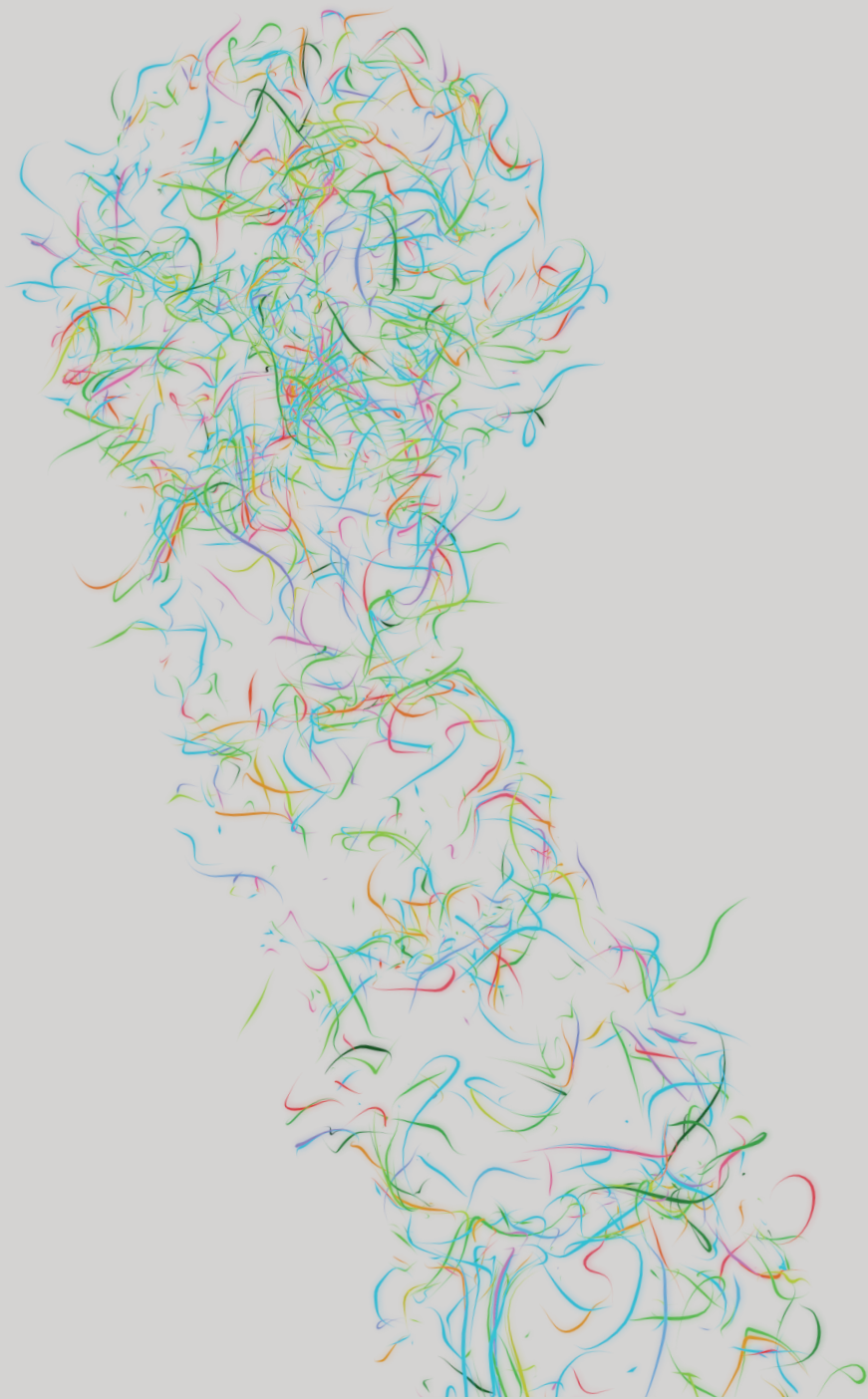
spindle poles and division plane by double preprophase bands in a BY-2 cell line expressing GFP-tubulin. *Plant and Cell Physiology*. <https://doi.org/10.1093/pcp/pci055>

Yoshida, S., Barbier de Reuille, P., Lane, B., Bassel, G. W., Prusinkiewicz, P., Smith, R. S., & Weijers, D. (2014). Genetic control of plant development by overriding a geometric division rule. *Developmental Cell*, 29(1), 75–87. <https://doi.org/10.1016/j.devcel.2014.02.002>

Yoshida, S., van der Schuren, A., van Dop, M., van Galen, L., Saiga, S., Adibi, M., ... Weijers, D. (2019). A SOSEKI-based coordinate system interprets global polarity cues in Arabidopsis. *Nature Plants*. <https://doi.org/10.1038/s41477-019-0363-6>

Yruela, I. (2015). Plant development regulation: Overview and perspectives. *Journal of Plant Physiology*. <https://doi.org/10.1016/j.jplph.2015.05.006>





## Chapter 2

# Tissue and organ initiation in the plant embryo: A first time for everything

Joakim Palovaara<sup>1\*</sup>, Thijs de Zeeuw<sup>1\*</sup>, and Dolf Weijers<sup>1</sup>

A version of this chapter has been published as:

**Palovaara, J, de Zeeuw, T. and Weijers, D. 2016.** Tissue and organ initiation in the plant embryo: A first time for everything. *Annual Review of cell and developmental biology* 32

1. Laboratory of Biochemistry, Wageningen University, Stippeneng 4, 6708 WE. Wageningen, the Netherlands

\* These authors contributed equally



## Abstract

Land plants can grow to tremendous body sizes, yet even the most complex architectures are the result of iterations of the same developmental processes: organ initiation, growth, and pattern formation. A central question in plant biology is how these processes are regulated and coordinated to allow for the formation of ordered, 3D structures. All these elementary processes first occur in early embryogenesis, during which, from a fertilized egg cell, precursors for all major tissues and stem cells are initiated, followed by tissue growth and patterning. Here we discuss recent progress in our understanding of this phase of plant life. We consider the cellular basis for multicellular development in 3D and focus on the genetic regulatory mechanisms that direct specific steps during early embryogenesis.

## Introduction

Embryogenesis is the process in which an embryo, a rudimentary multicellular diploid eukaryote, develops from a fertilized egg cell, the zygote<sup>1</sup>. In land plants (embryophytes), this process initiates a framework of cell fate<sup>2</sup> decisions and patterning steps that necessitate the coordination of oriented cell division, cell-cell communication (positional signaling), and genetic regulatory mechanisms. As the embryo develops, the first tissue precursors and stem cells are established to set up the basic body pattern of the plant. This invariably results in a mature embryo (seedling) that consist of the epidermis, vasculature (in tracheophytes), and ground tissues, i.e., the basic tissue types of the postembryonic structure (Johnson & Wardlaw, 1956; Johri, 1984; Johri et al., 1992; Vasil, 1979). Thus, embryogenesis and the intrinsic specification events that occur are fundamental for postembryonic plant development.

In seed plants, the stereotyped seedling displays a body plan of an overlapping apical-basal and radial pattern<sup>3</sup> (Johri, 1984; Johri et al., 1992; Vasil, 1979). Along the apical-basal axis of polarity, the primary apical meristems<sup>4</sup> are located at the shoot [shoot apical meristem (SAM)], flanked by one or more cotyledons<sup>5</sup>, and at the root [root apical meristem (RAM)]. The basic tissue types form concentric layers in a perpendicular radial pattern. The meristems contain niches in which pluripotent stem cells continuously divide to produce differentiated cells for organ formation and in which neighboring organizer cells prevent differentiation of the stem cells (Van Den Berg et al., 1997; Weigel & Jürgens, 2002). Although this basic body plan of the seedling is similar in different species, the developmental path often varies. In many seed plants, early embryogenesis is characterized by seemingly irregular and random cell divisions (Johri, 1984; Johri et al., 1992; Vasil, 1979). In contrast, members of the Brassicaceae family of flowering plants, including *Arabidopsis thaliana*, display highly regular and predictable patterns (Gooh et al., 2015; Jürgens & Mayer, 1994; Mansfield & Briarty, 1991; Yoshida et al., 2014). Due to such regularity, the origin of mature embryo and seedling structures can be traced back to specific cell types in the early embryo. Because *Arabidopsis* also has a small genome and is relatively easy to genetically manipulate, it has become the de facto model organism to

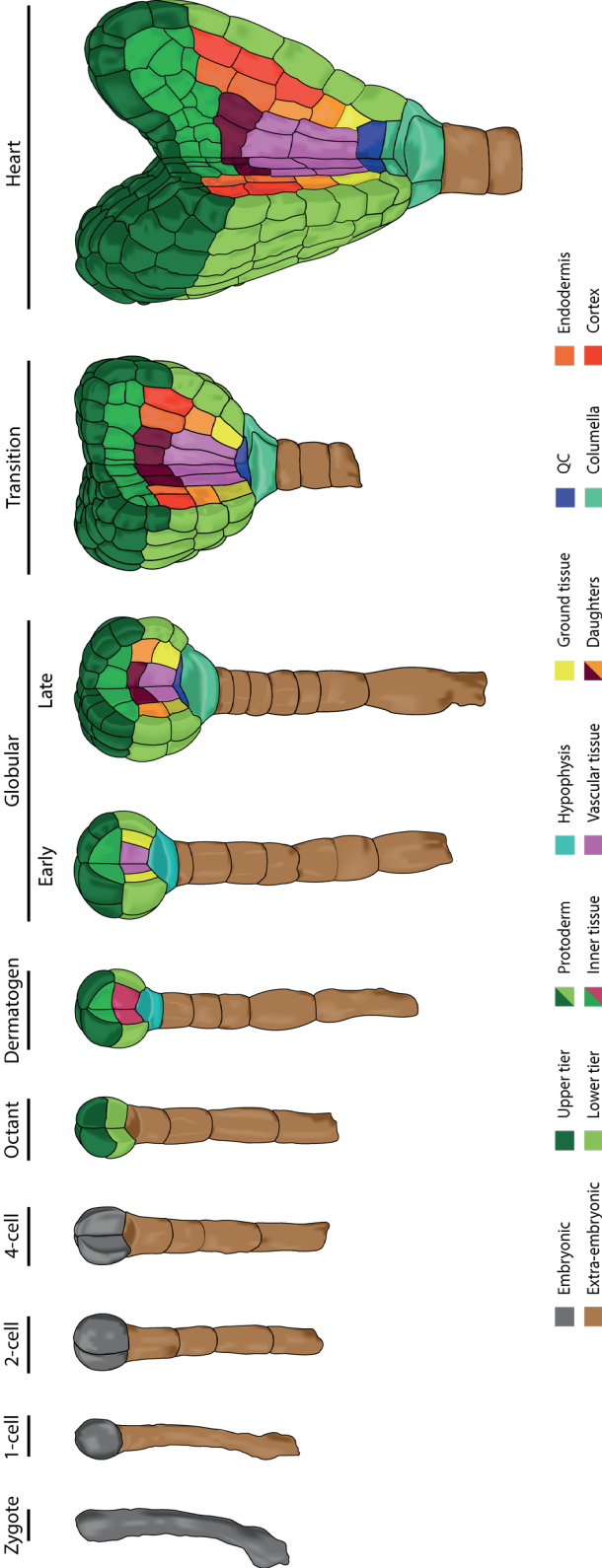
<sup>1</sup>**Zygote:** the fertilized egg cell

<sup>2</sup>**Cell fate:** the differentiated state to which a cell has become committed

<sup>3</sup>**Apical-basal and radial axis:** anatomical terminology to describe the polarity and orientation around a central plant body axis

<sup>4</sup>**Meristem:** a region that sustains plant growth through stem cell niche activity

<sup>5</sup>**Cotyledon:** an embryonic leaf



**Figure 1:** 3D view of early embryo development in *Arabidopsis thaliana*. Cells are colored according to their lineage. Upper-tier cells will become the shoot and lower-tier cells will become the hypocotyl and root of the future seedling. QC denotes quiescent center. Based on imaging data described in Yoshida et al. (2014).

study the molecular and cellular mechanisms underlying pattern formation during seed plant embryo development. Accordingly, although morphological studies of the embryos of a range of species date back nearly a century, most of the genetic (and all of the genomic) advances have been made in the past 20 years, largely from *Arabidopsis*.

This review covers current knowledge and advances with regard to the cellular basis of embryo development in 3D and the genetic control of key developmental transitions that—through positional signaling, cell fate decisions, and (apical-basal/radial) patterning—shape the embryo. Our focus is on major determination events rather than on their maintenance, and thus on early embryogenesis when tissue precursors and stem cells are first specified. Because most of what is currently known regarding this topic is based on *Arabidopsis* studies, this review mainly explores early *Arabidopsis* embryo development, although other seed plant species are considered, when appropriate, to broaden the scope. Finally, the outstanding questions this field faces, as well as the possible ways forward, are discussed.

## The fundamentals: Ontogeny and cell biology of the embryo

The ontogeny of the plant embryo can be divided into different defined stages of development, from the time of fertilization of the egg cell to its mature form. Due to the invariant cell lineage in the embryo, this process is very distinct in *Arabidopsis* (Figure 1) (Gooh et al., 2015; Jürgens & Mayer, 1994; Mansfield & Briarty, 1991; Yoshida et al., 2014). The fertilized zygote elongates and divides to produce a smaller apical cell and a larger basal cell. The apical cell forms the eight-cell (octant-stage) proembryo<sup>1</sup> through two rounds of longitudinal divisions and a transverse division. Through a series of transverse divisions, the basal cell generates the extraembryonic suspensor<sup>2</sup>, a file of seven to nine cells that anchors the embryo to the surrounding embryo sac and ovule tissue (Mansfield

<sup>1</sup>**Proembryo:** cell collective that will form the majority of the embryo

<sup>2</sup>**Suspensor:** an extraembryonic structure that connects the proembryo to the ovule

<sup>3</sup>**Protoderm:** surface cell layer of the proembryo that differentiates into the epidermis

<sup>4</sup>**Ground tissue initials:** primordium that will generate the endodermis and cortex of the ground tissue

<sup>5</sup>**Vascular initials:** primordium that will form xylem, phloem, and (pro)cambium of the vascular bundle

<sup>6</sup>**Hypophysis:** the top cell of the *Arabidopsis* suspensor that differentiates into the quiescent center and columella stem cells of the root apical meristem

<sup>7</sup>**Asymmetric cell division:** division that results in two daughter cells unequal in size and/or in distribution of cellular components or molecules (RNA, protein)

<sup>8</sup>**Quiescent center (QC):** the organizer cells of the root apical meristem

## AUXIN SIGNALING

*The transcriptional response to auxin, a key regulator of plant development, is orchestrated through auxin response factor (ARF) DNA-binding proteins and AUX/IAA (IAA) transcriptional repressors. Auxin binds the F-box protein TRANSPORTER INHIBITOR RESPONSE1 (TIR1) to promote proteasome-mediated degradation of IAAs through the SCF<sup>TIR1/AFB</sup> ubiquitin ligase complex (reviewed in in (Wang & Estelle, 2014)). Upon IAA protein degradation, ARFs are released to regulate the expression of auxin-responsive genes. ARFs contain a conserved DNA-binding domain (DBD) at their N termini that targets generic auxin response elements (AuxRE) (Ulmasov et al., 1999), a middle region to activate or repress transcription (Tiwari et al., 2003), and a C-terminal domain (domain III/IV) that mediates ARF/IAA and ARF/ARF interactions (Han et al., 2014; Korasick et al., 2014; Nanao et al., 2014). Dimerization of the ARF DBDs leads to cooperative binding to adjacent AuxRE sites (Boer et al., 2014), with the spacing between sites determining ARF binding affinity. Because ARFs can also dimerize through domain III/IV, DNA-bound ARF dimers can form higher-order complexes that can be disrupted or weakened by IAA/ARF interaction (Han et al., 2014). Together, these findings suggest a model in which specificity and diversification of gene expression in response to auxin depend on the properties of dimeric and, possibly, oligomeric ARF complexes.*

& Briarty, 1991). The octant-stage proembryo can be separated into upper- and lower-tier cells along the apical-basal axis. The upper-tier cells will give rise to the SAM and most of the cotyledons (i.e., the shoot), whereas the lower-tier cells will form the RAM (i.e., the hypocotyl and root) (Jürgens & Mayer, 1994; Mansfield & Briarty, 1991). A radial axis emerges at the 16-cell (dermatogen) stage, when periclinal divisions generate eight outer protodermal<sup>3</sup> cells (epidermis precursor cells) and eight inner cells. The four inner cells in the lower hemisphere form ground tissue<sup>4</sup> and (inner) vascular initial cells<sup>5</sup> after subsequent periclinal divisions during the transition to the early globular stage. Concurrently, the uppermost cell of the suspensor is specified as the hypophysis<sup>6</sup>. The hypophysis divides asymmetrically<sup>7</sup> to form a smaller lens-shaped apical cell and a larger basal cell. Both of these cells are incorporated into the embryo to form the organizer center, i.e., the quiescent center<sup>8</sup> (QC), and columella root cap cells, respectively, of the RAM (Hamann et al., 1999; Scheres et al., 1994). The SAM is first recognizable as a group of small cells between the cotyledon primordia at the torpedo stage (Barton & Poethig, 1993; Laux et al., 1996).

From this limited set of initial cells, the plant ultimately generates a complex, multicellular body pattern. In contrast to animal cells, plant cells have rigid cell walls

<sup>1</sup>**Shortest-wall rule:** states that a new division wall will form according to local energy minima in a cell; this orientation is considered to be the default division orientation

preventing cell migration, meaning that correct division orientation and growth are essential. The coordination of cell division is executed individually in each cell, raising the question of how the collective of individual cellular decisions generate identical, or at least similar, 3D tissues and organs. Little is known about the underlying mechanisms that ensure uniform division patterns that form the mature plant body from the simple embryonic structure. Therefore, this phase of plant life offers an excellent opportunity for exploring the fundamental principles that determine organized 3D development in plants.

Formation of an ordered 3D structure can be orchestrated through genetic regulation or, alternatively, uniform geometric rules for cell behavior and the self-organization of cells into defined shapes. The early embryo, because of its simplicity, is a good model to address the role of geometric and genetic input to cell division orientation. Simulations and abstractions of plant cell division are based mostly on classical rules proposed in the nineteenth century (de Wildeman, 1893; Errera, 1888; Hofmeister & West, 2012; Sachs, 1877). The most prominent geometric rule, formulated by Errera (1888) and de Wildeman (1893), states that, upon cell division, a cell will divide along the plane of least area that encloses a fixed cellular volume. Such division was later defined as the shortest-wall rule<sup>1</sup> and can be considered the default orientation that is directed primarily by geometric principles. Experimental data support this rule but suggest that selection of the plane of division involves a competition between alternative division plane configurations whose geometries represent local area minima, transforming this rule to a probabilistic rule (Besson & Dumais, 2011). Recent developments in 3D and live imaging, combined with those in modeling, have provided important new information regarding division patterns and shape changes during embryogenesis and postembryonic organogenesis in plants (Gooh et al., 2015; Von Wangenheim et al., 2016; Yoshida et al., 2014). Similar to the case of previously described stomatal divisions (Galatis & Apostolakos, 2004), these studies report asymmetric cell divisions that deviate from the default geometric shortest-wall rule. These findings indicate that such divisions are in some way regulated, possibly by mechanical stresses (Louveaux & Hamant, 2013) and/or the hormone auxin<sup>1</sup> [indole-3-acetic acid (IAA)] (Yoshida et al., 2014), whose signaling mechanism is detailed in the **box “Auxin Signaling”**.

<sup>1</sup>**Auxins:** a class of plant signaling molecules; the main auxin is indole-3-acetic acid

<sup>2</sup>**Actin filaments (AFs) and microtubules (MTs):** cytoskeletal filaments that form the cytoskeleton matrix in plant cells

<sup>3</sup>**Preprophase band (PPB):** an array of cortical microtubules and actin filaments that predicts cell plate formation and division in a plant cell

With the exception of the formative asymmetric divisions, most division in the *Arabidopsis* embryo can be explained using a 3D version of the shortest-wall principle. However, in embryos insensitive to auxin, formative divisions are suppressed, and all divisions follow the geometric default rule. This observation suggests that auxin is required to suppress default divisions (Yoshida et al., 2014), raising the question of what underlying mechanisms alter the division plane orientation in response to auxin signaling. (Lloyd, 1991) proposed that actin filaments<sup>2</sup> (AFs) interact with cortical microtubules<sup>2</sup> (MTs) to guide the future plane of divisions to a configuration of minimal area. Later, (Besson & Dumais, 2014) linked probabilistic geometric rules to the arrangement of cytoskeletal structures within cells, possibly revealing the key structures responsible for regulation of division plane orientation.

MTs and AFs are the two major cytoskeletal structures that are essential for cell division and expansion in plants (Kost et al., 1999; Vanstraelen et al., 2006). The site of cell plate formation and subsequent cell division is first marked by the position of a transient ring of cortical MTs and AFs termed the preprophase band<sup>3</sup> (PPB) (Mineyuki, 1999). Given that the PPB accurately predicts the division plane orientation, events leading to its positioning may give insight into the mechanisms determining division plane orientation. In premitotic cells, MT and AF strands connect the nucleus to the cell surface (Lloyd, 1991). These strands are under tension, which helps maintain the position of the nucleus in the cell and possibly underlies the tendency for these strands to span the shortest distance to the cell surface (Besson & Dumais, 2011). The same strands stabilize cortical MTs recruited for PPB formation. In contrast to animals, plants lack centrosomes as microtubule-organizing centers (reviewed in (Masoud et al., 2013)). However, a phosphatase 2A (PP2A) complex termed TTP—composed of TONNEAU1 (TON1), TON1 recruiting motif (TRM), and PP2A, all of which share similarities with animal centrosomal proteins (Azimzadeh et al., 2008; Drevensek et al., 2012; Spinner et al., 2013)—has been identified in *Arabidopsis*. TRM1 binds to and recruits TON1 to the cortical microtubules, where it forms a multiprotein complex with PP2A (Spinner et al., 2013). This complex is essential for correct PPB formation, and mutations of complex members lead to defects in division plane orientation and PPB assembly.

Other MT-associated proteins involved in PPB formation have been identified (reviewed in (Rasmussen et al., 2013)). These proteins include the SABRE (SAB) and CLASP proteins (Ambrose et al., 2007; Pietra et al., 2013). SAB stabilizes CLASP-dependent MT orientation in the PPB to ensure correct division plane direction in *Arabidopsis* roots (Pietra

## PARENT-OF-ORIGIN EFFECTS AND ZYGOTIC GENOME ACTIVATION

Two models have been proposed for the maternal-to-zygotic transition in plants. The prevailing model proposes that most mRNAs in the early embryo are maternally derived (Autran et al., 2011; Pillot et al., 2010), whereas an alternative model suggests that both maternal and paternal alleles generate the early embryonic transcriptome (Ingouff et al., 2010; Meyer & Scholten, 2007; Nodine & Bartel, 2012; Weijers et al., 2001). Can these two different models of parent-of-origin effects be reconciled?

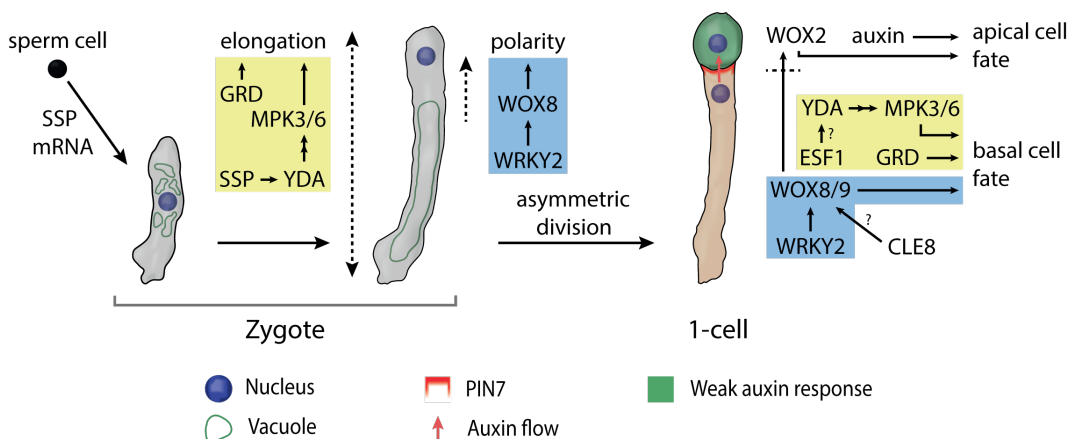
(Del Toro-De León et al., 2014) showed that significant variance in parental allele activation is observed in hybrid embryos with parents of different *Arabidopsis* ecotypes, which could explain the conflicting results of previous transcriptomics studies (Autran et al., 2011; Meyer & Scholten, 2007; Nodine & Bartel, 2012). In nonhybrid embryos, zygotic genome activation (ZGA) roughly correlates with the first division of the zygote (reviewed in (Del Toro-De León et al., 2016)). Functional evidence suggests that initial zygotic transcription shows a maternal bias and that progressive release of gene silencing gradually increases many paternal alleles as embryogenesis proceeds (Autran et al., 2011; Baroux et al., 2001; Del Toro-De León et al., 2014; Vielle-Calzada et al., 2000). In *Arabidopsis*, the embryo fully relies on zygotic expression by the globular stage (Del Toro-De León et al., 2014). Consistent with this observation, it has been proposed that minor and major activation waves characterize gradual ZGA (Baroux et al., 2001). Under this proposal, ZGA is not uniform, and the number of transcribed loci increases during development, which could resolve the conflicting reports of paternal gene activity in the plant embryo.

et al., 2013). CLASP mediates planar cell polarity upstream of Rho-of-plastid (ROP) GTPases (Ambrose et al., 2007; Pietra et al., 2013), several of which function in both MT and AF cytoskeleton organization (Fu et al., 2005; T. Xu et al., 2011). This finding suggests that CLASP potentially guides PPB orientation also through AFs. Whereas depolymerization of MTs prevents both AF and MT formation, depolymerization of AFs results in broadening of the MT PPB and in randomization of division plane orientation (Vanstraelen et al., 2006). Thus, both cytoskeletal structures and their interaction, substantiated by the recent identification of multiple regulatory MT/AF-interacting proteins (Li et al., 2010; J. Tian et al., 2015), may have an indispensable role in PPB orientation.

The necessity of cytoskeletal components and their regulation for plant embryogenesis is highlighted in mutants with defects in cell division orientation. Loss-of-function mutations in the genes encoding TON1, TON2/FASS (a regulatory subunit in the TTP complex), RopGEF7 (an activator of ROPs), and ROP3 cause abnormal cell

**'Zygotic genome activation':** the time point/developmental stage at which zygotic mRNA is first detected or highly transcribed

division patterns in the *Arabidopsis* embryo (Chen et al., 2014, 2011; Spinner et al., 2013; Torres-Ruiz & Jürgens, 1994; Yoshida et al., 2014). ROP3 is transcriptionally induced by auxin and regulates the polarity of PIN-FORMED (PIN) auxin efflux transporters and, thus, auxin maxima formation (Chen et al., 2014). This feed-forward mechanism integrates ROP signaling and auxin-dependent pattern formation in the embryo. Although auxin was previously suggested to regulate cell division orientation (Fukaki et al., 2002; Hamann et al., 1999; Hardtke & Berleth, 1998; Yoshida et al., 2014), linking transcriptional control to the cell biological processes underlying the rearrangement of the cytoskeleton will be critical to further unraveling the mechanistic basis of oriented cell division in plants. Even though the embryo is an excellent model for studying the regulation of oriented cell division due to its simple cellular architecture, its small size and encapsulation in seed and fruit make the embryo a challenge for cell biology. Thus, novel approaches will have to be developed to visualize subcellular structures, and dedicated genetic tools will be required to dissect the role that the cytoskeleton plays in controlling the oriented, formative divisions that shape the plant embryo.



**Figure 2:** Zygote development and apical and basal cell fate determination. Sperm cell–provided SHORT SUSPENSOR (SSP) triggers the YODA (YDA) MAP kinase (MAPK) signaling pathway [involving GROUNDED (GRD)] to induce zygote elongation, and WRKY DNA-BINDING PROTEIN2 (WRKY2) activates *WUSCHEL RELATED HOMEBOX8* (*WOX8*) expression to initiate the polarization of organelle position in the zygote. Following asymmetric zygote division, PIN-FORMED7 (PIN7)-mediated auxin transport establishes a weak auxin response maximum in the apical cell of the one-cell embryo. Here, auxin response and the WRKY2/*WOX* pathway, through *WOX2*, regulate apical cell fate. The WRKY2/*WOX* and YDA MAPK pathways regulate basal cell fate. Furthermore, *CLAVATA3/ENDOSPERM SURROUNDING REGION8* (CLE8) and maternally derived *EMBRYO SURROUNDING FACTOR1* (ESF1) are involved in suspensor development, likely by inducing *WOX8* expression (CLE8) and through the YDA MAPK pathway (ESF1).

## Setting up the body axis

### *Zygote fertilization: genome activation, polarity, and elongation*

In seed plants, the zygote is formed inside the future seed after the egg cell of the female gametophyte is fertilized by a sperm cell delivered through the pollen tube (reviewed in (Bleckmann et al., 2014)). Subsequent zygotic genome activation<sup>1</sup> marks the beginning of a gradual process termed maternal-to-zygote transition wherein the zygote emancipates itself from parental developmental control by activation of de novo expression of the inherited parental alleles. For years there has been a debate regarding this transition and the varying importance of parental transcripts and de novo zygote expression in early plant embryogenesis (detailed in the **box “Parent-of-Origin Effects and Zygotic Genome Activation”**). There are several examples, some of which are presented in this review, of both parental and zygotic genes that have been shown by mutational analyses to be required for early embryo development.

With regard to morphology, the zygote of many flowering plants maintains the asymmetric distribution of cellular components observed in the egg cell (Mansfield & Briarty, 1991; Mogensen & Suthar, 1979; Schulz & Jensen, 1968; Zhao et al., 2011): The nucleus is located at the chalazal end of the female gametophyte (i.e., apically), and a large vacuole is generally located at the micropylar end (i.e., basally) (reviewed in (Drews & Koltunow, 2011)). It is not clear how this polarity is initially established (Ceccato et al., 2013; Lituiev et al., 2013; Pagnussat et al., 2009). Although this distribution would indicate that polarity persists after fertilization, in *Arabidopsis* this is not the case, because the zygote is repolarized from a transient symmetric state in which the nucleus is in a central position and the vacuoles are evenly distributed (Ueda et al., 2011). Zygote repolarization, i.e., the apical localization of the nucleus and the basal localization of a large vacuole, requires WRKY DNA-BINDING PROTEIN2 (WRKY2), partly via de novo transcription of *WUSCHEL RELATED HOMEODOMAIN 8* (*WOX8*) in the zygote, to initiate a shift in organelle position (Figure 2). WRKY2 is not needed to establish or maintain egg cell polarity, and similar to *Arabidopsis*, other flowering plants exhibit altered polarity after fertilization, including complete reversals, followed by zygote repolarization (Dumas & Rogowsky, 2008; Sato et al., 2010). Thus, zygote polarity appears to be established independently of egg cell polarity, and despite differing cellular appearances, the inherent embryonic apical-basal polarity, discussed in depth below, appears identical in many seed plants.

Zygote repolarization in *Arabidopsis* is followed by a threefold cell elongation

along the cell's apical-basal axis (Mansfield & Briarty, 1991) that seems to depend largely on a MITOGEN-ACTIVATED PROTEIN (MAP) kinase (MAPK) signaling pathway in which the MAPKK YODA (YDA) is the principal component (Figure 2) (Lukowitz et al., 2004; Wang et al., 2007). Mutants for *YDA* and the downstream MAPKs *MPK3* and *MPK6* block zygote elongation. YDA is activated by the paternally (sperm cell) provided receptor-like cytoplasmic kinase SHORT SUSPENSOR (SSP) (Bayer et al., 2009), which links fertilization to zygote elongation. *NIMNA* (*NMA*), a polygalacturonase gene whose mutation impedes cell elongation in the zygote, also shows a paternal effect similar to that of *SSP* (Babu et al., 2013). Although no direct targets of the YDA MAPK signaling pathway have been identified, the RWP-PK-type transcription factor GROUNDED (*GRD*)/RKD4 was recently identified as a crucial component because the loss of *GRD* blocks YDA signaling (Jeong et al., 2011).

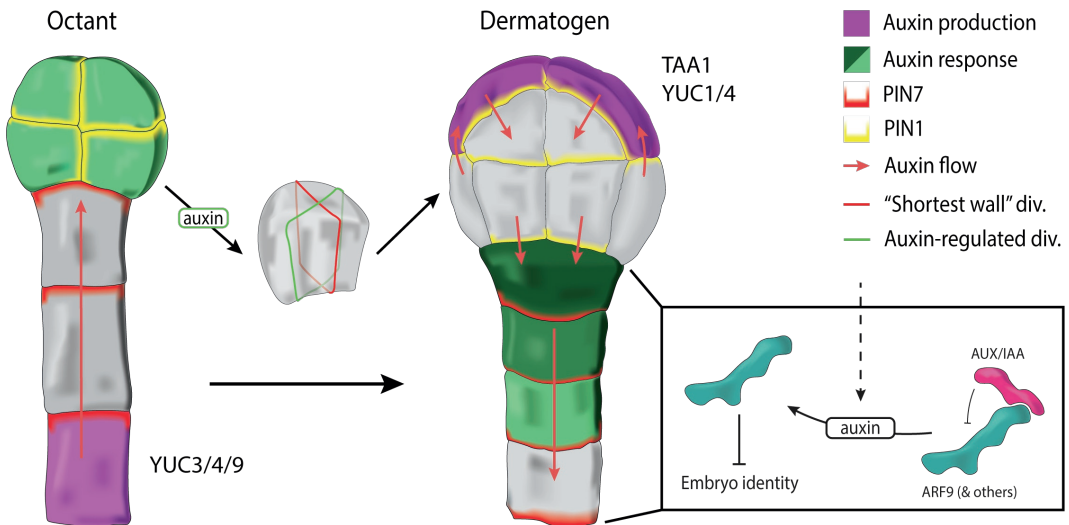
#### *Zygote division: apical and basal cell fate*

The first cleavage of the zygote occurs in a transverse manner in nearly all surveyed flowering plants (Johri, 1984). Depending on the plant species, the zygote divides either symmetrically or asymmetrically to produce an apical daughter cell and a basal daughter cell with varying size and volume ratios (Kumlehn et al., 1999; Sivaramakrishna, 1978; Yu & Zhao, 2012). The division is asymmetric in Arabidopsis, and the small apical cell and the larger basal cell adopt divergent cell fates (Figure 1) (Gooh et al., 2015; Jürgens & Mayer, 1994; Mansfield & Briarty, 1991; Yoshida et al., 2014). Although the mechanistic basis for asymmetric (or symmetric) zygote division remains to be determined, research shows that the YDA MAPK signaling pathway and the WRKY2/WOX transcription cascade are critically and interdependently involved with an auxin-dependent pathway in Arabidopsis apical and basal cell determination.

In the YDA MAPK signaling pathway, aborted zygote elongation in the *ssp*, *yda*, *mpk3*, *mpk6*, and *grd* mutants results in an atypical symmetric division of the zygote that generates a normal-sized apical cell and an abnormally short basal cell (Bayer et al., 2009; Jeong et al., 2011; Lukowitz et al., 2004). Subsequently, the extraembryonic suspensor fails to develop normally, suggesting that the YDA MAPK signaling pathway plays an important role in specifying basal cell fate (Figure 2). Interestingly, a positive-feedback loop between the YDA MAPK cascade and BREAKING OF ASYMMETRY IN THE STOMATAL LINEAGE (BASL) constitute a polarity module that connects cell polarity

to fate differentiation during stomatal asymmetric division in *Arabidopsis* (Zhang et al., 2015b). The polarization of a similar system could be a deciding factor in asymmetric division of the zygote and cell fate determination of the basal lineage. In addition, a small, cysteine-rich peptide family member, EMBRYO SURROUNDING FACTOR1 (ESF1), has been proposed to act synergistically with SSP to regulate suspensor development through the YDA MAPK signaling pathway (Figure 2) (Costa et al., 2014). Before fertilization, ESF1 peptides accumulate in the female central cell gametes and, thus, may represent an additional unique parental factor that regulates early embryogenesis in a manner similar to that of SSP, except that ESF1 is maternally derived.

The WRKY2/WOX transcription cascade affects both apical and basal cell fate from the one-cell stage onward. Similar to *WOX8*, *WOX2* is expressed in the egg cell and zygote, but after the first zygote division it becomes predominant in the apical daughter cells (Haecker, 2004). In contrast, following WRKY2 activation, *WOX8* (also known as STIMPY-LIKE; (Wu et al., 2007)) and its close homolog *WOX9* (*STIMPY*; (Wu et al., 2007)) are expressed primarily in the basal daughter cells (Haecker, 2004; Ueda et al.,



**Figure 3:** Auxin production, transport, and response in the early embryo. At the octant stage, suspensor-specific YUCCA (YUC)3/4/6 activity provides an auxin source for PIN-FORMED (PIN)1/7-dependent establishment of the auxin response maximum in the proembryo. Auxin response suppresses the shortest-wall division (considered to be the default division orientation) and is required for the asymmetric division that sets apart the protoderm and inner cells. At the dermatogen stage, TRYPTOPHAN AMINOTRANSFERASE OF ARABIDOPSIS1 (TAA1) and YUC4/6 activities initiate auxin production in the proembryo apex, and PIN1 and PIN7 mediate auxin transport downward to establish a new basal auxin response maximum. Here, auxin suppresses embryonic identity through AUXIN RESPONSE FACTOR9 (ARF9) (and other ARFs). IAA denotes indole-3-acetic acid. Shades of green represent different intensities of auxin response (*darker green* represents higher intensity). Schemes are based on data from Robert et al. (2013) and Yoshida et al. (2014).

2011). *WOX8* and *WOX9* are crucial for cell determination in the basal lineage because *wox8 wox9* double mutants exhibit abnormal suspensor development (Breuninger et al., 2008). However, different *wox9/stimpy* alleles were reported to cause embryo lethality (Wu et al., 2007), and thus the function of the *WOX8* and *WOX9* genes during embryogenesis may extend beyond suspensor development. Indeed, in the apical cell lineage, *WOX2* is non-cell-autonomously activated by *WOX8/9* and promotes pattern formation and proper auxin response (Figure 2) (Breuninger, 2008; Lie et al., 2012). Interestingly, the *CLAVATA3/ENDOSPERM SURROUNDING REGION (CLE)* family polypeptide *CLE8* induces *WOX8* expression in the upper half of the suspensor, which affects suspensor cell division, proliferation, and elongation (Fiume & Fletcher, 2012). These findings suggest a *CLE/WOX8* module that, independently of the *WRKY2/WOX* transcription cascade, regulates suspensor development (Figure 2). *CLE8* and *ESF1* are two key examples of our emerging understanding of the importance of peptide signaling during plant embryo development (Fletcher, 1999; Schoof et al., 2000; Xu et al., 2015); reviewed in (Grienenberger & Fletcher, 2015)).

Although MAPKs have been shown to phosphorylate WRKY factors (Ishihama et al., 2011; Mao et al., 2011), there is no evidence that the YDA MAP and *WRKY2/WOX* pathways interact. Nevertheless, with components from both pathways, the zygote expresses a mixture of cell regulators that, after asymmetric division, establish distinct apical and basal cell fates in the zygotic daughter cells. The early distinction between apical and basal cells is further supported by comparative transcription analyses in *Arabidopsis* (Slane et al., 2014) and *Nicotiana tabacum* (Hu et al., 2010, 2011), which have revealed distinct and uneven apical and basal distribution of specific transcripts following zygote division. For a more extensive review on tissue- and cell type-specific transcriptomics approaches in plant embryo research, we refer readers to (Palovaara et al., 2013).

The auxin-dependent pathway is initiated after zygote division, when auxin is transported from the basal daughter cell to the apical daughter cell via suspensor-specific PIN7 to form a weak auxin response maximum (Figure 2) (Friml et al., 2003; Robert et al., 2013). Because disruption of auxin transport and response results in a transverse rather than a longitudinal division of the apical cell (reviewed in (Möller et al., 2009)), this maximum likely contributes to apical cell fate specification. Early suspensor-specific expression of *YUCCA3 (YUC3)*, *YUC4*, and *YUC9*, all components of the tryptophan-dependent IAA biosynthetic pathway (reviewed in (Tivendale et al., 2014)), provide a likely source of auxin because corresponding loss-of-function mutants show defects in apical descendants (Figure

3) (Robert et al., 2015). At the dermatogen stage, TRYPTOPHAN AMINOTRANSFERASE OF ARABIDOPSIS1 (TAA1) and YUC4/6 initiate auxin production at the proembryo apex, and PIN1 is polarized in the inner proembryonic cells to mediate basal auxin transport. This development, together with redundant AUXIN RESISTANT1 (AUX1) and LIKE AUXIN RESISTANT1 (LAX1) auxin influx carriers (Robert et al., 2015), helps establish a new basal auxin response maximum (Figure 3) (Friml et al., 2003). Regulation of both auxin efflux (*PIN1*) and influx (*AUX1*, *LAX1*, and *LAX2*) by ARF5/MONOPTEROS (MP) is required for this process (Robert et al., 2015). These results are supported by computational modeling, in which the auxin sources predict the observed PIN7 and PIN1 polarity and auxin response maxima (Wabnik et al., 2013a).

## 2

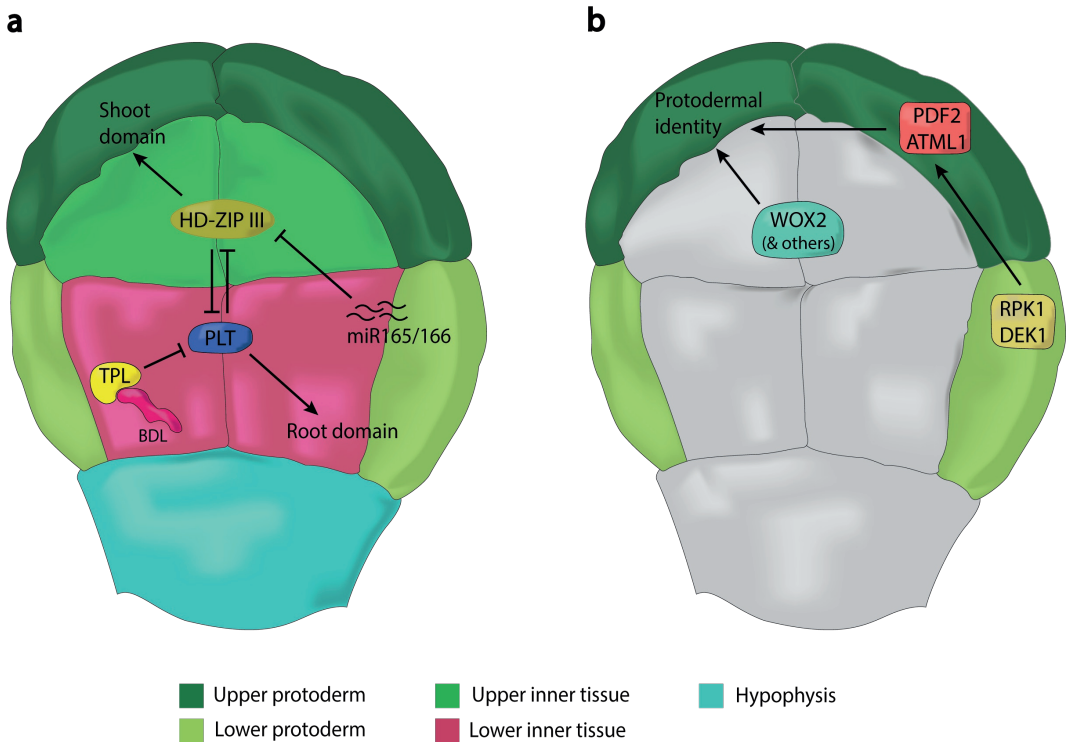
### *Embryo versus suspensor identity*

The basal auxin maximum is required for the specification of basal embryo structures, such as the hypophysis (discussed in depth below) and suspensor cell fate (Friml et al., 2003; Rademacher et al., 2012; Robert et al., 2013; Schlereth et al., 2010). Inhibiting the auxin response machinery in the Arabidopsis suspensor, of which ARF9 and IAA10 are the main interacting components, causes extraembryonic suspensor cells to lose their identity and, at least partially, convert to embryonic cell fate (Rademacher et al., 2012). This finding suggests that proembryo-derived auxin acts as a cell-autonomous inhibitory signal to maintain suspensor cell identity in these cells (Figure 3).

In a landmark technical achievement, Gooch et al., (2015) developed an in vitro culture system that allows for live-cell imaging and optical manipulation of early Arabidopsis embryos. Using this setup, they applied laser irradiation to disrupt the basal cell of a one-cell embryo and observed aberrant cell divisions in apical descendants, confirming the role of the basal cell and its derivatives in providing growth regulators and proper pattern formation in the early proembryo. In contrast, apical cell ablation induced apical cell properties in the uppermost basal descendants, which gave rise to a morphologically and molecularly distinct dermatogen-stage embryo. This cell fate conversion, from extraembryonic cells into embryonic cells, was also observed when Liu et al., (2015), using a similar laser ablation technique, detached the proembryo from the suspensor at the octant and globular stages. Thus, suspensor cells possess embryonic potential that is suppressed by the embryo during normal embryogenesis. After ablation, auxin accumulates in the free end of the suspensor, where it likely reprograms cell fate to initiate embryogenesis (Liu et

al., 2015). Supporting this hypothesis, suspensor-derived embryogenesis in *Brassica napus* microspore cultures is dependent on PIN7-directed flow of auxin to the most apical cell (Soriano et al., 2014). The expression patterns of *PIN7*, *PIN1*, and the auxin response reporter *DR5* are very similar in *B. napus* and *Arabidopsis*, indicating that the inferences from *B. napus* likely apply to *Arabidopsis* as well.

Together, these findings imply a dual role for auxin signaling in cell identity regulation because it can either suppress or induce embryo cell identity in the suspensor, depending on the presence of the proembryo and, in extension, on the flow direction and response maximum of auxin. Although the response mechanisms underlying these differences are not fully understood, it is known that ARFs are differentially expressed and control distinct developmental processes during *Arabidopsis* embryogenesis (Rademacher et al., 2012, 2011; Schlereth et al., 2010; reviewed in Chandler & Werr, 2015). ARFs likely



**Figure 4:** Determination of protodermal identity and shoot and root domains. **a** Repression by TOPLESS (TPL) restricts PLETHORA (PLT) family members to the lower-tier cells, whereas HD-ZIP III members are restricted to the upper-tier cells following posttranscriptional regulation by *miR165/166*. Here, HD-ZIP III and PLT members antagonistically regulate shoot and root determination. BDL denotes BODENLOS. **b** Both WUSCHEL RELATED HOMEODOMAIN (WOX2) (and other WOXs) and ARABIDOPSIS THALIANA MERISTEM LAYER 1 (ATML1) [with PROTODERMAL FACTOR 2 (PDF2)] are required for protodermal identity. *ATML1* is regulated by DEFECTIVE KERNEL 1 (DEK1), RECEPTOR-LIKE PROTEIN KINASE 1 (RPK1), and TOADSTOOL 2 (TOAD2) (the last is not shown here because it is first expressed in the later stages of embryogenesis).

acquire specificity by forming dimeric complexes with specific DNA spacing preferences (see the **box “Auxin Signaling”**) (Boer et al., 2014). Thus, the contrasting role of auxin may be due to the unique composition of ARFs that either suppress or activate genes required for initiation of embryogenesis. Notably, *GRD/RKD4* and possibly other RWP-PK family members are in this group of important genes (Jeong et al., 2011; Lawit, Chamberlin, Agee, Caswell, & Albertsen, 2013; Waki, Hiki, Watanabe, Hashimoto, & Nakajima, 2011; reviewed in Radoeva & Weijers, 2014).

### *Shoot and root domain determination*

2

As a direct consequence of zygote polarity and transverse division of the zygote, additional cell divisions separate the *Arabidopsis* octant proembryo into a developmentally distinct shoot domain (upper-tier cells) and root domain (lower-tier cells) (Figure 1). This separation effectively sets up the polarized apical-basal body axis of the embryo. Two transcription factor families, the class III HD-ZIP family (Prigge et al., 2005) and the AP2 domain PLETHORA (PLT) family (Aida et al., 2004; Galinha et al., 2007), are crucial for retaining the identity of these domains (Figure 4a).

Expression of several HD-ZIP III family members—i.e., *PHABULOSA* (*PHB*), *PHAVOLUTA* (*PHV*), *REVOLUTA* (*REV*), *ARABIDOPSIS THALIANA* *HOMEBOX8* (*ATHB8*), and *ATHB15* [also known as *CORONA* (*CNA*)]—is spatially restricted to the upper tier of cells at the dermatogen and globular stages following posttranscriptional regulation by the basally and peripherally located microRNAs *miR165* and *miR166* (Emery et al., 2003; Floyd & Bowman, 2004; Mallory et al., 2004; Miyashima et al., 2013; Williams et al., 2005; Zhou et al., 2015). In contrast, the PLT family members *PLT1*, *PLT2*, *PLT3/AINTEGUMENTA-LIKE6* (*PLT3*), and *PLT4/BABY BOOM* (*BBM*) localize to the lower cell tier from the octant stage onward (Aida et al., 2004; Galinha et al., 2007). Misexpression of microRNA-resistant HD-ZIP III transcripts using the *PLT2* promoter completely transforms the root pole into a secondary shoot pole (Smith & Long, 2010), whereas ubiquitous expression of PLT genes induces ectopic roots in the shoot apex (Aida et al., 2004; Galinha et al., 2007). *PLT1* and *PLT2* are direct targets of *TOPLESS* (*TPL*), a transcriptional corepressor that binds to the IAA12/BODENLOS (*BDL*) ARF inhibitor (Long et al., 2006; Smith & Long, 2010; Szemenyei et al., 2008). In *tpl-1* mutants, both genes are misexpressed in the shoot domain and induce a second root pole (Smith & Long, 2010). Gain-of-function mutations in the miRNA target motif of HD-ZIP III genes, which

lead to the ectopic activity of these genes, repress the *PLT* pathway in the shoot domain and restore apical fate. Thus, HD-ZIP III and PLT transcription factors can be considered as antagonistic master regulators of embryonic shoot and root determination, respectively. Although recent research has provided additional data regarding HD-ZIP III and *PLT* regulation (e.g., Gu, Wang, Huang, & Cui, 2012; Kanei, Horiguchi, & Tsukaya, 2012), further investigations are required to elucidate the interaction of these factors, especially with regard to maintaining boundaries between the shoot domain and the root domain.

## Radial patterning: Defining the three major tissue types

### *The protoderm*

The first formative division of the eight cells in the octant-stage embryo marks the onset of radial patterning in *Arabidopsis* (Figure 1) (Gooh et al., 2015; Jürgens & Mayer, 1994; Mansfield & Briarty, 1991; Yoshida et al., 2014). At the same time, the embryo switches to a mode of growth in which the contribution of expansion to overall growth increases (Yoshida et al., 2014). After division, the eight outer cells act as protoderm founder cells, whereas the four inner lower-tier cells will establish the ground and vascular tissues (Scheres et al., 1994; Yoshida et al., 2014). The mechanism behind these first asymmetric divisions is not clear, although auxin signaling and WOX transcription factors have been linked to this process. Inhibition of auxin response by expression of a nondegradable version of BDL inhibits the asymmetric divisions (Yoshida et al., 2014), but eventually, the embryos still form a separate outer layer. This indicates that auxin response is required for the asymmetric divisions during the transition from the octant stage to the dermatogen stage (Figure 3) but is not required for subsequent protoderm formation (Rademacher et al., 2012). In conjunction with this pathway, *WOX2*, *WOX8*, and other (redundant) *WOX* genes are also crucial for asymmetric divisions at this stage (Figure 4b) because single, double, triple, and quadruple loss-of-function mutants (i.e., *wox2*, *wox2 wox8*, *wox1 wox2 prs*, and *wox1 wox2 wox8 prs*) fail to correctly separate the protodermal layer by periclinal divisions, resulting in increasingly severe shoot developmental phenotypes in seedlings (Breuninger et al., 2008). This function appears to be conserved between angiosperms and gymnosperms because RNAi-assisted downregulation of a *WOX2* ortholog in the gymnosperm *Picea abies* results in the failure to form a protoderm in (somatic) embryos (Zhu et al., 2016).

The protoderm-specific marker *ARABIDOPSIS THALIANA MERISTEM LAYER1* (*ATML1*), which encodes an HD-ZIP IV transcription factor, is expressed in Arabidopsis as early as the one-cell embryo stage (Mukherjee et al., 2009). At the octant-dermatogen transition, however, its expression becomes restricted to the outer layer, which is the incipient protoderm and epidermis precursor (Takada & Jürgens, 2007) (Figure 4b). Overexpression of *ATML1* induces epidermal gene expression and epidermis-related traits such as stomatal guard cell and trichome-like cell formation in nonepidermal tissues (Peterson et al., 2013; Takada et al., 2013). Furthermore, mutations in *ATML1* and its closest homolog, *PROTODERMAL FACTOR 2* (*PDF2*) (Abe et al., 2003), cause either defects in protodermal cell fate or complete developmental arrest in globular stage embryos, depending on *atml1* allele strength (Ogawa et al., 2014; San-Bento et al., 2014). *ATML1* orthologs localizing preferably to the protoderm have been identified in other species (Ingram et al., 2000, 1999; Ito et al., 2002), suggesting a deep origin of this factor in protoderm formation. It has been proposed that *ATML1* and *PDF2* positively regulate the expression of epidermis-specific genes through the L1 box, a *cis*-regulatory element that is also included in their own promoter regions (Abe et al., 2003, 2001). This L1 box is required for protodermal expression of *PDF2*, but not *ATML1* (Abe et al., 2001; Takada & Jürgens, 2007). Thus, other factors, which appear to be auxin and microRNA independent (Nodine & Bartel, 2010), initiate *ATML1* expression. Several candidate *ATML1* regulators—including *DEFECTIVE KERNEL1* (*DEK1*), *RECEPTOR-LIKE PROTEIN KINASE1* (*RPK1*), and *RPK2/TOADSTOOL2* (*TOAD2*) (Johnson et al., 2005; Nodine et al., 2007)—and a downstream target gene, *ARABIDOPSIS CRINKLY4* (*ACR4*) (San-Bento et al., 2014; Tanaka et al., 2002), are involved in the formation and/or maintenance of epidermal cell fate (Takada & Jürgens, 2007; reviewed in Takada & Iida, 2014). Thus, *ATML1*, whose transcription is required and sufficient for protodermal identity, can be regarded as a master transcriptional regulator of epidermal cell fate in the plant embryo (Figure 4b).

### *The ground tissue*

Following the formation of ground tissue initials at the early globular stage, subsequent periclinal divisions generate the endodermis and cortex, two layers that collectively constitute the ground tissue (Petricka et al., 2009). Critical components of ground tissue subspecification and maintenance have been identified in embryonic and postembryonic Arabidopsis development (see below). However, the mechanisms underlying ground tissue

initiation in the embryo remain largely unknown (Figure 5).

Both the GRAS family transcription factor SHORT-ROOT (SHR) and its target SCARECROW (SCR) are essential for the periclinal divisions underlying formation of the endodermis and cortex cell layers during root development ((Helariutta et al., 2000; Nakajima et al., 2001; Scheres et al., 1995). SHR moves from the stele to the ground tissue, where it, together with SCR, localizes to the nucleus (Nakajima et al., 2001; Vatén et al.,

2

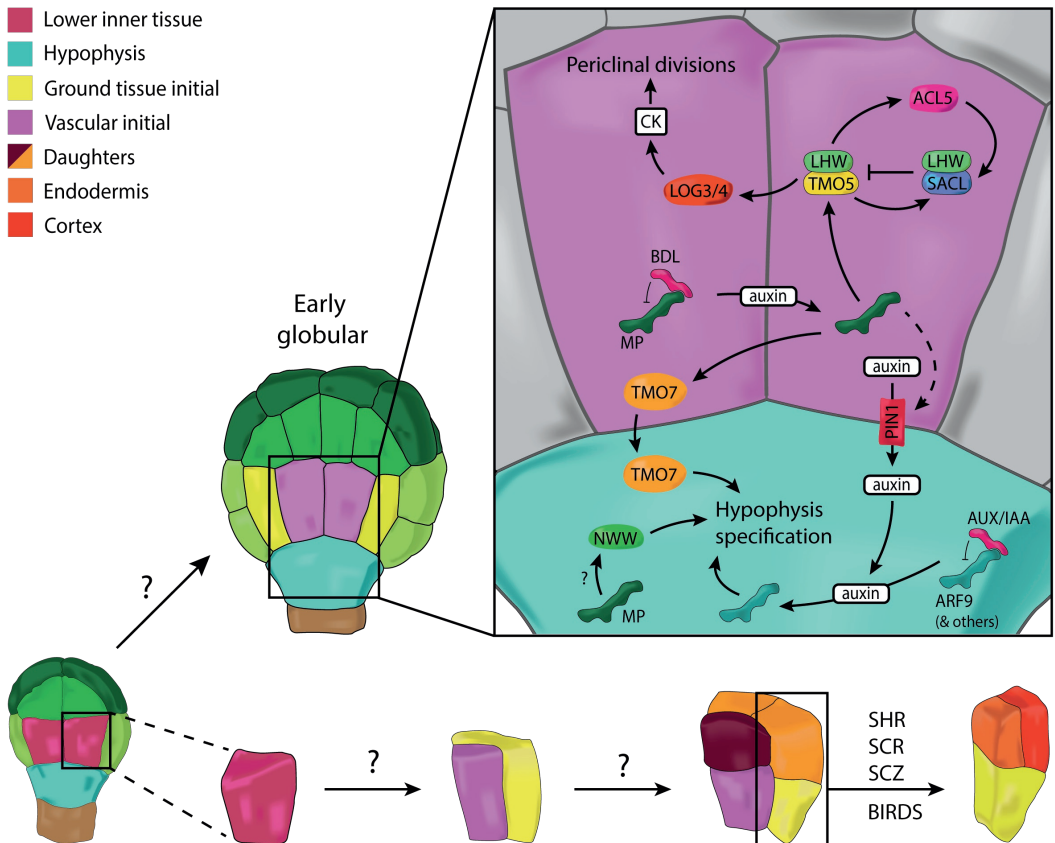


Figure 5: Establishment of vascular tissue, ground tissue, and the hypophysis. At the globular stage, vascular tissue, ground tissue, and hypophysis identity is initiated, followed by cell-specific division patterns. Auxin triggers *TARGET OF MONOPTEROS5* (*TMO5*) expression through *MONOPTEROS* (MP) in the vascular initials. *TMO5* dimerizes with *LONESOME HIGHWAY* (*LHW*) to promote periclinal divisions by inducing *LONELY GUY3/4* (*LOG3/4*) expression and, thus, cytokinin (CK) biosynthesis. A negative-feedback module that includes *SUPPRESSOR OF ACAULIS5-LIKE* (*SACL*) and *ACAULIS5* (*ACL5*) controls *TMO5/LHW* activity. Concurrently, MP activates *TMO7*, which moves from the vascular initials to the hypophysis. Also, MP promotes *PIN-FORMED1* (*PIN1*)-dependent auxin transport to the same cell. Here *TMO7*, auxin response [through *AUXIN RESPONSE FACTOR9* (*ARF9*) and other ARFs], and *NO TRANSMITTING TRACT*, *WIP DOMAIN PROTEIN4*, and *WIP DOMAIN PROTEIN5* (collectively referred to as *NWW*) converge to promote hypophysis specification and division. MP regulates *NWW* either indirectly or directly in this cell. A regulatory network consisting of *SHORT-ROOT* (*SHR*), *SCARECROW* (*SCR*), *BIRDS*, and *SCHIZORIZA* (*SCZ*) is required to govern proper periclinal divisions and specification of endodermis and cortex of the ground tissue. Other abbreviations: *BDL*, *BODENLOS*; *IAA*, indole-3-acetic acid.

2011). This relocalization of SHR between cell layers is required for the periclinal division forming the endodermis and cortex (Gallagher et al., 2004; Vatén et al., 2011). Both *SHR* and *SCR* are expressed in the globular-stage embryo, although loss-of-function mutants first display a phenotype only at the early heart stage, when a single ground tissue layer is formed (Helariutta et al., 2000; Scheres et al., 1995; Wysocka-Diller et al., 2000). Other factors that are involved in the SHR/SCR regulatory network, including SCHIZORIZA (SCZ), a heat shock transcription factor, have been identified (Mylona et al., 2002; Pernas et al., 2010; ten Hove et al., 2010). Similar to *shr* and *scr* mutants, *scz* mutants start to show defects only after ground tissue has been established, which suggests a role for all three of these factors after initiation.

2 Recently, SCZ has been identified as a target of a transcription factor network composed of SCR and BIRD proteins in roots (Moreno-Risueno et al., 2015). The BIRD family consists of JACKDAW (JKD), MAGPIE (MGP), NUTCRACKER (NUC), BLUEJAY (BLJ), and IMPERIAL EAGLE (IME). JKD and its close homolog BALD-IBIS (BIB) regulate SHR movement by promoting its nuclear migration (Long et al., 2015) and, together with MGP and NUC, are required for the periclinal divisions that pattern the ground tissue. The BIRDS, together with SCR, appear to be critical for maintaining ground tissue identity in the root by specifying the cortex/endodermis stem cells (Moreno-Risueno et al., 2015). In addition, following SHR activation these proteins promote periclinal cell divisions that pattern the ground tissue stem cell initials. Although *JKD*, *MGP*, and *NUC* are already expressed in the ground tissue in the globular-stage embryo (Levesque et al., 2006; Welch et al., 2007), *blj jkd scr* embryos do develop ground tissue (Moreno-Risueno et al., 2015). This observation indicates that, as with SCZ, the combined activity of the BIRDS and SCR is crucial only for ground tissue subspecification.

Although the major components of ground tissue subspecification and maintenance are known, no critical components of embryonic ground tissue initiation have been identified. Initiation may depend on entirely different factors, or alternatively, early roles for late-acting factors may be obscured by genetic redundancy.

### *The vascular tissue*

During the transition from the dermatogen stage to the globular stage, formative divisions generate four vascular initials that will eventually develop into a vascular bundle composed

of a central xylem axis and two phloem poles that are separated by (pro)cambium (reviewed in De Rybel, Mähönen, Helariutta, & Weijers, 2016). Three aspects are crucial for vascular tissue formation. First, vascular identity needs to be instructed. Second, the four initials need to generate an entire vascular bundle. Third, this bundle needs to be partitioned into xylem, phloem, and cambium domains. Unfortunately, essentially nothing is known about the critical first step. However, much has recently been learned about the following growth and patterning steps.

Auxin response through MP is crucial for the correct development of the vascular tissue and specification of the hypophysis (Figure 5). Indeed, *mp* mutants show abnormal division of the vascular cells, and they fail to establish an embryonic root (De Rybel et al., 2013; Hardtke & Berleth, 1998). MP directly activates *TARGET OF MONOPTEROS5* (*TMO5*) (Schlereth et al., 2010), whose product dimerizes with another bHLH transcription factor, LONESOME HIGHWAY (LHW) (De Rybel et al., 2013; Ohashi-Ito et al., 2013). In the four vascular initials, the TMO5/LHW complex triggers, at the early globular stage, biosynthesis of the hormone cytokinin through direct activation of *LONELY GUY3/4* (*LOG3/4*) (De Rybel et al., 2013; Ohashi-Ito et al., 2013), which encodes enzymes in the final step of cytokinin biosynthesis (Kuroha et al., 2009). Loss of either TMO5 (and its homologs) or LHW (and its homologs) results in a strong decrease in the number of vascular cell files in the embryo, whereas ectopic coexpression results in an excess of cell file numbers primarily (but not only) in the vasculature (De Rybel, 2013; Ohashi-Ito, 2013). Thus, both TMO5 and LHW are necessary and sufficient for promoting periclinal cell divisions. In addition, *LOG* genes control cell numbers within the root vascular bundle (Tokunaga et al., 2012). Together, these observations suggest that auxin promotes local cytokinin biosynthesis through the TMO5/LHW complex to control the periclinal divisions of the first vascular initials and their daughter cells and, hence, establishment of a vascular bundle from four initial cells.

The TMO5/LHW dimer is a potent inducer of periclinal divisions (De Rybel et al., 2013), which implies that its activity needs to be strictly controlled. Recently, the thermospermine synthase *ACAULIS5* (*ACL5*) was shown to limit TMO5/LHW activity by promoting the translation of SUPPRESSOR OF ACAULIS5-LIKE (*SACL*) bHLH transcription factors (Hanzawa, 2000; Vera-Sirera et al., 2015). Mutations in the *ACL5* gene result in a dramatic increase in vascular bundle size (Hanzawa et al., 1997), and genetic screens for suppressors of the *acl5* phenotype revealed the involvement of *SAC51* in limiting the vascular bundle (Imai et al., 2006). *SACL* proteins can bind LHW and, thus,

likely antagonize TMO5/LHW interactions to prevent overproliferation of vascular cells (Vera-Sirera et al., 2015). The TMO5/LHW complex likely directly activates *SACL* genes (Vera-Sirera et al., 2015) and promotes *SACL* translation by activating *ACL5* expression (Katayama et al., 2015). This activity creates a dedicated negative-feedback module. Together, these processes connect auxin, through the coordinated activation of TMO5 and *SACL*, and negative feedback to the control of vascular cell divisions and tissue growth. Because *SACL3* is expressed in the vascular initials from the globular stage onward and thus overlaps with *TMO5* and *LHW* expression domains (Vera-Sirera et al., 2015), it is likely that these regulatory interactions are already established in the early embryo (Figure 5).

2

In addition to its role in vascular tissue growth, cytokinin is necessary for dividing the vascular bundle into distinct domains (Bishopp et al., 2011). Because auxin promotes cytokinin biosynthesis through LOG3/4 (De Rybel et al., 2014; Ohashi-Ito et al., 2014), auxin/cytokinin cross talk seems to be important for vascular bundle growth and patterning. Recently, different modeling strategies have been implemented to understand the dynamics and interaction of auxin and cytokinin during embryonic and postembryonic vascular development in *Arabidopsis* (De Rybel et al., 2014; el-Showk et al., 2015; Muraro et al., 2014). For example, De Rybel et al., (2014) modeled the auxin/cytokinin interaction onto a growing cellular template of the embryonic vascular tissue, starting at the stage at which there are four initials. Simulations suggested that a core network of auxin/cytokinin interactions could account for generating a sharp boundary between high-auxin and high-cytokinin response domains in the vascular tissue. Thus, both experimental evidence and computational modeling support the conclusion that auxin/cytokinin cross talk is vital for both growth and patterning of the vascular tissue in the embryo.

## Initiation of stem cell niches

The distinctive ability of plants to continuously generate new organs throughout life originates from stem cells in the RAM, SAM, and procambium. Establishment of the RAM and SAM stem cell niches<sup>1</sup> (stem and organizer cells) in the early embryo is thus pivotal for postembryonic development (Van Den Berg et al., 1997; Weigel & Jürgens, 2002). Here the

<sup>1</sup>**Stem cell niche:** a microenvironment in which continuously dividing (undifferentiated) stem cells are maintained by so-called organizer cells

first determination steps of these stem cell niches are discussed. For discussions concerning the maintenance and the genetic regulation of cotyledon primordium initiation, we refer to other recent reviews (Drisch & Stahl, 2015; Lau et al., 2012; Perales & Reddy, 2012).

### *The root*

A basal auxin maximum in the early *Arabidopsis* embryo is necessary not only for the specification of suspensor cell fate but also for the hypophysis (Figure 5) (Friml et al., 2003; Rademacher et al., 2012; Robert et al., 2013; Schlereth et al., 2010; Wabnik et al., 2013b). The hypophysis is the precursor to the QC (Figure 1), and both are marked by *WOX5* expression (Haecker, 2004; Scheres et al., 1994). *WOX5* is required for QC maintenance (Pi et al., 2015; Sarkar et al., 2007; Zhang et al., 2015a), and thus, hypophysis specification can be regarded as the de facto initiating step of RAM formation. The hypophysis is, however, not essential for root formation, because many seed plants do not have a cell comparable to that of the *Arabidopsis* hypophysis (Johri, 1984; Johri et al., 1992; Vasil, 1979). Nevertheless, these species seem to use signaling pathways similar to those in *Arabidopsis* (Hedman et al., 2013; Kamiya et al., 2003; Lim et al., 2005). Therefore, the developmental significance of the hypophysis presumably relates to its position rather than its clonal origin. Supporting this, in the *hanaba taranu* (*han*) mutant, the future root pole develops from the lower-tier cell(s) of the *Arabidopsis* proembryo, and not from the hypophysis (Nawy et al., 2010). Mutation in *HAN* causes the boundary between suspensor and proembryo to shift apically and redistributes auxin to create a new auxin maximum within the proembryo.

In *Arabidopsis*, the specification of the hypophysis and subsequent distal stem cell fate involves *TMO7* (Figure 5) (Schlereth et al., 2010). Similar to *TMO5*, *TMO7* is directly regulated by MP in the vascular initials. Subsequently, the MP protein moves to the hypophysis, where it contributes to correct division and, in extension, QC formation through an as-yet-unidentified pathway. Recently, the transcription factor *NO TRANSMITTING TRACT* (*NTT*) and its two paralogs *WIP DOMAIN PROTEIN4* (*WIP4*) and *WIP5*, all expressed in the hypophysis, were identified as critical regulators of auxin-dependent root formation (Crawford et al., 2015). Triple mutants exhibit abnormal hypophysis divisions and a rootless phenotype. Furthermore, *NTT* misexpression is sufficient to induce root cap cell identity, and because little to no *NTT* can be detected in the hypophysis of the *mp* mutant, it likely acts downstream of MP. That MP activity in the proembryo is sufficient for normal development (Schlereth et al., 2010; Weijers et al., 2006) suggests an indirect

regulation of NTT by MP or, alternatively, the existence of multiple MP-dependent pathways contributing to hypophysis specification and division (Figure 5).

Additional auxin-dependent factors have been identified as key components in hypophysis specification. ARF9 and IAA10 not only maintain suspensor cell identity but also participate in hypophysis auxin response because both the downregulation of *ARF9* (and *ARF13*) and the induction of *IAA10* result in defects in hypophysis division (Figure 5) (Rademacher et al., 2012, 2011). Also, the loss of *PLT1*, *PLT2*, *PLT3*, and *BBM* function (resulting in the *plt1 plt2 plt3 bbm* quadruple mutant) leads to aberrant hypophysis division and, consequently, a rootless seedling phenotype (Galinha et al., 2007). *PLT1*, *PLT2*, *PLT3*, and *BBM* are restricted to the apical descendants following asymmetric hypophysis division (Aida et al., 2004; Galinha et al., 2007). MP does not directly regulate *PLT* genes (Schlereth et al., 2010). However, auxin slowly promotes *PLT* transcription, and both *PLT1* expression and *PLT2* expression depend on the presence of MP (Aida et al., 2004; Mähönen et al., 2014). Thus, at least four molecular components downstream of auxin—*TMO7*, *NTT*/*WIP4*/*WIP5*, *ARF9*, and the *PLT* genes—appear to participate in hypophysis specification. A future challenge will be to elucidate how these components converge to trigger correct hypophysis development.

The QC is defined by its low frequency of division and ability to prevent differentiation of adjoining stem cells (Clowes, 1956; Fujie et al., 1993; Van Den Berg et al., 1997). It was recently proposed that, in addition to the role of *WOX5* in maintaining QC identity, *WOX5* activity also maintains quiescence in the QC by restricting cell divisions through *CYCLIN D* (*CYCD*) suppression (Forzani et al., 2014). Ectopic *CYCD3*;3 expression in the QC is sufficient to induce cell division, and *WOX5* binds to the *CYCD3*;3 promoter to repress its expression. Thus, core cell cycle components and transcription factors can be directly linked in RAM organization. Cytokinin is a key component in cell cycle regulation, and *CYCD3* seems to act downstream of cytokinin in this process (reviewed in Schaller, Street, & Kieber, 2014). Ectopic cytokinin signaling in the basal derivative of the hypophysis interferes with the stereotypical cell division pattern of the root pole (Müller & Sheen, 2008). Auxin dampens this signaling via two negative cytokinin regulators, *ARABIDOPSIS RESPONSE REGULATOR7* (*ARR7*) and *ARR15*. Together, these observations indicate that auxin/cytokinin cross talk and *WOX5* activity converge to regulate analogous cell cycle components and, subsequently, cell division in the root stem cell niche. However, even though research on auxin/cytokinin interaction is rapidly progressing (Růžicka et al., 2009; Šimášková et al., 2015; reviewed in Chandler & Werr,

2015), greater effort is required to fully understand the role of such interaction in early embryo development and WOX5 function, especially because emerging evidence indicates a role for auxin and the ARF/IAA machinery in WOX5 regulation (Ding & Friml, 2010; Tian et al., 2014).

### *The shoot*

In contrast to the RAM, the SAM is morphologically delineated in the later stages of embryo development. In Arabidopsis, the SAM is first recognized at the torpedo stage after the initiation of cotyledon primordia (Barton & Poethig, 1993; Laux et al., 1996), even though the expression of *WUS*, a marker for shoot organizer cells, can be detected in the four inner apical cells of the proembryo at the dermatogen stage (Mayer et al., 1998). *WUS* maintains organizer cell identity in the Arabidopsis SAM (Laux et al., 1996; Mayer et al., 1998) and likely plays a similar role in many other species (Kieffer et al., 2006; Nardmann et al., 2009; Nardmann & Werr, 2006; Stuurman et al., 2002). Several other molecular factors, such as *SHOOT MERISTEMLESS (STM)* and HD-ZIP III family members (Long et al., 1996; Prigge et al., 2005), have been identified to regulate SAM organization. However, very little is known regarding the mechanisms controlling stem cell establishment in the SAM during embryo development. Nevertheless, many of the genes involved in maintenance are expressed in the early embryo and can thus be considered as putative candidates in regulating SAM initiation.

For example, the triple loss-of-function mutant of the HD-ZIP II genes *HOMEODOMAIN ARABIDOPSIS THALIANA3 (HAT3)*, *ARABIDOPSIS THALIANA HOMEODOMAIN BOX2 (ATHB2)*, and *ATHB4*, all of which are expressed in the early embryo, lacks an active SAM, and defects are enhanced when *hat3 athb4* is combined with the HD-ZIP III mutant *phv*, *phb*, or *rev* (Luana Turchi et al., 2013). The expression patterns of HD-ZIP II and HD-ZIP III family members overlap, and these genes likely interact at the molecular level because REV directly regulates several HD-ZIP II genes (Brandt et al., 2012; Reinhart et al., 2013; Turchi et al., 2013; reviewed in L. Turchi, Baima, Morelli, & Ruberti, 2015). The implication is that HD-ZIP III genes control SAM activity through the HD-ZIP II genes. Because PHB, PHV, and CNA act independently of WUS to control stem cell initiation and function in postembryonic vegetative SAMs (Lee & Clark, 2015), this pathway may operate in parallel to WUS in the embryo. The protoderm acts as a positional signaling source to define a region of stem cell competence during SAM formation in the embryo.

A mobile microRNA, *miR394*, non-cell-autonomously represses the F-box protein LEAF CURLING RESPONSIVENESS (LCR) (Jones-Rhoades & Bartel, 2004; Knauer et al., 2013) in underlying protodermal cell layers (L2/L3) to enhance WUS activity. However, although *WUS* is not maintained in the *mir394b* mutant, its expression is correctly initiated (Knauer et al., 2013). This finding suggests that the protodermal *miR394*/LCR signaling pathway is crucial only for the maintenance and localization of the SAM, and not for the establishment of the SAM during embryogenesis.

To summarize, several important regulators of postembryonic SAM and shoot stem cell function have been identified, and many of these regulators are expressed in relevant cells of the embryo. However, there is no coherent framework for how the SAM is initiated.

## 2

## Outlook

In this review, we discuss the progress toward understanding the regulation of early plant embryogenesis. We review the cellular basis for pattern formation, as well as the regulatory pathways that direct each of the major cellular decisions that shape the embryo. Here, we list several areas that we find particularly interesting for future research, as well as challenges that need to be overcome to address important outstanding questions.

### *Cell geometry and division*

Technical advances in imaging techniques, image analysis, and modeling approaches have provided us with exciting information regarding the regulation of cell division patterns in plants (Gooh et al., 2015; Von Wangenheim et al., 2016; Yoshida et al., 2014). These studies suggest that transcriptional control and mechanical stress regulate formative divisions in plant development and direct the orientation away from purely geometrically defined cell division planes. A major open question, however, is how genetic regulators subvert the cell division machinery. In future studies, combining these technical advances with clever transcriptomics approaches and detailed cell biology could connect mechanisms that regulate orientation of the division plane to the cell biological processes underlying the changes in division orientation.

*Hormonal control and transcriptional networks*

Patterning in the embryo is dependent on auxin and cytokinin control. The recent discovery of how auxin response specificity is achieved in the embryo (Boer et al., 2014; Rademacher et al., 2011) and the cumulative evidence of close auxin/cytokinin interaction during specification events (De Rybel et al., 2014; el-Showk et al., 2015; Muraro et al., 2014; Růžicka et al., 2009; Šimášková et al., 2015) lead us closer to discovering the necessary transcriptional networks that underlie patterning in the early embryo. With the development of novel and more precise reporters for sensitive and quantitative auxin response measurement (e.g., Liao et al., 2015) and the fast progress of transcriptomics approaches that can be applied to the embryo at the single-cell scale (reviewed in Palovaara et al., 2013), we should be able to define and analyze the gene sets that are locally expressed to trigger cell identity and pattern.

2

*Epigenetic control of embryo development*

As shown in this review, many transcriptional regulators are essential for correct cell division and differentiation in embryonic and postembryonic structures. Recently, key transcriptional regulators were shown to be spatially regulated at the epigenetic level through locus-specific histone modifications (Pi et al., 2015; Saiga et al., 2012; Sang et al., 2012; Weiste & Dröge-Laser, 2014; Zhang et al., 2015a). Yet very little is known about how epigenetic control impacts plant embryo development. It will be interesting to see how epigenetic regulation is modified and how different epigenetic factors function together with transcriptional regulators in the establishment of complex 3D structure.

*Evolution of embryo patterning*

Morphology of plant embryos shares many common features, some dating back to the divergence of the earliest land plants. Yet, because most molecular-genetic studies have been performed in *Arabidopsis*, it is not clear to what extent the genetic regulators identified in *Arabidopsis* are representative of conserved, general mechanisms. The advent of increasing availability of genome and transcriptome information in land plants and beyond provides a good starting point to address this problem. Specifically, tracing the origin of auxin-mediated patterning could help us further dissect this mechanism in plant

development. Recent studies have shown roles for transcriptional auxin response in general development throughout the evolution of multicellular land plants (Finet & Jaillais, 2012; Flores-Sandoval et al., 2015; Kato et al., 2015; Lavy et al., 2012; Pires et al., 2013; Plavskin et al., 2016; Prigge et al., 2010; Tam et al., 2015). Thus, exploring the genes controlled by auxin throughout the plant kingdom may help us better understand not only the evolution and origin of auxin action, but also the genetic wiring of embryo patterning.

## Acknowledgements

2 We would like to thank Kuan-Ju Lu, Margo Smit, and Maritza van Dop for critical comments on the manuscript, as well as Saiko Yoshida for providing the original embryo stacks on which the embryos in Figure 1 were based. In addition, we like to thank our colleagues in the SIREN network for useful discussions that have inspired our writing of this review. This work was supported by the Earth and Life Sciences Council (open competition grant 824.14.009) of the Netherlands Organization for Scientific Research, ERA-CAPS project EURO-PEC (grant 849.13.006), and the Federation of European Biochemical Societies.

## References

- Abe, M., Takahashi, T., & Komeda, Y. (2001). Identification of a cis-regulatory element for L1 layer-specific gene expression, which is targeted by an L1-specific homeodomain protein. *Plant Journal*. <https://doi.org/10.1046/j.1365-313X.2001.01047.x>
- Abe, Mitsutomo, Katsumata, H., Komeda, Y., & Takahashi, T. (2003). Regulation of shoot epidermal cell differentiation by a pair of homeodomain proteins in Arabidopsis. *Development*. <https://doi.org/10.1242/dev.00292>
- Aida, M., Beis, D., Heidstra, R., Willemsen, V., Blilou, I., Galinha, C., ... Scheres, B. (2004). The PLETHORA genes mediate patterning of the Arabidopsis root stem cell niche. *Cell*. <https://doi.org/10.1016/j.cell.2004.09.018>
- Ambrose, J. C., Shoji, T., Kotzer, A. M., Pighin, J. A., & Wasteneys, G. O. (2007). The Arabidopsis CLASP gene encodes a microtubule-associated protein involved in cell expansion and division. *Plant Cell*. <https://doi.org/10.1105/tpc.107.053777>
- Autran, D., Baroux, C., Raissig, M. T., Lenormand, T., Wittig, M., Grob, S., ... Grossniklaus, U. (2011). Maternal epigenetic pathways control parental contributions to Arabidopsis early embryogenesis. *Cell*, 145(5), 707–719. <https://doi.org/10.1016/j.cell.2011.04.014>
- Azimzadeh, J., Nacry, P., Christodoulidou, A., Drevensek, S., Camilleri, C., Amiour, N., ... Boucheza, D. (2008). Arabidopsis Tonneau1 proteins are essential for preprophase band formation and interact with centrin. *Plant Cell*. <https://doi.org/10.1105/tpc.107.056812>
- Babu, Y., Musielak, T., Henschen, A., & Bayer, M. (2013). Suspensor length determines developmental progression of the embryo in Arabidopsis. *Plant Physiology*. <https://doi.org/10.1104/pp.113.217166>
- Baroux, C., Blanvillain, R., & Gallois, P. (2001). Paternally inherited transgenes are down-regulated but retain low activity during early embryogenesis in Arabidopsis. *FEBS Letters*. [https://doi.org/10.1016/S0014-5793\(01\)03097-6](https://doi.org/10.1016/S0014-5793(01)03097-6)
- Barton, M. K., & Poethig, R. S. (1993). Formation of the shoot apical meristem in Arabidopsis thaliana: An analysis of development in the wild type and in the shoot meristemless mutant. *Development*.
- Bayer, M., Nawy, T., Giglione, C., Galli, M., Meinnel, T., & Lukowitz, W. (2009). Paternal

control of embryonic patterning in *Arabidopsis thaliana*. *Science*. <https://doi.org/10.1126/science.1167784>

Besson, S., & Dumais, J. (2011). Universal rule for the symmetric division of plant cells. *Proceedings of the National Academy of Sciences of the United States of America*, 108(15), 6294–6299. <https://doi.org/10.1073/pnas.1011866108>

Besson, S., & Dumais, J. (2014). Stochasticity in the symmetric division of plant cells: When the exceptions are the rule. *Frontiers in Plant Science*. <https://doi.org/10.3389/fpls.2014.00538>

Bishopp, A., Help, H., El-Showk, S., Weijers, D., Scheres, B., Friml, J., ... Helariutta, Y. (2011). A mutually inhibitory interaction between auxin and cytokinin specifies vascular pattern in roots. *Current Biology*. <https://doi.org/10.1016/j.cub.2011.04.017>

Bleckmann, A., Alter, S., & Dresselhaus, T. (2014). The beginning of a seed: Regulatory mechanisms of double fertilization. *Frontiers in Plant Science*. <https://doi.org/10.3389/fpls.2014.00452>

Boer, D. R., Freire-Rios, A., Van Den Berg, W. A. M., Saaki, T., Manfield, I. W., Kepinski, S., ... Coll, M. (2014). Structural basis for DNA binding specificity by the auxin-dependent ARF transcription factors. *Cell*. <https://doi.org/10.1016/j.cell.2013.12.027>

Brandt, R., Salla-Martret, M., Bou-Torrent, J., Musielak, T., Stahl, M., Lanz, C., ... Wenkel, S. (2012). Genome-wide binding-site analysis of REVOLUTA reveals a link between leaf patterning and light-mediated growth responses. *Plant Journal*. <https://doi.org/10.1111/j.1365-313X.2012.05049.x>

Breuninger, H., Rikirsch, E., Hermann, M., Ueda, M., & Laux, T. (2008). Differential Expression of WOX Genes Mediates Apical-Basal Axis Formation in the Arabidopsis Embryo. *Developmental Cell*. <https://doi.org/10.1016/j.devcel.2008.03.008>

Ceccato, L., Masiero, S., Sinha Roy, D., Bencivenga, S., Roig-Villanova, I., Ditengou, F. A., ... Colombo, L. (2013). Maternal Control of PIN1 Is Required for Female Gametophyte Development in Arabidopsis. *PLoS ONE*. <https://doi.org/10.1371/journal.pone.0066148>

Chandler, J. W., & Werr, W. (2015). Cytokinin-auxin crosstalk in cell type specification. *Trends in Plant Science*. <https://doi.org/10.1016/j.tplants.2015.02.003>

Chen, M., Liu, H., Chen, M., Li, X., Wang, M., Yang, Y., ... Tao, L. Z. (2014). ROP3 GTPase contributes to polar auxin transport and auxin responses and is important for embryogenesis and seedling growth in Arabidopsis. *Plant Cell*. <https://doi.org/10.1105/tpc.114.127902>

Chen, M., Liu, H., Kong, J., Yang, Y., Zhang, N., Li, R., ... Tao, L. Z. (2011). RopGEF7 regulates PLETHORA-dependent maintenance of the root stem cell niche in Arabidopsis. *Plant Cell*. <https://doi.org/10.1105/tpc.111.085514>

Clowes, F. A. L. (1956). Nucleic acids in root apical meristems of zea. *New Phytologist*. <https://doi.org/10.1111/j.1469-8137.1956.tb05264.x>

Costa, L. M., Marshall, E., Tesfaye, M., Silverstein, K. A. T., Mori, M., Umetsu, Y., ... Gutierrez-Marcos, J. F. (2014). Central cell-derived peptides regulate early embryo patterning in flowering plants. *Science*. <https://doi.org/10.1126/science.1243005>

Crawford, B. C. W., Sewell, J., Golembeski, G., Roshan, C., Long, J. A., & Yanofsky, M. F. (2015). Genetic control of distal stem cell fate within root and embryonic meristems. *Science*. <https://doi.org/10.1126/science.aaa0196>

De Rybel, B., Adibi, M., Breda, A. S., Wendrich, J. R., Smit, M. E., Novák, O., ... Weijers, D. (2014). Plant development. Integration of growth and patterning during vascular tissue formation in Arabidopsis. *Science (New York, N.Y.)*, 345(6197), 1255215. <https://doi.org/10.1126/science.1255215>

De Rybel, B., Mähönen, A. P., Helariutta, Y., & Weijers, D. (2016). Plant vascular development: From early specification to differentiation. *Nature Reviews Molecular Cell Biology*. <https://doi.org/10.1038/nrm.2015.6>

De Rybel, B., Möller, B., Yoshida, S., Grabowicz, I., Barbier de Reuille, P., Boeren, S., ... Weijers, D. (2013). A bHLH Complex Controls Embryonic Vascular Tissue Establishment and Indeterminate Growth in Arabidopsis. *Developmental Cell*, 24(4), 426–437. <https://doi.org/10.1016/j.devcel.2012.12.013>

de Wildeman, E. (1893). Études sur l'attache des cloisons cellulaires. *Mémoires Couronnés et Mémoires Des Savants Étrangers*, 53, 1–84.

Del Toro-De León, G., García-Aguilar, M., & Gillmor, C. S. (2014). Non-equivalent contributions of maternal and paternal genomes to early plant embryogenesis. *Nature*.

<https://doi.org/10.1038/nature13620>

Del Toro-De León, G., Lepe-Soltero, D., & Gillmor, C. S. (2016). Zygotic genome activation in isogenic and hybrid plant embryos. *Current Opinion in Plant Biology*. <https://doi.org/10.1016/j.pbi.2015.12.007>

Ding, Z., & Friml, J. (2010). Auxin regulates distal stem cell differentiation in Arabidopsis roots. *Proceedings of the National Academy of Sciences of the United States of America*. <https://doi.org/10.1073/pnas.1000672107>

Drevensek, S., Goussot, M., Duroc, Y., Christodoulidou, A., Steyaert, S., Schaefer, E., ... Pastuglia, M. (2012). The Arabidopsis TRM1-TON1 interaction reveals a recruitment network common to plant cortical microtubule arrays and eukaryotic centrosomes. *The Plant Cell*, 24(1), 178–191. <https://doi.org/10.1105/tpc.111.089748>

Drews, G. N., & Koltunow, A. M. . (2011). The Female Gametophyte. *The Arabidopsis Book*. <https://doi.org/10.1199/tab.0155>

Drisch, R. C., & Stahl, Y. (2015). Function and regulation of transcription factors involved in root apical meristem and stem cell maintenance. *Frontiers in Plant Science*. <https://doi.org/10.3389/fpls.2015.00505>

Dumas, C., & Rogowsky, P. (2008). Fertilization and early seed formation. *Comptes Rendus - Biologies*. <https://doi.org/10.1016/j.crv.2008.07.013>

el-Showk, S., Help-Rinta-Rahko, H., Blomster, T., Siligato, R., Marée, A. F. M., Mähönen, A. P., & Grieneisen, V. A. (2015). Parsimonious Model of Vascular Patterning Links Transverse Hormone Fluxes to Lateral Root Initiation: Auxin Leads the Way, while Cytokinin Levels Out. *PLoS Computational Biology*. <https://doi.org/10.1371/journal.pcbi.1004450>

Emery, J. F., Floyd, S. K., Alvarez, J., Eshed, Y., Hawker, N. P., Izhaki, A., ... Bowman, J. L. (2003). Radial Patterning of Arabidopsis Shoots by Class III HD-ZIP and KANADI Genes. *Current Biology*. <https://doi.org/10.1016/j.cub.2003.09.035>

Errera, L. (1888). Über Zellformen und Siefenblasen. *Bot. Centralbl.*, 34, 395–399.

Finet, C., & Jaillais, Y. (2012). AUXOLOGY: When auxin meets plant evo-devo. *Developmental Biology*. <https://doi.org/10.1016/j.ydbio.2012.05.039>

- Fiume, E., & Fletcher, J. C. (2012). Regulation of Arabidopsis embryo and endosperm development by the polypeptide signaling molecule CLE8. *Plant Cell*. <https://doi.org/10.1105/tpc.111.094839>
- Fletcher, J. C. (1999). Signaling of cell fate decisions by CLAVATA3 in Arabidopsis shoot meristems. *Science*. <https://doi.org/10.1126/science.283.5409.1911>
- Flores-Sandoval, E., Eklund, D. M., & Bowman, J. L. (2015). A Simple Auxin Transcriptional Response System Regulates Multiple Morphogenetic Processes in the Liverwort *Marchantia polymorpha*. *PLoS Genetics*. <https://doi.org/10.1371/journal.pgen.1005207>
- Floyd, S. K., & Bowman, J. L. (2004). Ancient microRNA target sequences in plants. *Nature*. <https://doi.org/10.1038/428485a>
- Forzani, C., Aichinger, E., Sornay, E., Willemsen, V., Laux, T., Dewitte, W., & Murray, J. A. H. (2014). WOX5 suppresses CYCLIN D activity to establish quiescence at the Center of the root stem cell niche. *Current Biology*. <https://doi.org/10.1016/j.cub.2014.07.019>
- Friml, J., Vieten, A., Sauer, M., Weijers, D., Schwarz, H., Hamann, T., ... Jürgens, G. (2003). Efflux-dependent auxin gradients establish the apical-basal axis of Arabidopsis. *Nature*. <https://doi.org/10.1038/nature02085>
- Fu, Y., Gu, Y., Zheng, Z., Wasteneys, G., & Yang, Z. (2005). Arabidopsis interdigitating cell growth requires two antagonistic pathways with opposing action on cell morphogenesis. *Cell*. <https://doi.org/10.1016/j.cell.2004.12.026>
- Fujie, M., Kuroiwa, H., Kawano, S., & Kuroiwa, T. (1993). Studies on the behavior of organelles and their nucleoids in the root apical meristem of *Arabidopsis thaliana* (L.) *Col*. *Planta*. <https://doi.org/10.1007/BF00194444>
- Fukaki, H., Tameda, S., Masuda, H., & Tasaka, M. (2002). Lateral root formation is blocked by a gain-of-function mutation in the solitary-root/IAA14 gene of Arabidopsis. *Plant Journal*. <https://doi.org/10.1046/j.0960-7412.2001.01201.x>
- Galatis, B., & Apostolakis, P. (2004). The role of the cytoskeleton in the morphogenesis and function of stomatal complexes. *New Phytologist*. <https://doi.org/10.1046/j.1469-8137.2003.00986.x>
- Galinha, C., Hofhuis, H., Luijten, M., Willemsen, V., Blilou, I., Heidstra, R., & Scheres,

B. (2007). PLETHORA proteins as dose-dependent master regulators of Arabidopsis root development. *Nature*. <https://doi.org/10.1038/nature06206>

Gallagher, K. L., Paquette, A. J., Nakajima, K., & Benfey, P. N. (2004). Mechanisms regulating SHORT-ROOT intercellular movement. *Current Biology*. <https://doi.org/10.1016/j.cub.2004.09.081>

Gooh, K., Ueda, M., Aruga, K., Park, J., Arata, H., Higashiyama, T., & Kurihara, D. (2015). Live-Cell Imaging and Optical Manipulation of Arabidopsis Early Embryogenesis. *Developmental Cell*. <https://doi.org/10.1016/j.devcel.2015.06.008>

Grienenberger, E., & Fletcher, J. C. (2015). Polypeptide signaling molecules in plant development. *Current Opinion in Plant Biology*. <https://doi.org/10.1016/j.pbi.2014.09.013>

Gu, X. L., Wang, H., Huang, H., & Cui, X. F. (2012). SPT6L encoding a putative WG/GW-repeat protein regulates apical-basal polarity of embryo in Arabidopsis. *Molecular Plant*. <https://doi.org/10.1093/mp/ssr073>

Haecker, A. (2004). Expression dynamics of WOX genes mark cell fate decisions during early embryonic patterning in Arabidopsis thaliana. *Development*. <https://doi.org/10.1242/dev.00963>

Hamann, T., Mayer, U., & Jürgens, G. (1999). The auxin-insensitive bodenlos mutation affects primary root formation and apical-basal patterning in the Arabidopsis embryo. *Development*.

Han, M., Park, Y., Kim, I., Kim, E. H., Yu, T. K., Rhee, S., & Suh, J. Y. (2014). Structural basis for the auxin-induced transcriptional regulation by Aux/IAA17. *Proceedings of the National Academy of Sciences of the United States of America*. <https://doi.org/10.1073/pnas.1419525112>

Hanzawa, Y. (2000). ACAULIS5, an Arabidopsis gene required for stem elongation, encodes a spermine synthase. *The EMBO Journal*. <https://doi.org/10.1093/emboj/19.16.4248>

Hanzawa, Yoshie, Takahashi, T., & Komeda, Y. (1997). ACL5: An Arabidopsis gene required for internodal elongation after flowering. *Plant Journal*. <https://doi.org/10.1046/j.1365-313X.1997.12040863.x>

Hardtke, C. S., & Berleth, T. (1998). The Arabidopsis gene MONOPTEROS encodes a

transcription factor mediating embryo axis formation and vascular development. *EMBO Journal*. <https://doi.org/10.1093/emboj/17.5.1405>

Hedman, H., Zhu, T., von Arnold, S., & Sohlberg, J. J. (2013). Analysis of the WUSCHEL-RELATED HOMEODOMAIN gene family in the conifer *Picea abies* reveals extensive conservation as well as dynamic patterns. *BMC Plant Biology*. <https://doi.org/10.1186/1471-2229-13-89>

Helariutta, Y., Fukaki, H., Wysocka-Diller, J., Nakajima, K., Jung, J., Sena, G., ... Benfey, P. N. (2000). The SHORT-ROOT gene controls radial patterning of the Arabidopsis root through radial signaling. *Cell*. [https://doi.org/10.1016/S0092-8674\(00\)80865-X](https://doi.org/10.1016/S0092-8674(00)80865-X)

Hofmeister, W., & West, T. (2012). On the germination, development, and fructification of the higher Cryptogamia : and on the fructification of the Coniferæ /. In On the germination, development, and fructification of the higher Cryptogamia : and on the fructification of the Coniferæ /. <https://doi.org/10.5962/bhl.title.60930>

Hu, T. X., Yu, M., & Zhao, J. (2010). Comparative transcriptional profiling analysis of the two daughter cells from tobacco zygote reveals the transcriptome differences in the apical and basal cells. *BMC Plant Biology*.

Hu, T. X., Yu, M., & Zhao, J. (2011). Comparative transcriptional analysis reveals differential gene expression between asymmetric and symmetric zygotic divisions in tobacco. *PLoS ONE*. <https://doi.org/10.1371/journal.pone.0027120>

Imai, A., Hanzawa, Y., Komura, M., Yamamoto, K. T., Komeda, Y., & Takahashi, T. (2006). The dwarf phenotype of the Arabidopsis *ac15* mutant is suppressed by a mutation in an upstream ORF of a bHLH gene. *Development*. <https://doi.org/10.1242/dev.02535>

Ingouff, M., Rademacher, S., Holec, S., Šoljić, L., Xin, N., Readshaw, A., ... Berger, F. (2010). Zygotic resetting of the HISTONE 3 variant repertoire participates in epigenetic reprogramming in Arabidopsis. *Current Biology*. <https://doi.org/10.1016/j.cub.2010.11.012>

Ingram, G. C., Boissard-Lorig, C., Dumas, C., & Rogowsky, P. M. (2000). Expression patterns of genes encoding HD-ZipIV homeo domain proteins define specific domains in maize embryos and meristems. *Plant Journal*. <https://doi.org/10.1046/j.1365-313X.2000.00755.x>

Ingram, G. C., Magnard, J. L., Vergne, P., Dumas, C., & Rogowsky, P. M. (1999). ZmOCL1,

an HDGL2 family homeobox gene, is expressed in the outer cell layer throughout maize development. *Plant Molecular Biology*. <https://doi.org/10.1023/A:1006271332400>

Ishihama, N., Yamada, R., Yoshioka, M., Katou, S., & Yoshioka, H. (2011). Phosphorylation of the nicotiana benthamiana WRKY8 transcription factor by MAPK functions in the defense response. *Plant Cell*. <https://doi.org/10.1105/tpc.110.081794>

Ito, M., Sentoku, N., Nishimura, A., Hong, S. K., Sato, Y., & Matsuoka, M. (2002). Position dependent expression of gl2-type homeobox gene, *roc1*: Significance for protoderm differentiation and radial pattern formation in early rice embryogenesis. *Plant Journal*. <https://doi.org/10.1046/j.1365-313x.2002.01234.x>

2

Jeong, S., Palmer, T. M., & Lukowitz, W. (2011). The RWP-RK factor GROUNDED promotes embryonic polarity by facilitating YODA MAP kinase signaling. *Current Biology*. <https://doi.org/10.1016/j.cub.2011.06.049>

Johnson, K. L., Degnan, K. A., Ross Walker, J., & Ingram, G. C. (2005). AtDEK1 is essential for specification of embryonic epidermal cell fate. *Plant Journal*. <https://doi.org/10.1053/j.jfas.2005.01.003>

Johnson, M. A., & Wardlaw, C. W. (1956). Embryogenesis in Plants. *Bulletin of the Torrey Botanical Club*. <https://doi.org/10.2307/2482745>

Johri, B.M. (1984). Embryology of Angiosperms. *Springer-Verlag Berlin Heidelberg*.

Johri, Brij M., Ambegaokar, K. B., & Srivastava, P. S. (1992). Comparative Embryology of Angiosperms. In *Comparative Embryology of Angiosperms*. <https://doi.org/10.1007/978-3-642-76395-3>

Jones-Rhoades, M. W., & Bartel, D. P. (2004). Computational identification of plant MicroRNAs and their targets, including a stress-induced miRNA. *Molecular Cell*. <https://doi.org/10.1016/j.molcel.2004.05.027>

Jürgens, G., & Mayer, U. (1994). “Arabidopsis,” in A colour Atlas of Developing Embryos. *Harcourt Health Sciences*.

Kamiya, N., Nagasaki, H., Morikami, A., Sato, Y., & Matsuoka, M. (2003). Isolation and characterization of a rice WUSCHEL-type homeobox gene that is specifically expressed in the central cells of a quiescent center in the root apical meristem. *Plant Journal*. <https://doi.org/10.1046/j.1365-3113.2003.02000.x>

org/10.1046/j.1365-313X.2003.01816.x

Kanei, M., Horiguchi, G., & Tsukaya, H. (2012). Stable establishment of cotyledon identity during embryogenesis in *Arabidopsis* by *ANGUSTIFOLIA3* and *HANABA TARANU*. *Development (Cambridge)*. <https://doi.org/10.1242/dev.081547>

Katayama, H., Iwamoto, K., Kariya, Y., Asakawa, T., Kan, T., Fukuda, H., & Ohashi-Ito, K. (2015). A negative feedback loop controlling bHLH complexes is involved in vascular cell division and differentiation in the root apical meristem. *Current Biology*. <https://doi.org/10.1016/j.cub.2015.10.051>

Kato, H., Ishizaki, K., Kouno, M., Shirakawa, M., Bowman, J. L., Nishihama, R., & Kohchi, T. (2015). Auxin-Mediated Transcriptional System with a Minimal Set of Components Is Critical for Morphogenesis through the Life Cycle in *Marchantia polymorpha*. *PLoS Genetics*. <https://doi.org/10.1371/journal.pgen.1005084>

Kieffer, M., Stern, Y., Cook, H., Clerici, E., Maulbetsch, C., Laux, T., & Davies, B. (2006). Analysis of the transcription factor *WUSCHEL* and its functional homologue in *Antirrhinum* reveals a potential mechanism for their roles in meristem maintenance. *Plant Cell*. <https://doi.org/10.1105/tpc.105.039107>

Knauer, S., Holt, A. L., Rubio-Somoza, I., Tucker, E. J., Hinze, A., Pisch, M., ... Laux, T. (2013). A Protodermal miR394 Signal Defines a Region of Stem Cell Competence in the *Arabidopsis* Shoot Meristem. *Developmental Cell*. <https://doi.org/10.1016/j.devcel.2012.12.009>

Korasick, D. A., Westfall, C. S., Lee, S. G., Nanao, M. H., Dumas, R., Hagen, G., ... Strader, L. C. (2014). Molecular basis for AUXIN RESPONSE FACTOR protein interaction and the control of auxin response repression. *Proceedings of the National Academy of Sciences of the United States of America*. <https://doi.org/10.1073/pnas.1400074111>

Kost, B., Mathur, J., & Chua, N. H. (1999). Cytoskeleton in plant development. *Current Opinion in Plant Biology*. [https://doi.org/10.1016/S1369-5266\(99\)00024-2](https://doi.org/10.1016/S1369-5266(99)00024-2)

Kumlehn, J., Lörz, H., & Kranz, E. (1999). Monitoring individual development of isolated wheat zygotes: A novel approach to study early embryogenesis. *Protoplasma*. <https://doi.org/10.1007/BF01279086>

Kuroha, T., Tokunaga, H., Kojima, M., Ueda, N., Ishida, T., Nagawa, S., ... Sakakibara,

H. (2009). Functional analyses of LONELY GUY cytokinin-activating enzymes reveal the importance of the direct activation pathway in Arabidopsis. *Plant Cell*. <https://doi.org/10.1105/tpc.109.068676>

Lau, S., Slane, D., Herud, O., Kong, J., & Jürgens, G. (2012). Early embryogenesis in flowering plants: setting up the basic body pattern. *Annual Review of Plant Biology*, 63, 483–506. <https://doi.org/10.1146/annurev-arplant-042811-105507>

Laux, T., Mayer, K. F. X., Berger, J., & Jürgens, G. (1996). The WUSCHEL gene is required for shoot and floral meristem integrity in Arabidopsis. *Development*.

Lavy, M., Prigge, M. J., Tigyi, K., & Estelle, M. (2012). The cyclophilin DIAGEOTROPICA has a conserved role in auxin signaling. *Development*. <https://doi.org/10.1242/dev.074831>

Lawit, S. J., Chamberlin, M. A., Agee, A., Caswell, E. S., & Albertsen, M. C. (2013). Transgenic manipulation of plant embryo sacs tracked through cell-type-specific fluorescent markers: Cell labeling, cell ablation, and adventitious embryos. *Plant Reproduction*. <https://doi.org/10.1007/s00497-013-0215-x>

Lee, C., & Clark, S. E. (2015). A WUSCHEL-independent stem cell specification pathway is repressed by PHB, PHV and CNA in arabidopsis. *PLoS ONE*. <https://doi.org/10.1371/journal.pone.0126006>

Levesque, M. P., Vernoux, T., Busch, W., Cui, H., Wang, J. Y., Blilou, I., ... Benfey, P. N. (2006). Whole-genome analysis of the short-root developmental pathway in Arabidopsis. *PLoS Biology*. <https://doi.org/10.1371/journal.pbio.0040143>

Li, Y., Shen, Y., Cai, C., Zhong, C., Zhu, L., Yuan, M., & Ren, H. (2010). The type II Arabidopsis formin14 interacts with microtubules and microfilaments to regulate cell division. *Plant Cell*. <https://doi.org/10.1105/tpc.110.075507>

Liao, C. Y., Smet, W., Brunoud, G., Yoshida, S., Vernoux, T., & Weijers, D. (2015). Reporters for sensitive and quantitative measurement of auxin response. *Nature Methods*. <https://doi.org/10.1038/nmeth.3279>

Lie, C., Kelsom, C., & Wu, X. (2012). WOX2 and STIMPY-LIKE/WOX8 promote cotyledon boundary formation in Arabidopsis. *Plant Journal*. <https://doi.org/10.1111/j.1365-313X.2012.05113.x>

- Lim, J., Jung, J. W., Chae, E. L., Lee, M. H., Bong, J. K., Kim, M., ... Benfey, P. N. (2005). Conservation and diversification of SCARECROW in maize. *Plant Molecular Biology*. <https://doi.org/10.1007/s11103-005-0578-y>
- Lituiev, D. S., Krohn, N. G., Müller, B., Jackson, D., Hellriegel, B., Dresselhaus, T., & Grossniklaus, U. (2013). Theoretical and experimental evidence indicates that there is no detectable auxin gradient in the angiosperm female gametophyte. *Development (Cambridge)*. <https://doi.org/10.1242/dev.098301>
- Liu, Y., Li, X., Zhao, J., Tang, X., Tian, S., Chen, J., ... Sun, M. X. (2015). Direct evidence that suspensor cells have embryogenic potential that is suppressed by the embryo proper during normal embryogenesis. *Proceedings of the National Academy of Sciences of the United States of America*. <https://doi.org/10.1073/pnas.1508651112>
- Lloyd, D. (1991). The cytoskeletal basis of plant growth and form. *London: Academic*.
- Long, J. A., Moan, E. I., Medford, J. I., & Barton, M. K. (1996). A member of the KNOTTED class of homeodomain proteins encoded by the STM gene of Arabidopsis. *Nature*. <https://doi.org/10.1038/379066a0>
- Long, J. A., Ohno, C., Smith, Z. R., & Meyerowitz, E. M. (2006). TOPLESS regulates apical embryonic fate in Arabidopsis. *Science*. <https://doi.org/10.1126/science.1123841>
- Long, Y., Smet, W., Cruz-Ramírez, A., Castelijns, B., De Jonge, W., Mähönen, A. P., ... Blilou, I. (2015). Arabidopsis BIRD zinc finger proteins jointly stabilize tissue boundaries by confining the cell fate regulator SHORT-ROOT and contributing to fate specification. *Plant Cell*. <https://doi.org/10.1105/tpc.114.132407>
- Louveaux, M., & Hamant, O. (2013). The mechanics behind cell division. *Current Opinion in Plant Biology*. <https://doi.org/10.1016/j.pbi.2013.10.011>
- Lukowitz, W., Roeder, A., Parmenter, D., & Somerville, C. (2004). A MAPKK Kinase Gene Regulates Extra-Embryonic Cell Fate in Arabidopsis. *Cell*. [https://doi.org/10.1016/S0092-8674\(03\)01067-5](https://doi.org/10.1016/S0092-8674(03)01067-5)
- Mähönen, A. P., Tusscher, K. Ten, Siligato, R., Smetana, O., Díaz-Triviño, S., Salojärvi, J., ... Scheres, B. (2014). PLETHORA gradient formation mechanism separates auxin responses. *Nature*. <https://doi.org/10.1038/nature13663>

Mallory, A. C., Reinhart, B. J., Jones-Rhoades, M. W., Tang, G., Zamore, P. D., Barton, M. K., & Bartel, D. P. (2004). MicroRNA control of PHABULOSA in leaf development: Importance of pairing to the microRNA 5' region. *EMBO Journal*. <https://doi.org/10.1038/sj.emboj.7600340>

Mansfield, S. G., & Briarty, L. G. (1991). Early embryogenesis in *Arabidopsis thaliana*. II. The developing embryo. *Canadian Journal of Botany*. <https://doi.org/10.1139/b91-063>

Mao, G., Meng, X., Liu, Y., Zheng, Z., Chen, Z., & Zhang, S. (2011). Phosphorylation of a WRKY transcription factor by two pathogen-responsive MAPKs drives phytoalexin biosynthesis in *Arabidopsis*. *Plant Cell*. <https://doi.org/10.1105/tpc.111.084996>

2

Masoud, K., Herzog, E., Chabouté, M. E., & Schmit, A. C. (2013). Microtubule nucleation and establishment of the mitotic spindle in vascular plant cells. *Plant Journal*. <https://doi.org/10.1111/tpj.12179>

Mayer, K. F. X., Schoof, H., Haecker, A., Lenhard, M., Jürgens, G., & Laux, T. (1998). Role of WUSCHEL in regulating stem cell fate in the *Arabidopsis* shoot meristem. *Cell*. [https://doi.org/10.1016/S0092-8674\(00\)81703-1](https://doi.org/10.1016/S0092-8674(00)81703-1)

Meyer, S., & Scholten, S. (2007). Equivalent Parental Contribution to Early Plant Zygotic Development. *Current Biology*. <https://doi.org/10.1016/j.cub.2007.08.046>

Mineyuki, Y. (1999). The preprophase band of microtubules: Its function as a cytokinetic apparatus in higher plants. *International Review of Cytology*.

Miyashima, S., Honda, M., Hashimoto, K., Tatematsu, K., Hashimoto, T., Sato-Nara, K., ... Nakajima, K. (2013). A comprehensive expression analysis of the *arabidopsis* MICRORNA165/6 gene family during embryogenesis reveals a conserved role in meristem specification and a non-cell-autonomous function. *Plant and Cell Physiology*. <https://doi.org/10.1093/pcp/pcs188>

Mogensen, H. L., & Suthar, H. K. (1979). Ultrastructure of the Egg Apparatus of *Nicotiana tabacum* (Solanaceae) Before and After Fertilization. *Botanical Gazette*. <https://doi.org/10.1086/337073>

Möller, B., Weijers, D., Mo, B., & Weijers, D. (2009). Auxin Control of Embryo Patterning. 1–13. <https://doi.org/10.1101/cshperspect.a001545>

Moreno-Risueno, M. A., Sozzani, R., Yardimci, G. G., Petricka, J. J., Vernoux, T., Blilou, I., ... Benfey, P. N. (2015). Transcriptional control of tissue formation throughout root development. *Science*. <https://doi.org/10.1126/science.aad1171>

Mukherjee, K., Brocchieri, L., & Bürglin, T. R. (2009). A comprehensive classification and evolutionary analysis of plant homeobox genes. *Molecular Biology and Evolution*. <https://doi.org/10.1093/molbev/msp201>

Müller, B., & Sheen, J. (2008). Cytokinin and auxin interaction in root stem-cell specification during early embryogenesis. *Nature*. <https://doi.org/10.1038/nature06943>

Muraro, D., Mellor, N., Pound, M. P., Help, H., Lucas, M., Chopard, J., ... Bishopp, A. (2014). Integration of hormonal signaling networks and mobile microRNAs is required for vascular patterning in Arabidopsis roots. *Proceedings of the National Academy of Sciences of the United States of America*. <https://doi.org/10.1073/pnas.1221766111>

Mylona, P., Linstead, P., Martienssen, R., & Dolan, L. (2002). Schizoriza controls an asymmetric cell division and restricts epidermal identity in the Arabidopsis root. *Development*.

Nakajima, K., Sena, G., Nawy, T., & Benfey, P. N. (2001). Intercellular movement of the putative transcription factor SHR in root patterning. *Nature*. <https://doi.org/10.1038/35095061>

Nanao, M. H., Vinos-Poyo, T., Brunoud, G., Thévenon, E., Mazzoleni, M., Mast, D., ... Dumas, R. (2014). Structural basis for oligomerization of auxin transcriptional regulators. *Nature Communications*. <https://doi.org/10.1038/ncomms4617>

Nardmann, J., Reisewitz, P., & Werr, W. (2009). Discrete shoot and root stem cell-promoting WUS/WOX5 functions are an evolutionary innovation of angiosperms. *Molecular Biology and Evolution*. <https://doi.org/10.1093/molbev/msp084>

Nardmann, J., & Werr, W. (2006). The shoot stem cell niche in angiosperms: Expression patterns of WUS orthologues in rice and maize imply major modifications in the course of mono- and dicot evolution. *Molecular Biology and Evolution*. <https://doi.org/10.1093/molbev/msl125>

Nawy, T., Bayer, M., Mravec, J., Friml, J., Birnbaum, K. D., & Lukowitz, W. (2010). The GATA Factor HANABA TARANU Is Required to Position the Proembryo Boundary

in the Early Arabidopsis Embryo. *Developmental Cell*. <https://doi.org/10.1016/j.devcel.2010.06.004>

Nodine, M. D., & Bartel, D. P. (2010). MicroRNAs prevent precocious gene expression and enable pattern formation during plant embryogenesis. *Genes and Development*. <https://doi.org/10.1101/gad.1986710>

Nodine, M. D., & Bartel, D. P. (2012). Maternal and paternal genomes contribute equally to the transcriptome of early plant embryos. *Nature*, 482(7383), 94–97. <https://doi.org/10.1038/nature10756>

Nodine, M. D., Yadegari, R., & Tax, F. E. (2007). RPK1 and TOAD2 Are Two Receptor-like Kinases Redundantly Required for Arabidopsis Embryonic Pattern Formation. *Developmental Cell*. <https://doi.org/10.1016/j.devcel.2007.04.003>

Ogawa, E., Yamada, Y., Sezaki, N., Kosaka, S., Kondo, H., Kamata, N., ... Takahashi, T. (2014). ATML1 and PDF2 play a redundant and essential role in arabidopsis embryo development. *Plant and Cell Physiology*. <https://doi.org/10.1093/pcp/pcv045>

Ohashi-Ito, K., Matsukawa, M., & Fukuda, H. (2013). An atypical bHLH transcription factor regulates early xylem development downstream of auxin. *Plant and Cell Physiology*. <https://doi.org/10.1093/pcp/pct013>

Ohashi-Ito, K., Saegusa, M., Iwamoto, K., Oda, Y., Katayama, H., Kojima, M., ... Fukuda, H. (2014). A bHLH complex activates vascular cell division via cytokinin action in root apical meristem. *Current Biology: CB*, 24(17), 2053–2058. <https://doi.org/10.1016/j.cub.2014.07.050>

Pagnussat, G. C., Alandete-Saez, M., Bowman, J. L., & Sundaresan, V. (2009). Auxin-dependent patterning and gamete specification in the Arabidopsis female gametophyte. *Science*. <https://doi.org/10.1126/science.1167324>

Palovaara, J., Saiga, S., & Weijers, D. (2013). Transcriptomics approaches in the early Arabidopsis embryo. *Trends in Plant Science*. <https://doi.org/10.1016/j.tplants.2013.04.011>

Perales, M., & Reddy, G. V. (2012). Stem cell maintenance in shoot apical meristems. *Current Opinion in Plant Biology*. <https://doi.org/10.1016/j.pbi.2011.10.008>

Pernas, M., Ryan, E., & Dolan, L. (2010). SCHIZORIZA Controls Tissue System

Complexity in Plants. *Current Biology*. <https://doi.org/10.1016/j.cub.2010.02.062>

Peterson, K. M., Shyu, C., Burr, C. A., Horst, R. J., Kanaoka, M. M., Omae, M., ... Torii, K. U. (2013). Arabidopsis homeodomain-leucine zipper IV proteins promote stomatal development and ectopically induce stomata beyond the epidermis. *Development (Cambridge)*. <https://doi.org/10.1242/dev.090209>

Petricka, J. J., Van Norman, J. M., & Benfey, P. N. (2009). Symmetry breaking in plants: molecular mechanisms regulating asymmetric cell divisions in Arabidopsis. *Cold Spring Harbor Perspectives in Biology*.

Pi, L., Aichinger, E., van der Graaff, E., Llavata-Peris, C. I., Weijers, D., Hennig, L., ... Laux, T. (2015). Organizer-Derived WOX5 Signal Maintains Root Columella Stem Cells through Chromatin-Mediated Repression of CDF4 Expression. *Developmental Cell*. <https://doi.org/10.1016/j.devcel.2015.04.024>

Pietra, S., Gustavsson, A., Kiefer, C., Kalmbach, L., Hörstedt, P., Ikeda, Y., ... Grebe, M. (2013). Arabidopsis SABRE and CLASP interact to stabilize cell division plane orientation and planar polarity. *Nature Communications*, 4(7317), 2779. <https://doi.org/10.1038/ncomms3779>

Pillot, M., Baroux, C., Vazquez, M. A., Autran, D., Leblanc, O., Vielle-Calzada, J. P., ... Grimanelli, D. (2010). Embryo and endosperm inherit distinct chromatin and transcriptional states from the female gametes in Arabidopsis. *Plant Cell*. <https://doi.org/10.1105/tpc.109.071647>

Pires, N. D., Yi, K., Breuninger, H., Catarino, B., Menand, B., & Dolan, L. (2013). Recruitment and remodeling of an ancient gene regulatory network during land plant evolution. *Proceedings of the National Academy of Sciences of the United States of America*. <https://doi.org/10.1073/pnas.1305457110>

Plavskin, Y., Nagashima, A., Perroud, P. F., Hasebe, M., Quatrano, R. S., Atwal, G. S., & Timmermans, M. C. P. (2016). Ancient trans-Acting siRNAs Confer Robustness and Sensitivity onto the Auxin Response. *Developmental Cell*. <https://doi.org/10.1016/j.devcel.2016.01.010>

Prigge, M. J., Lavy, M., Ashton, N. W., & Estelle, M. (2010). Physcomitrella patens auxin-resistant mutants affect conserved elements of an auxin-signaling pathway. *Current Biology*.

<https://doi.org/10.1016/j.cub.2010.08.050>

Prigge, M. J., Otsuga, D., Alonso, J. M., Ecker, J. R., Drews, G. N., & Clark, S. E. (2005). Class III homeodomain-leucine zipper gene family members have overlapping, antagonistic, and distinct roles in Arabidopsis development. *Plant Cell*. <https://doi.org/10.1105/tpc.104.026161>

Rademacher, E. H., Lokerse, A. S., Schlereth, A., Llavata-Peris, C. I., Bayer, M., Kientz, M., ... Weijers, D. (2012). Different Auxin Response Machineries Control Distinct Cell Fates in the Early Plant Embryo. *Developmental Cell*. <https://doi.org/10.1016/j.devcel.2011.10.026>

Rademacher, E. H., Möller, B., Lokerse, A. S., Llavata-Peris, C. I., Van Den Berg, W., & Weijers, D. (2011). A cellular expression map of the Arabidopsis AUXIN RESPONSE FACTOR gene family. *Plant Journal*. <https://doi.org/10.1111/j.1365-313X.2011.04710.x>

Radoeva, T., & Weijers, D. (2014). A roadmap to embryo identity in plants. *Trends in Plant Science*. <https://doi.org/10.1016/j.tplants.2014.06.009>

Rasmussen, C. G., Wright, A. J., & Müller, S. (2013). The role of the cytoskeleton and associated proteins in determination of the plant cell division plane. *The Plant Journal: For Cell and Molecular Biology*, 75(2), 258–269. <https://doi.org/10.1111/tpj.12177>

Reinhart, B. J., Liu, T., Newell, N. R., Magnani, E., Huang, T., Kerstetter, R., ... Barton, M. K. (2013). Establishing a framework for the ad/abaxial regulatory network of Arabidopsis: Ascertaining targets of class III HOMEODOMAIN LEUCINE ZIPPER and KANADI regulation. *Plant Cell*. <https://doi.org/10.1105/tpc.113.111518>

Robert, H. S., Grunewald, W., Sauer, M., Cannoot, B., Soriano, M., Swarup, R., ... Friml, J. (2015). Plant embryogenesis requires AUX/LAX-mediated auxin influx. *Development*. <https://doi.org/10.1242/dev.115832>

Robert, Hélène S., Grones, P., Stepanova, A. N., Robles, L. M., Lokerse, A. S., Alonso, J. M., ... Friml, J. (2013). Local auxin sources orient the apical-basal axis in Arabidopsis embryos. *Current Biology: CB*, 23(24), 2506–2512. <https://doi.org/10.1016/j.cub.2013.09.039>

Růžicka, K., Šimášková, M., Duclercq, J., Petrášek, J., Zažímalová, E., Simon, S., ... Benková, E. (2009). Cytokinin regulates root meristem activity via modulation of the polar auxin transport. *Proceedings of the National Academy of Sciences of the United States of America*. <https://doi.org/10.1073/pnas.0900060106>

- Sachs, J. (1877). Über die Anordnung der Zellen in jüngsten Pflanzentheilen. *Stahel'shen*.
- Saiga, S., Möller, B., Watanabe-Taneda, A., Abe, M., Weijers, D., & Komeda, Y. (2012). Control of embryonic meristem initiation in Arabidopsis by PHD-finger protein complexes. *Development*. <https://doi.org/10.1242/dev.074492>
- San-Bento, R., Farcot, E., Galletti, R., Creff, A., & Ingram, G. (2014). Epidermal identity is maintained by cell-cell communication via a universally active feedback loop in Arabidopsis thaliana. *Plant Journal*. <https://doi.org/10.1111/tpj.12360>
- Sang, Y., Silva-Ortega, C. O., Wu, S., Yamaguchi, N., Wu, M. F., Pfluger, J., ... Wagner, D. (2012). Mutations in two non-canonical Arabidopsis SWI2/SNF2 chromatin remodeling ATPases cause embryogenesis and stem cell maintenance defects. *Plant Journal*. <https://doi.org/10.1111/tpj.12009>
- Sarkar, A. K., Luijten, M., Miyashima, S., Lenhard, M., Hashimoto, T., Nakajima, K., ... Laux, T. (2007). Conserved factors regulate signalling in Arabidopsis thaliana shoot and root stem cell organizers. *Nature*. <https://doi.org/10.1038/nature05703>
- Sato, A., Toyooka, K., & Okamoto, T. (2010). Asymmetric cell division of rice zygotes located in embryo sac and produced by in vitro fertilization. *Sexual Plant Reproduction*. <https://doi.org/10.1007/s00497-009-0129-9>
- Schaller, G. E., Street, I. H., & Kieber, J. J. (2014). Cytokinin and the cell cycle. *Current Opinion in Plant Biology*. <https://doi.org/10.1016/j.pbi.2014.05.015>
- Scheres, B., Di Laurenzio, L., Willemsen, V., Hauser, M. T., Janmaat, K., Weisbeek, P., & Benfey, P. N. (1995). Mutations affecting the radial organisation of the Arabidopsis root display specific defects throughout the embryonic axis. *Development*.
- Scheres, Ben, Wolkenfelt, H., Willemsen, V., Terlouw, M., Lawson, E., Dean, C., & Weisbeek, P. (1994). Embryonic origin of the Arabidopsis primary root and root meristem initials. *Development*.
- Schlereth, A., Möller, B., Liu, W., Kientz, M., Flipse, J., Rademacher, E. H., ... Weijers, D. (2010). MONOPTEROS controls embryonic root initiation by regulating a mobile transcription factor. *Nature*, 464(7290), 913–916. <https://doi.org/10.1038/nature08836>
- Schoof, H., Lenhard, M., Haecker, A., Mayer, K. F. X., Jürgens, G., & Laux, T. (2000).

The stem cell population of Arabidopsis shoot meristems is maintained by a regulatory loop between the CLAVATA and WUSCHEL genes. *Cell*. [https://doi.org/10.1016/S0092-8674\(00\)80700-X](https://doi.org/10.1016/S0092-8674(00)80700-X)

Schulz, R., & Jensen, W. A. (1968). Capsella Embryogenesis: The Egg, Zygote, and Young Embryo. *American Journal of Botany*. <https://doi.org/10.2307/2440969>

Šimášková, M., O'Brien, J. A., Khan, M., Van Noorden, G., Ötvös, K., Vieten, A., ... Benková, E. (2015). Cytokinin response factors regulate PIN-FORMED auxin transporters. *Nature Communications*. <https://doi.org/10.1038/ncomms9717>

Sivaramakrishna, D. (1978). Size relationships of apical cell and basal cell in two-celled embryos in angiosperms. *Canadian Journal of Botany*. <https://doi.org/10.1139/b78-166>

Slane, D., Kong, J., Berendzen, K. W., Kilian, J., Henschen, A., Kolb, M., ... Jürgens, G. (2014). Cell type-specific transcriptome analysis in the early arabidopsis thaliana embryo. *Development (Cambridge)*. <https://doi.org/10.1242/dev.116459>

Smith, Z. R., & Long, J. A. (2010). Control of Arabidopsis apical-basal embryo polarity by antagonistic transcription factors. *Nature*. <https://doi.org/10.1038/nature08843>

Soriano, M., Li, H., Jacquard, C., Angenent, G. C., Krochko, J., Offringa, R., & Boutilier, K. (2014). Plasticity in cell division patterns and auxin transport dependency during in vitro embryogenesis in Brassica napus. *Plant Cell*. <https://doi.org/10.1105/tpc.114.126300>

Spinner, L., Gadeyne, A., Belcram, K., Goussot, M., Moison, M., Duroc, Y., ... Pastuglia, M. (2013). A protein phosphatase 2A complex spatially controls plant cell division. *Nature Communications*, 4, 1863. <https://doi.org/10.1038/ncomms2831>

Stuurman, J., Jäggi, F., & Kuhlemeier, C. (2002). Shoot meristem maintenance is controlled by a GRAS-gene mediated signal from differentiating cells. *Genes and Development*. <https://doi.org/10.1101/gad.230702>

Szemenyei, H., Hannon, M., & Long, J. A. (2008). TOPLESS mediates auxin-dependent transcriptional repression during Arabidopsis embryogenesis. *Science*. <https://doi.org/10.1126/science.1151461>

Takada, S., & Iida, H. (2014). Specification of epidermal cell fate in plant shoots. *Frontiers in Plant Science*. <https://doi.org/10.3389/fpls.2014.00049>

Takada, S., & Jürgens, G. (2007). Transcriptional regulation of epidermal cell fate in the Arabidopsis embryo. *Development*. <https://doi.org/10.1242/dev.02803>

Takada, S., Takada, N., & Yoshida, A. (2013). ATML1 promotes epidermal cell differentiation in Arabidopsis shoots. *Development (Cambridge)*. <https://doi.org/10.1242/dev.094417>

Tam, T. H. Y., Catarino, B., & Dolan, L. (2015). Conserved regulatory mechanism controls the development of cells with rooting functions in land plants. *Proceedings of the National Academy of Sciences of the United States of America*. <https://doi.org/10.1073/pnas.1416324112>

Tanaka, H., Watanabe, M., Watanabe, D., Tanaka, T., Machida, C., & Machida, Y. (2002). A cr4, a putative receptor kinase gene of arabidopsis thaliana, that is expressed in the outer cell layers of embryos and plants, is involved in proper embryogenesis. *Plant and Cell Physiology*. <https://doi.org/10.1093/pcp/pcf052>

ten Hove, C. A., Willemsen, V., de Vries, W. J., van Dijken, A., Scheres, B., & Heidstra, R. (2010). SCHIZORIZA Encodes a Nuclear Factor Regulating Asymmetry of Stem Cell Divisions in the Arabidopsis Root. *Current Biology*. <https://doi.org/10.1016/j.cub.2010.01.018>

Tian, H., Wabnik, K., Niu, T., Li, H., Yu, Q., Pollmann, S., ... Ding, Z. (2014). WOX5-IAA17 feedback circuit-mediated cellular auxin response is crucial for the patterning of root stem cell niches in arabidopsis. *Molecular Plant*. <https://doi.org/10.1093/mp/sst118>

Tian, J., Han, L., Feng, Z., Wang, G., Liu, W., Ma, Y., ... Kong, Z. (2015). Orchestration of microtubules and the actin cytoskeleton in trichome cell shape determination by a plant-unique kinesin. *ELife*. <https://doi.org/10.7554/eLife.09351>

Tivendale, N. D., Ross, J. J., & Cohen, J. D. (2014). The shifting paradigms of auxin biosynthesis. *Trends in Plant Science*. <https://doi.org/10.1016/j.tplants.2013.09.012>

Tiwari, S. B., Hagen, G., & Guilfoyle, T. (2003). The roles of auxin response factor domains in auxin-responsive transcription. *Plant Cell*. <https://doi.org/10.1105/tpc.008417>

Tokunaga, H., Kojima, M., Kuroha, T., Ishida, T., Sugimoto, K., Kiba, T., & Sakakibara, H. (2012). Arabidopsis lonely guy (LOG) multiple mutants reveal a central role of the LOG-dependent pathway in cytokinin activation. *Plant Journal*. <https://doi.org/10.1111/j.1365-313X.2011.04795.x>

Torres-Ruiz, R. A., & Jürgens, G. (1994). Mutations in the FASS gene uncouple pattern formation and morphogenesis in Arabidopsis development. *Development*.

Turchi, L., Baima, S., Morelli, G., & Ruberti, I. (2015). Interplay of HD-Zip II and III transcription factors in auxin-regulated plant development. *Journal of Experimental Botany*. <https://doi.org/10.1093/jxb/erv174>

Turchi, Luana, Carabelli, M., Ruzza, V., Possenti, M., Sassi, M., Peñalosa, A., ... Ruberti, I. (2013). Arabidopsis HD-Zip II transcription factors control apical embryo development and meristem function. *Development (Cambridge)*. <https://doi.org/10.1242/dev.092833>

Ueda, M., Zhang, Z., & Laux, T. (2011). Transcriptional Activation of Arabidopsis Axis Patterning Genes WOX8/9 Links Zygote Polarity to Embryo Development. *Developmental Cell*. <https://doi.org/10.1016/j.devcel.2011.01.009>

Ulmasov, T., Hagen, G., & Guilfoyle, T. J. (1999). Activation and repression of transcription by auxin-response factors. *Proceedings of the National Academy of Sciences of the United States of America*. <https://doi.org/10.1073/pnas.96.10.5844>

Van Den Berg, C., Willemsen, V., Hendriks, G., Weisbeek, P., & Scheres, B. (1997). Short-range control of cell differentiation in the Arabidopsis root meristem. *Nature*. <https://doi.org/10.1038/36856>

Vanstraelen, M., Van Damme, D., De Rycke, R., Mylle, E., Inzé, D., & Geelen, D. (2006). Cell cycle-dependent targeting of a kinesin at the plasma membrane demarcates the division site in plant cells. *Current Biology*. <https://doi.org/10.1016/j.cub.2005.12.035>

Vasil, V. (1979). Embryology of Gymnosperms. Encyclopedia of Plant Anatomy, Volume X, Part 2. Hardev Singh . *The Quarterly Review of Biology*. <https://doi.org/10.1086/411361>

Vatén, A., Dettmer, J., Wu, S., Stierhof, Y. D., Miyashima, S., Yadav, S. R., ... Helariutta, Y. (2011). Callose Biosynthesis Regulates Symplastic Trafficking during Root Development. *Developmental Cell*. <https://doi.org/10.1016/j.devcel.2011.10.006>

Vera-Sirera, F., De Rybel, B., Úrbez, C., Kouklas, E., Pesquera, M., Álvarez-Mahecha, J. C., ... Blázquez, M. A. (2015). A bHLH-Based Feedback Loop Restricts Vascular Cell Proliferation in Plants. *Developmental Cell*. <https://doi.org/10.1016/j.devcel.2015.10.022>

Vielle-Calzada, J. P., Baskar, R., & Grossniklaus, U. (2000). Delayed activation of the

paternal genome during seed development. *Nature*. <https://doi.org/10.1038/35003595>

Von Wangenheim, D., Fangerau, J., Schmitz, A., Smith, R. S., Leitte, H., Stelzer, E. H. K., & Maizel, A. (2016). Rules and self-organizing properties of post-embryonic plant organ cell division patterns. *Current Biology*. <https://doi.org/10.1016/j.cub.2015.12.047>

Wabnik, K., Robert, H. S., Smith, R. S., & Friml, J. (2013a). Modeling framework for the establishment of the apical-basal embryonic axis in plants. *Current Biology*. <https://doi.org/10.1016/j.cub.2013.10.038>

Wabnik, K., Robert, H. S., Smith, R. S., & Friml, J. (2013b). Modeling framework for the establishment of the apical-basal embryonic axis in plants. *Current Biology: CB*, 23(24), 2513–2518. <https://doi.org/10.1016/j.cub.2013.10.038>

Waki, T., Hiki, T., Watanabe, R., Hashimoto, T., & Nakajima, K. (2011). The arabidopsis RWP-RK protein RKD4 triggers gene expression and pattern formation in early embryogenesis. *Current Biology*. <https://doi.org/10.1016/j.cub.2011.07.001>

Wang, H., Ngwenyama, N., Liu, Y., Walker, J. C., & Zhang, S. (2007). Stomatal development and patterning are regulated by environmentally responsive mitogen-activated protein kinases in Arabidopsis. *Plant Cell*. <https://doi.org/10.1105/tpc.106.048298>

Wang, R., & Estelle, M. (2014). Diversity and specificity: Auxin perception and signaling through the TIR1/AFB pathway. *Current Opinion in Plant Biology*. <https://doi.org/10.1016/j.pbi.2014.06.006>

Weigel, D., & Jürgens, G. (2002). Stem cells that make stems. *Nature*. <https://doi.org/10.1038/415751a>

Weijers, D., Geldnert, N., Offringa, R., & Jürgens, G. (2001). Seed development: Early paternal gene activity in Arabidopsis. *Nature*. <https://doi.org/10.1038/414709a>

Weijers, D., Schlereth, A., Ehrismann, J. S., Schwank, G., Kientz, M., & Jürgens, G. (2006). Auxin triggers transient local signaling for cell specification in Arabidopsis embryogenesis. *Developmental Cell*. <https://doi.org/10.1016/j.devcel.2005.12.001>

Weiste, C., & Dröge-Laser, W. (2014). The Arabidopsis transcription factor bZIP11 activates auxin-mediated transcription by recruiting the histone acetylation machinery. *Nature Communications*. <https://doi.org/10.1038/ncomms4883>

Welch, D., Hassan, H., Blilou, I., Immink, R., Heidstra, R., & Scheres, B. (2007). Arabidopsis JACKDAW and MAGPIE zinc finger proteins delimit asymmetric cell division and stabilize tissue boundaries by restricting SHORT-ROOT action. *Genes and Development*. <https://doi.org/10.1101/gad.440307>

Williams, L., Grigg, S. P., Xie, M., Christensen, S., & Fletcher, J. C. (2005). Regulation of Arabidopsis shoot apical meristem and lateral organ formation by microRNA miR166g and its AtHD-ZIP target genes. *Development*. <https://doi.org/10.1242/dev.01942>

Wu, X., Chory, J., & Weigel, D. (2007). Combinations of WOX activities regulate tissue proliferation during Arabidopsis embryonic development. *Developmental Biology*. <https://doi.org/10.1016/j.ydbio.2007.07.019>

Wysocka-Diller, J. W., Helariutta, Y., Fukaki, H., Malamy, J. E., & Benfey, P. N. (2000). Molecular analysis of SCARECROW function reveals a radial patterning mechanism common to root and shoot. *Development*.

Xu, T., Nagawa, S., & Yang, Z. (2011). Uniform auxin triggers the Rho GTPase-dependent formation of interdigitation patterns in pavement cells. *Small GTPases*. <https://doi.org/10.4161/sgtp.2.4.16702>

Xu, T. T., Ren, S. C., Song, X. F., & Liu, C. M. (2015). CLE19 expressed in the embryo regulates both cotyledon establishment and endosperm development in Arabidopsis. *Journal of Experimental Botany*. <https://doi.org/10.1093/jxb/erv293>

Yoshida, S., Barbier de Reuille, P., Lane, B., Bassel, G. W., Prusinkiewicz, P., Smith, R. S., & Weijers, D. (2014). Genetic control of plant development by overriding a geometric division rule. *Developmental Cell*, 29(1), 75–87. <https://doi.org/10.1016/j.devcel.2014.02.002>

Yu, M., & Zhao, J. (2012). The cytological changes of tobacco zygote and proembryo cells induced by beta-glucosyl Yariv reagent suggest the involvement of arabinogalactan proteins in cell division and cell plate formation. *BMC Plant Biology*. <https://doi.org/10.1186/1471-2229-12-126>

Zhang, Ying, Wang, P., Shao, W., Zhu, J. K., & Dong, J. (2015). The BASL Polarity Protein Controls a MAPK Signaling Feedback Loop in Asymmetric Cell Division. *Developmental Cell*. <https://doi.org/10.1016/j.devcel.2015.02.022>

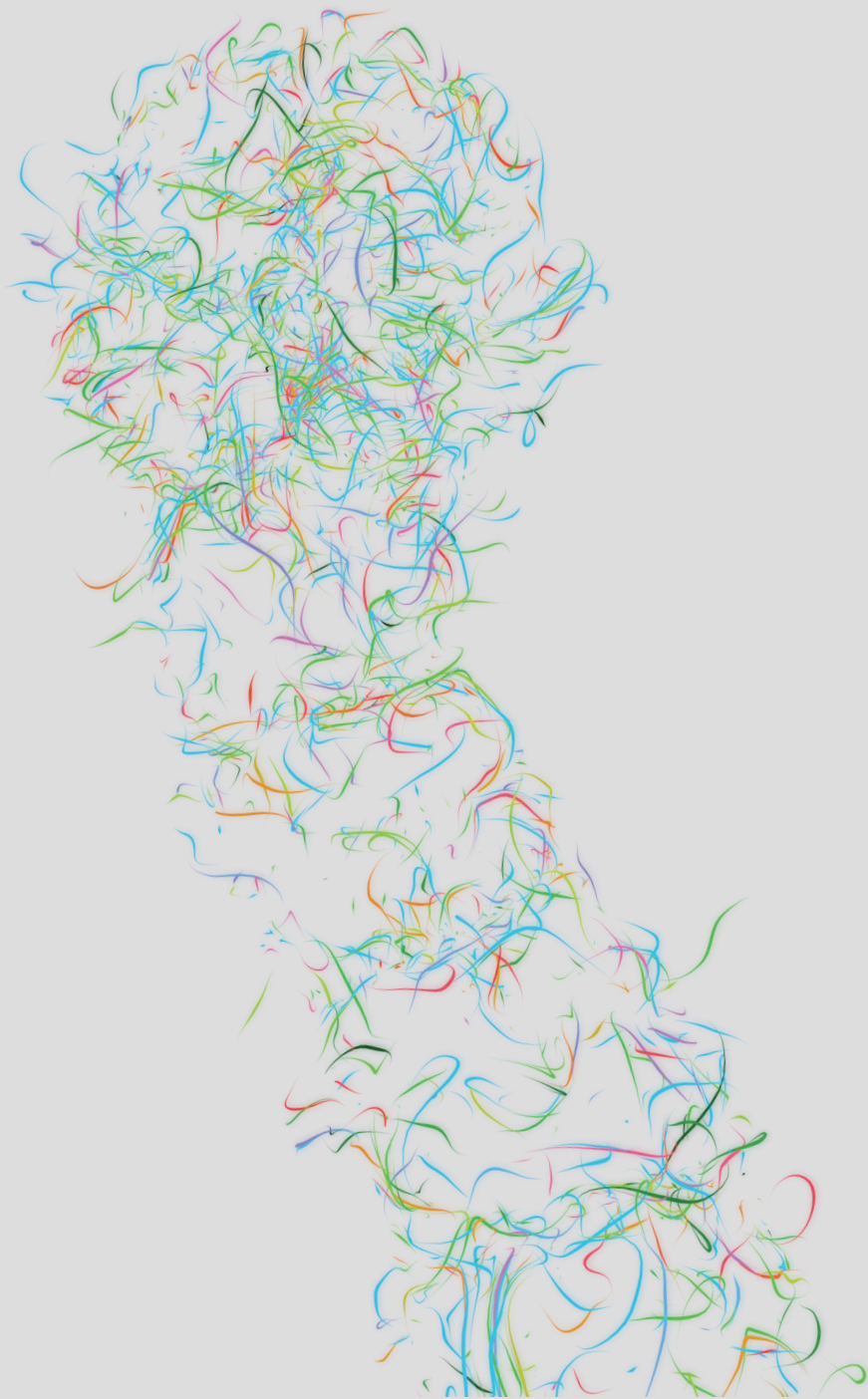
Zhang, Yuzhou, Jiao, Y., Liu, Z., & Zhu, Y. X. (2015). ROW1 maintains quiescent centre

identity by confining WOX5 expression to specific cells. *Nature Communications*. <https://doi.org/10.1038/ncomms7003>

Zhao, J., Xin, H., Qu, L., Ning, J., Peng, X., Yan, T., ... Sun, M. X. (2011). Dynamic changes of transcript profiles after fertilization are associated with de novo transcription and maternal elimination in tobacco zygote, and mark the onset of the maternal-to-zygotic transition. *Plant Journal*. <https://doi.org/10.1111/j.1365-313X.2010.04403.x>

Zhou, Y., Honda, M., Zhu, H., Zhang, Z., Guo, X., Li, T., ... Zhang, X. (2015). Spatiotemporal sequestration of miR165/166 by arabidopsis argonaute10 promotes shoot apical meristem maintenance. *Cell Reports*. <https://doi.org/10.1016/j.celrep.2015.02.047>

Zhu, T., Moschou, P. N., Alvarez, J. M., Sohlberg, J. J., & Arnold, S. (2016). WUSCHEL-RELATED HOMEODOMAIN 2 is important for protoderm and suspensor development in the gymnosperm Norway spruce. *BMC Plant Biology*. <https://doi.org/10.1186/s12870-016-0706-7>



# Chapter 3

## A microtubule-based mechanism predicts cell division orientation in plant embryogenesis

Bandan Chakraborty<sup>1,2</sup>, Viola Willemsen<sup>1\*</sup>, Thijs de Zeeuw<sup>4\*</sup>, Che-Yang Liao<sup>4</sup>, Dolf Weijers<sup>4</sup>, Bela Mulder<sup>2,3\*\*</sup> and Ben Scheres<sup>1\*\*</sup>

A version of this chapter has been published as:

**Chakraborty, B, Willemsen, V, de Zeeuw, T, Liao, C, Weijers, D, Mulder, B, Scheres, B. 2018.**  
A plausible microtubule-based mechanism for cell division orientation in plant embryogenesis.  
*Current biology* 28, 3031-3043

1. Plant Developmental Biology, Wageningen University, Wageningen 6708PB, the Netherlands.
2. Institute AMOLF, Science Park 104, 1098 XG, Amsterdam, the Netherlands.
3. Cell Biology, Wageningen University, Wageningen 6708PB, the Netherlands.
4. Laboratory of Biochemistry, Wageningen University, Dreijenlaan 3, 6703HA Wageningen, the Netherlands

\* These authors contributed equally

\*\* joint corresponding authors: mulder@amolf.nl ; ben.scheres@wur.nl



## Abstract

Oriented cell divisions are significant in plant morphogenesis because plant cells are embedded in cell walls and cannot relocate. Cell divisions follow various regular orientations, but the underlying mechanisms have not been clarified. We show that cell-shape dependent self-organisation of cortical microtubule arrays is crucial for determining planes of early tissue-generating divisions and forms the basis for robust control of cell division orientation in the embryo. To achieve this, we simulate microtubules on actual cell surface shapes from which we derive a minimal set of three rules for proper array orientation. The first rule captures the effects of cell shape alone on microtubule organisation, the second rule describes the regulation of microtubule stability at cell edges and the third rule includes the differential effect of auxin on local microtubule stability. These rules explain early embryonic division plane orientations and offer a framework for understanding patterned cell divisions in plant morphogenesis.

## Introduction

Plant cell division patterns show striking regularities. A prime example is the early stage embryo in *Arabidopsis thaliana* (Campilho et al., 2006; Grandjean et al., 2004; Yoshida et al., 2014), which starting from the single-cell stage undergoes a few rounds of remarkably robust and geometrically precise internal divisions, setting the stage for further development through differentiation and growth. For already more than a century these regularities have spurred the formulation of heuristic geometric rules for oriented cell divisions. These rules relate the selection division planes e.g. to the principal direction of growth, geometric relations to existing cell walls and the nucleus, or minimum cell surface energy (Besson & Dumais, 2011; Dupuy et al., 2010; Errera, 1886; Hofmeister, 1868; Sachs, 1878; Smith et al., 2006). With the advent of modern cell biology, however, division plane orientation in plants has been connected with the orientation of the ordered ensemble of microtubules (MTs) associated with the plasma membrane, the cortical microtubule array (CMA) (Ehrhardt & Shaw, 2006; Wasteneys, 2002). Shortly before cell division, the cortical MTs, while keeping their net orientation, become spatially restricted to a plane that is closely associated with the nucleus, forming the so-called pre-prophase band (PPB). The orientation of the PPB and, by extension that of the CMA, is an indicator of cell division orientation (Mineyuki, 1999; Müller et al., 2009). Some variability between PPB and cell plate orientation may occur (e.g. Oud and Nanninga (Oud & Nanninga, 1992)) and recent evidence suggests that the PPB is not strictly required for division plane orientation (Schaefer et al., 2017), but nevertheless the link of cell division plane to CMA orientation is maintained. The question of how the CMA is organised is therefore of prime importance to understanding division plane orientation.

Here we address this question in the early *Arabidopsis* embryo. Apart from the intrinsic biological interest of the tissue-separating ('formative') cell divisions that occur in this system, it provides a unique, well-defined and yet highly non-trivial "laboratory" for studying the interplay between the molecular mechanisms driving CMA organisation and the developmental context. This holds a fortiori as previous analysis of *Arabidopsis* embryogenesis surprisingly shows that auxin-insensitive embryos misexpressing a truncated version of the BODENLOS (BDL) protein do divide consistent with proposed geometric rules, whereas wild-type (WT) divisions seem to require additional control (Yoshida et al., 2014), possibly through auxin-mediated CMA regulation. This indicates the need to elucidate to what extent the geometrical rules are in fact consistent with concrete molecular mechanisms.

There is a broad consensus that orientational ordering in the CMA is the collective outcome of the local effects of “collisions” between MTs driven by their dynamical instability mechanism (Dixit & Cyr, 2004). Moreover, there is evidence gleaned from root epidermis cells that specific geometric features such as sharps edges between relatively flat cell faces, can influence the orientation of the CMA by effectively blocking the passage of MTs from one cell face to the other, and that this effect is possibly modulated by Microtubule Associated Protein (MAP) CLASP (Ambrose et al., 2011). However, we as yet lack a full understanding of how cell shape in general impacts CMA organisation. This is especially salient in the early *Arabidopsis* embryo, which in its first 4 division cycles displays a gamut of cell shapes, ranging from almost spherical, to halves of spherical-wedges with a sharp opening angle. Recently, tensile stress has also been shown to influence CMA orientation (Louveau et al., 2016), leading to the proposal of a new general rule for division plane orientation along on the direction of maximal wall tension. However, to date the molecular mechanism by which MTs “sense” the direction of wall tension remains elusive, although the activity of the MT severing protein Katanin appears to be implicated (Zhang et al., 2013). Finally, as cortical MTs co-align with cellulose microfibrils, growing cells exhibit a complex interplay between CMA orientation, the deposition of microfibrils in the cell wall and growth (Lloyd & Chan, 2004; Paredez, 2006), so that growth by itself could influence division plane orientation, potentially underpinning one of the phenomenological rules (Hejnowicz, 2014).

Here, we utilize a recently developed computational framework that simulates the dynamics of MT ordering on realistic cell shapes (Chakraborty et al., 2018). We specifically focussed on the impact of shape in a geometrical sense, including the described edge effects, on the collective dynamics of MTs that lead a global orientation of the CMA. This provides a clearly defined default model to which other effects may be added incrementally. As it is at present infeasible to directly measure or predict stress patterns in the embryo, and in the absence of a concrete molecular mechanism to implement the feedback of tension on MT dynamics, we parsimoniously chose to disregard these effects at this stage. Finally, as only a very limited amount of volumetric growth occurs during the considered embryonic developmental phase, potential growth-related effects were also ignored.

Combining our in-silico results with high-resolution visualization of both cell-outline and cortical MTs in WT *Arabidopsis* embryos and selected mutants enabled us to show that hitherto unanticipated constraints due to cell shape alone, in combination with cell edge-catastrophe protection and auxin-mediated MT stability, can already provide

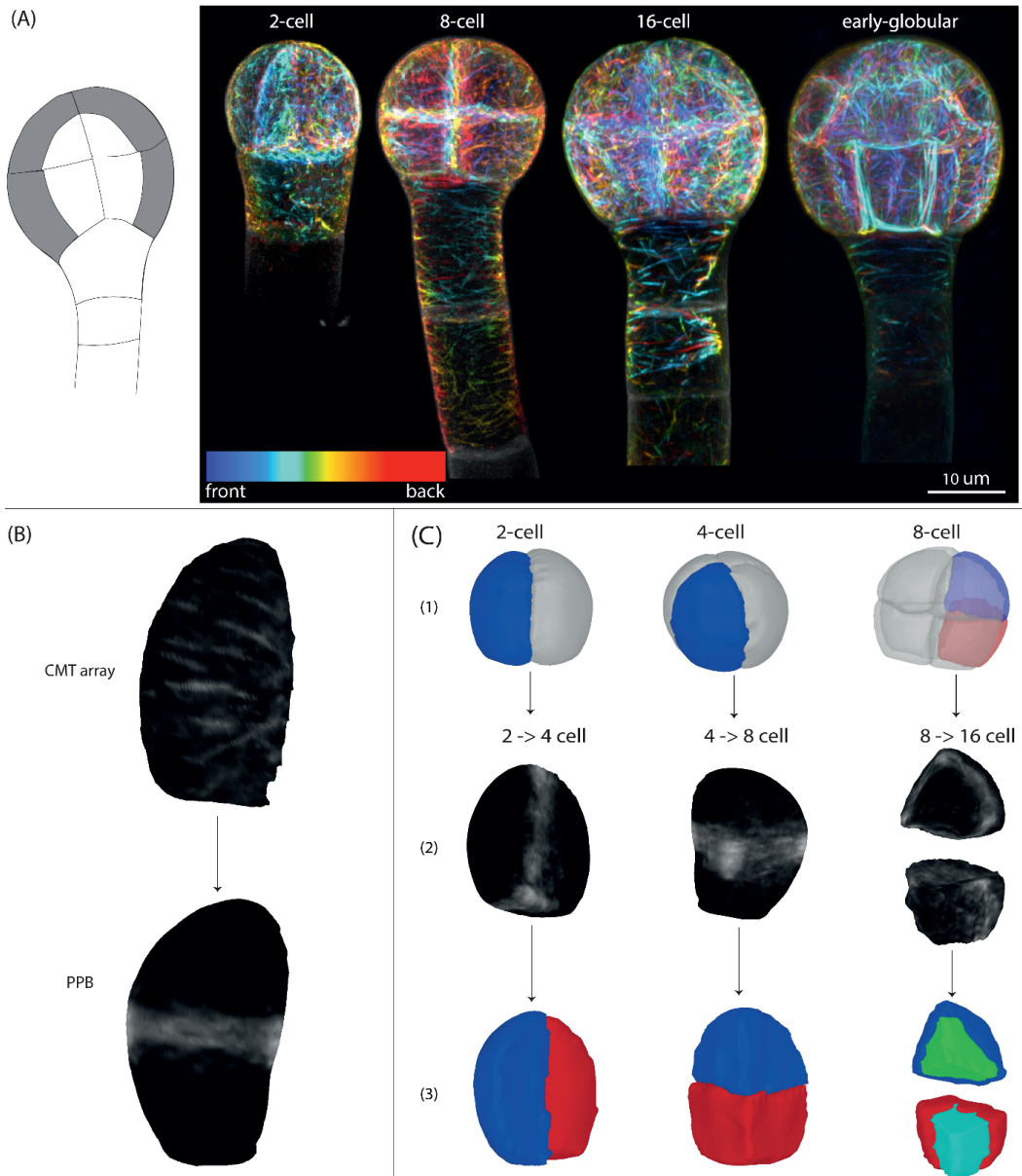
a sufficient explanation for cell division patterns in 1- to 16-cell stage embryos. Thus, our minimal MT-based molecular statistical mechanism correctly predicts division plane orientations, recapitulates many of the proposed geometric rules, and establishes a basis for specific experimental validations and the incorporation of additional mechanism when necessary in the future.

## Results

### *First principle-based MT modelling on realistic cell shapes*

Our approach for understanding rules of cell division in cells that undergo formative cell divisions was to model cortical MT dynamics during the first four division cycles in the Arabidopsis embryo proper, which have been documented in detail (Jürgens et al., 1991; Mansfield & Briarty, 1991; Scheres et al., 1994; Yoshida et al., 2014). These characteristic divisions lead to the formation of inner and outer tissue layers (Figure 1A, left). Our starting assumption was that embryonic cells, like most cell types previously considered, have a regular CMA orientation that predicts the orientation of cell division. To test this assumption, we utilized an optimized imaging methodology for high-resolution 3D-imaging of the CMA which preserves MT orientation throughout the different stages of Arabidopsis embryogenesis (Liao & Weijers, 2018). We expressed TUA6-GFP from the embryo specific *WUSCHEL RELATED HOMEODOMAIN 2* (*WOX2*) promoter. Maximum projections of high-resolution Z-stacks reveal the overall topology of the MT array, including the CMA, for embryos from the 1-cell stage to globular stage (Figure 1A, right). Cell segmentation allowed the extraction of individual cell surfaces for the different embryonic cells. Analysis of cortical MT signals projected on these extracted cell surfaces shows the ordered orientation of CMA on individual cells. The CMAs collapse to form PPB structures (Cleary et al., 1992), and we found this to likely also be the case in embryos (Figure 1B), thus correctly predicting future division plane orientation (Figure 1C). Our observations validated the early embryo as a suitable model system to investigate how cortical MT ordering is established in cells with varying geometries.

To enable the exploration of a number of factors that, given observations in other cell types, are likely to govern CMA orientation in the early embryo, we designed a computational framework to simulate the key properties of MT dynamics on arbitrary shaped cellular surfaces. CMAs in animal cells have also been shown to be sensitive to cell



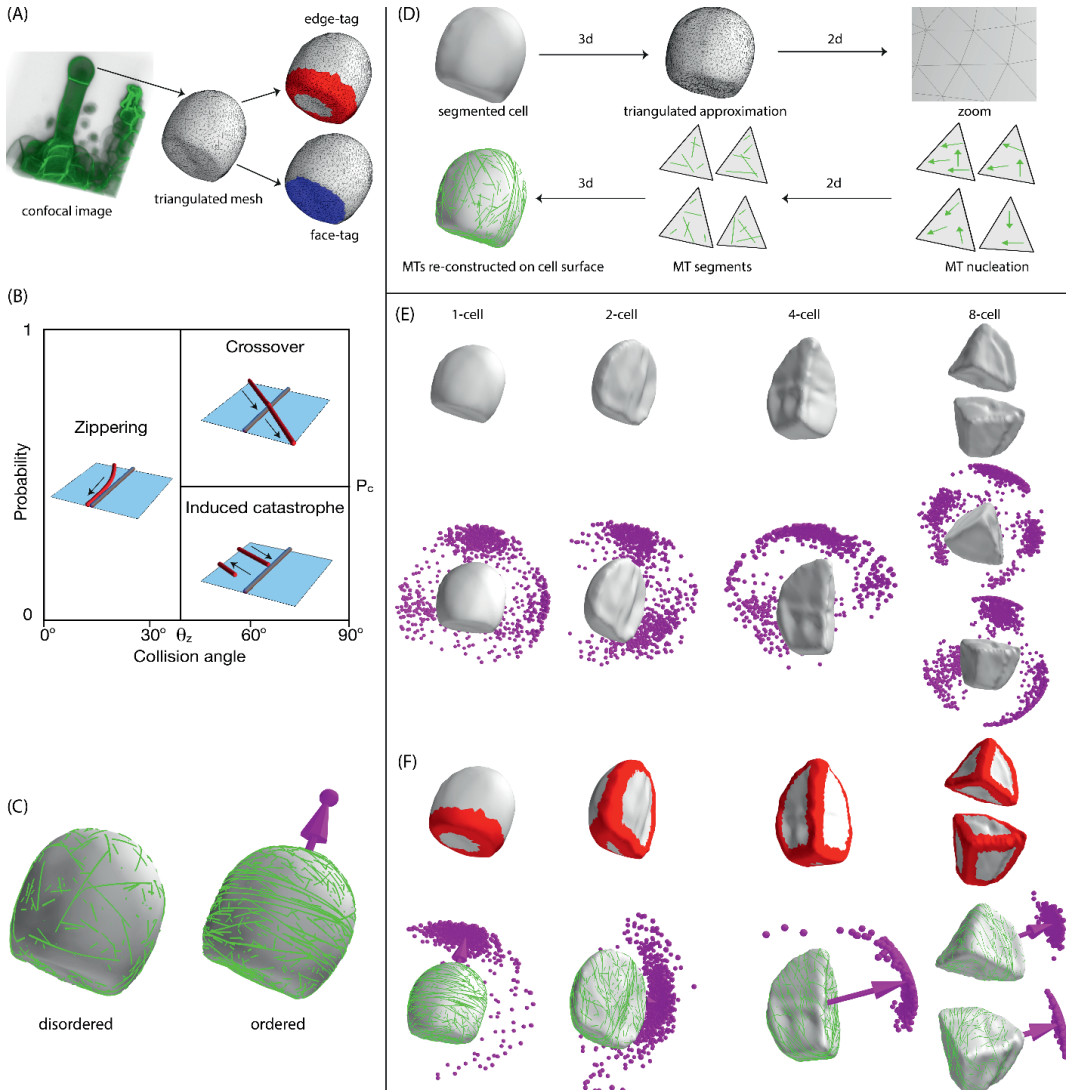
**Figure 1.** Experimental visualization of CMA and PPB during Arabidopsis early embryonic development. **a** Characteristic divisions lead to the formation of inner and outer tissue layers (left), maximum projection of depth-coded stacks of MTs visualized using a pWOX2::TUA6-GFP reporter line show an ordered orientation of MT array (right). The look-up table shows color values corresponding to the depth of the image in the z-dimension. **b** Sequential imaging of cortical MTs and the SR2200 membrane stain allows for extraction of cell shapes for separate embryonic cells. Projection of cortical MT signal on extracted cell shapes shows orientation of CMA that predicts the orientation of PPB (7 cells were analysed; note that the images are taken from different cells in the same embryo, not from live imaging the same cell over time). **c** PPB predicts the location and orientation of the division plane: (1) Representative single cell from 2-cell stage and 4-cell stage embryo, and representative single cell from upper tier and lower tier of 8-cell stage embryo are highlighted, (2) Projection of PPB on the corresponding cell templates during 2- to 4-cell stage (3 cells were analysed), 4- to 8-cell stage (5 cells were analysed) and 8- to 16-cell stage (5 cells were analysed) transitions, and (3) Pair of daughter cells during 2- to 4-, 4- to 8- and 8- to 16-cell stage transitions.

shape (Gomez et al., 2016). Therefore, we used the actual embryonic cell shapes obtained by segmenting high-resolution confocal images of fluorescently stained Arabidopsis embryos to extract cell surfaces, approximated through fine-grained triangulation (Figure 2A). To simulate MT dynamics on individual planar triangles we adapted a previously developed event-driven algorithm (Tindemans et al., 2014, 2010) that implements all key MT properties with biophysical significance, such as nucleation and dynamic instability (Mitchison & Kirschner, 1984). In the latter mechanism MTs alternate between states of steady growth or shrinkage, stochastically switching between these states at constant rates in events termed *catastrophes* and *rescues* respectively. We also encoded three possible results from MT-MT collisions that have been observed (Dixit & Cyr, 2004), *zippering*, in which an impinging growing MT bends and continues growing along an obstructing MT, *crossover*, in which an impinging MT simply passes over an obstructing MT and *induced-catastrophe*, in which the impinging MT switches to a shrinking state and retreats from the obstructing MT (Figure 2B). Although additional factors are known to influence MT dynamics, most notably directional nucleation from existing MTs (Chan et al., 2009) and severing by katanin (Burk et al., 2013; Zhang et al., 2013), previous modelling work has shown that these additional effects mainly modify the range of parameters for which ordered arrays develop spontaneously, but have less impact on the nature of the ordered state per se (Deinum & Mulder, 2013; Deinum et al., 2017, 2011). Likewise, MTs that are nucleated in the bulk cytosol, but become entrained to the cortex by binding to the cell membrane (see e.g. (Mirabet et al., 2018)) effectively only increase the nucleation rate. Parsimony therefore led us to omit these features here. The simulations on individual triangles are linked together by ensuring that the trajectories of MTs crossing from a triangle to a neighbouring one are propagated in a manner consistent with the 3D geometry of the cell surface, as illustrated in Figure 2D. The technical details of our simulation procedure, its validation against known results and illustrative background results on the interplay between geometry and CMA organization on simple shapes are more fully explained in a recently published method paper (Chakraborty et al., 2018)..

Earlier work has shown that all parameters of individual MT behaviour, excluding collision parameters, can be absorbed in a single dimensionless control parameter ( $G$ ) that controls the frequency of MT interactions (Deinum, 2013; Hawkins et al., 2010):

$$G = ((2(v_+ - v^{tm})(v_- + v^{tm})) / (r_n(v_+ + v_-)))^{1/3} ((r_r / (v_- + v^{tm})) - (r_c / (v_+ - v^{tm})))$$

where  $v_+$ ,  $v_-$  and  $v^{tm}$  are the growth, shrinkage and minus-end treadmilling speeds of the



**Figure 2.** MT modelling on Arabidopsis early embryonic cell templates. **a** The confocal image of embryonic 1-cell shape is extracted as a triangulated surface mesh via image segmentation software MorphoGraphX (Barbier de Reuille et al., 2015). The edge of the mesh is tagged (red colour) by assigning all triangles belonging to this edge with a unique edge-tag index. The flat bottom face (faint blue) and the curved top face (faint grey) are tagged by assigning all their triangles with a unique face-tag index. Edge-tags and face-tags are used for simulation implementation of edge-catastrophe and face specific MT stabilization. **b** Basic MT-MT interactions. Two dimensional attachment of MTs to cell cortex allows MTs to interact with each other via collisions. Shallow angles ( $\leq 40^\circ$ ) of collision lead to zippering and steeper angles ( $\geq 40^\circ$ ) of collision lead to crossover or induced-catastrophe. **c** Order parameter to quantify the degree of MT order and array orientation. A disordered state results in  $Q^{(2)} = 0$  without formation of MT array. An ordered state indicates the formation of MT array with significant degree of MT order,  $Q^{(2)} \sim 1$ . Perpendicular to the MT array, a vector ( $\Omega$ ) is defined which quantifies the orientation of the MT array. The tip of this vector will be used to represent the MT array orientation. **d** A schematic overview of the simulation approach, where geometrically correct propagation of growing MT ends between the neighbouring triangles lead to the reconstruction of MT dynamics on the cell surfaces. Simulated orientation of MT array on 1- to 8-cell stage WT cell templates: **e** Default cell shapes, which showed a diverse but not randomly distributed MT array orientation, and **f** With edge-catastrophe in MT dynamics, which showed one unique cluster of MT array orientation in each cell stage. Simulations were performed for  $\approx 1000$  independent configura-

rations of stochastic MT dynamics. The arrow vectors represent mean orientation of the associated MT array.

MTs,  $r_c$  and  $r_r$  the catastrophe- and rescue rates, and  $r_n$  the rate of MT nucleations per unit of cell surface area. By convention the sign of  $G$  is chosen such that  $G < 0$  when the MTs are in the biologically relevant bounded growth regime. If  $G$  increases beyond a threshold value the interacting cortical MTs will spontaneously form an ordered array.  $G$  can be increased (i.e. brought closer to 0) in several ways. For example, the higher nucleation rate  $r_n$ , the more MTs are present, which increases the frequency of collisions in the cortex. Likewise, decreasing the catastrophe rate  $r_c$ , making the MTs longer on average, which makes them more likely to interact through collisions. As the value of  $G$  can be freely chosen on each triangle, we are able to modulate MT behaviour on selected areas of the cell surface corresponding to biologically controlled effects e.g. developmentally distinct cell faces and/or highly curved edge regions between cell faces.

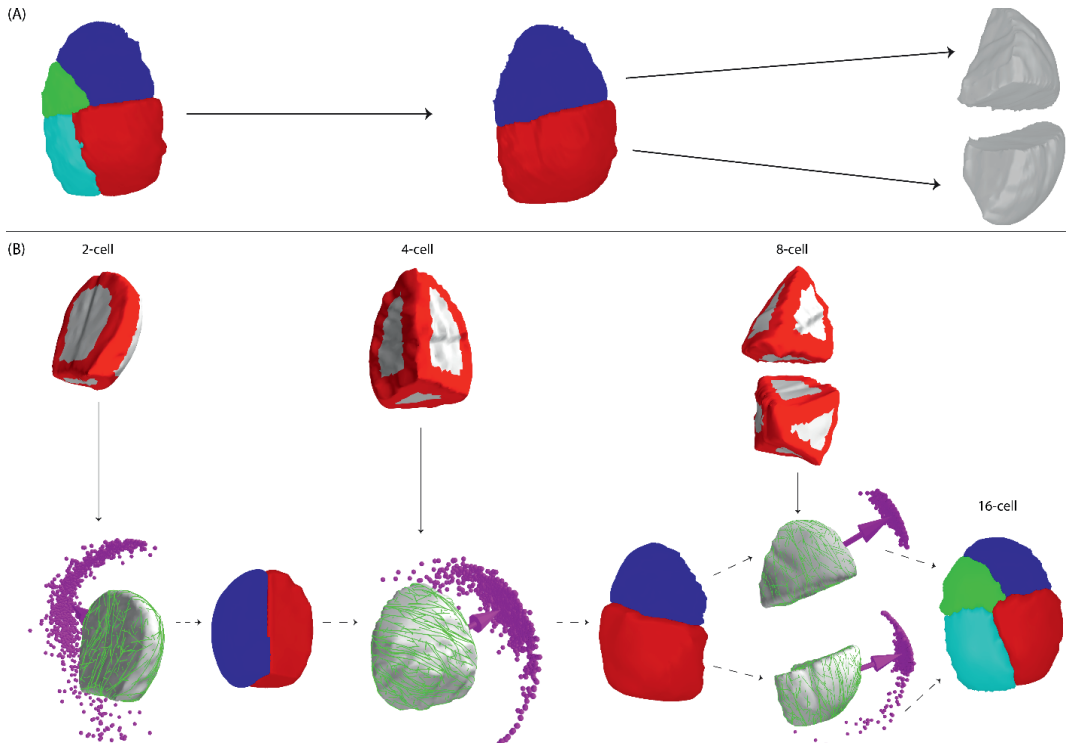
3

To read out the order of the steady-state CMA, we employed a tensorial order parameter  $Q(2)$  (for details of its definition see (Chakraborty et al., 2018), whose absolutely smallest eigenvalue  $Q(2)$  characterizes the degree of ordering:  $Q(2) = 0$  when MT orientation is random and  $Q(2) \sim 1$  when MTs are fully aligned. The normalized eigenvector  $\hat{\Omega}$  associated with the eigenvalue  $Q(2)$  characterizes the global orientation of the MT array. Its direction is perpendicular to the plane in which on average the MTs are pointing, i.e. if the MTs form a dense band around the “equator” of a cell,  $\hat{\Omega}$  will point to one of the “poles”. In all simulation images,  $\hat{\Omega}$  is represented by a dot marking the end point of the vector (Figure 2C).

*Shape and edge-catastrophe can explain early embryo cell division patterns in an auxin response mutant*

We performed  $\approx 1000$  stochastically independent simulations of MT dynamics per cell on cell surfaces extracted from WT embryos from 1- to 8-cell stage, ensuring throughout that a steady state was reached. The resulting CMAs displayed a diverse but not randomly distributed orientation (Figure 2E, quantification in Figure 7A). Thus, cell shape significantly impacted, but could not uniquely specify the orientation of the CMAs on a given cell template. It has been reported that cell edges may hinder the propagation of MTs in plant cells depending on their degree of curvature (Ambrose et al., 2011). We were curious whether this reported property of MT behaviour could further reduce the diversity

of CMA orientations in our simulations. We implemented a local enhanced catastrophe in those cell edges that have high curvature. In the various WT cells, this implementation robustly reduced the possible CMA orientations to a single sharply defined cluster for each cell stage (Figure 2F). However, the resultant inferred division patterns were non-WT and instead appeared to match those of the auxin insensitive embryos ectopically expressing *BDL* protein (*RPS5A>>bdl*) (Yoshida et al., 2014). Moreover, the simulations predicted a preference for slightly oblique division at the 4-cell stage in auxin-insensitive embryos, hitherto not described. We experimentally verified this preference of oblique division for 4- to 8-cell stage transition in *RPS5A>>bdl* embryos as well as their aberrant divisions in 8- to 16-cell stage transition (Yoshida et al., 2014) (Figure S1). Note that, at the 1- to 2-cell transition, all simulations yielded horizontal divisions, whereas only 18% of the original *bdl* mutant (non-overexpressed) divide in this direction (Hamann et al., 1999). To exclude that the mapping to *bdl* division patterns was a coincidental effect of using WT cell templates,



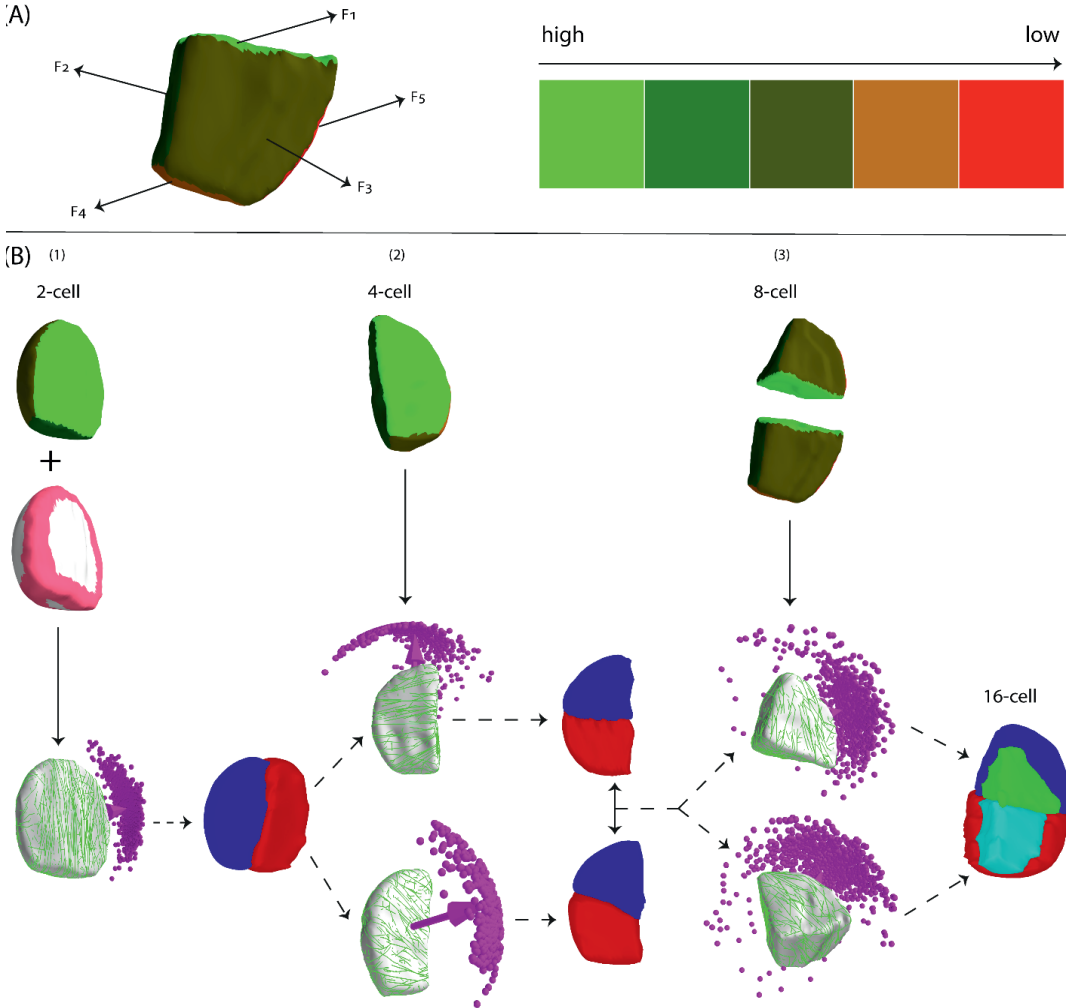
**Figure 3.** Recapitulation of *bdl* division patterns in Arabidopsis early embryonic development. **a** Reconstruction of mother cell by merging the corresponding daughter cell pair. In this example, the daughter pair of both upper and lower tier of Arabidopsis *bdl* 16-cell template were merged to reconstruct the corresponding mother 8-cell template. Such re-created mother cells were separated out for simulating MT dynamics. **b** Simulated MT arrays on 2- to 8-cell stage of *bdl* cell template, which were reconstructed by merging the corresponding daughter cell pair of the next cell stage. Simulations were performed with edge-catastrophe, yielding one unique cluster of MT array orientation in each cell stage, which correctly predicted the corresponding *bdl* division plane orientation. Cell edges are coloured red to indicate that in simulation MTs were subjected to edge-catastrophes.

we extracted cell templates from 4- to 16-cell stages *RPS5A>>bdl* embryos, reconstructed progenitor 2- to 8-cell stage cell surfaces by merging corresponding daughter cell pairs and ran simulations on these reconstructed ‘mother cells’ (Figure 3A). The steady state CMA orientation in all these simulations correctly predicted the division plane, confirming that shape effects and edge-catastrophe were sufficient to explain *bdl* divisions between 2- to 16-cell stages (Figure 3B). For a quantification of the predicted division plane angles with respect to the basal plane compared to experimentally measured values, see Figure 7B.

### *Face stability and edge-catastrophe reduction explain WT early embryo cell division patterns*

The highly characteristic WT division pattern at the 8- to 16-cell stage transition that separates inner and outer cell layers did not follow the rules based on cell shape and edge-catastrophe only. To search for an additional rule that might explain the WT division pattern, we first focused on the divisions between 2- to 16-cell stages, which were correctly predicted in *bdl*-mutant cells. We asked whether the observed defects with respect to WT were associated with aberrant CMA formation. In *RPS5A>bdl* embryos, the cytosolic (non-polymerized) TUA6:GFP fraction was significantly higher, suggesting that MTs were more often depolymerized compared to WT. This indicates that reduced auxin signalling affects MT polymerization or stability in embryo cells (Figure S2). We implemented this observation in our simulations by allowing auxin-dependent cell face-specific changes in the *G* parameter, leading to locally enhanced average MT stability (Figure S3). The resulting simulations therefore implemented, next to the basic rules for MT dynamics, effects of two biological control parameters: auxin-regulated face stability (Figure 4A) and edge-catastrophe. We investigated multiple combinations of the strength of these two effects yielding different behavioural regimes. A complete match with WT division patterns (Figure 4B, Figure 7C, Figure S4) was obtained by simulating MT dynamics on ‘original’ or ‘reconstructed mother’ 2- to 8-cell stage cell templates under the following adaptations of our initial rules: (1) enhanced cell face stability that is strongest in recent division faces and (2) reduced edge-catastrophe (for simulation parameters see Table S1). These specific rules conceivably result from concrete molecular processes. First, auxin-mediated enhanced face stability could be transiently established at each new division site. Second, edge-catastrophe could be reduced, for example, by the activity of proteins that stabilize bending MTs (Ambrose et al., 2011).

As an initial test of the requirement of edge-catastrophe reduction for obtaining correctly oriented CMAs between 2- to 16-cell stages in WT, we analysed embryos homozygous for two different mutations in the *CLASP* gene, reported to influence MT edge-catastrophe (Ambrose et al., 2011). To support our assumption that edge-catastrophe is regulated in WT embryos by CLASP, its mutations should affect division plane orientation in



**Figure 4.** WT division pattern in Arabidopsis early embryonic development. **a** Developmental age of cell faces  $F5 > F4 > F3 > F2 > F1$  as depicted by the colour scale. MT dynamic catastrophe rate increases with developmental age, yielding a corresponding decrease in average MT length i.e. lower MT stability (see also Figure S3). **b** Simulated orientation of MT array on WT cell templates taken from different cell stages: (1) 2-cell stage with reduced edge-catastrophe in MT dynamics and enhanced MT stabilization at developmentally new cell faces, resulting in one unique cluster of MT array orientation correctly predicting the WT division plane orientation, (2) 4-cell stage without edge-catastrophe in MT dynamics and enhanced MT stabilization at developmentally new cell faces, resulting in two clusters of MT array orientation correctly predicting the two observed phenotypes of WT division plane orientation, and (3) 8-cell stage without edge-catastrophe in MT dynamics and enhanced MT stabilization at developmentally new cell faces, resulting in one unique cluster of MT array orientation for both upper and lower tier cells correctly predicting the WT division plane orientation.

a manner predicted by our simulations. Indeed, in both mutant alleles, division orientations were severely skewed compared to WT (Figure 5A for 4- to 8-cell stage; Figure S5 for all 1- to 16-cell stage). To test whether we could correctly predict division planes in *clasp* mutant embryos, we first focused on the resulting sister cells of 4- to 8-cell stage transition in the *clasp* mutant to reconstruct mother cell and then simulated CMA orientation on the resulting cell shape. We used WT settings for auxin-mediated face stability, assumed to be unaffected, but introduced increased edge-catastrophes to simulate loss of CLASP. Under these conditions, the observed CMA orientations indeed robustly predicted the observed division planes in the *clasp* mutant (Figure 5B, quantification in Figure 7D). In conclusion, the model assumptions that result in WT division pattern also yield, *mutatis mutandis*, the aberrant division pattern of *clasp* at the critical 4- and 8-cell stage transition.

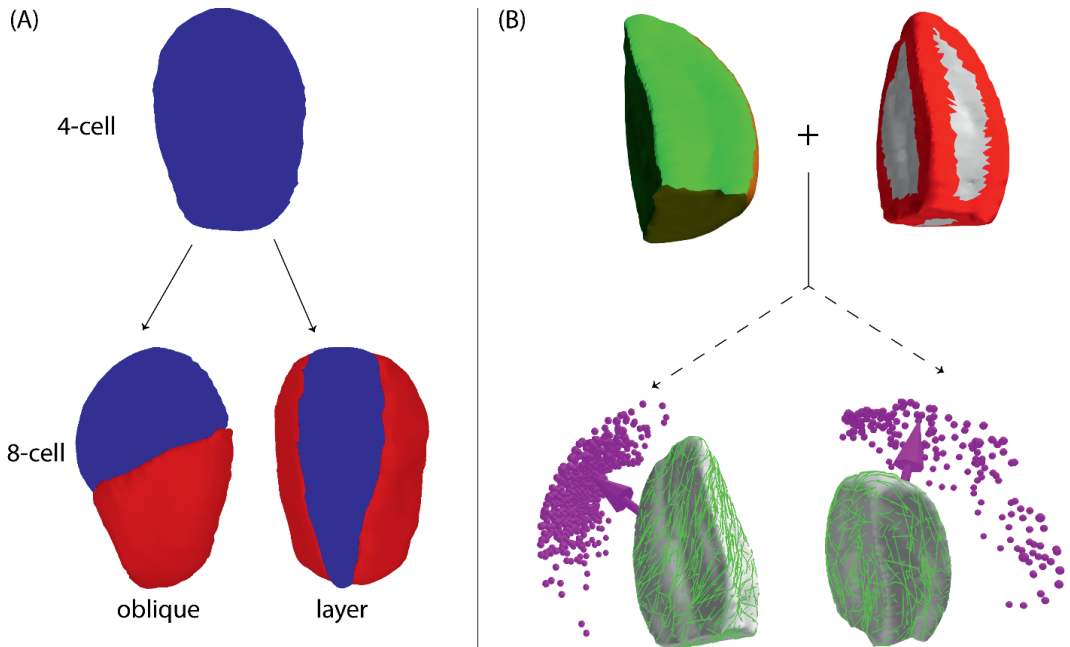
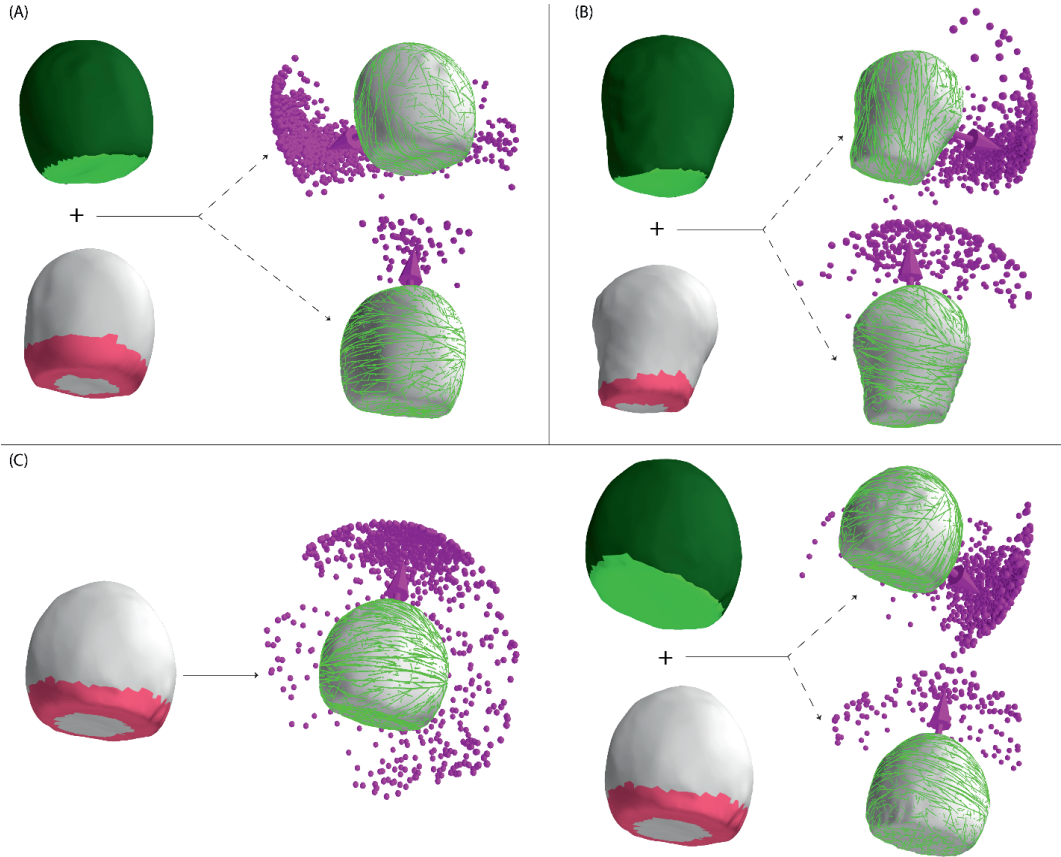


Figure 5. Simulating *clasp* mutant division patterns in Arabidopsis early embryonic development. **a** Representative *clasp* (*clasp 1* and *clasp 2*) division phenotypes during 4- to 8-cell stage transition (detailed quantification in Figure S5). **b** Simulated MT arrays on *clasp 2* cell template of 4-cell stage, reconstructed by merging the corresponding 8-cell daughter cell pair. Simulations were performed with edge-catastrophe and enhanced MT stabilization at developmentally new cell faces, yielding two clusters of MT array orientation correctly predicting the two *clasp* division phenotypes. Cell edges coloured red indicate presence of edge-catastrophes and different colour coding of the cell faces represents the degree of MT stabilization (see Figure S3).

## Tuning of face stability and edge-catastrophe allows prediction of all early embryo cell division patterns

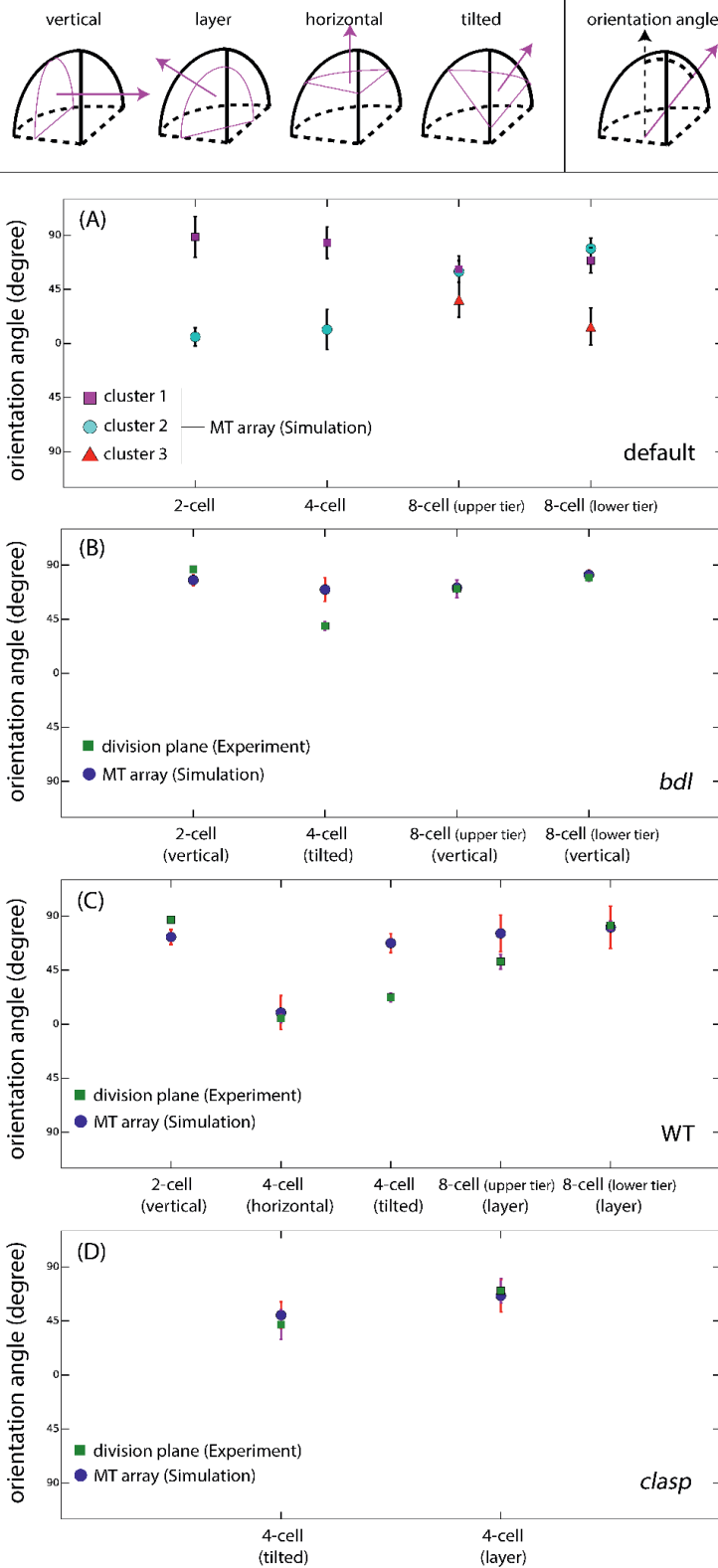
Our model so far predicted correct WT division patterns between the 2- to 16-cell stage when both auxin-mediated face stability and CLASP-mediated edge-catastrophe reduction



**Figure 6.** Fine-tuning of the 1- to 2-cell stage WT, *clasp* and *bdl* division patterns in Arabidopsis early embryos. **a** Simulations on WT cell template with reduced edge-catastrophe in MT dynamics and enhanced MT stabilization at developmentally new cell faces, showing a large cluster of a unique vertical MT array orientation ( $\approx 92\%$ ) that matched with the WT division plane orientation (top). A sparse cluster of horizontal MT array orientation ( $\approx 8\%$ ) was also observed (bottom). **b** Simulations on the *clasp* (*clasp 2*) cell template combining reduced edge-catastrophe and enhanced MT stabilization at developmentally new cell faces showed a majority cluster of vertical MT array orientations ( $\approx 75\%$ ) matching the *clasp* division plane orientation (top), and a sparse cluster of horizontal MT array orientations ( $\approx 25\%$ ), indicating stochasticity in division plane orientation under genetic perturbation (bottom). **c** Simulations on the *bdl* cell template with reduced edge-catastrophe resulted in a dominant horizontal orientation of MT array recapitulating the observed fraction ( $\approx 18\%$ ) of horizontal division plane orientation (left). Combination of reduced edge-catastrophe and enhanced MT stabilization at developmentally new cell faces produced a large cluster of MT array orientation ( $\approx 80\%$ ) which reflects the experimentally observed major vertical and unique division plane orientation (right, top) observed in *bdl* mutant. The remaining horizontal arrays ( $\approx 20\%$ ) indicate possible stochasticity in division plane orientation (right, bottom) under genetic perturbation, as actually observed and quantified<sup>26</sup>. Pink edges indicate reduced edge-catastrophes and colour coding of the cell faces represents the degree of MT stabilization (see Figure S3).

are implemented. This same implementation of the model also correctly predicted the vertical orientation of the cell division plane in the 1- to 2-cell transition, albeit not fixing its in-plane direction (Figure S6A for WT cell template and Figure S6B for *clasp* cell template). Notably, even in the presence of edge-catastrophe (simulated as the *clasp* mutant) the correct vertical orientation is maintained (Figure 6A for WT cell template and Figure 6B for *clasp* cell template). Moreover, with moderate edge-catastrophe the division axis was constrained to a single specific direction, reminiscent of the true WT situation. This led us to hypothesise that CLASP is less active at the 1-cell stage than at later stages. Strikingly, when we implemented this stage-specific reduced CLASP activity without the auxin-mediated face stability rule (i.e., simulating a *bdl* mutant under this new condition), we obtained a proportion of horizontal and vertical divisions that closely matched the 18% horizontal divisions observed in the original *bdl* mutant (Figure 6C). In conclusion, auxin-mediated face stability from the 1-cell stage onward and CLASP-mediated edge-catastrophe reduction from the 2-cell stage onward can robustly and consistently recapitulate cell division orientations between the 1- to 16-cell stage in WT and *bdl* embryos, and between 1- to 8-cell stage in *clasp* embryos.

It is important to note that our quantification of the observed variation in the simulated CMA orientation (Figure 7) confirms the experimentally observed variation in division plane orientation in other cell types where PPB formation had been disturbed using *trm678* mutant, i.e. in epidermis, cortex and endodermis (Schaefer et al., 2017). Finally, we noted that under these rules only a fraction of division predictions for the 8- to 16-cell transition of *clasp* mutants was correct. To assess this discrepancy, we looked at the growth rates of cells at this stage, inferred from the calculated cell volume increases between cell stages (Figure S6D and Figure S6E). We observed that the correctness of prediction negatively correlated with the growth rates of cell volume. Indeed, when, instead of using a re-created mother cell of the 4-cell stage embryo (by merging the corresponding daughter cell pair from 8-cell stage), we simulated MT dynamics on a true single cell of the 4-cell stage, the prediction of cell division plane orientation correlated better with the experimentally observed ones (Figure S6C). This result indicated that, in *clasp* mutants, cell growth becomes relevant. In this case, mechanisms that influence MT stability depending on direction of growth induced mechanical stress may become dominant factors in CMA orientation (Hamant & Traas, 2010). Hence, tissue growth rates define an upper bound below which the rules here described can successfully explain formative cell divisions.



## Discussion

Here we used a modelling framework on actual cell surface shapes and combined this with high-resolution imaging of both cell-outline and MTs to derive a plausible model that explains the orientation of formative cell divisions in the Arabidopsis embryo from first principles on a molecular basis. When comparing predictions of division plane orientation based on basic MT-MT interaction rules and edge catastrophe with the predictions of the heuristic geometrical rules, it is striking that the minimal set of rules that couple intrinsic MT dynamics to the local and global geometry of the cell are by themselves already sufficient to correctly predict divisions in auxin insensitive *bdl* cells (Figure S7). The difference between *bdl* and WT division patterns indicates that, in addition, auxin-mediated regulation is crucial to establish the WT division pattern in Arabidopsis embryos. In order to explain the orientation of cell division up to the 16-cell stage of WT, we parsimoniously implemented, besides the basic MT dynamics, two other factors influencing MT stability that are under biological control.

The first biological control mechanism is an auxin-dependent face stability rule, derived from our observed MT patterns on *bdl* mutant cells. The assumption that transient cortical MT stability is most strongly associated with new cell walls is not without precedence. Several observations indicate that peripheral marks instrumental for cell division orientation can transiently accumulate

at specific cell faces in different organisms. In plants, Arabidopsis BASL marks are positioned away from the previous division wall (Robinson et al., 2011). In yeast, Bud8p and Bud9p proteins mark opposite division sites during bipolar budding (Harkins et al., 2001). In order to assess to what extent this hypothesis leads to a robust mechanism, we have performed an extensive, and computationally intensive, parameter analysis (see Figure S3B). This revealed that the transient stability mechanism yields consistently correct predictions over an appreciable range of parameter values.

The second biological control mechanism is a CLASP dependent edge-catastrophe reduction rule, based on published analyses of MTs at cell edges (Ambrose et al., 2011) and our own analysis of division planes in *clasp* mutant embryos. CLASP-like proteins in mammalian cells provide resistance to MTs under traction (Logarinho et al., 2012) and it is therefore conceivable that plant CLASPs in similar ways stabilize MT under torsion. Our parameter analysis (Figure S3A) indicates that, in contrast to the auxin-based mechanism, the activity of CLASP must be tightly regulated in order to achieve the correct divisions.

It will therefore be interesting to investigate whether mutations in transcription factors that specifically change early embryo division patterns, such as BDL (Yoshida et al., 2014) and WOX2 (Breuninger et al., 2008), can be explained by their transcriptional control of MT regulators.

Our results clearly only provide evidence for sufficiency of the proposed rules, and, hence, at most arguments for their plausibility. However, the fact that we were able to obtain these results, without invoking other likely mechanisms such as the role of the direction of maximal wall stress in orienting the CMA at the very least raises an interesting question. This holds in particular in view of the *bdl* mutant results, which required the minimal number of additional assumptions over and above the bare MT collision mechanism to recapitulate all successive division plane orientation decisions up to the 16-cell stage. If stress-dependent CMA orientation is indeed the dominant mechanism at this stage, why does the autonomous mechanism proposed here, which only requires the basic features of entrainment of MTs to the cell membrane and their usual (de)polymerization behaviour to be operative, lead to essentially the same results? In our view, our findings suggest that the two mechanisms may well turn out to be synergistic. It is therefore interesting to see whether the stress related mechanism can help in explaining the apparently systematic disagreement between predicted division plane angle and the experimentally observed one for the specific case of the 4-cell stage tilted divisions (see Figure 7).

In rapidly growing tissues, the sensitivity of katanin-mediated MT severing to tensile stress has been proposed as an additional array orienting mechanism (Hamant et al., 2008; Uyttewaald et al., 2012). This may explain the preferred orientation of cell division planes transverse to the main direction of growth in meristems, and potentially in later-stage embryos, where most divisions are also oriented orthogonal to the main growth axes. It is a striking observation that our minimal model appears to be no longer sufficient exactly for the fastest growing cells, i.e. the 8- to 16-cell stage in the *clasp* mutant. Although explicit molecular hypotheses explaining katanin-mediated effects on array orientation have yet to be formulated, the local modulation of severing activity can be readily implemented within our framework (Deinum et al., 2017).

Finally, it should be noted that our model is cell autonomous and does not incorporate any explicit feedback control. It essentially implements an open-ended sequence; mother cell shape dictates CMA orientation, which determines division plane orientation, which determines daughter cell shape. However, there is evidence that MT ordering contributes,

through its relation with the cell wall synthesis machinery, to the anisotropy of plant cell growth (Paradez et al., 2006; Uyttewaal et al., 2012). This suggests that a coupling of shape-dependent and tension-dependent MT organization to cell growth may create both intracellular and multicellular pathways for feedback, with changes in cell shape feeding back on the MT localization process.

In summary, our work provides a theoretical framework for fundamental understanding of formative cell divisions in plants, which are not restricted to embryogenesis but continuously occur in stem cell niches where tissue growth is reduced compared to surrounding zones (e.g. (Grandjean et al., 2004)). Live-cell imaging methods for Arabidopsis embryogenesis have recently been established (Gooh et al., 2015; Kurihara et al., 2017). Our model makes clear predictions on the key effects of auxin signalling and CLASP protein in specific cell faces and edges of the embryo and by extension other slow growing cells, such as those in stem cells niches. It will now be a challenge to further develop high-resolution live imaging of the CMA in these cells in order to test the proposed molecular control mechanisms.

We envision that a combination of the basic rules of CMA organisation presented here, supplemented by moderating rules involving the mechanics of wall tension and growth will ultimately provide a complete picture of cell division control in plants, and potentially the means to modify these divisions for agricultural purposes.

## Material and methods

### *Plant growth conditions*

Arabidopsis seeds were surface-sterilized and dried seeds were subsequently sown on half-strength Murashige and Skoog (MS) medium. After a 48 hour cold treatment at 4 °C without light, seedlings were grown at 22 °C in standard long-day (16:8 h light:dark) growth conditions. After two weeks of growth, seedlings were transferred to soil and further grown under the same conditions. Siliques were harvested from mature plants for imaging. pRPS5A>>*bdl* embryos were generated by pollination of homozygous RPS5A-GAL4 pistils (Weijers et al., 2003) with homozygous UAS-*bdl* (Weijers et al., 2006) pollen. For *bdl* mutant MT-imaging, pWOX2::TUA6-GFP was transformed into the RPS5A-GAL4 line. Homozygous RPS5A-GAL4 X pWOX2::TUA6-GFP pistils were subsequently pollinated using either Col-0 or UAS-*bdl*.

### Staining and imaging conditions

3D stacks: Arabidopsis ovules of Col-0, *clasp 1* (SALK\_120061) and *clasp 2* (SALK\_83034) have been isolated from siliques in SCRI Renaissance 2200 solution on an objective slide (Ambrose et al., 2007; Musielak et al., 2015). The embryos have been popped out of the ovules by applying gentle pressure on the coverslip. 3D stacks of the embryos have been made using of Zeiss LSM710 with the 405nm laser. For generating 3D stacks of *bdl* embryos, we adapted the procedure described in Yoshida *et al.* (Yoshida et al., 2014).

cortical MT: Arabidopsis siliques were cut open using a fine needle and ovules were mounted and stained in a MT imaging solution (10% glucose, 10  $\mu$ M Taxol, 0.1 M Pipes, pH 6.8, 1 mM EGTA, 1 mM  $\text{MgSO}_4$ ) containing 0.1% Renaissance (SR2200; Renaissance Chemicals; stock solution of the supplier was considered as 100%) cell wall counter-stain. Embryos were separated from ovules by gently pressing the coverslip. Images were taken within 30 minutes after release from the ovule. Sequential images were taken with 0.2  $\mu$ m intervals to create high-resolution Z-stacks. Images were obtained using the Leica SP5 confocal laser scanning microscope equipped with photon-counting HyD detector and x63 water immersion objective. GFP and SR2200 signals were detected at 488nm excitation/500-530nm emission or 405nm excitation/520-560nm emission wavelength, respectively.

Measurement of cytosolic mGFP: TUA6 signal in individual cells: The optical section containing the great circle of the nucleus was visually defined, a maximum projection containing 5 optical sections, 2 above, 2 beneath the optical section with the great circle, and the optical section containing the great circle, was then generated from the raw image stack. A 0.2 to 0.4  $\mu\text{m}^2$  region of interest (ROI) in the cell of interest was given at where no distinguishable microtubule structure was found. The average mGFP fluorescence signal intensity in this ROI was documented and defined as the cytosolic mGFP: TUA6 signal of the cell of interest. The difference in average cytosolic mGFP: TUA6 signals were tested via two-tailed student t-test with MS Excel™.

### Cell segmentation and cortical MT projection

Cell segmentation and cortical MT projection are performed in MorphoGraphX (version 2.0) (de Reuille et al., 2015). SR2200 stacks (tiff) were Gaussian blurred using Sigma 0.3  $\mu$ m. Blurred stacks were segmented using ITK watershed auto seeded segmentation with

levels ranging from 500-1500. From segmented cells, meshes were created using Marching cubes 3D with Cube size in the range 0.5-1.0. cortical MT (pWOX2::TUA6-GFP) stacks (tiff) were loaded and overlaid with created corresponding cell meshes. Absolute cortical MT signal with a distance of 0-1  $\mu\text{m}$  relative to the cell surface was projected on the cell mesh.

*Number of embryonic cells used in the simulations*

Phenotype	1-cell stage	2-cell stage	4-cell stage	8-cell stage
WT	4	4	4	4
<i>bdl</i>	4	4	4	4
<i>clasp 1</i>		2	2	
<i>clasp 2</i>	1	4	4	

**Acknowledgements**

We thank Thomas Laux and Martin Hülskamp for critical reading of an earlier version of the manuscript. The work of BC was supported by a Wageningen University IPOP grant. The work of BMM is part of the research programme of the Netherlands Organisation for Scientific Research (NWO).

**Author contributions**

BC developed the computational framework and performed the simulations. BS and BM developed the questions and conceptual approach underlying the study. VW produced 3D stacks for WT and *clasp*, and analysed cell division phenotypes. TdZ and CYL produced 3D stacks of *bdl* embryos and performed MT imaging in WT and *bdl*, and analysed the relation between MT, PPB and cell division orientation. BC, VW, TdZ, CYL, DW, BM and BS wrote the paper.

## References

- Ambrose, C., Allard, J. F., Cytrynbaum, E. N., & Wasteneys, G. O. (2011). A CLASP-modulated cell edge barrier mechanism drives cell-wide cortical microtubule organization in *Arabidopsis*. *Nature Communications*. <https://doi.org/10.1038/ncomms1444>
- Ambrose, J. C., Shoji, T., Kotzer, A. M., Pighin, J. A., & Wasteneys, G. O. (2007). The *Arabidopsis* CLASP gene encodes a microtubule-associated protein involved in cell expansion and division. *Plant Cell*. <https://doi.org/10.1105/tpc.107.053777>
- Barbier de Reuille, P., Routier-Kierzkowska, A.-L., Kierzkowski, D., Bassel, G. W., Schüpbach, T., Tauriello, G., ... Smith, R. S. (2015). MorphoGraphX: A platform for quantifying morphogenesis in 4D. *ELife*, 4, 05864. <https://doi.org/10.7554/eLife.05864>
- Besson, S., & Dumais, J. (2011). Universal rule for the symmetric division of plant cells. *Proceedings of the National Academy of Sciences*. <https://doi.org/10.1073/pnas.1011866108>
- Breuninger, H., Rikirsch, E., Hermann, M., Ueda, M., & Laux, T. (2008). Differential Expression of WOX Genes Mediates Apical-Basal Axis Formation in the *Arabidopsis* Embryo. *Developmental Cell*. <https://doi.org/10.1016/j.devcel.2008.03.008>
- Burk, D. H., Liu, B., Zhong, R., Morrison, W. H., Ye, Z.-H., Zhang, Q., ... Mulder, B. M. (2013). How selective severing by katanin promotes order in the plant cortical microtubule array. *Proceedings of the National Academy of Sciences*, 114(21), 56002. <https://doi.org/10.1105/tpc.13.4.807>
- Campilho, A., Garcia, B., Toorn, H., Wijk, H., & Scheres, B. (2006). Time-lapse analysis of stem cell divisions in the *Arabidopsis thaliana* root meristem. *The Plant Journal*, Vol. 48, pp. 619–627.
- Chakraborty, B., Blilou, I., Scheres, B., & Mulder, B. M. (2018). A computational framework for cortical microtubule dynamics in realistically shaped plant cells. *PLoS Computational Biology*. <https://doi.org/10.1371/journal.pcbi.1005959>
- Chan, J., Sambade, A., Calder, G., & Lloyd, C. (2009). *Arabidopsis* Cortical Microtubules Are Initiated along, as Well as Branching from, Existing Microtubules. *Plant Cell*, 12(8), 2298–2306.
- Cleary, A. L., Gunning, B. E. S., Wasteneys, G. O., & Hepler, P. K. (1992). Microtubule

and F-actin dynamics at the division site in living *Tradescantia* stamen hair cells. *Journal of Cell Science*, 103(4), 977 LP – 988.

de Reuille, P. B., Routier-Kierzkowska, A. L., Kierzkowski, D., Bassel, G. W., Schüpbach, T., Tauriello, G., ... Smith, R. S. (2015). MorphoGraphX: A platform for quantifying morphogenesis in 4D. *ELife*. <https://doi.org/10.7554/eLife.05864>

Deinum, E. E., & Mulder, B. M. (2013). Modelling the role of microtubules in plant cell morphology. *Curr. Opin. Plant Biol.*, Vol. 16, pp. 688–692. <https://doi.org/10.1016/j.pbi.2013.10.001>

Deinum, E. E., Tindemans, S. H., Lindeboom, J. J., & Mulder, B. M. (2017). How selective severing by katanin promotes order in the plant cortical microtubule array. *Proceedings of the National Academy of Sciences*, 114(27), 6942–6947. <https://doi.org/10.1073/pnas.1702650114>

3

Deinum, E. E., Tindemans, S. H., & Mulder, B. M. (2011). Taking directions: the role of microtubule-bound nucleation in the self-organization of the plant cortical array. *Phys Biol*, 8(5), 56002. <https://doi.org/10.1088/1478-3975/8/5/056002>

Dixit, R., & Cyr, R. (2004). Encounters between dynamic cortical microtubules promote ordering of the cortical array through angle-dependent modifications of microtubule behavior. *Plant Cell*. <https://doi.org/10.1105/tpc.104.026930>

Dupuy, L., Mackenzie, J., & Haseloff, J. (2010). Coordination of plant cell division and expansion in a simple morphogenetic system. *Proceedings of the National Academy of Sciences*, 107(6), 2711 LP – 2716.

Ehrhardt, D. W., & Shaw, S. L. (2006). Microtubule Dynamics and Organization in the Plant Cortical Array. *Annual Review of Plant Biology*, 57(1), 859–875. <https://doi.org/10.1146/annurev.arplant.57.032905.105329>

Errera, L. (1886). Sur une condition fondamentale d'équilibre des cellules vivantes. *C R Hebd Seances Acad Sci*, 103, 822–824.

Gomez, J. M., Chumakova, L., Bulgakova, N. A., & Brown, N. H. (2016). Microtubule organization is determined by the shape of epithelial cells. *Nat. Com.*, Vol. 7, p. 13172.

Gooh, K., Ueda, M., Aruga, K., Park, J., Arata, H., Higashiyama, T., & Kurihara, D.

(2015). Live-Cell Imaging and Optical Manipulation of Arabidopsis Early Embryogenesis. *Developmental Cell*. <https://doi.org/10.1016/j.devcel.2015.06.008>

Grandjean, O., Vernoux, T., & Laufs, P. (2004). In vivo analysis of cell division, cell growth, and differentiation at the shoot apical meristem in Arabidopsis. *The Plant Cell*, 16(1), 74–87. <https://doi.org/10.1105/tpc.017962>.(ANT)

Hamann, T., Mayer, U., & Jürgens, G. (1999). The auxin-insensitive bodenlos mutation affects primary root formation and apical-basal patterning in the Arabidopsis embryo. *Development*.

Hamant, O., Heisler, M. G., Jönsson, H., Krupinski, P., Uyttewaal, M., Bokov, P., ... Traas, J. (2008). Developmental patterning by mechanical signals in Arabidopsis. *Science*. <https://doi.org/10.1126/science.1165594>

Hamant, O., & Traas, J. (2010). The mechanics behind plant development. *New Phytologist*, 185(2), 369–385. <https://doi.org/10.1111/j.1469-8137.2009.03100.x>

Harkins, H. A., Pagé, N., Schenkman, L. R., De Virgilio, C., Shaw, S., Bussey, H., & Pringle, J. R. (2001). Bud8p and Bud9p, proteins that may mark the sites for bipolar budding in yeast. *Molecular Biology of the Cell*, 12(8), 2497–2518. <https://doi.org/10.1091/MBC.12.8.2497>

Hawkins, R. J., Tindemans, S. H., & Mulder, B. M. (2010). Model for the orientational ordering of the plant microtubule cortical array. *Physical Review E*, 82(1), 011911. <https://doi.org/10.1103/PhysRevE.82.011911>

Hejnowicz, Z. (2014). Trajectories of principal directions of growth, natural coordinate system in growing plant organ. *Acta Societatis Botanicorum Poloniae*, 53(1), 29–42. <https://doi.org/10.5586/asbp.1984.004>

Hofmeister, W. (1868). Allgemeine morphologie der Gewächse. Engelmann.

Jürgens, G., Mayer, U., Torres Ruiz, R. A., Berleth, T., & Miséra, S. (1991). Genetic analysis of pattern formation in the Arabidopsis embryo. *Development*, 113, 27–38.

Kurihara, D., Kimata, Y., Higashiyama, T., & Ueda, M. (2017). In vitro ovule cultivation for live-cell imaging of zygote polarization and embryo patterning in Arabidopsis thaliana. *Journal of Visualized Experiments*. <https://doi.org/10.3791/55975>

Liao, C. Y., & Weijers, D. (2018). A toolkit for studying cellular reorganization during early

embryogenesis in *Arabidopsis thaliana*. *Plant Journal*. <https://doi.org/10.1111/tpj.13841>

Lloyd, C., & Chan, J. (2004). Microtubules and the shape of plants to come. *Nature Reviews. Molecular Cell Biology*, 5(1), 13–22. <https://doi.org/10.1038/nrm1277>

Logarinho, E., Maffini, S., Barisic, M., Marques, A., Toso, A., Meraldi, P., & Maiato, H. (2012). CLASPs prevent irreversible multipolarity by ensuring spindle-pole resistance to traction forces during chromosome alignment. *Nature Cell Biology*, 14(3), 295–303. <https://doi.org/10.1038/ncb2423>

Louveaux, M., Rochette, S., Beauzamy, L., Boudaoud, A., & Hamant, O. (2016). The impact of mechanical compression on cortical microtubules in *Arabidopsis*: a quantitative pipeline. *The Plant Journal*. <https://doi.org/10.1111/tpj.13290>

Mansfield, S. G., & Briarty, L. G. (1991). Early embryogenesis in *Arabidopsis thaliana*. II. The developing embryo. *Canadian Journal of Botany*. <https://doi.org/10.1139/b91-063>

Mineyuki, Y. (1999). The preprophase band of microtubules: Its function as a cytokinetic apparatus in higher plants. *International Review of Cytology*.

Mirabet, V., Krupinski, P., Hamant, O., Meyerowitz, E. M., Jönsson, H., & Boudaoud, A. (2018). The self-organization of plant microtubules inside the cell volume yields their cortical localization, stable alignment, and sensitivity to external cues. *PLOS Computational Biology*, 14(2), e1006011. <https://doi.org/10.1371/journal.pcbi.1006011>

Mitchison, T., & Kirschner, M. (1984). Dynamic instability of microtubule growth. *Nature*, 312(5991), 237–242. <https://doi.org/10.1038/312237a0>

Müller, S., Wright, A. J., & Smith, L. G. (2009). Division plane control in plants: new players in the band. *Trends Cell Biol*, 19(4), 180–188. <https://doi.org/10.1016/j.tcb.2009.02.002>

Musielak, T. J., Schenkel, L., Kolb, M., Henschen, A., & Bayer, M. (2015). A simple and versatile cell wall staining protocol to study plant reproduction. *Plant Reproduction*, 28(3–4), 161–169. <https://doi.org/10.1007/s00497-015-0267-1>

Oud, J. L., & Nanninga, N. (1992). Cell shape, chromosome orientation and the position of the plane of division in *Vicia faba* root cortex cells. *Journal of Cell Science*.

Paradez, A., Wright, A., & Ehrhardt, D. W. (2006). Microtubule cortical array organization and plant cell morphogenesis. *Current Opinion in Plant Biology*. <https://doi.org/10.1016/j>

pbi.2006.09.005

Paredez, A. R. (2006). Visualization of Cellulose Synthase Demonstrates Functional Association with Microtubules. *Science*, 312(5779), 1491–1495. <https://doi.org/10.1126/science.1126551>

Robinson, S., De Reuille, P. B., Chan, J., Bergmann, D., Prusinkiewicz, P., & Coen, E. (2011). Generation of spatial patterns through cell polarity switching. *Science*. <https://doi.org/10.1126/science.1202185>

Sachs, J. (1878). Über die Anordnung der Zellen in jüngsten Pflanzentheilen. *Arbeiten Des Botanischen Instituts in Würzburg*, 2, 46–104.

Schaefer, E., Belcram, K., Uyttewaal, M., Duroc, Y., Goussot, M., Legland, D., ... Bouchez, D. (2017). The preprophase band of microtubules controls the robustness of division orientation in plants. *Science*. <https://doi.org/10.1126/science.aal3016>

Scheres, B., Wolkenfelt, H., Willemsen, V., Terlouw, M., Lawson, E., Dean, C., & Weisbeek, P. (1994). Embryonic origin of the Arabidopsis primary root and root meristem initials. *Development*.

Smith, R. S., Guyomarc'h, S., Mandel, T., Reinhardt, D., Kuhlemeier, C., & Prusinkiewicz, P. (2006). A plausible model of phyllotaxis. *Proceedings of the National Academy of Sciences*, 103(5), 1301–1306. <https://doi.org/10.1073/pnas.0510457103>

Tindemans, S. H., Deinum, E. E., Lindeboom, J. J., & Mulder, B. M. (2014). Efficient event-driven simulations shed new light on microtubule organization in the plant cortical array. *Frontiers in Physics*. <https://doi.org/10.3389/fphy.2014.00019>

Tindemans, S. H., Hawkins, R. J., & Mulder, B. M. (2010). Survival of the aligned: Ordering of the plant cortical microtubule array. *Physical Review Letters*. <https://doi.org/10.1103/PhysRevLett.104.058103>

Uyttewaal, M., Burian, A., Alim, K., Landrein, B. B., Borowska-WykrÄt, D., Dedieu, A., ... Hamant, O. (2012). Mechanical stress acts via katanin to amplify differences in growth rate between adjacent cells in Arabidopsis. *Cell*, 149(2), 439–451. <https://doi.org/10.1016/j.cell.2012.02.048>

Wasteneys, G. O. (2002). Microtubule organization in the green kingdom: chaos or self-

order? *J. Cell Sci.*, 115(Pt 7), 1345–1354.

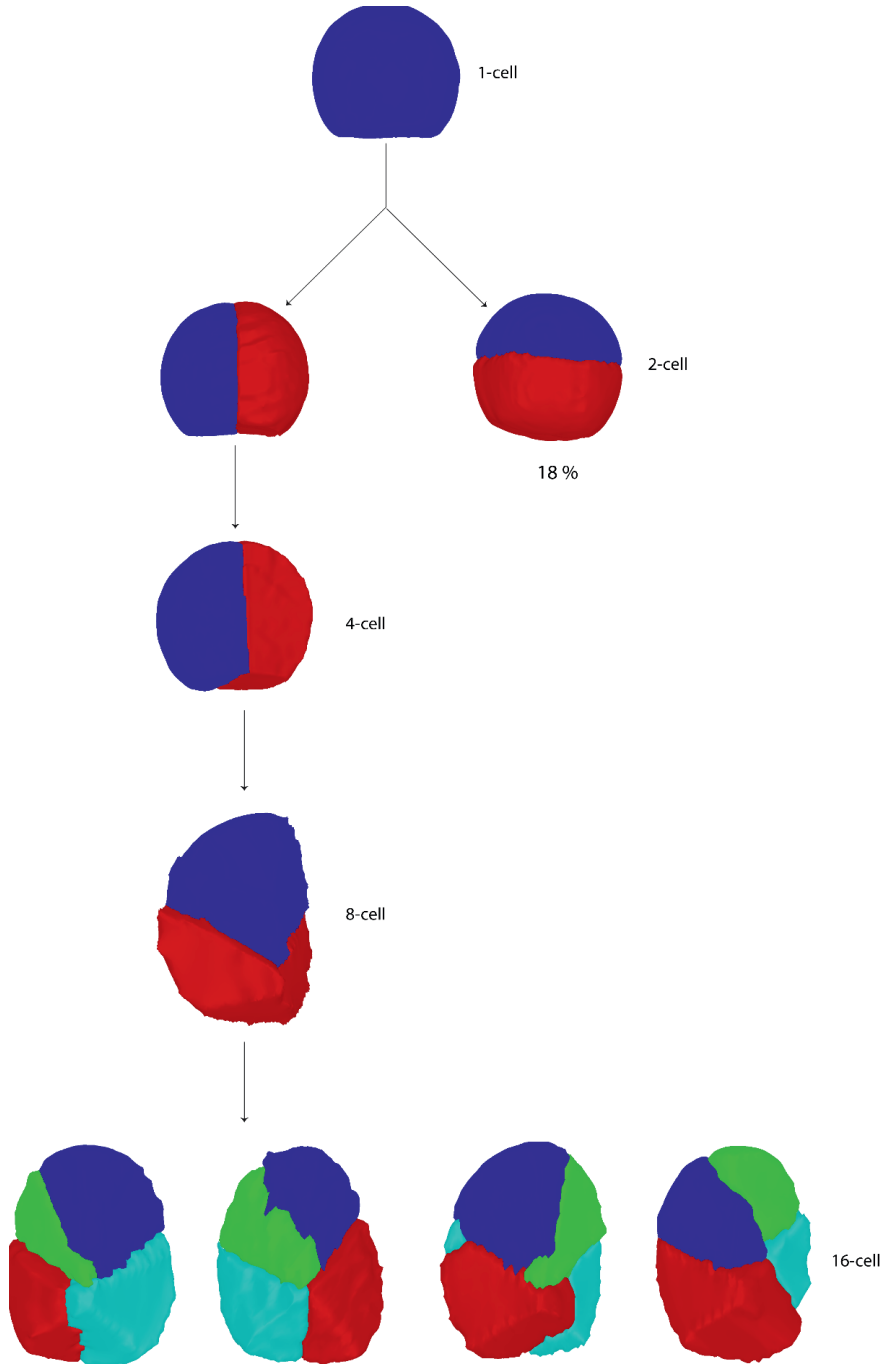
Weijers, D., Schlereth, A., Ehrismann, J. S., Schwank, G., Kientz, M., & Jürgens, G. (2006). Auxin triggers transient local signaling for cell specification in Arabidopsis embryogenesis. *Developmental Cell*. <https://doi.org/10.1016/j.devcel.2005.12.001>

Weijers, D., Van Hamburg, J. P., Van Rijn, E., Hooykaas, P. J. J., & Offringa, R. (2003). Diphtheria Toxin-Mediated Cell Ablation Reveals Interregional Communication during Arabidopsis Seed Development. *Plant Physiology*. <https://doi.org/10.1104/pp.103.030692>

Yoshida, S., Barbier de Reuille, P., Lane, B., Bassel, G. W., Prusinkiewicz, P., Smith, R. S., & Weijers, D. (2014). Genetic control of plant development by overriding a geometric division rule. *Developmental Cell*, 29(1), 75–87. <https://doi.org/10.1016/j.devcel.2014.02.002>

Zhang, Q., Fishel, E., Bertroche, T., & Dixit, R. (2013). Microtubule severing at crossover sites by katanin generates ordered cortical microtubule arrays in Arabidopsis. *Current Biology : CB*, 23(21), 2191–2195. <https://doi.org/10.1016/j.cub.2013.09.018>

## Supplementary materials



**Figure S1.** Arabidopsis early embryonic *bdl* division phenotype. A notable oblique division during 4- to 8-cell stage transition and aberrant divisions during 8- to 16 cell-stage transition. In analysis, 5 different embryos were used and only the correctly segmented cells were considered. We clearly observed these phenotypes, except the 18% horizontal divisions during 1-2-cell stage transition. However, such horizontal division phenotype has been reported in heterozygous *BDL/bdl* background (Hamann et al., 1999).

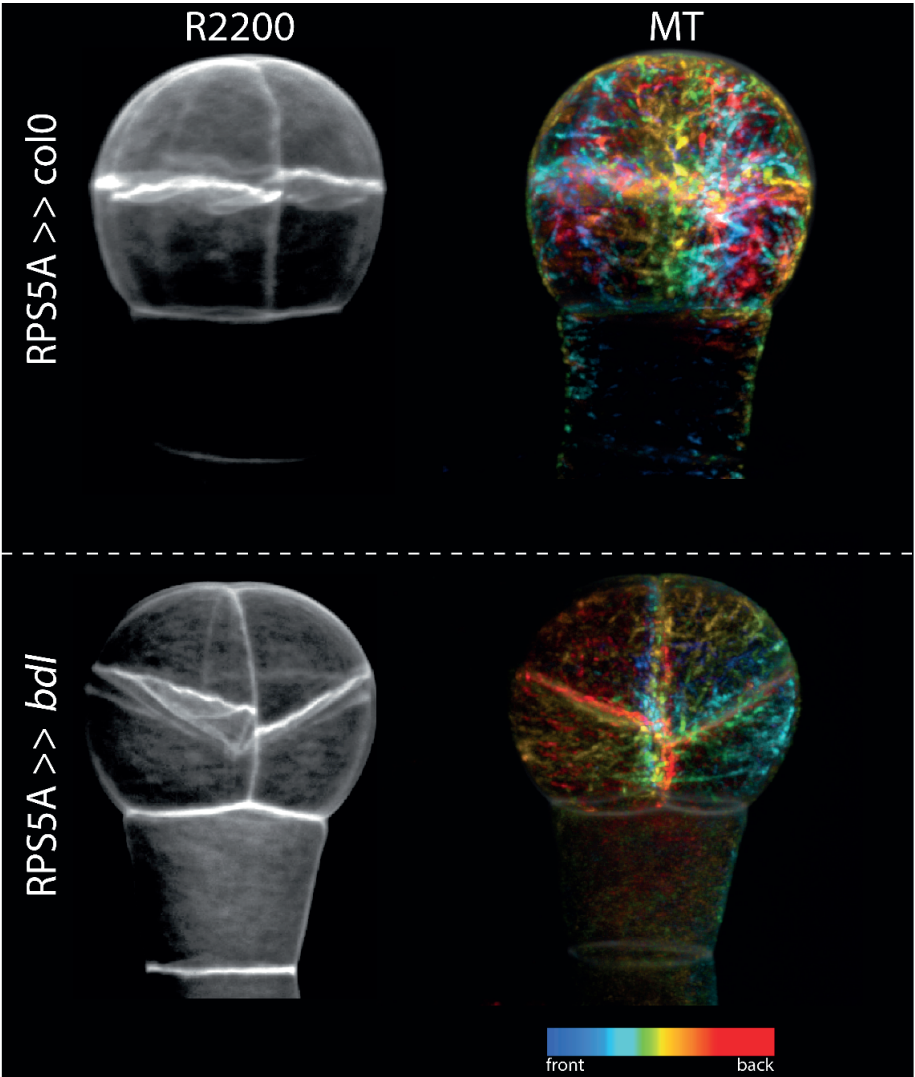
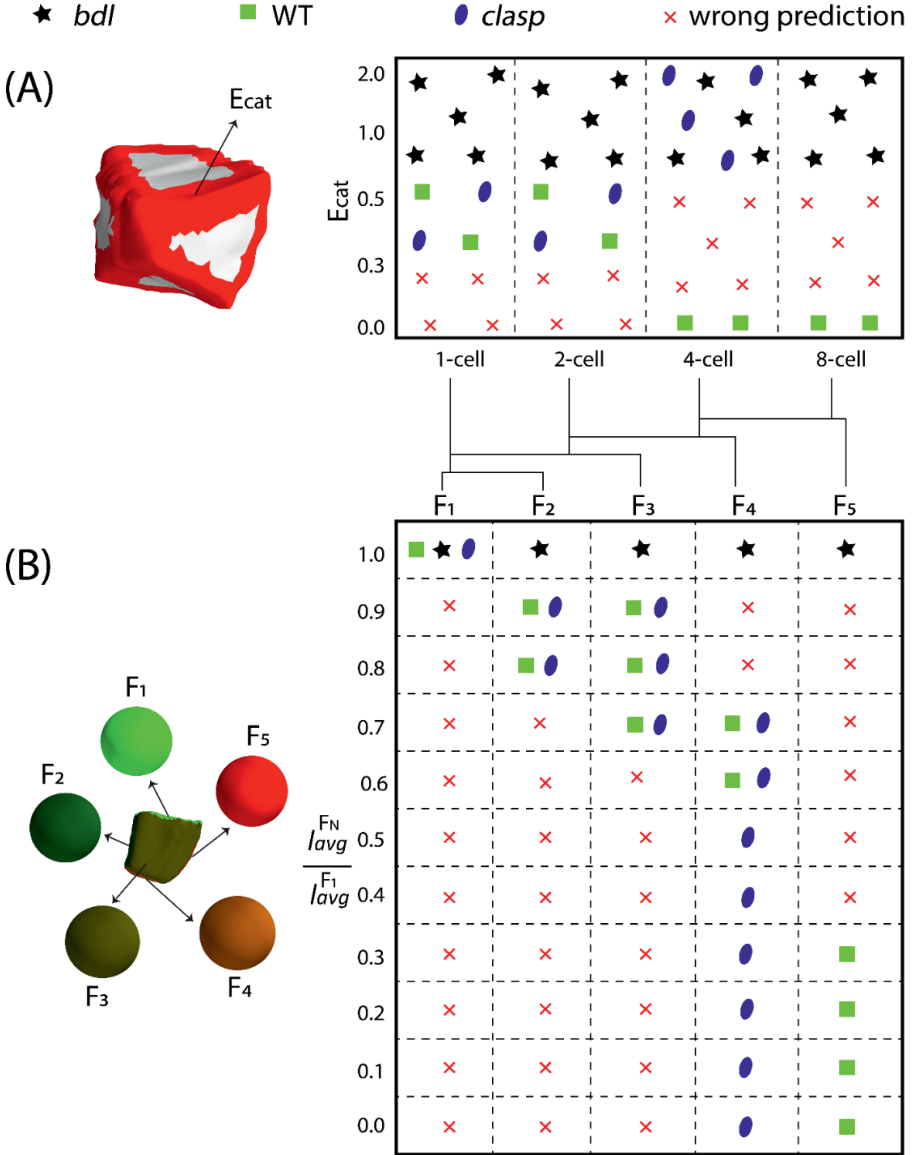


Table: Cytosolic mGFP: TUA6 signal in each cell of 8-cell embryos

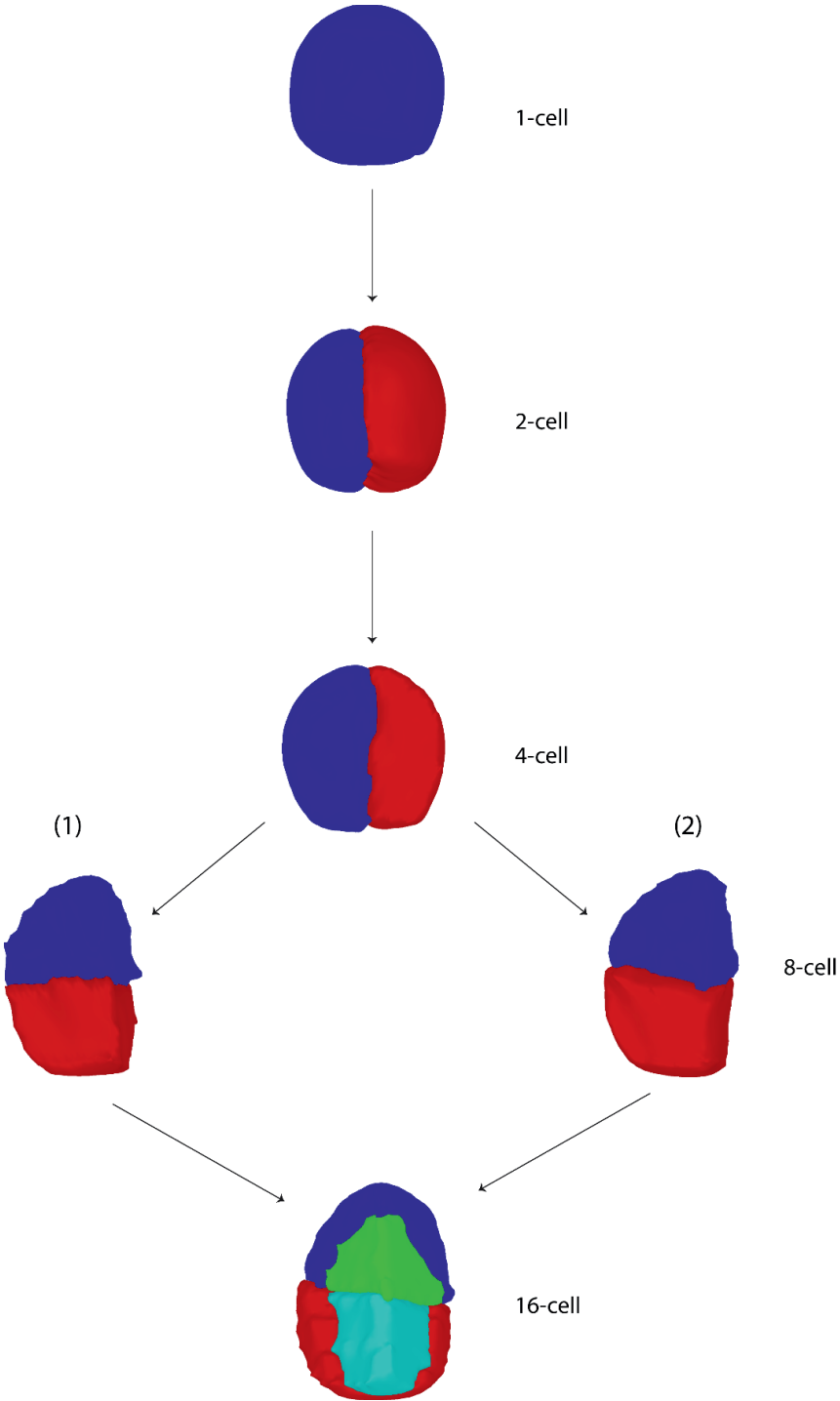
Phenotype	Signal intensity
WT	10.82 ± 4.42 (n = 148)
pRPS5A >> <i>bdl</i>	17.08 ± 6.70 (n = 132)
p-value*	1.57E-17

\* Two-tail student t-test

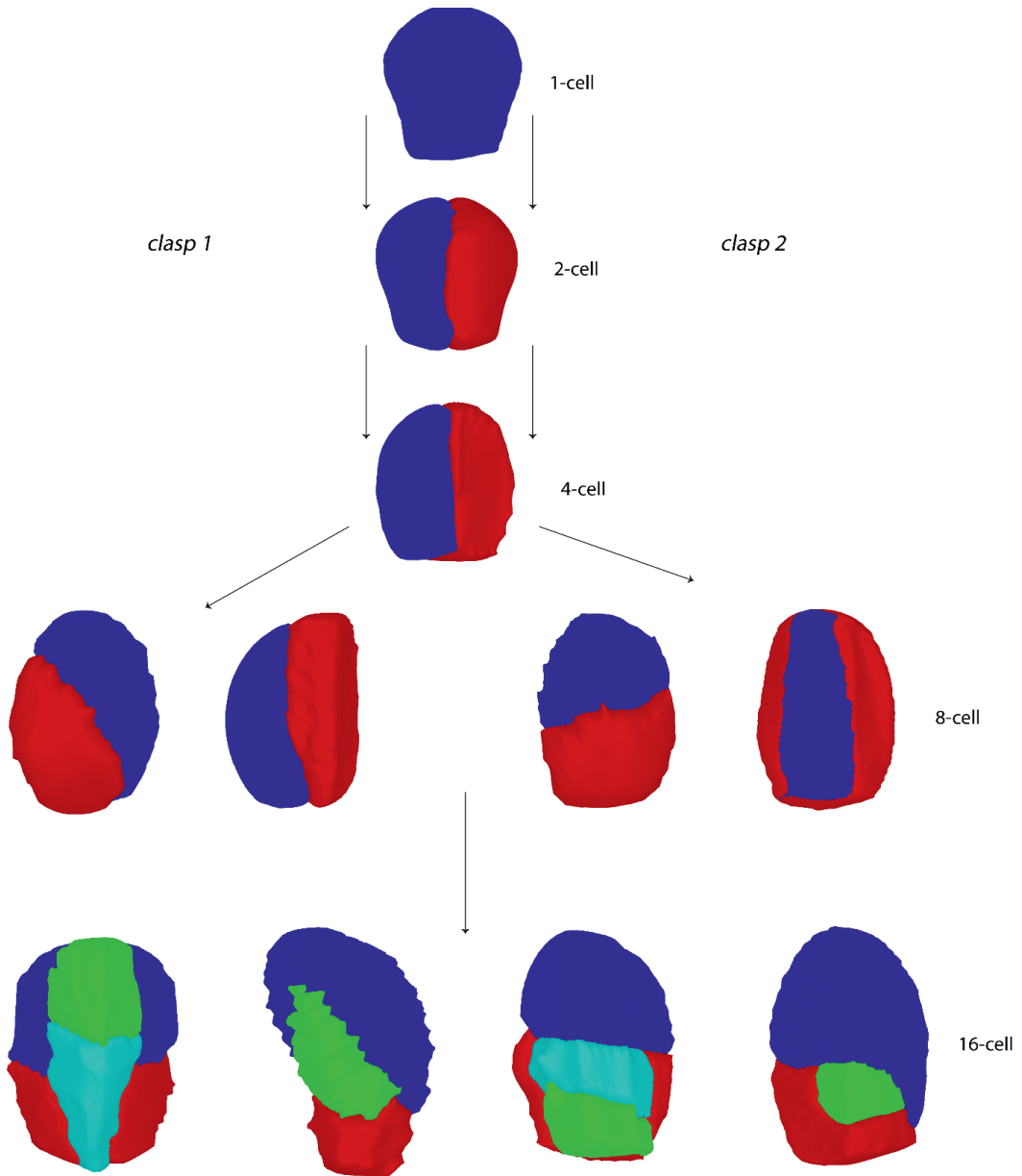
**FigureS2.** Maximum projection of depth-coded stacks of MTs visualized using a pWOX2::TUA6-GFP reporter line in RPS5A>>Col-0 (WT) and RPS5A>>bdl and quantification of the cytosolic (non-polymerized) TUA6:GFP fraction.



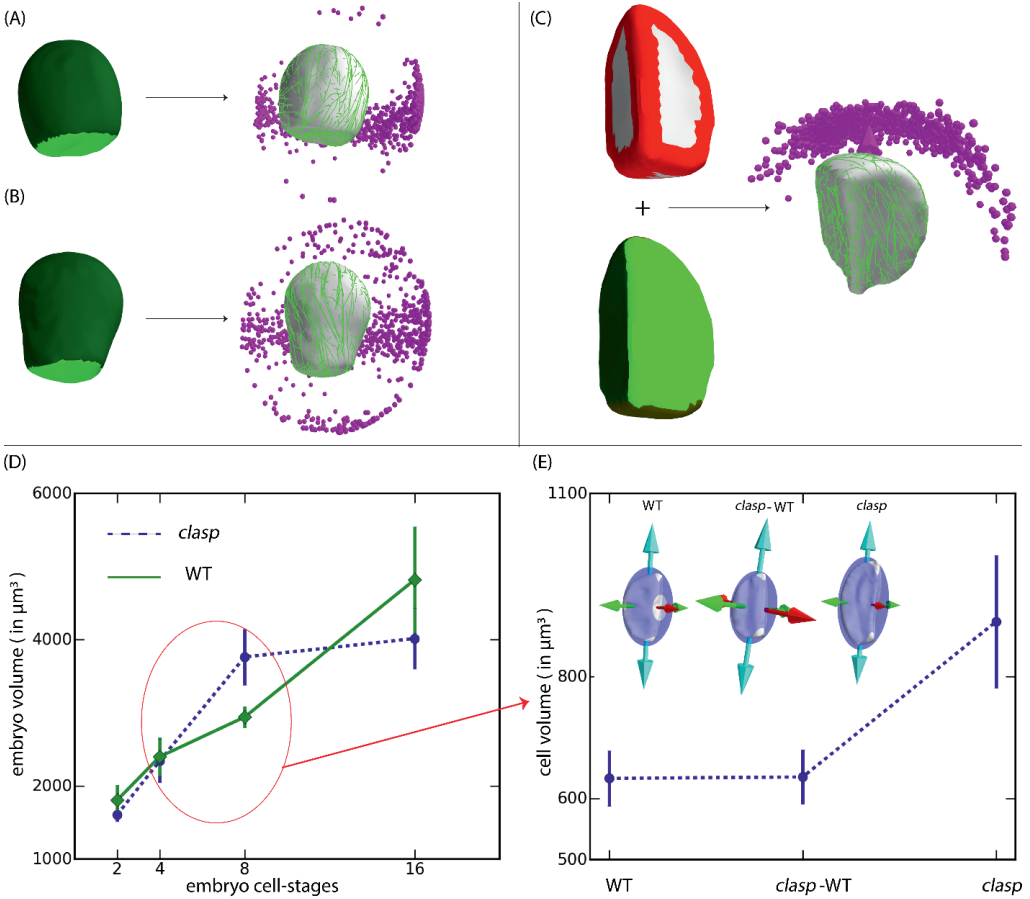
**Figure S3.** Simulation parameterization in terms of average MT length ( $l_{avg}^F$ ) at different cell faces (F) and edge-catastrophe multiplier (Ecat) at the cell edges. **a** Schematic representation of cell-edge tagging. Strength of edge-catastrophe at the cell-edges is represented by Ecat (Chakraborty et al., 2018), higher is the value more is the probability of encountering edge-catastrophe. Parameter space was explored for all possible values of Ecat ( $0.0 \leq E_{cat} \leq 2.0$ ). **b** Schematic diagram of cell shape (a lower tier cell of 8-cell stage Arabidopsis embryo). This cell has five developmentally different faces (N = 5), which we named as F1, F2, F3, F4 and F5 in the order of increased developmental age. Corresponding to each face, we created a sphere of radius  $\approx 6 \mu m$  (average radius of an embryonic cell between 1- to 16-cell stages). Stability of MTs at any cell-face (FN) is measured as a ratio of steady state value of average MT length ( $l_{avg}^{FN}$ ) at this face with respect to that at the developmentally youngest face ( $l_{avg}^{F1}$ ). For any cell stage,  $l_{avg}^{F1}$  at F1 is calculated by using default shape simulation parameters (Chakraborty et al., 2018) and on other faces the MT dynamics catastrophe rate was tuned to vary  $l_{avg}^{FN}$  where  $N = 2, 3, 4, 5$ . Parameter space was explored systematically for all possible values of face-stability ( $l_{avg}^{FN}/l_{avg}^{F1}$ ) and for each cell-faces. We discovered a well-defined regime of parameters (edge-catastrophe and face stabilization) for a robust biological conclusion.



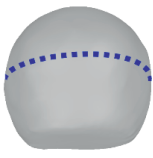
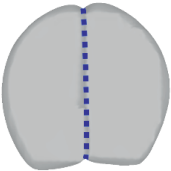

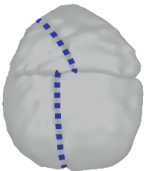
**Figure S4.** Arabidopsis early embryonic WT division phenotype. Notably, 4- to 8-cell stage transition reveals two types of division plane orientation phenotypes: (1) horizontal and (2) tilted horizontal division. Further quantification indicates that out of all observed divisions  $\approx 46\%$  (6/13) were horizontal and  $\approx 54\%$  (7/13) were tilted horizontal. Divisions during the 8- to 16-cell stage transition generate inner and outer tissue layers. In our analysis, 5 different embryos were used and only correctly segmented cells were considered.



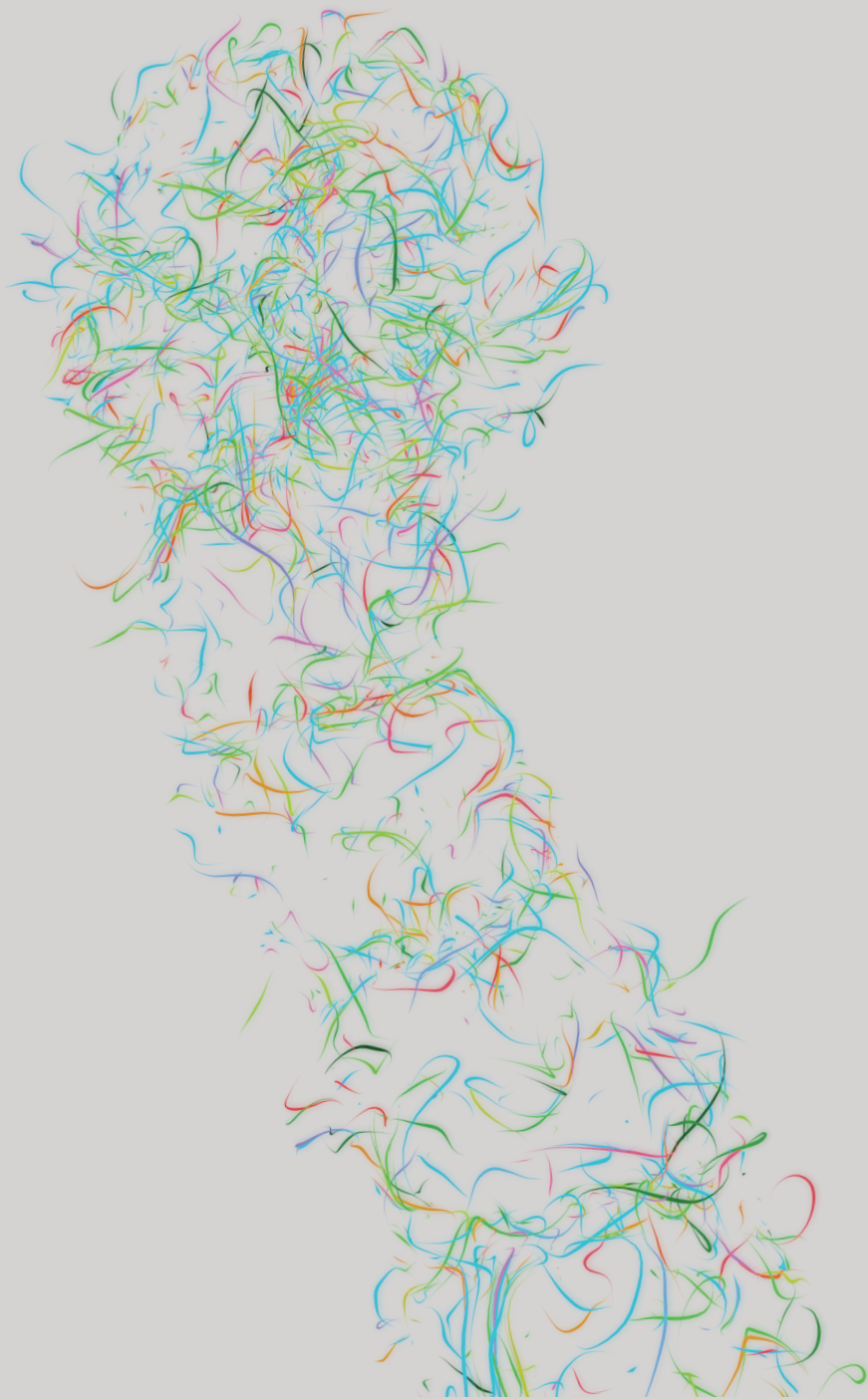
**Figure S5.** Arabidopsis early embryonic *clasp* division phenotype. Left branch corresponds to the *clasp 1* mutant allele and right to the *clasp 2* allele. Notably, 4- to 8-cell stage transition reveals division plane orientations which were skewed compared to WT. Out of all observed skewed divisions  $\approx 65\%$  (15/23) were oblique and  $\approx 45\%$  (8/23) generated the inward-outward layer. Further, 8- to 16-cell stage transition reveals aberrant division plane orientation.



**Figure S6.** Simulating MT dynamics on 1-cell stage WT, 1- and 4-cell stage *clasp2* cell templates of Arabidopsis early embryo, and correlating the *clasp* division prediction with cell growth. For both **a** WT and **b** *clasp2*, MT dynamics was simulated by considering enhanced MT stabilization at the developmentally new basal cell face (green) than the apical face (dark green); see Figure S3 and Table S1. Predicted division was vertical which matched with the experimental observation but with full symmetry in the horizontal plane, i.e. a ring-shaped cluster of MT array orientation on the horizontal plane. The symmetry in MT array orientation actually reflects the default symmetry of these cell shapes. **c** MT simulation on an ‘original’ *clasp* 4-cell instead ‘reconstructed mother’ from 8-cell stage cell template. In these simulations, strong indication of a vertical division that creates inward-outward layer was revealed compare to rather weak prediction of such layering on merged cell templates (see Figure 5). **d** Comparison of embryonic volumes between WT (solid line) and *clasp* (mixture of *clasp 1* and *clasp 2* embryos, dashed line), during 2- to 16-cell stage transitions. **e** Comparative studies for changes in cell volume and cell shape anisotropy at the critical 4- to 8-cell stage transition in WT and *clasp* cells. At a given embryonic cell-stage not all cells were affected by loss of CLASP (i.e. *clasp* mutation), therefore we categorized the embryonic cells present in a *clasp* embryo into two sets: cells that showed normal WT like division phenotype were categorized as *clasp*-WT cells and the cells that gave typical *clasp* phenotype, i.e. formation of premature inner-outer layer at the 4- to 8-cell stage transition were categorized as (normal) *clasp* cells. Cell volume was calculated by re-creating about to divide 4-cell and therefore accounting post growth effect during 4- to 8-cell stage transition, by merging the corresponding 8-cell. Statistical analysis on cell volumes showed  $p < 0.05$ , indicating clear increase in cell volume in *clasp* affected cells than WT/*clasp*-WT cells. Further analysis via best fit ellipsoid showed a larger major to minor axis length ratio ( $k$ ) in *clasp* ( $k \approx 2.0$ ) than WT/*clasp*-WT ( $k \approx 1.7$ ) cells, a possible reflection of growth induced change in shape anisotropy. This plot indicates in *clasp* already a significant growth in the average embryonic volume occurs during 4- to 8-cell stage transition, while in WT a significant growth in embryonic volume starts during 8- to 16-cell stage transition.

Division rules	1-cell	2-cell	4-cell	8-cell
				
Hofmeister	*	*	*	*
Sachs	✗	✓	✗	✗
Errera	✗	✓	✗	✓
Dupuy	✗	✓	✗	✓
cortical MT simulation	✓	✓	✓	✓

**Figure S7.** Comparison of the different rules of cell division when auxin signalling, a key genetic controller of *Arabidopsis* early embryonic cell division is compromised. Experimentally observed division plane orientations are shown by blue (dotted) lines. The symbols used in the table stands for: ✓ = correct prediction (green), ✗ = incorrect prediction (red) and \* = not applicable, which holds uniformly for the Hofmeister rule, which is applicable for anisotropically growing cells only.



# Chapter 4

## **Cell biology of auxin-regulated control of division orientation in the Arabidopsis embryo**

Thijs de Zeeuw<sup>1</sup>, Che-Yang Liao<sup>1</sup>, Soeren Strauss<sup>2</sup>, Richard Smith<sup>2</sup>, Dolf Weijers<sup>1\*</sup>

1. Laboratory of Biochemistry, Wageningen University, Stippeneng 4, 6708 WE Wageningen, the Netherlands

2. Laboratory of Computational modelling of morphogenesis and biomechanisms, Max Planck Institute, Carl-von-Linne-Weg 10, D-50829, Cologne, Germany

\* Corresponding Author: [dolf.weijers@wur.nl](mailto:dolf.weijers@wur.nl)



## Abstract

Pattern formation in plants is often accompanied by tightly controlled regulation of cell division orientation, an example of which is the highly invariant division pattern in *Arabidopsis thaliana* embryos. Asymmetric, formative divisions in the early embryo give rise to protoderm, ground tissue and vascular tissue layer. These divisions are affected in mutants impaired in auxin signalling or transport, suggesting that this hormone controls asymmetric divisions in the embryo. A major unanswered question is how, and through what cellular processes, the auxin hormone regulates division plane orientation. Here, we exploit a set of previously generated subcellular marker lines, and combine these with a computational approach to analyse cell-biological differences underlying cell division defects in the auxin-insensitive *bdl*-mutant. We show that F-actin organisation and perinuclear actin arches are affected in the *bdl*-mutant, which is accompanied by increased cell expansion. Furthermore, we find that the position of the nucleus is an unlikely determinant to create the invariant cell division pattern observed in the *Arabidopsis* embryo.

## Introduction

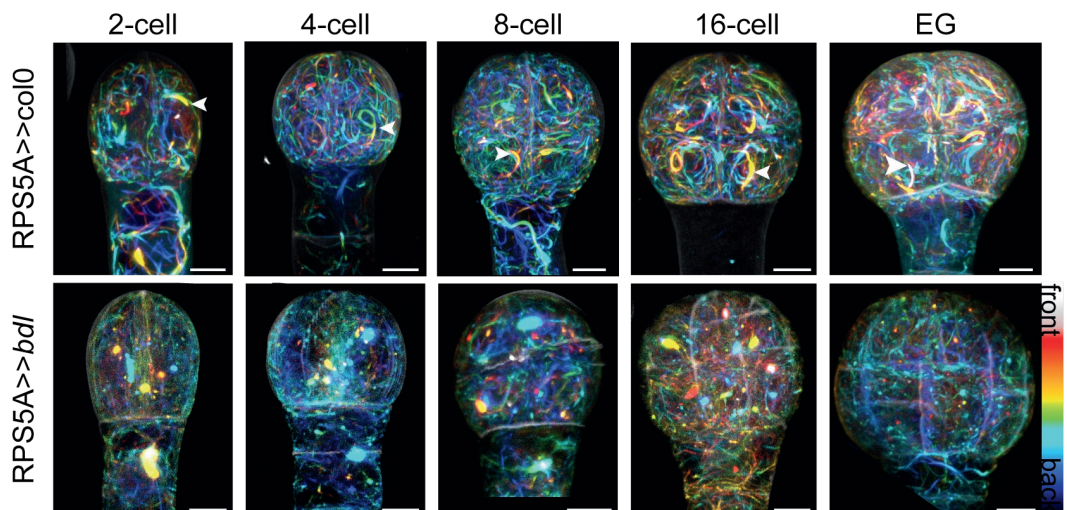
Correct cell division orientation is a crucial property of all plant species. Cell movement is restricted by the pectocellulosic cell wall, making division orientation the determining factor for plant development and ultimately plant shape. As a consequence, control of cell division orientation is connected to the establishment of new cell types (Di Ruocco et al., 2018) and new or lateral organs (Dubrovsky et al., 2000; Shapiro et al., 2015). Research focusing on the mechanisms for molecular regulation of plant cell division orientation is mainly hindered by the complexity of plant structures and tissues, and the lethality of many mutants with defects in the cell division machinery (Gillmor et al., 2016). These restrictions make the *Arabidopsis thaliana* embryo, with its highly regulated division pattern and limited number of cells, an attractive model system to study factors regulating cell division orientation. Arabidopsis development starts from a single zygote cell which undergoes a series of highly robust divisions that form all future tissue types during embryogenesis (reviewed in (Palovaara et al., 2016)). Cell division orientation has been extensively studied and modelled, which has led to the formation of heuristic geometric rules explaining oriented cell divisions based on geometric- and surface area cues (de Wildeman, 1893; Errera, 1888; Thompson & Bonner, 2014). The most prominent division rule, termed the default “shortest wall” division rule states that a cell will divide along the path with minimal surface area within the confined volume (Besson & Dumais, 2014; Errera, 1888).

In Arabidopsis embryos, there is a clear distinction in regulation between divisions following the default “shortest wall” geometric rules, or multiple formative divisions that need additional regulation (Yoshida et al., 2014). Inhibition of auxin response in the embryo through expression of a nondegradable version of the Aux/IAA protein BODENLOS/IAA12 (BDL) under control of the *RPS5A* promoter (*RPS5A>>bdl*; henceforth referred to as “*bdl*-mutant”) inhibits all formative divisions during early embryogenesis, suggesting that auxin signalling is involved in the regulation of cell division orientation control (Yoshida et al., 2014). Thus, BDL-controlled cell division orientation is a strong model system for dissecting the mechanisms underlying the control of cell division orientation by a developmental regulator. In this chapter, we explore the role of modulating the cytoskeleton in BDL-dependent division control.

Microtubule (MT) and fine-actin (F-actin) cytoskeletal structures have been shown to have essential roles during plant cell division (Rasmussen et al., 2013), and may possibly

also play determining roles in division orientation control (Spinner et al., 2010; Wright et al., 2009). Prior to cell division, cortical MT arrays (CMA) and actin filaments become spatially restricted to a plane surrounding the nucleus, forming the pre-prophase band (PPB) and actin-depleted zone (Vos et al., 2004), which predict the future division plane of the cell (Chan et al., 2003; Lloyd & Chan, 2004). Microtubules and actin act cooperatively to change cell wall mechanics leading to cell expansion (Yanagisawa et al., 2015). Based on imaging microtubules and modelling their behaviour on embryo cell geometries, there are indications that regulation of the CMA downstream of auxin-signalling is involved in division plane orientation regulation in formative divisions (Chakraborty et al., 2018). It is however unclear if Actin regulation mediates the control of these formative divisions, and if so, to what effect.

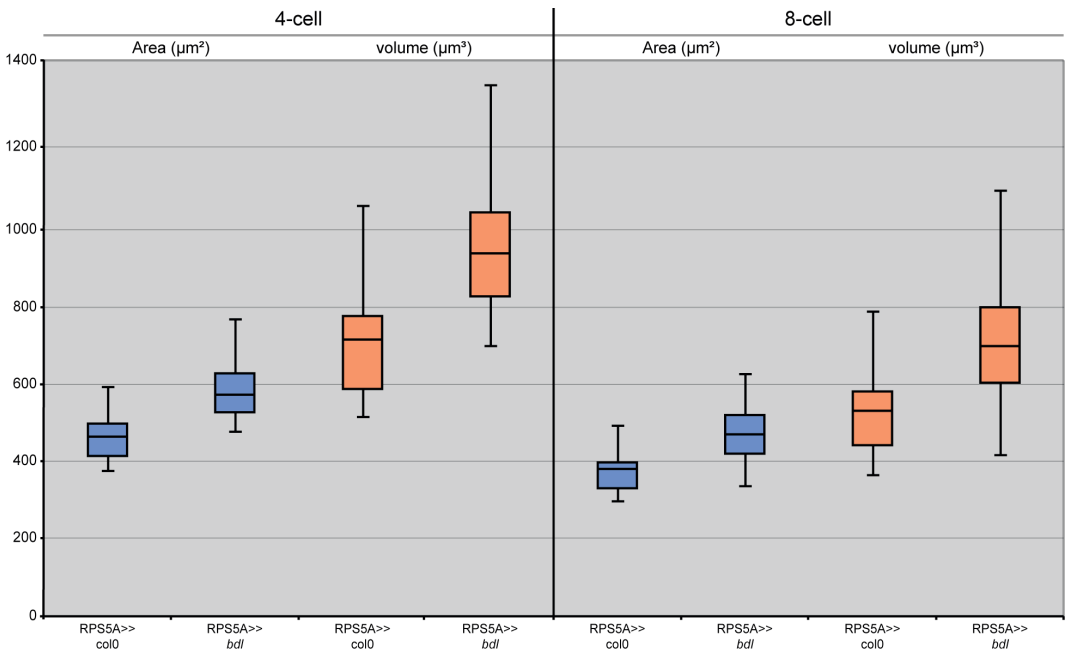
Actin filaments were previously already shown to be part of a broader network which define local mechanical properties of the cell wall, and ultimately growth (Zerzour et al., 2009). Furthermore, actin filaments are involved in nuclear movement and vacuole distribution within the cell (Iwabuchi et al., 2019; Kimata et al., 2016, 2019), which in turn is essential for cell division position and possibly cell division plane orientation control (Iwabuchi et al., 2019; Kimata et al., 2019). As the involvement in a diversity of cellular processes linked to cell division regulation is clear, unravelling of actin filament regulation



**Figure 1:** Visualization of F-actin organisation in Arabidopsis 2-cell to early globular wild-type (*RPS5A>>col-0*) and *bd1*-mutant (*RPS5A>>bd1*) embryos. Depth colour-coded F-actin stacks visualized using a *pWOX2::Lifeact::tdTomato* reporter line merged with membrane stacks visualized using SCRI Renaissance Stain 2200 (SR2200) show F-actin bundles throughout the embryonic cells and peri-nuclear F-actin bundles surrounding nuclei. F-actin structures are disorganised in the *bd1*-mutant. Arrowheads indicate peri-nuclear rings observed in wild-type embryos. Scale bars indicate 5  $\mu$ m distance. Colour scale indicates depth of individual images within the stack from front to back.

is crucial to understand their involvement in regulation of cell division orientation.

Here, we implement a previously established high-quality imaging protocol optimized for early embryogenesis, using embryo-specific subcellular markers (Liao & Weijers, 2018) to dissect the role of actin filaments and downstream regulation of nuclear position in division plane regulation by comparing their sub-cellular organisation in *bdl*-mutant embryos to wild-type Columbia (*col-0*) embryos. Our results show that F-actin organisation is affected in the auxin-insensitive mutant embryos, which we hypothesize could influence cell morphology and nuclear position. We show that cell morphology is indeed affected in the mutant background and observe a large variation in nuclear position relative to the cellular space, which makes it unlikely that this is a determining factor in cell division plane control.

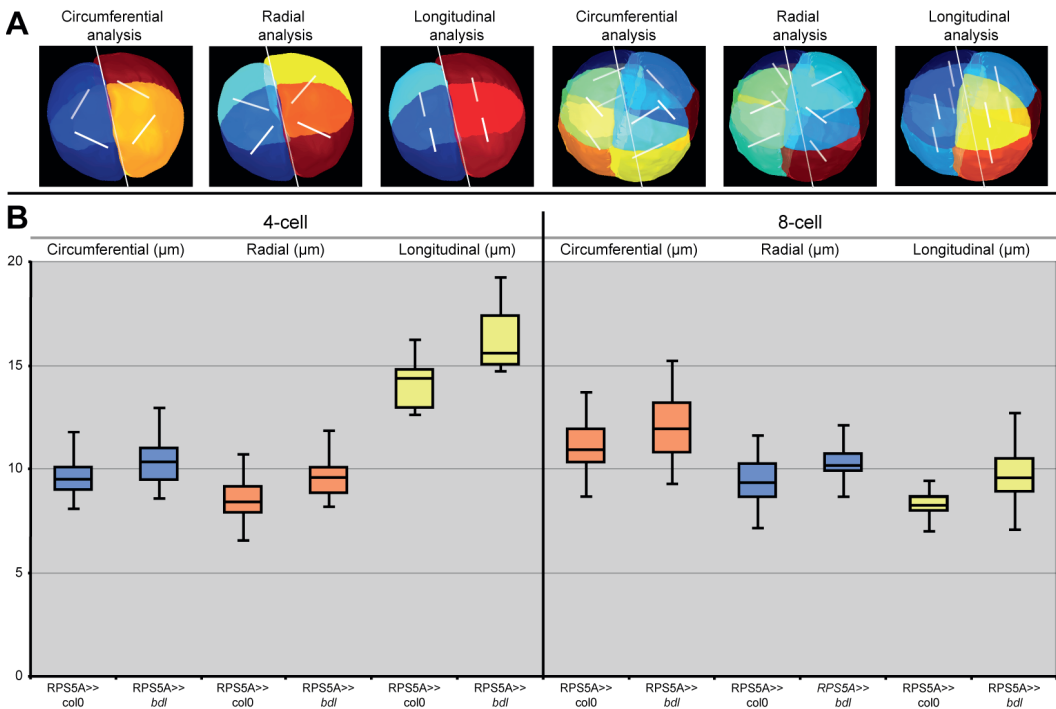


**Figure 2:** 3D cell surface area- and cell volume analysis of Arabidopsis 4-cell and 8-cell wild-type (RPS5A>>col-0) and *bdl*-mutant (RPS5A>>*bdl*) embryos. Average cell surface area (in µm<sup>2</sup>) and cell volume (in µm<sup>3</sup>) are shown for individual cells of 4-cell and 8-cell wild-type and *bdl*-mutant embryos. Based on two-sided student t-tests, all comparisons are statistically significant ( $P < 0.001$ ). Measurements were done on 20- to 56 individual embryonic cells from at least 5 individual embryos per condition.

## Results

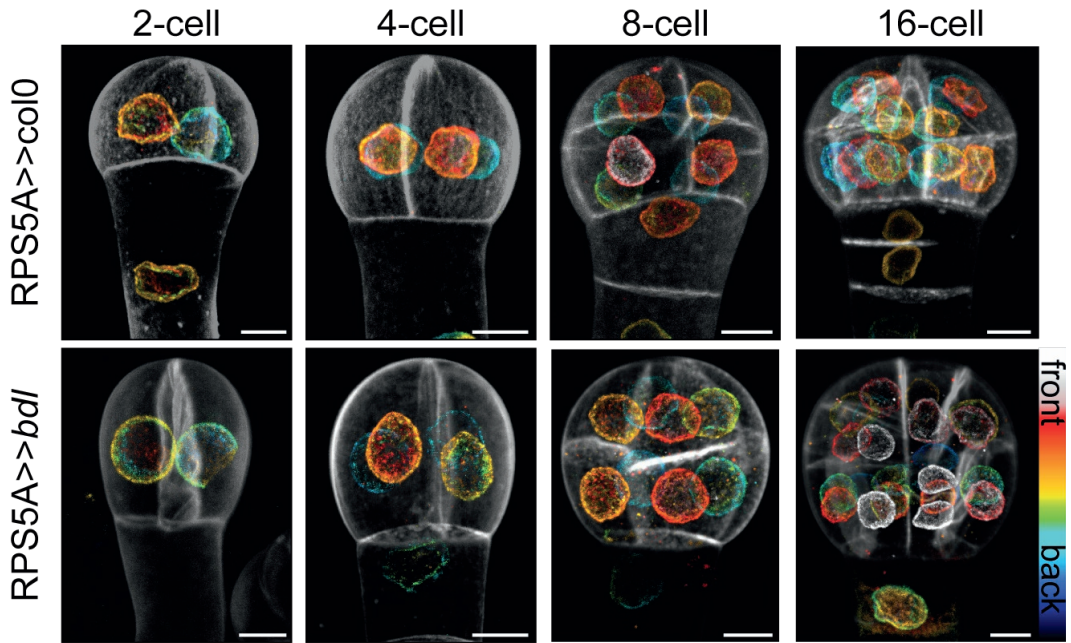
### *Actin filament network organisation is affected in auxin-insensitive mutant embryos*

Previously, using the *bdl*-mutant, we showed that auxin-mediated regulation of the MT-cytoskeleton contributes to regulated asymmetrical cell divisions during Arabidopsis embryogenesis (chapter 2 of this thesis; (Chakraborty et al., 2018)). Since interplay between the MT- and actin-cytoskeleton is essential for correct preprophase band formation and cell division site determination (Hamada, 2014; Takáč et al., 2017; Wu & Bezanilla, 2018), we studied the actin cytoskeleton in the early Arabidopsis embryo using a previously established transgenic line expressing a tandem-Tomato-tagged version of LIFEACT (*Liao & Weijers, 2018; pWOX2::lifeact-TdTomato*), which labels F-actin specifically in Arabidopsis embryos. Since the expression of *bdl* protein induces strong developmental defects throughout development (Hamann et al., 1999; Weijers et al., 2005; Rademacher et al., 2012), we had to use a two-component gene expression system (GAL4-UAS), in



**Figure 3:** 3D cell size analysis of Arabidopsis 4-cell and 8-cell wild-type (*RPS5A>>col-0*) and *bdl*-mutant (*RPS5A>>bdl*) embryos. **a** Illustrates the defined axis for performed measurements. First, a central axis was defined for the pro-embryo. Relative from this axis, circumferential, radial, and longitudinal measurements were performed through the cell centre. **b** circumferential size (in μm), radial size (in μm) and longitudinal size (in μm) are shown for individual cells of 4-cell and 8-cell wild-type and *bdl*-mutant embryos. Based on two-sided student t-tests, all comparisons are statistically significant ( $P < 0.03$ ). Measurements were done on 20- to 48 individual embryonic cells from at least 5 individual embryos per condition.

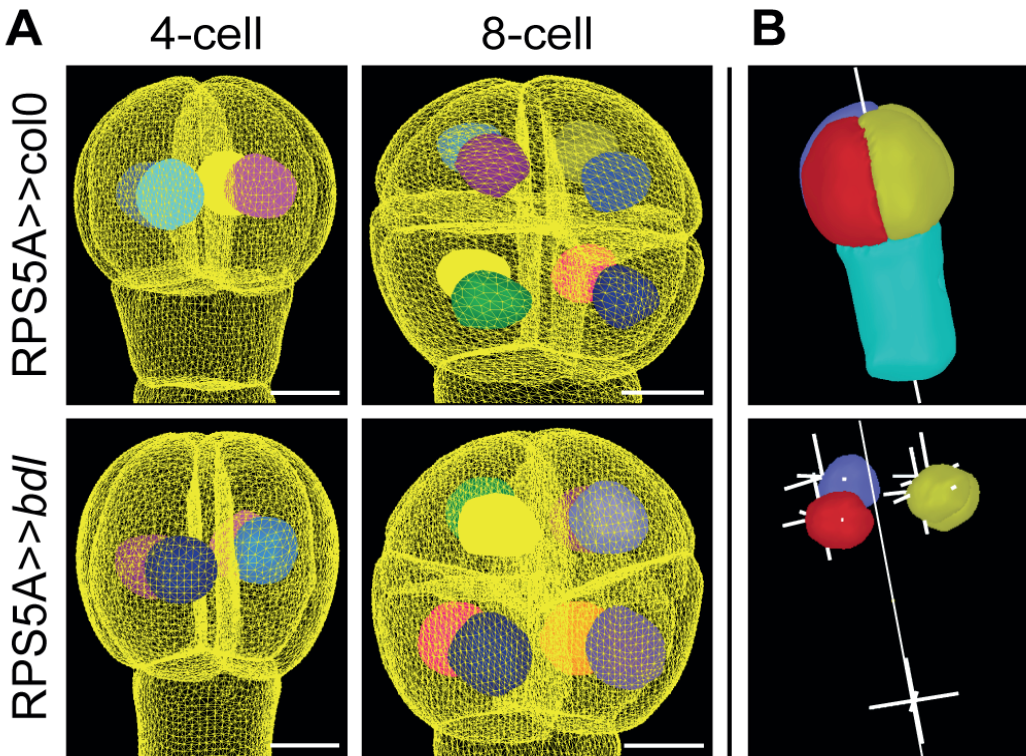
which expression of *bd1*, driven by the *RPS5A* promoter (Weijers et al., 2001), is only induced after fertilization. This strategy has previously been used to analyse the effect of *bd1* expression on cell division (Yoshida et al., 2014). We introduced the *pWOX2::lifeact-TdTomato* transgene into the *RPS5A-GAL4* driver line and crossed this with *UAS-bd1* plants to study auxin-mediated regulation of F-actin organisation. As an isogenic control, lines were crossed to Col-0 wild-type.



**Figure 4:** Visualization of nuclei in Arabidopsis 2-cell to 16-cell wild-type (*RPS5A>>col-0*) and *bd1*-mutant (*RPS5A>>bd1*) embryos. Depth colour-coded nucleus stacks visualized using a *pWOX2::NUP54-GFP* reporter line merged with membrane stacks visualized using SCRI Renaissance Stain 2200 (SR2200) show nuclear position within the embryonic cell volume for both wild-type – and *bd1*-mutant embryos. Scale bars indicate 5  $\mu$ m distance. Colour scale indicates depth of individual images within the stack from front to back.

As previously reported in wild-type embryos, F-actin organises in a dense network with thick bundles throughout the cytoplasm (Fig. 1; Liao & Weijers, 2018). In all stages, bright, thick arches of bundled actin are observed around the nuclei (Fig.1; arrowheads). These peri-nuclear arches were previously observed in Arabidopsis embryos and *Nicotiana benthamiana* BY-2 cells (Liao & Weijers, 2018; Yu et al., 2006), and were suggested to be involved in regulation of nuclear movement. In the *bd1*-mutant background, the actin-network is less dense with fewer visible bundles and more cytosolic signal (Fig. 1). Most notably, although there are still aggregates of bright Lifeact-tdTomato signal, there are no distinctive arches surrounding the nuclei. These results suggest that auxin signalling is required for the stability of the actin cytoskeletal network and for the formation

of specialized actin-structures, comparable to what we showed for cortical MTs in the Arabidopsis embryo (chapter 2 of this thesis; (Chakraborty et al., 2018)). Since actin, together with the MT cytoskeleton functions in cell- elongation, expansion and shape (Hiwatashi et al., 2014; Peñalva et al., 2017; Wu & Bezanilla, 2018), destabilization could change cell geometry, which in turn could affect cell division patterns. The function of the peri-nuclear actin arch is not known, but we hypothesize that this peri-nuclear ring could function in regulation of nuclear position (Yu et al., 2006), which has been correlated with the division plane localization in plant cells (Kimata et al., 2016; Robinson et al., 2011).



**Figure 5:** Visualization and analysis of segmented nuclei within segmented cell meshes in Arabidopsis 4-cell and 8-cell wild-type (*RPS5A>>col-0*) and *bdl*-mutant (*RPS5A>>bdl*) embryos. **a** Nuclei visualized using a *pWOX2::NUP54-GFP* reporter line and membranes visualized using SCR1 Renaissance Stain 2200 (SR2200) stain are separately segmented using the MorphographX (MgX; (de Reuille et al., 2015)) software for both wild-type – and *bdl*-mutant embryos. Colours of nuclei refer to different labels assigned to segmented nuclei. The yellow triangular mesh is created from segmented cell volumes. Scale bars indicate 5  $\mu$ m distance. **b** A central axis is defined through the embryo proper for analysis of nuclear position within the cell. From this axis, longitudinal and radial distance from the cell centroid are defined.

## Auxin response inhibition alters cell shape

To test if destabilization of the cytoskeleton is associated with alteration in cell shape, we analysed cell volumes of the wild-type and *bdl*-mutant embryonic cells. Both cell division patterns and cytoskeletal structures are affected in 4-cell and 8-cell stage embryos (this thesis; (Chakraborty et al., 2018; Yoshida et al., 2014). Therefore we chose to analyse these stages by segmenting high-resolution z-stacks of Propidium Iodide (PI) stained embryos as described in (Yoshida et al., 2014). Meshes were made for the segmented cells of the pro-embryo, and measurements for volume and membrane surface area were performed using the MorphoGraphX (MGX) software (Barbier de Reuille et al., 2015). Both membrane surface area and cell volume are significantly larger in both 4-cell and 8-cell *bdl*-mutant embryos (Fig. 2), indicating that cell geometry is indeed affected in the *bdl*-mutant. To determine if the observed cell expansion is random or directed in either of the cellular directions, we measured circumferential-, radial-, and longitudinal cell lengths of the same embryonic cell volumes (Fig. 3A). Although cell length was slightly increased in all measured directions, the majority of expansion is in the longitudinal direction in both 4-cell and 8-cell embryonic cells (fig. 3B). The dominant longitudinal expansion could be due to affected cell polarity in the pro-embryo, or destabilization of the cytoskeleton, since both actin filaments and MTs have been reported to be involved in directional cell expansion and control of cell wall mechanics (Nakajima et al., 2004; Sedbrook et al., 2004; Yanagisawa et al., 2015; Zerzour et al., 2009).

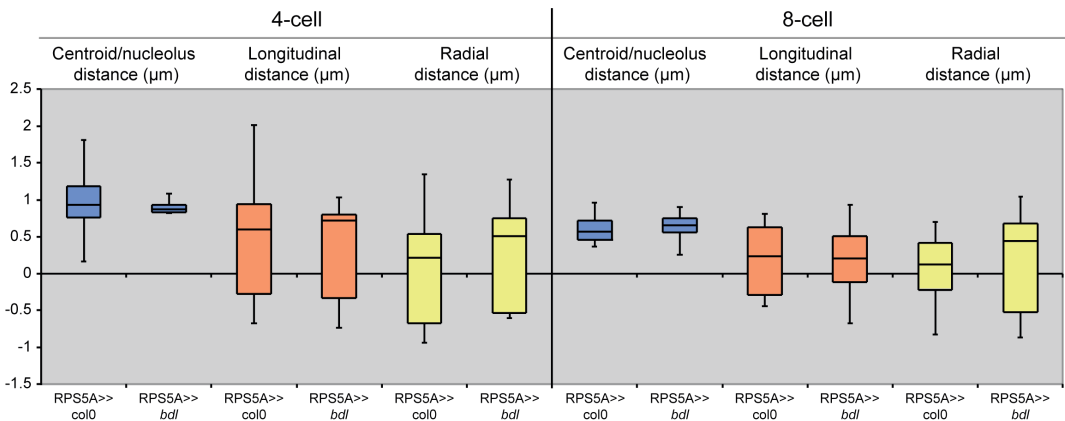


Figure 6: 3D-analysis of nucleolus position relative to cellular centroid position within Arabidopsis 4-cell and 8-cell wild-type (*RPS5A>>col-0*) and *bdl*-mutant (*RPS5A>>bdl*) embryos. Averages for overall centroid/nucleolus distance (in  $\mu\text{m}$ ), longitudinal centroid/nucleolus distance (in  $\mu\text{m}$ ), and radial centroid/nucleolus distance (in  $\mu\text{m}$ ) are shown for individual cells of 4-cell and 8-cell wild-type and *bdl*-mutant embryos. Based on two-sided student t-tests, none of the comparisons are statistically significant ( $P>0.3$ ). Measurements were done on 7- to 25 individual embryonic cells and corresponding nuclei from at least 4 different individual embryos per condition.

*Nuclear position in embryonic cells is not a determinant for cell division orientation*

The position of the nucleus in plant cells has been associated with division plane placement, and there is indeed a clear link between nuclear movement and division placement in Arabidopsis leaf epidermal cells (Elsner et al., 2012), lateral root primordia (Ramakrishna et al., 2019; Von Wangenheim et al., 2016) and zygotes (Kimata et al., 2019; Kurihara et al., 2017). It was also suggested that nuclear position can be a driver for division orientation in the early Arabidopsis embryos (Moukhtar et al., 2019), where displacement of the nucleus would render the asymmetric division that gives rise to the 16-cell embryo one of the “default” divisions. Under this scenario, the primary regulation exerted by auxin response could be nuclear repositioning. Given that actin has a profound role in nuclear movement (Iwabuchi et al., 2019; Kimata et al., 2019), this is a clear and testable hypothesis. However, if nuclear position is to be a reliable cue for division placement, its localization would have to be tightly controlled in wild-type. To test if nuclear position could be a determinant for cell division orientation downstream of cytoskeletal regulation, we used a previously generated and optimized line expressing a GFP-tagged version of NUP54 ((Liao & Weijers, 2018); *pWOX2::NUP54-GFP*) which labels nuclear envelopes specifically in Arabidopsis embryos. We introduced this transgene in the *RPS5A-GAL4* driver line and crossed this with either wild-type Col-0 plants or UAS-*bdl* plants to study nuclear position in 4-cell and 8-cell wild-type and *bdl*-mutant embryos. As described previously, nuclei in mutants from 2-cell until 16-cell stage contain nuclei with either a smooth- or a wavy surface, depending on the cellular developmental stage (Fig. 4a)(Liao & Weijers, 2018). Qualitatively, there is no difference in nuclear phenotype in the *bdl*-mutant (Fig. 4b), but since space is very limited in embryonic cells (Liao & Weijers, 2018; Yoshida et al., 2014), small differences in nuclear position could influence division plane position.

We set out to analyse nuclear position in detail by segmenting high resolution Z-stacks of the nuclear GFP (*pWOX2::NUP54-GFP*) signal and SCR1 Renaissance (R2200) cell wall staining of the same embryonic cells. Creating meshes for both segmented stacks provided us with the nuclear volume positioned within the cellular volume (Fig. 5a). Using the MGX software, we defined the cellular (CC) and nuclear centroid (NC) to calculate nuclear position relative to the centroid of the cell. Defining a central axis through the embryo, we could measure general distance of NC to CC, as well as specifying the direction of displacement in longitudinal- and radial directions (Fig. 5b). For both 4-cell and 8-cell embryos, we could not find significant differences in nuclear position between wild-type – and *bdl*-mutant embryos (Fig. 6). Additionally, from our data we can conclude that the

variation in nuclear position is relatively high in these embryonic cells. Opposed to the high variation in nuclear position within the cellular volume, the cell division patterns in the *Arabidopsis* embryo is highly invariant (Natho, 1998). These findings in both wild-type and *bdl*-mutant embryos argues against a determining role for nuclear position in cell division orientation control.

## Discussion

In this chapter, we analysed F-actin organisation in auxin-insensitive *Arabidopsis* embryos relative to the wild-type organisation. Our high-resolution imaging using a fluorescent F-actin marker reveals that actin stability is severely affected in early stage auxin-insensitive embryos, illustrated by reduced interphase actin uniformity and loss of the peri-nuclear arches observed in wild-type plants. Previously, we have shown that stability of the CMT-array in interphase embryonic cells is also affected in auxin-insensitive embryos (Chapter 3 of this thesis; (Chakraborty et al., 2018)). Therefore, we hypothesise that the aberrant division plane phenotype observed in the *bdl*-mutant is caused by cytoskeletal defects downstream of auxin signalling.

The actin cytoskeleton has been shown to regulate nuclear position in the *Arabidopsis* embryos (Iwabuchi et al., 2019), and nuclear position is an important determinant for cell division in plants (Kimata et al., 2016; Robinson et al., 2011). Therefore, we hypothesized that nuclear position could be a factor contributing to cell division plane orientation determination. However, our results show that nuclear position is highly variable in both wild-type and *bdl*-mutant embryos, with no significant differences between embryos for these conditions. We could argue that the variation in nuclear position is due to a difference in cell cycle stage per individual cell, but since the variation is also high in the developmentally invariable wild-type embryos, we conclude that the variation in nuclear position is a true feature of embryonic *Arabidopsis* cells. The high amount of variation in nuclear position relative to the cell membrane indicates that nuclear position cannot be determining for division plane orientation control in the embryo with its highly invariable division pattern (Yoshida et al., 2014).

Interplay between the actin- and MT cytoskeleton has been shown to be essential for plant cell shape at different developmental stages (Wu & Bezanilla, 2018). Considering the importance of geometric input in plant cell division control (Besson & Dumais, 2014;

Iwabuchi et al., 2019; Yoshida et al., 2014), it is evident that physical- and positional properties of cell membranes play an important role in development. Here, we analysed 3D cell morphology in 4-cell and 8-cell embryos of the *bdl*-mutant to determine if embryonic cell morphology is affected downstream of auxin-signalling and cytoskeletal control. Our results show that cell volume and membrane surface are significantly larger in 4-cell and 8-cell *bdl*-mutant embryos. Cells size measurements on the same embryonic cells revealed that cells were elongated primarily in the longitudinal direction, indicating that cell morphology is indeed affected in the *bdl*-mutant. Since classically, cell division orientation control has been described by division rules based on geometry (Besson & Dumais, 2014; de Wildeman, 1893; Errera, 1888), the affected cell shape in auxin-insensitive embryos could be a factor in determining division plane position and orientation (Alim et al., 2012; Besson, 2014). However, previous studies show that the division pattern observed in 8-cell and 16-cell Arabidopsis embryos cannot be explained solely based on cell geometry (Yoshida et al., 2014), suggesting that the observed cell morphological differences observed here are not enough to change division plane orientation.

Individual plant cells are polarized, and based on data obtained in yeast and mammalian cells, polarity information is used for local cell outgrowth and proper cell division orientation (Chant, 1994; Johnston, 2018; Nakamura et al., 2012). Additionally, the high number of directional changes during Arabidopsis embryogenesis suggest that the initiation and maintenance of cellular polarity is an essential part of plant embryo development (Dhonukshe et al., 2005). The observed cell outgrowth in the longitudinal direction and division defect in 4-cell and 8-cell *bdl*-mutant embryos could be a consequence of affected polarity in cells of the pro-embryo. In mammalian cells, cell division orientation is determined mainly by polar cues that control cytoskeletal reorganization (Wodarz, 2002). However, inversely, microtubule disruption causes cell polarity defects including aberrant polar localization of polar proteins (Martin & Chang, 2003). In Arabidopsis, auxin-regulated polarly localized SOSEKI proteins have recently been identified (Yoshida et al., 2019), and shows that auxin response is capable of altering the cell polarity system in the embryo. Importantly, SOSEKI1 can alter division orientation when misexpressed (Yoshida et al., 2019). This, together with the observed defects in cytoskeletal organisation in the auxin-insensitive *bdl*-mutant (chapter 2 of this thesis) links auxin-dependent organismal axes, cell polarity and cytoskeletal regulation to cell division orientation. Cell polarity-related research in plants has been hampered by the lack of polarity-markers and possible embryonic lethality of polarity-defective mutants. It will be interesting to see if

future research can overcome these challenges and directly link cell polarity to cellular mechanisms underlying plant morphogenesis.

## Methods

### *Plant material*

*pGIIN/pWOX2::Lifeact-tdTomato:tNOS* (ACE14) and *pGIIN/pWOX2::NUP54-GFP:tNOS* (ACE11), previously described in (Liao & Weijers, 2018), were introduced into homozygous *pRPS5A::GAL4:VP16* driver line (Weijers et al., 2003) in the Columbia (Col-0) ecotype. T3 homozygous transgenic plants with representative expression level across their corresponding cellular structures were used for crossing with Col-0 plant or *UAS-bdl* plants (Weijers et al., 2006). *RPS5A::GAL4:VP16* plants were used as female parent.

After seed sterilization, seedlings were plated on half-strength Murashige-Skoog (MS) plates containing 0.8% Dashin agar (Duchefa), 1% sucrose, and Norflurazon (Supelco) (Misawa et al., 1993) for transgenic plant selection. After two weeks of growth on plates, seedlings were transferred to soil and further grown at a constant temperature of 22°C under long-day conditions (16 hours light/8 hours dark).

### *Microscopy and image analysis*

Embryo samples were prepared as described in (Liao, 2018). Images for qualitative purpose were acquired in 8-bit format, images for segmentation were acquired in 16-bit format. Images were acquired using a Leica TCS SP5II confocal laser scanning microscope with 63x NA=1.2 water objective with pinhole set to 1.0 Airy unit. mGFP was excited by an Argon-ion laser and tdTomato and SCRI Renaissance Stain 2200 (SR2200) (Renaissance Chemicals, <http://www.renchem.co.uk/>) were excited using a diode laser, and their emissions were detected sequentially with a Leica HyD in photon counting mode. Excitation and detection of fluorophores were configured as follows: mGFP was excited at 488 nm and detected at 498–528 nm; tdTomato was excited at 561 nm and detected at 571–630 nm; Renaissance 2200 was excited at 405 nm and detected at 430–470 nm. Line accumulation was set to 4, 4, and 2 for mGFP, tdTomato, and SR2200, respectively.

For qualitative results description of F-actin and nuclear structures, maximum

projections were generated. For these stacks, background signal outside of the embryo were subtracted, and remaining embryonic signal was multiplied 2-4 times up until signal saturation. All image processes and measurements were conducted via Fiji (Schindelin et al., 2012)

### *3D cell segmentation and nuclear position measurements*

For segmentation, in MophoGraphX (de Reuille et al., 2015), confocal image stacks (TIF) were Gaussian blurred using sigma value 0.6  $\mu\text{m}$ , subsequently we applied the ITK watershed auto-seeding with level threshold value in the range 300–1500 and default smoothing levels. Segmented bitmap stacks were manually corrected for oversegmentation errors within MGX by fusing together multiple labels into the single cells, which were represented using a combination of the select and paint bucket tools in MGX (Roeder et al., 2012). Then, we approximated the segmented cells by creating triangulated surface meshes using marching cubes 3D with cube size of 1.

Nuclear measurements were performed on segmented meshes created using the same segmentation method described above using the nuclei marker channel. Cell and nucleus centroid positions were determined in MGX by calculating the centre of gravity of their triangulated surface meshes.

Organ centric directions were determined in the same way as described in the 3D Cell Atlas Add-on for MGX (Montenegro-Johnson et al., 2015) by manually placing a straight line through the embryo using the “Bezier line” in MGX. For each cell then 3 directions relative to this central line were calculated: a longitudinal direction that is identical with the direction defined by the central line, a radial direction that was defined by the cell centroid and its closest point on the central line, and a circumferential direction that was defined by the cross product of the previous two directions.

To calculate the distances between cell centroid and nucleus centroid along the longitudinal and radial direction, the scalar product of the vector defined by the centroids and the vector of the respective direction was computed.

### *3D cell morphology measurements*

Cell sizes along longitudinal, radial and circumferential directions were computed as described in Montenegro-Johnson et al. (2015) by shooting rays from the cell centroid along the respective cell directions and their opposites and measure the distance of the two intersection points of the rays with the cellular mesh.

## **Acknowledgements**

We would like to thank dr. Prasad Vaddepalli and dr. Soeren Strauss for critical comments on the manuscript. This work was supported by a Netherlands Organization for Scientific Research (NWO) grant (ALW 824.14.009) to D.W.

## References

- Alim, K., Hamant, O., & Boudaoud, A. (2012). Regulatory Role of Cell Division Rules on Tissue Growth Heterogeneity. *Frontiers in Plant Science*. <https://doi.org/10.3389/fpls.2012.00174>
- Barbier de Reuille, P., Routier-Kierzkowska, A.-L., Kierzkowski, D., Bassel, G. W., Schüpbach, T., Tauriello, G., ... Smith, R. S. (2015). MorphoGraphX: A platform for quantifying morphogenesis in 4D. *ELife*, 4, 05864. <https://doi.org/10.7554/eLife.05864>
- Besson, S., & Dumais, J. (2014). Stochasticity in the symmetric division of plant cells: When the exceptions are the rule. *Frontiers in Plant Science*. <https://doi.org/10.3389/fpls.2014.00538>
- Chakraborty, B., Willemsen, V., de Zeeuw, T., Liao, C. Y., Weijers, D., Mulder, B., & Scheres, B. (2018). A Plausible Microtubule-Based Mechanism for Cell Division Orientation in Plant Embryogenesis. *Current Biology*. <https://doi.org/10.1016/j.cub.2018.07.025>
- Chan, J., Calder, G. M., Doonan, J. H., & Lloyd, C. W. (2003). EB1 reveals mobile microtubule nucleation sites in Arabidopsis. *Nature Cell Biology*, 5(11), 967–971. <https://doi.org/10.1038/ncb1057>
- Chant, J. (1994). Cell polarity in yeast. *Trends in Genetics*. [https://doi.org/10.1016/0168-9525\(94\)90036-1](https://doi.org/10.1016/0168-9525(94)90036-1)
- de Reuille, P. B., Routier-Kierzkowska, A. L., Kierzkowski, D., Bassel, G. W., Schüpbach, T., Tauriello, G., ... Smith, R. S. (2015). MorphoGraphX: A platform for quantifying morphogenesis in 4D. *ELife*. <https://doi.org/10.7554/eLife.05864>
- de Wildeman, E. (1893). Études sur l'attache des cloisons cellulaires. *Mémoires Couronnés et Mémoires Des Savants Étrangers*, 53, 1–84.
- Dhonukshe, P., Kleine-Vehn, J., & Friml, J. (2005). Cell polarity, auxin transport, and cytoskeleton-mediated division planes: Who comes first? *Protoplasma*. <https://doi.org/10.1007/s00709-005-0104-8>
- Di Ruocco, G., Di Mambro, R., & Ioio, R. Dello. (2018). Building the differences: A case for the ground tissue patterning in plants. *Proceedings of the Royal Society B: Biological Sciences*. <https://doi.org/10.1098/rspb.2018.1746>

Dubrovsky, J. G., Doerner, P. W., Colón-Carmona, A., & Rost, T. L. (2000). Pericycle cell proliferation and lateral root initiation in *Arabidopsis*. *Plant Physiology*. <https://doi.org/10.1104/pp.124.4.1648>

Elsner, J., Michalski, M., & Kwiatkowska, D. (2012). Spatiotemporal variation of leaf epidermal cell growth: A quantitative analysis of *Arabidopsis thaliana* wild-type and triple cyclinD3 mutant plants. *Annals of Botany*. <https://doi.org/10.1093/aob/mcs005>

Errera, L. (1888). Über Zellformen und Siefenblasen. *Bot. Centralbl.*, 34, 395–399.

Gillmor, C. S., Roeder, A. H. K., Sieber, P., Somerville, C., & Lukowitz, W. (2016). A genetic screen for mutations affecting cell division in the *Arabidopsis thaliana* embryo identifies seven loci required for cytokinesis. *PLoS ONE*. <https://doi.org/10.1371/journal.pone.0146492>

Hamada, T. (2014). Microtubule organization and microtubule-associated proteins in plant cells. In *International Review of Cell and Molecular Biology*. <https://doi.org/10.1016/B978-0-12-800178-3.00001-4>

Hiwatashi, Y., Sato, Y., & Doonan, J. H. (2014). Kinesins Have a Dual Function in Organizing Microtubules during Both Tip Growth and Cytokinesis in *Physcomitrella patens*. *The Plant Cell*. <https://doi.org/10.1105/tpc.113.121723>

Iwabuchi, K., Ohnishi, H., Tamura, K., Fukao, Y., Furuya, T., Hattori, K., ... Hara-Nishimura, I. (2019). ANGUSTIFOLIA Regulates Actin Filament Alignment for Nuclear Positioning in Leaves. *Plant Physiology*. <https://doi.org/10.1104/pp.18.01150>

Johnston, D. S. (2018). Establishing and transducing cell polarity: common themes and variations. *Current Opinion in Cell Biology*. <https://doi.org/10.1016/j.ceb.2017.10.007>

Kimata, Y., Higaki, T., Kawashima, T., Kurihara, D., Sato, Y., Yamada, T., ... Ueda, M. (2016). Cytoskeleton dynamics control the first asymmetric cell division in *Arabidopsis* zygote. *Proceedings of the National Academy of Sciences*. <https://doi.org/10.1073/pnas.1613979113>

Kimata, Y., Kato, T., Higaki, T., Kurihara, D., Yamada, T., Segami, S., ... Ueda, M. (2019). Polar vacuolar distribution is essential for accurate asymmetric division of *Arabidopsis* zygotes. *Proceedings of the National Academy of Sciences of the United States of America*. <https://doi.org/10.1073/pnas.1814160116>

- Kurihara, D., Kimata, Y., Higashiyama, T., & Ueda, M. (2017). In vitro ovule cultivation for live-cell imaging of zygote polarization and embryo patterning in *Arabidopsis thaliana*. *Journal of Visualized Experiments*. <https://doi.org/10.3791/55975>
- Liao, C. Y., & Weijers, D. (2018). A toolkit for studying cellular reorganization during early embryogenesis in *Arabidopsis thaliana*. *Plant Journal*. <https://doi.org/10.1111/tpj.13841>
- Lloyd, C., & Chan, J. (2004). Microtubules and the shape of plants to come. *Nature Reviews. Molecular Cell Biology*, 5(1), 13–22. <https://doi.org/10.1038/nrm1277>
- Martin, S. G., & Chang, F. (2003). Cell polarity: A new mod(e) of anchoring. *Current Biology*. <https://doi.org/10.1016/j.cub.2003.08.046>
- Misawa, N., Yamano, S., Linden, H., De Felipe, M. R., Lucas, M., Ikenaga, H., & Sandmann, G. (1993). Functional expression of the *Erwinia uredovora* carotenoid biosynthesis gene *crtl* in transgenic plants showing an increase of  $\beta$ -carotene biosynthesis activity and resistance to the bleaching herbicide norflurazon. *Plant Journal*. <https://doi.org/10.1046/j.1365-313X.1993.04050833.x>
- Moukhtar, J., Trubuil, A., Belcram, K., Legland, D., Khadir, Z., Urbain, A., ... Andrey, P. (2019). Cell geometry determines symmetric and asymmetric division plane selection in arabidopsis early embryos. *PLoS Computational Biology*. <https://doi.org/10.1371/journal.pcbi.1006771>
- Nakajima, K., Furutani, I., Tachimoto, H., Matsubara, H., & Hashimoto, T. (2004). SPIRAL1 Encodes a Plant-Specific Microtubule-Localized Protein Required for Directional Control of Rapidly Expanding Arabidopsis Cells. *The Plant Cell*. <https://doi.org/10.1105/tpc.017830>
- Nakamura, M., Kiefer, C. S., & Grebe, M. (2012). Planar polarity, tissue polarity and planar morphogenesis in plants. *Current Opinion in Plant Biology*. <https://doi.org/10.1016/j.pbi.2012.07.006>
- Natho, G. (1998). B. M. Johri; K. B. Ambegaokar & P. S. Srivastava, Comparative Embryology of Angiosperms, 2 Bde., XXV + 1221 S., 362 Abb., 32 Tab. Springer-Verlag, Berlin, Heidelberg, New York, London, Paris, Tokyo, Hong Kong, Barcelona, Budapest, 1992. ISBN 3-540-53633-7. Feddes Repertorium. <https://doi.org/10.1002/fedr.4921090108>
- Palovaara, J., de Zeeuw, T., & Weijers, D. (2016). Tissue and Organ Initiation in the

Plant Embryo: A First Time for Everything. *Annual Review of Cell and Developmental Biology*, 32(1), annurev-cellbio-111315-124929. <https://doi.org/10.1146/annurev-cellbio-111315-124929>

Peñalva, M. A., Zhang, J., Xiang, X., & Pantazopoulou, A. (2017). Transport of fungal RAB11 secretory vesicles involves myosin-5, dynein/dynactin/p25, and kinesin-1 and is independent of kinesin-3. *Molecular Biology of the Cell*. <https://doi.org/10.1091/mbc.e16-08-0566>

Ramakrishna, P., Duarte, P. R., Rance, G. A., Schubert, M., Vordermaier, V., Vu, L. D., ... De Smet, I. (2019). EXPANSIN A1-mediated radial swelling of pericycle cells positions anticlinal cell divisions during lateral root initiation. *Proceedings of the National Academy of Sciences of the United States of America*. <https://doi.org/10.1073/pnas.1820882116>

Rasmussen, C. G., Wright, A. J., & Müller, S. (2013). The role of the cytoskeleton and associated proteins in determination of the plant cell division plane. *The Plant Journal: For Cell and Molecular Biology*, 75(2), 258–269. <https://doi.org/10.1111/tpj.12177>

Robinson, S., De Reuille, P. B., Chan, J., Bergmann, D., Prusinkiewicz, P., & Coen, E. (2011). Generation of spatial patterns through cell polarity switching. *Science*. <https://doi.org/10.1126/science.1202185>

Roeder, A. H. K., Cunha, A., Burl, M. C., & Meyerowitz, E. M. (2012). A computational image analysis glossary for biologists. *Development*. <https://doi.org/10.1242/dev.076414>

Schindelin, J., Arganda-Carreras, I., Frise, E., Kaynig, V., Longair, M., Pietzsch, T., ... Cardona, A. (2012). Fiji: An open-source platform for biological-image analysis. *Nature Methods*. <https://doi.org/10.1038/nmeth.2019>

Sedbrook, J. C., Ehrhardt, D. W., Fisher, S. E., Scheible, W.-R., & Somerville, C. R. (2004). The Arabidopsis SKU6 / SPIRAL1 Gene Encodes a Plus End–Localized Microtubule-Interacting Protein Involved in Directional Cell Expansion . *The Plant Cell*. <https://doi.org/10.1105/tpc.020644>

Shapiro, B. E., Tobin, C., Mjolsness, E., & Meyerowitz, E. M. (2015). Analysis of cell division patterns in the Arabidopsis shoot apical meristem. *Proceedings of the National Academy of Sciences of the United States of America*, 112(15), 4815–4820. <https://doi.org/10.1073/pnas.1502588112>

- Spinner, L., Pastuglia, M., Belcram, K., Pegoraro, M., Goussot, M., Bouchez, D., & Schaefer, D. G. (2010). The function of TONNEAU1 in moss reveals ancient mechanisms of division plane specification and cell elongation in land plants. *Development*. <https://doi.org/10.1242/dev.043810>
- Takáč, T., Šamajová, O., Pechan, T., Luptovčiak, I., & Šamaj, J. (2017). Feedback Microtubule Control and Microtubule-Actin Cross-talk in Arabidopsis Revealed by Integrative Proteomic and Cell Biology Analysis of KATANIN 1 Mutants . *Molecular & Cellular Proteomics*. <https://doi.org/10.1074/mcp.m117.068015>
- Thompson, D. W., & Bonner, J. T. (2014). On growth and form. *In On Growth and Form*. <https://doi.org/10.1017/CBO9781107589070>
- Von Wangenheim, D., Fangerau, J., Schmitz, A., Smith, R. S., Leitte, H., Stelzer, E. H. K., & Maizel, A. (2016). Rules and self-organizing properties of post-embryonic plant organ cell division patterns. *Current Biology*. <https://doi.org/10.1016/j.cub.2015.12.047>
- Vos, J. W., Dogterom, M., & Emons, A. M. C. (2004). Microtubules Become More Dynamic but Not Shorter during Preprophase Band Formation: A Possible “Search-and-Capture” Mechanism for Microtubule Translocation. *Cell Motility and the Cytoskeleton*. <https://doi.org/10.1002/cm.10169>
- Weijers, D., Schlereth, A., Ehrismann, J. S., Schwank, G., Kientz, M., & Jürgens, G. (2006). Auxin triggers transient local signaling for cell specification in Arabidopsis embryogenesis. *Developmental Cell*. <https://doi.org/10.1016/j.devcel.2005.12.001>
- Weijers, D., Van Hamburg, J. P., Van Rijn, E., Hooykaas, P. J. J., & Offringa, R. (2003). Diphtheria Toxin-Mediated Cell Ablation Reveals Interregional Communication during Arabidopsis Seed Development. *Plant Physiology*. <https://doi.org/10.1104/pp.103.030692>
- Wodarz, A. (2002). Establishing cell polarity in development. *Nature Cell Biology*. <https://doi.org/10.1038/ncb0202-e39>
- Wright, A. J., Gallagher, K., & Smith, L. G. (2009). discordial and alternative discordial Function Redundantly at the Cortical Division Site to Promote Preprophase Band Formation and Orient Division Planes in Maize. *The Plant Cell*. <https://doi.org/10.1105/tpc.108.062810>
- Wu, S. Z., & Bezanilla, M. (2018). Actin and microtubule cross talk mediates persistent

polarized growth. *The Journal of Cell Biology*. <https://doi.org/10.1083/jcb.201802039>

Yanagisawa, M., Desyatova, A. S., Belteton, S. A., Mallery, E. L., Turner, J. A., & Szymanski, D. B. (2015). Patterning mechanisms of cytoskeletal and cell wall systems during leaf trichome morphogenesis. *Nature Plants*. <https://doi.org/10.1038/nplants.2015.14>

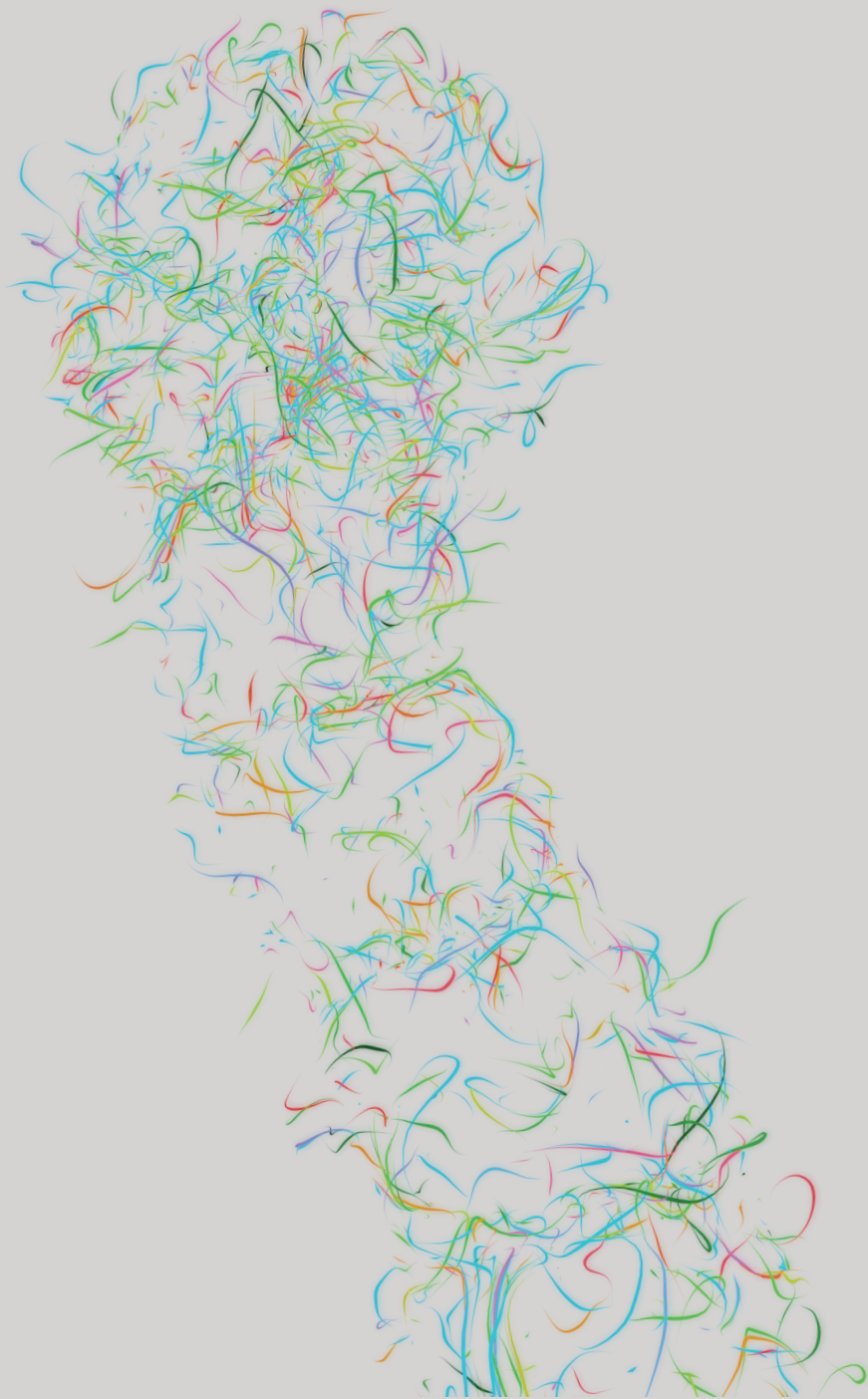
Yoshida, S., Barbier de Reuille, P., Lane, B., Bassel, G. W., Prusinkiewicz, P., Smith, R. S., & Weijers, D. (2014). Genetic control of plant development by overriding a geometric division rule. *Developmental Cell*, 29(1), 75–87. <https://doi.org/10.1016/j.devcel.2014.02.002>

Yoshida, S., van der Schuren, A., van Dop, M., van Galen, L., Saiga, S., Adibi, M., ... Weijers, D. (2019). A SOSEKI-based coordinate system interprets global polarity cues in Arabidopsis. *Nature Plants*. <https://doi.org/10.1038/s41477-019-0363-6>

Yu, M., Yuan, M., & Ren, H. (2006). Visualization of actin cytoskeletal dynamics during the cell cycle in tobacco (*Nicotiana tabacum* L. cv Bright Yellow) cells. *Biology of the Cell*. <https://doi.org/10.1042/bc20050074>

Zerzour, R., Kroeger, J., & Geitmann, A. (2009). Polar growth in pollen tubes is associated with spatially confined dynamic changes in cell mechanical properties. *Developmental Biology*. <https://doi.org/10.1016/j.ydbio.2009.07.044>





# Chapter 5

## **A reference transcriptome of early Arabidopsis embryogenesis**

Thijs de Zeeuw, Sumanth Mutte, Zhaodong Hao, Tatyana Radoeva, Margo Smit, Joakim Palovaara, Valentijn Jansen and Dolf Weijers

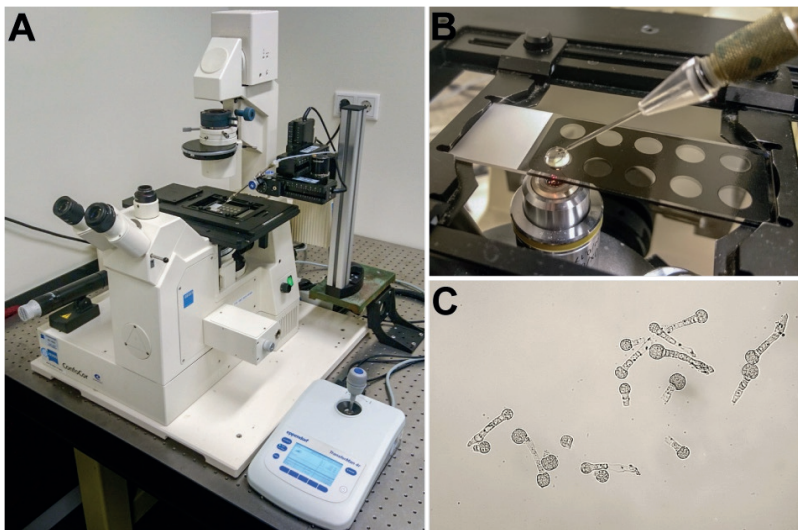


## Abstract

Precursors for all major plant cell types are formed during embryogenesis. Tight coordination of oriented cell division, cell-cell communication and genetic regulation are essential for correct establishment of these precursors. The establishment of different cell identities relies on the definition of unique transcript profiles for each cell type in the embryo. Therefore, analysing transcriptomes at high definition is essential for unravelling embryonic patterning and plant development in general. Because the embryo, containing a small number of cells, is embedded in endosperm and seed coat, it is a non-trivial challenge to generate high-quality embryo transcriptomes. Low efficiency of embryo isolation and contamination with maternal tissue- and endosperm-derived transcript are major impediments. Here, we optimize an embryonic transcriptome analysis pipeline and validate our developed method on a number of different genotypes. Using this approach, we can efficiently detect changes in the wild-type embryonic transcriptome during multiple stages of development, as well as in mutants in developmental regulators. Finally, we use our method to generate a reference transcriptome for early Arabidopsis embryogenesis which can be used to explore the genetic and regulatory basis underlying developmental processes during embryogenesis.

## Introduction

Multicellular land plants (Embryophytes) require numerous cell identity establishment- and coordination events for correct development. The basis for the major cell types and plant structures is established during embryogenesis. In the flowering plant *Arabidopsis thaliana*, all cell types develop from a single cell (the zygote) that undergoes a series of oriented cell divisions during embryogenesis to form all post-embryonic tissue layers (Jürgens & Mayer, 1994; Yoshida et al., 2014). The invariant cell division pattern during embryogenesis makes it possible to study the complex process of tissue formation in detail, and has shown that tight coordination of oriented cell divisions, cell-cell communication and genetic regulation is essential for correct establishment of all different cell types that make up the mature body pattern (Gooh et al., 2015; Laux, 2004; Palovaara et al., 2016; Yoshida et al., 2014). Differentiation of different cell types is largely defined by the presence of specific transcripts in this specific cell type (Hofmann et al., 2019; Palovaara et al., 2017; Xiang et al., 2011), making characterization of the embryonic transcriptome over the course of embryogenesis an essential task to unravel the machinery underlying correct cell-division control and specification of tissue identities. Flowering plant embryos are deeply embedded within the endosperm and the maternal seed coat, making it challenging to isolate quantities of embryos suitable for transcriptome studies in an efficient, straightforward manner without substantial seed coat- and endosperm contamination (Beeckman et al., 2006; Brown et al., 1999; Schon & Nodine, 2017). Advances in transcriptomics have now made it possible to generate more than 100 transcriptomes from *Arabidopsis* embryos using a variety of embryo isolation methods, but most of these datasets were shown to have



**Figure 1:** Isolation of *Arabidopsis* embryos. **a** Embryo isolation set-up with the Eppendorf transferman 4r installed on the Zeiss Confocor 1 inverted microscope. **b** Vacutip II microcapillaries are used to collect embryos from the ovule debris mixture. **c** *Arabidopsis* embryos from a variety of stages in the final wash drop (after 3 wash steps).

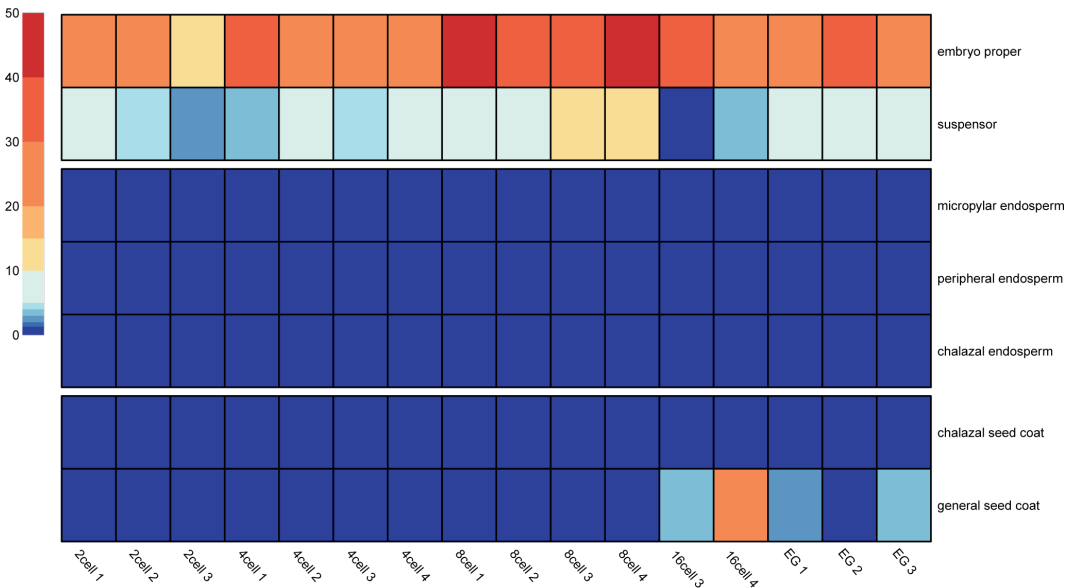
varying amounts of parental contamination (Schon & Nodine, 2017), hampering processing and detailed analysis of the data.

Here, we set out to establish a pipeline for efficient-, clean Arabidopsis embryo isolation for whole embryo transcriptomic analysis, using a microcapillary in combination with a micromanipulator to isolate and wash single embryos with visual microscopic confirmation. We test the viability of our method by generating transcriptome profiles for multiple different mutant backgrounds and different embryonic stages of Arabidopsis embryogenesis. Our developed early Arabidopsis reference dataset, together with the datasets used for validation provide embryo-specific transcriptomes that provide a resource to explore the genetic regulation underlying tissue initiation and developmental processes during embryogenesis.

## Results

### *Efficient isolation and RNA-sequencing of highly pure Arabidopsis embryos*

To set up a pipeline for clean Arabidopsis embryo isolation and RNAseq library preparation, we optimized the previously developed isolation method for the isolation of early-stage embryos (Raissig et al., 2013). To accelerate the procedure and ensure efficient collection of ovules from siliques, we implemented vacuum collection of ovules from collected



**Figure 2:** Heat map of tissue enrichment test results of 16 transcriptomes from wild-type embryos between 2-cell to early globular (EG) stages. Legend show tissue enrichment score values ( $-\log_{10}$  p-value), rows represent tissue subregions. Tissue enrichment tests are performed like described in (Schon & Nodine, 2017).

siliques (Palovaara et al., 2017). Following crushing of ovules, screening and collection of embryos was done using an inverted microscope with a microcapillary tip in combination with a micromanipulator. Commercially available high-quality microcapillaries with 60  $\mu\text{m}$  tip openings were used for all isolations. Use of the Eppendorf Celltram® microinjector system ensured efficient isolation and cleaning of embryos without the need for manual removal of ovule debris (fig. 1). Use of the inverted microscope during isolation also created the possibility to visually determine the embryonic stage during the isolation procedure, allowing to strongly enrich for embryos in a single stage. To fully ensure contamination-free isolation of embryos, we added an additional wash step to our isolation protocol before transferring the embryos to the destination buffer (fig. 1C). After optimization, we were able to isolate 2 samples, each containing approximately 30-40 visually clean embryos within 3 hours. For all subsequent analysis, we collected 4 replicates (each containing 30-40 embryos) to ensure statistical significance.

mRNA-seq libraries were prepared from total RNA isolated from 30-40 embryos using the non-commercial Smart-seq2 method (Picelli et al., 2014), and between 7473991 and 34784718 clusters were sequenced for all libraries using Illumina BGISEq-500, HiSeq-4000, or NovaSeq-6000 technology (Table S1). Tissue enrichment tests (Schon & Nodine, 2017) performed on the embryo transcriptome data showed that RNA-seq transcriptome datasets for early Arabidopsis embryos between 2-cell to early globular stage are highly embryo specific, with minimal seed-coat and endosperm contamination for most stages (fig. 2). Some 16-cell and early globular stage embryo datasets show general seed coat contamination, suggesting that qualitatively, our method works best for early stage embryo isolation and further optimization of our method could improve future datasets created for later stage embryos.

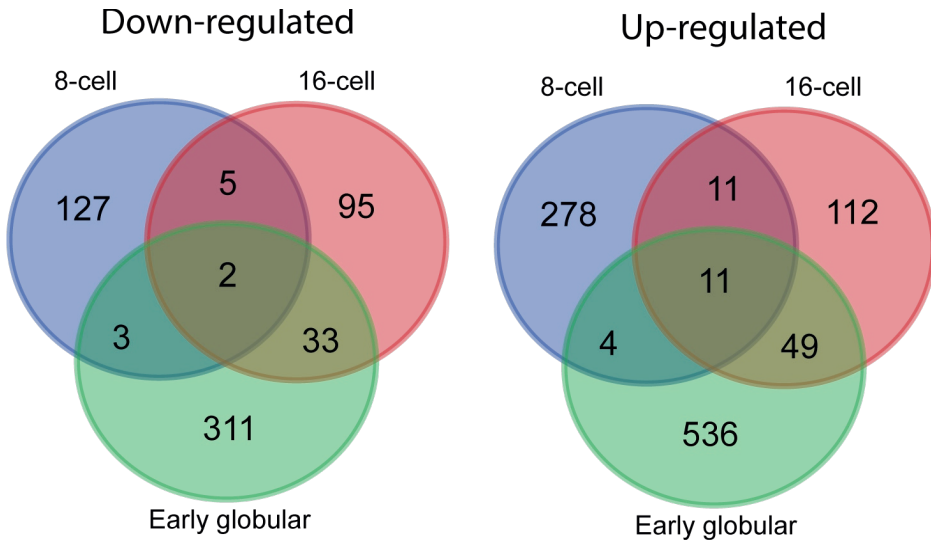
To test the viability of our generated early Arabidopsis embryo transcriptome pipeline we performed transcriptome profiling for mutants that are expected to have either severe- or subtle changes in transcriptomic profiles. The method was further validated by generating a transcriptome profile for five subsequent Arabidopsis embryonic stages, which are compared to previously generated data.

### *Transcriptomic analysis of strong developmental mutant embryos*

The auxin response inhibitor INDOLE-3-ACETIC ACID INDUCIBLE 12/BODENLOS

(BDL) protein is normally degraded in response to auxin. A Pro74Ser mutation in the BDL protein (*bdl*) prevents degradation and subsequent accumulation of the protein, rendering a cell expressing this mutant auxin insensitive. Using the two-component Galactose-induced gene 4/*Upstream Activation Sequence* (GAL4/*UAS*; (Weijers et al., 2006)) system to express *bdl* under control of the suspensor specific M0171 promoter (M0171>>*bdl*) induces an embryonic identity in suspensor cells (Rademacher et al., 2012). Previous transcriptional profiling of globular stage M0171>>*bdl* mutant embryos revealed misregulation of a large group of genes involved in re-establishing suspensor auxin activity and subsequent suspensor-derived embryogenesis (Radoeva et al., 2019). To benchmark our method, we generated transcriptomes of M0171>>*bdl* embryos at different stages, and compared results to the prior micro-array-based transcriptome data.

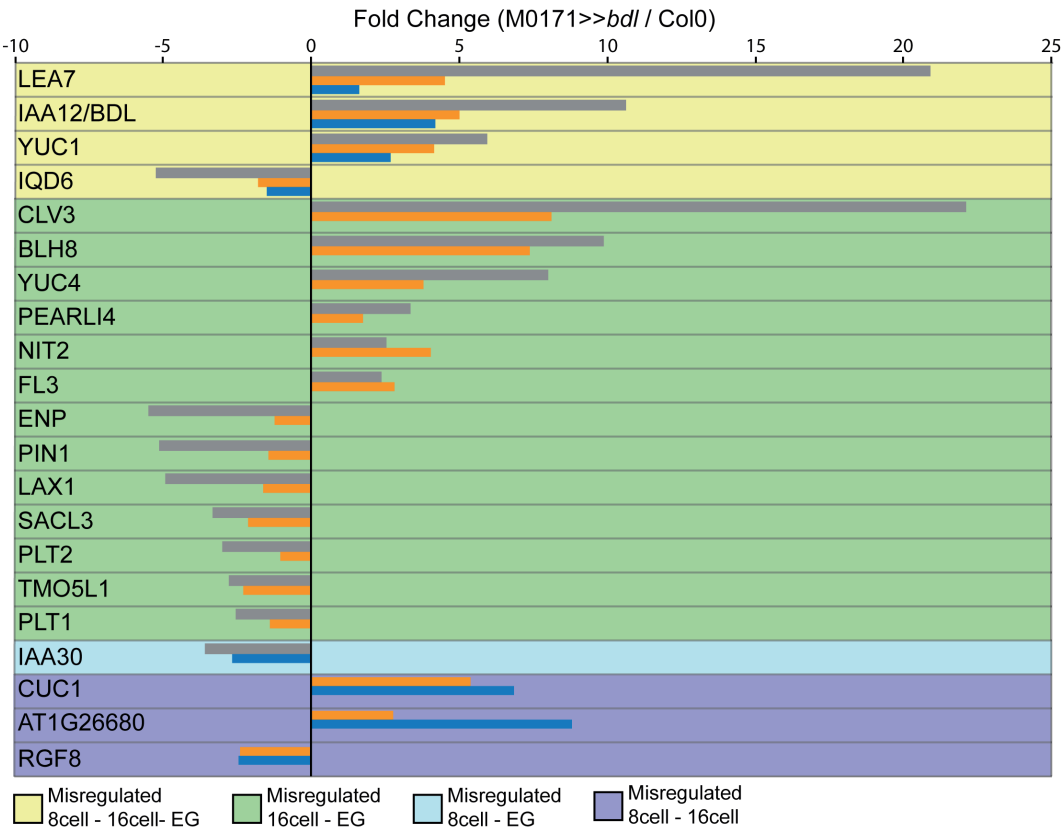
Embryos at 8- and 16 cell stage were isolated from siliques harvested 50 or 60 hours after hand pollination of M0171 pistils with either wild-type (control) or *UAS-bdl* pollen. After statistical analysis in all datasets, we were left with 4 highly-embryo specific replicates for all conditions (Fig. S1). the *BDL* gene was shown to be up-regulated at both stages, thus validating the quality of the performed transcriptome analysis. Comparing the two novel datasets with the prior dataset derived from globular-stage embryos revealed a majority of uniquely mis-regulated genes for each embryonic stage, but also a group of mis-regulated genes that is shared between the different embryonic stages (fig.3). The



**Figure 3:** Comparison of misregulated genes in the M0171>>*bdl* mutant in 8-, 16-, and early globular embryos (in fold change M0171>>*bdl*/M0171>>wild-type). All significantly downregulated and upregulated genes in our generated 8-, and 16-cell embryo transcriptomic datasets are compared to misexpressed genes identified in a transcriptomic dataset previously generated for early globular embryos (Radoeva et al., 2018).

majority of mis-regulated genes is shared between 16-cell and early globular embryos, and includes a variety of genes previously identified to be important in re-establishing auxin biosynthesis (*YUCCA* (*YUC*)1/4) and regulation of auxin transport (*PIN-FORMED* (*PIN*)1, *LIKE AUXIN RESISTANT* (*LAX*)1, *FL3*, *ENP*) (fig. 4). Although no morphological changes are yet observed in 8- and 16-cell M0171>>*bdl* suspensor cells (Radoeva et al., 2019), the transcriptomes reveal regulation of genes expressed in shoot apical meristems (*CLV3*, *BLH8*, *CUC1*), root stem cells (*PLT1/2*) and vascular tissue (*TMO5L1*, *SACL3*) (fig. 4). Regulation of these genes might provide evidence for activation of suspensor-derived embryogenesis at earlier stages of embryogenesis than previously thought.

Since morphological changes towards embryonic identity are observed in post-globular embryo suspensors, most studies to date focused on post-globular embryos. Our present dataset however shows a large group of severely mis-regulated genes already at 8-cell stage (fig. 5). Up-regulated genes could be involved in suspensor derived embryogenesis through transcriptional regulation of important pro-embryonic factors (fig. 5). A variety

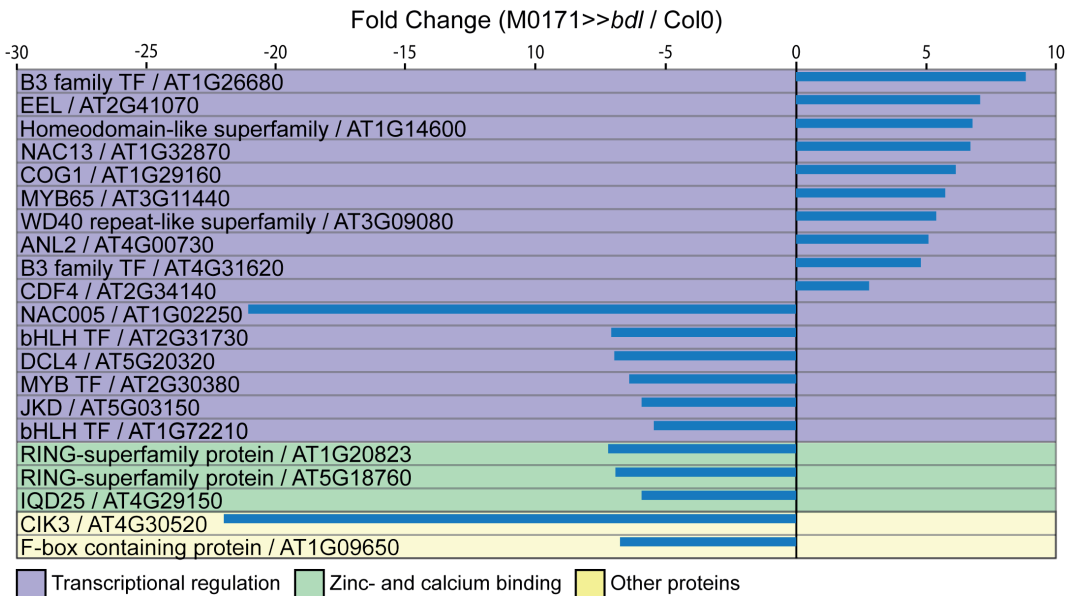


**Figure 4:** Misregulated genes in the different M0171>>*bdl* datasets (in fold change M0171>>*bdl*/M0171>>wild-type). Genes are grouped based on their shared misexpression in different datasets [shared misregulated in: 8cell-16cell and early globular, 16cell and early globular, 8cell and early globular, 8cell and 16cell].

of genes is heavily down-regulated in the mutant, suggesting a role for these genes in maintaining suspensor identity- or development. Additionally, as we show by comparing transcriptional profiles of different embryonic stages, these datasets enable us to study stage-specific aspects of transcriptomic regulation of the same developmental processes.

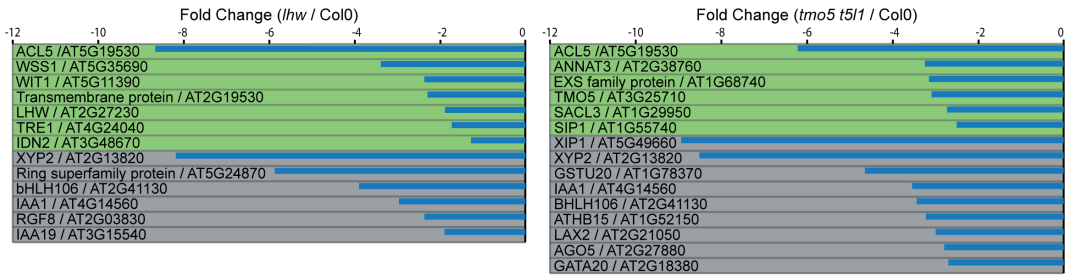
### Detection of subtle transcriptional changes in mutant embryos

The M0171>>*bdl* transcriptome is dramatically altered compared to wild-type embryos, and shows that such large changes can be detected using our optimized method. However, BDL misexpression likely inhibits multiple ARF transcription factors (Piya et al., 2014), and is thus not representative of the transcriptomic impact of knocking out a single regulator. We therefore turned to loss of function mutants in transcription factors to determine if the method is sensitive enough to detect subtle transcriptional effects. The TARGET OF MONOPTEROS5 (TMO5) bHLH transcription factor with its three TMO5-like (T5L1-3) homologs, together with the heterodimeric LONESOME HIGHWAY (LHW) bHLH transcription factor are essential for periclinal cell division in the vascular lineage (De Rybel et al., 2013b; Ohashi-Ito et al., 2014). Expression of TMO5 and LHW overlaps in early globular embryo provascular cells where they regulate cytokinin biosynthesis through activation of *LONELY GUY4* (*LOG4*) and its closest homolog *LOG3* (De Rybel



**Figure 5:** Uniquely misexpressed genes in 8-cell M0171>>*bdl* embryos (in fold change M0171>>*bdl*/M0171>>wild-type). Genes are grouped based on their protein function [Transcriptional regulation, Zinc- and calcium binding, Other].

et al., 2014; Ohashi-Ito et al., 2014). Transcriptional regulation by the TMO5/LHW dimer is regulated by ACAULIS5 (ACL5), which antagonizes TMO5/LHW heterodimer activity by promoting SAC51-LIKE (SACL) bHLH transcription factor activity (Vera-Sirera et al., 2015). By forming heterodimers with LHW, SACL competes with the TMO5/LHW interaction and reduces activity of TMO5/LHW target genes. Regulation and function for both TMO5 and LHW have been mainly described in the early globular embryo and post-embryonic roots, but both proteins are already expressed in 8-cell stage embryos (this thesis (fig. 8)). During the transition from 8- to 16-cell embryos the precursors for later vascular tissues are initially formed, and at this stage genes that are involved in vascular tissue initiation could potentially be regulated. Interestingly, transcriptomic analysis of TMO5/LHW-dependent genes has so far only been performed in post-embryonic tissues, and only using misexpression genotypes. Therefore, analysis of *tmo5* and *lhw* mutant embryos should also help resolve which genes critically require TMO5/LHW for their regulation.



**Figure 6:** Differential gene expression in 8-cell *tmo5 t5l1* (in fold change *tmo5 t5l1*/wild-type) and *lhw* (in fold change *lhw*/wild-type) mutant embryos. Genes colored green have been identified as *tmo5/lhw* targets in previous overexpression datasets on Arabidopsis roots and *Marchantia polymorpha* (Smet. W.M.S., 2018; Lu, K.J., unpublished).

We isolated 8-cell stage embryos of wild-type, *tmo5 t5l1* double mutant and *lhw* mutant. After statistical analysis, 3 highly embryo-specific replicates were available for wild-type and *tmo5tmo5l1* mutant, and 4 replicates for the *lhw* mutant (fig. S2). We retained a list of 29 down-regulated genes (-1-fold; FDR<0.05) in the *lhw* mutant, and 132 down-regulated genes in the *tmo5 t5l1* mutant. As done in available transcriptomic datasets generated from Dexamethasone (DEX)-induced LHW- and TMO5 overexpressing Arabidopsis root tissue and *Marchantia Polymorpha tissue* (Smet. W.M.S., 2018; Lu, K.J., unpublished), we chose to focus here on down-regulated genes because TMO5 and LHW seem to primarily act as transcriptional activators in most experiments. The identification of the known targets *ACL5* in both the *lhw*- and the *tmo5 t5l1* mutant and *SACL3* in the *tmo5 t5l1* mutant verifies the validity of our method to identify subtle changes in transcriptomic profiles. Our dataset does not show differential expression of the previously identified

targets *LOG3/4* or any other cytokinin-related factors, suggesting that TMO5 and LHW may not exert their function through cytokinin-mediated signalling at the earliest developmental stage, or indicating that sensitivity is not sufficient to detect small changes in expression levels (fig. 6). Additionally, both misregulated genes overlapping with identified targets in TMO5/LHW overexpression datasets (Smet. W.M.S., 2018; Lu, K.J., unpublished), and targets specific for 8-cell embryos could be identified. XYLOGEN PROTEIN 2 (XYP2), the auxin/indole3-acetic acid protein IAA1 and basic/helix-loop-helix 106 (bHLH106) transcription factor are down-regulated in 8-cell embryos of both the *lhw* and *tmo5 t5l* mutant. Polar xylogen deposition has been suggested to regulate vascular development, and *xyp1xyp2* double mutants show morphological defects in vascular development in roots, cotyledons and leaves (Motosé et al., 2004). Cell size of phloem and xylem are reduced in plants expressing a DEX-induced stabilized (domain II) version of IAA1 (Ku et al., 2009), suggesting involvement in vascular development. The down-regulation of the uncharacterized bHLH106 in both the mutants is interesting, since bHLH-transcription factors have been shown to have essential roles in the pathway regulating vascular tissue establishment (Ohashi-Ito et al., 2014; Vera-Sirera et al., 2015). XYLEM INTERMIXED WITH PHLOEM 1 (XIP1) is a receptor like kinase (RLK) specifically down-regulated in the *tmo5tmo5l* mutant, and is previously shown to be required for vascular patterning (Bryan et al., 2012). IAA19 is specifically regulated in the *lhw* mutant, indicating that there might be LHW-specific auxin-regulated regulation at this embryonic stage.

Further analysis and characterization of these misregulated genes in 8-cell Arabidopsis embryos should shed light on the function of LHW and TMO5, and their role in the initiation of vascular tissue development as early as the 8-cell stage of Arabidopsis embryogenesis.

### *A reference transcriptome for early Arabidopsis embryogenesis*

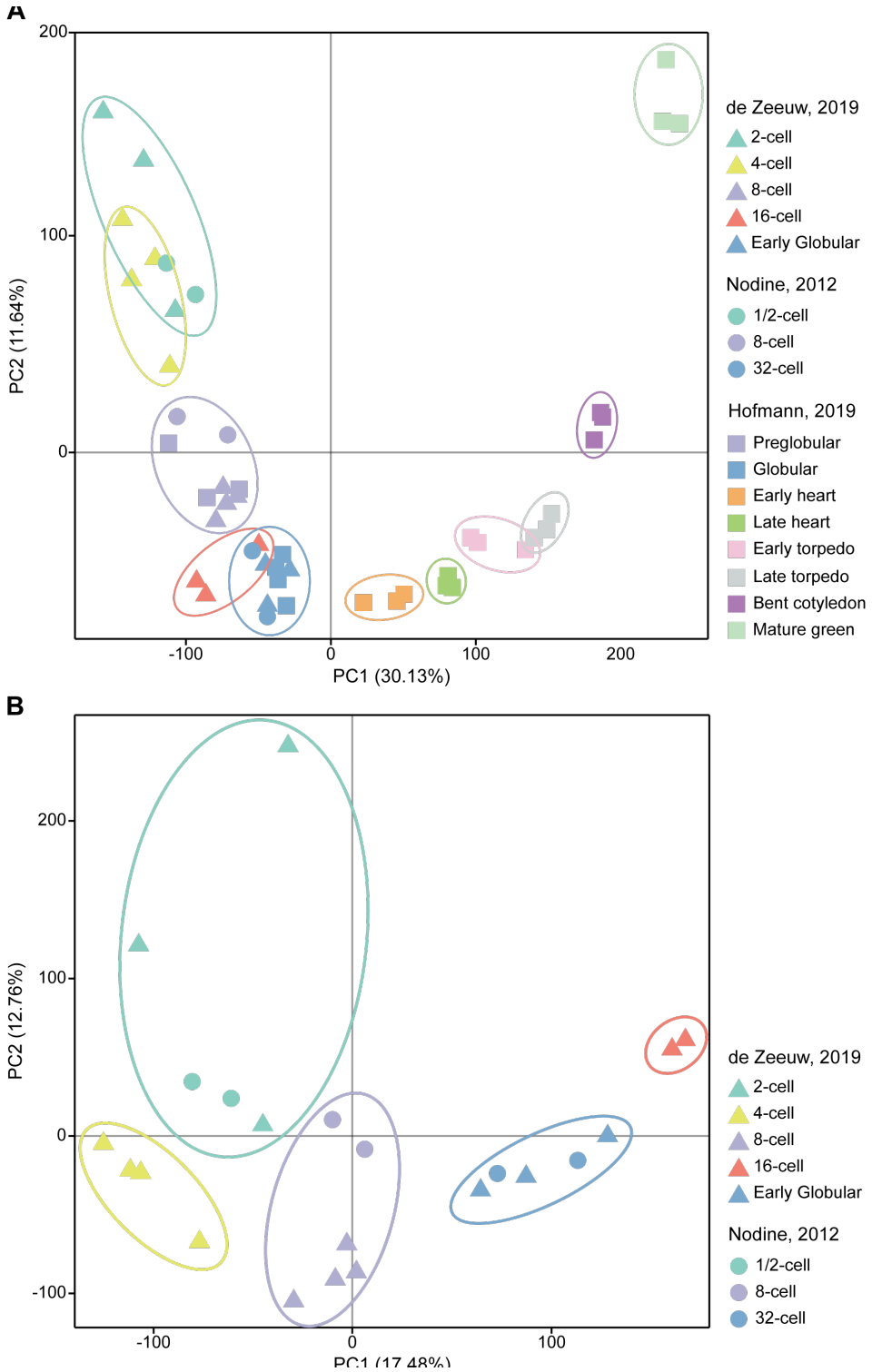
Key plant patterning events, including apical-basal and radial axis formation that occur during early embryogenesis are associated with changes in transcription (Laux, 2004; Mayer et al., 1991). Here we determined the transcriptome of the earliest stages of Arabidopsis embryogenesis to reveal changes in transcript populations per embryonic stage. To optimize the isolation of accurately staged embryos, hand-pollination was performed. Subsequent isolation at 60 and 65 hours after pollination increased the efficiency of separating 2-cell and 4-cell embryos. All subsequent stages were visually selected during the isolation

procedure.

After statistical analysis, 3 replicates were retained for 2-cell-, 16-cell- and globular stage embryos, and 4 replicates were retained for 4-cell-, 8-cell-embryos. These were sufficient to derive a high-quality temporal series of early *Arabidopsis* embryogenesis. The replicates of each stage cluster accurately in a Principle Component Analysis (PCA), and show perfect concordance with previously generated datasets for early *Arabidopsis* embryos (Hofmann et al., 2019; Nodine & Bartel, 2012), validating the quality of our dataset (fig. 7A). 2-cell and 4-cell transcriptomes overlapped in the PCA analysis, which could either mean that sampling and separation of 2- and 4-cell embryos was not efficient, or alternatively it may indicate that there are only limited differences in transcriptome profiles between these stages. A more detailed look at the earliest embryonic stages, comparing with most closely related published dataset (Nodine & Bartel, 2012) revealed clear differences between 2- and 4-cell transcriptome profiles, suggesting correct separation of these stages was achieved during sampling (Fig. 7B). This comparison does show that among the 2-cell samples the variation is high, suggesting that this group could be contaminated with 1-cell embryos. The transition from 8- to 16-cell embryos results in the biggest transcriptional change observed amongst the analysed stages. Developmentally this makes sense, since the initiation of the majority of future cell types takes place in 16-cell embryos, which would require the regulation of a large group of genes and genetic regulators (review in (Palovaara et al., 2016)).

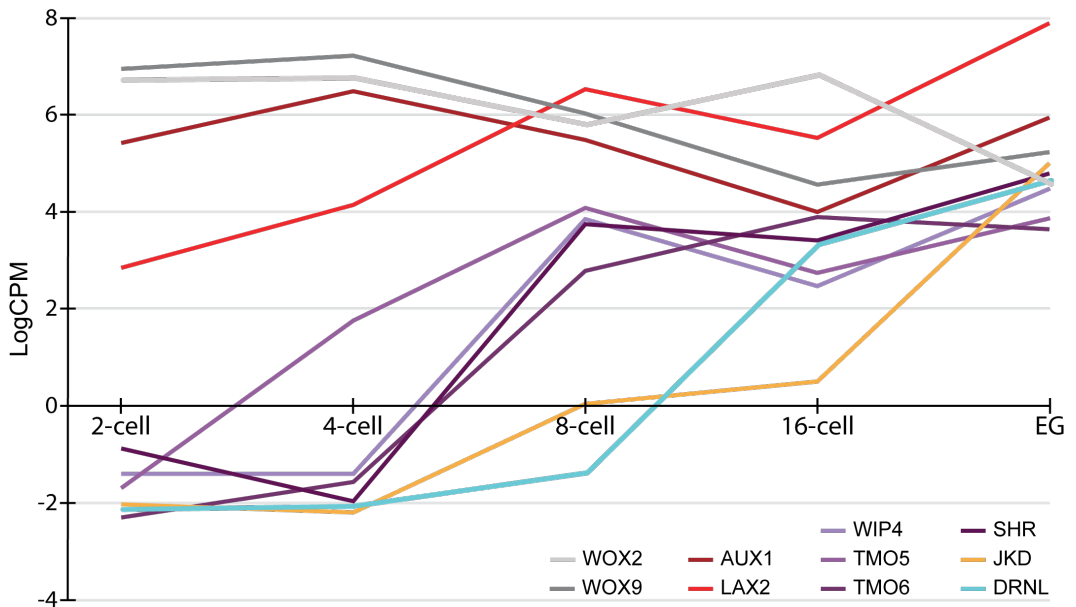
5

To further verify the quality of our dataset we determined expression patterns of genes with known expression patterns in different stages of early embryogenesis (fig. 8). *WUSCHEL RELATED HOMEODOMAIN 2* (*WOX2*), and *WOX9* are key players in early embryonic patterning and were previously shown to be expressed in the zygote and first stages of embryogenesis (Haecker, 2004). *WOX2* expression was previously detected in the zygote and later in the apical domain of the pro-embryo. *WOX9* expression was detected in the basal daughter cell of the zygote and later in the central domain of the embryo and hypophysis. In line with this data, our data shows high expression for both genes from 2-cell stage onward, and expression decreases slightly towards later stages (Fig. 8). The amino acid permease-like genes *AUX1* and *LIKE-AUX1 2* (*LAX2*) are auxin influx carriers crucial for auxin-dependent cell specification during embryogenesis (Robert et al., 2015). Expression of both genes was previously detected earliest in early-globular embryos where they are later specified to provascular cells (Robert et al., 2015). Our data shows moderate expression of both genes from 2-cell stage onward, with increasing expression towards the



**Figure 7:** PCA displaying the early Arabidopsis embryo time series generated in this study compared to other embryo transcriptomics data (Hofmann et al., 2019; Nodine & Bartel, 2012). **a** Comparison of all three datasets. **b** Comparison of our dataset to the most closely related dataset.

early-globular stage for LAX2 (Fig. 8). *WIP DOMAIN PROTEIN 4 (WIP4)*, is a zinc finger transcription factor required for correct formation of the lens-shaped cell during globular stage embryogenesis, which is vital for the formation of the root meristem. *WIP4* was previously detected from globular stage embryos onward, specifically in the hypophysis (Crawford et al., 2015). In line with this data, our data shows a strong increase in expression towards early-globular stage from 8-cell stage onward (Fig. 8). The bHLH transcription factor *TARGET OF MONOPTEROS 5 (TMO5)* and Dof-type transcription factor *TMO6* are crucial factors in regulating vascular tissue specification- and development. Both factors are previously detected from early-globular stage embryos onward, specifically in (pre)-vascular cells (Schlereth et al., 2010). In line with this data, our data shows a strong increase in expression towards early-globular stage from 8-cell stage onward (Fig. 8). The GRAS family transcription factor *SHORT-ROOT (SHR)* is a key factor in ground tissue initiation and maintenance, through control of oriented cell divisions. The C2H2 zinc finger *JACKDAW (JKD)* regulates ground tissue boundaries by constraining SHR movement to adjacent cell layers (Long et al., 2015). Both factors are previously detected from early-globular stage embryos onward, specifically in ground-tissue precursor cells (Welch et al., 2007). In line with this data our data shows a strong increase of *SHR* expression at the 8-cell stage and maintenance of this expression during subsequent stages. *JKD* expression is low during the earliest stages and is strongly increased at the 32-cell stage (Fig. 8). The AP2 ERF transcription factor *DORN RÖSCHEN-LIKE (DRNL)* redundantly controls



**Figure 8:** Gene expression values for known embryonic factors over the five different stages of our Arabidopsis embryo time series dataset. The log-counts-per-million (logCPM) values after mapping were used.

floral meristem (FM) maintenance and is previously detected from globular stage embryos onward (Chandler et al., 2007; Chandler & Werr, 2017). In line with this data, our data shows an increase in *DRNL* expression at 16-cell stage, and increases further to the early-globular stage (Fig. 8).

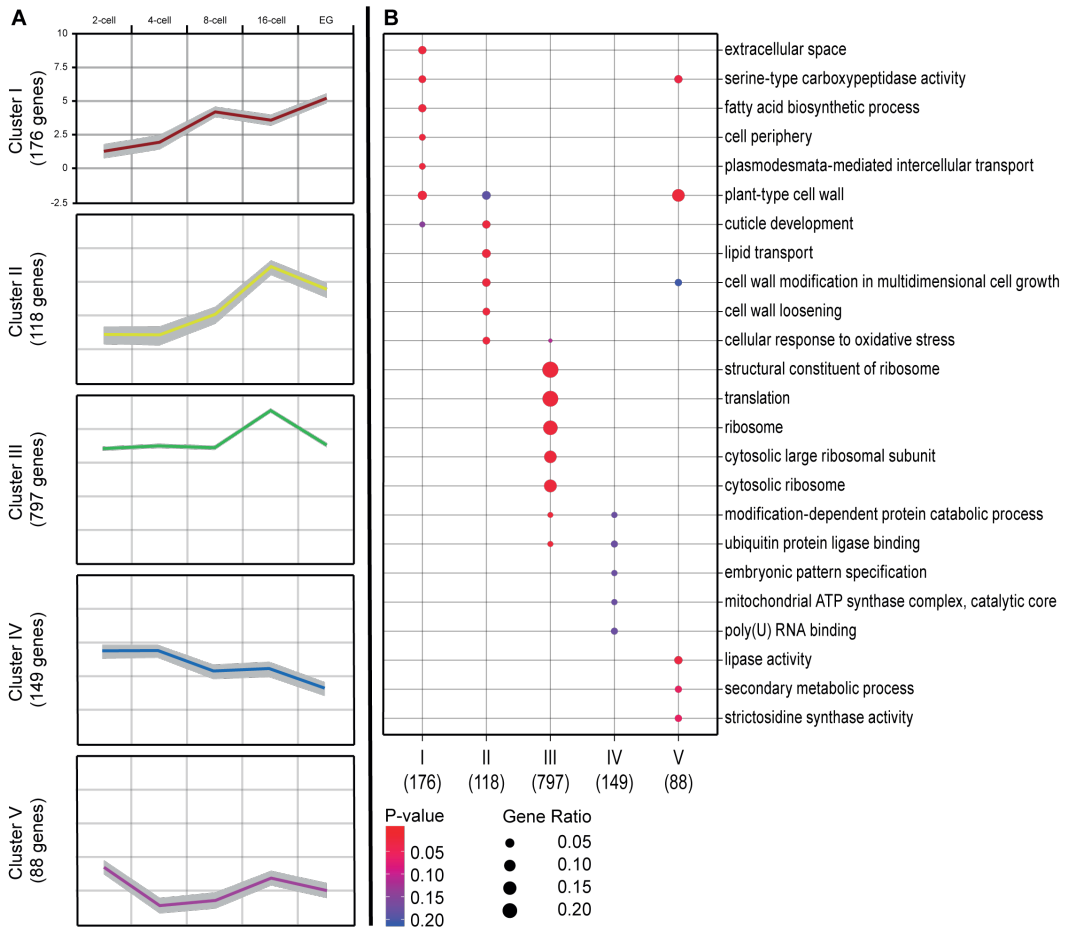
Given that several “marker” genes are correctly represented by the stage-specific transcriptomes, we explored the dataset to identify groups of genes with related expression patterns over the 5 consecutive embryonic stages. K-means clustering based on Log2CPM values revealed 5 major expression clusters (Fig. 9). These 5 clusters together represent the expression of 1328 genes, which corresponds to 15 % of the genes for which expression could be detected during at least one stage. Next, we analysed the enrichment of cellular functions in each cluster by calculating GO-term enrichments (fig. 9A). Importantly, different terms were enriched in each cluster (Fig. 9B).

In the first 2 clusters, expression is low during the two earliest embryonic stages, and increases towards early-globular stage embryos (Fig. 9A). The peak expression of cluster I is at 8-cell and early-globular stage, while maximal expression in cluster II is at 16-cell stage (fig. 9A). Genes in these clusters are mainly associated with cell wall (modification) and transport (fig.9B). These clusters contain a large group of known essential regulators in key developmental processes like stem cell maintenance (*WIP4/5*, *CLAVATA-RELATED16/17/19/25*), cell fate identity specification and maintenance (*TMO5/6*, *SHR*, *JKD*), auxin biosynthesis/transport (*YUC3*, *LAX2*) and transcriptional regulation (bHLH transcription factors *AT5G50915/AT1G29950* and *LBD18/40*).

In cluster III, expression is high throughout all stages, and increases in 16-cell embryos. This cluster contains a large part of detectable genes, and the majority of genes translates into ribosomal proteins or are involved in maintenance of translation and protein degradation (ubiquitins) (fig. 9). Remarkably, this cluster also contains a large group of  $\text{Ca}^{2+}$ -sensors and cytoskeleton related factors including all 7 Calmodulin genes, 5 Calmodulin-like genes, 3 Actin-related factors and the microtubule-associated gene *SPIRAL1* (*SPR1*).

In cluster IV, expression is moderately high in the two earlier stages, and decreases gradually over the later stages. In cluster V, expression is moderate in 2-cell embryos, but decreases in later stages and remains low. Because of their specific pattern, these clusters could identify genes that have specific functions in the earliest stages of embryogenesis. Genes in these clusters are mainly associated with embryonic pattern specification and protein degradation (fig. 9). Cluster IV contains the *WOX2* gene, which was shown to

be essential for correct embryonic patterning during the earliest stages of embryogenesis (Breuninger et al., 2008). Within cluster IV and V, genes like *RALF-LIKE18* (*RALFL18*), *CELLULASE3* (*CEL3*), *PATELLINI* (*PATL1*), *RWP-RK DOMAIN-CONTAINING3* (*RKD3*), and *NITRILASE2* (*NIT2*) are possible novel candidates for functions during early embryogenesis based on this expression pattern and their function in cell wall organisation, membrane trafficking, embryonic transcriptional control, IAA hydrolysis, and general plant physiology (Campbell & Turner, 2017; Kőszegi et al., 2011; Lewis et al., 2013; Peterman, 2004; Vorwerk et al., 2001).



**Figure 9:** Expression pattern clustering and GO-enrichment studies across the Arabidopsis embryo time series dataset. **a** K-means clustering using log-counts-per-million (logCPM) values for all genes in each of the five clusters generated. The number of genes grouping in the cluster is indicated on the left. Polygons represent  $\pm 1$  standard deviation. **b** Plot of gene ontology (GO) term enrichment in all 5 clusters. P-value cut-off is 0.1

## Discussion

A variety of methods has been developed for Arabidopsis embryo isolation and subsequent low-input mRNA-seq analysis (Gehring et al., 2011; Hsieh et al., 2011; Hu et al., 2011; Nodine & Bartel, 2010). Here, we combined high-throughput isolation of Arabidopsis ovules and efficient isolation of early-stage embryos with the low-input Smart-seq2 mRNA-seq protocol which ensures an increased number of detectable genes and relatively uniform coverage along the transcripts (Hofmann et al., 2019; Nodine & Bartel, 2012). Evaluating the quality of the obtained data showed that we are able to isolate Arabidopsis embryos from 2-cell to early-globular stage that are of high quality and, for most stages, contain minimal amounts of seed coat and endosperm contamination. The seed coat contamination detected in later-stage embryo samples shows that future efforts in method optimization should be aimed at the reduction of seed coat contamination, which could be achieved by adding an extra wash step for these samples.

Using the M0171>>*bd1* mutant, which has a dramatic change in transcriptomic profile, we showed that our method is suitable to detect substantial groups of misexpressed genes in early embryonic stages with known functions in downstream suspensor specific auxin signalling (Radoeva et al., 2019). The extra-embryonic suspensor is crucial for nutrient transport and mechanical support of the pro-embryo (Laux, 1997). The quiescent suspensor cells have the ability to adopt an embryonic fate when response to the signalling molecule auxin is specifically blocked in the suspensor (M0171>>*bd1*) (Rademacher et al., 2012). Transcriptome analysis comparing globular WT- and M0171>>*bd1* Arabidopsis embryos revealed an auxin-dependent Helix-Loop-Helix transcription factor network that mediates the activity of auxin itself, subsequently suppressing embryo identity in the suspensor (Radoeva et al., 2018). Here, we compare between this previously generated globular stage M0171>>*bd1* dataset (Radoeva et al., 2018) to our own M0171>>*bd1* datasets generated from 8- and 16 cell embryos. This data gives a unique chance to analyse the transcriptomic changes underlying a developmental process over different developmental stages. The comparison revealed a majority of uniquely mis-regulated genes for each embryonic stage, but also a significant group of mis-regulated genes shared between the different embryonic stages. In accordance with previous finding (Radoeva et al., 2018), the majority of factors shared between the different stages are involved in re-establishment of auxin biosynthesis and regulation of auxin transport. Since morphological changes towards embryonic identity are observed in post-globular embryo suspensors, most studies to date focused on post-globular embryos. Our present dataset however shows a large group of severely

mis-regulated genes already in 8- and 16-cell stage embryos. Identified upregulated genes could be involved in suspensor derived embryogenesis through transcriptional regulation of important pro-embryonic factors. On the contrary, identified downregulated could be involved in maintaining suspensor identity- or development during the earliest stages of embryogenesis.

Using the *tmo5 t5l* and *lhw* mutants, which have subtle effects on transcriptomic profile, we showed that our method is sensitive enough to detect substantial groups of misexpressed genes in early embryonic stages with known functions in cell fate specification downstream of auxin. The identification of the known targets verifies the viability of our dataset, but misregulation of known key targets LOG3/4 (De Rybel et al., 2013a; Ohashi-Ito et al., 2014; Schlereth et al., 2010) or any other cytokinin-related factors are not observed in 8-cell transcriptome datasets. This result reveals an unexpected function for TMO5 and LHW at the 8-cell stage, well before vascular tissue is initiated. Expression of LHW starts early during embryogenesis, but TMO5 expression has not been found before the 16/32-cell stage (Rademacher et al., 2012). It is possible that low-level expression below detection limit of the fluorescent reporter lines occurs at 8-cell stage, and that this expression is biologically relevant. Given that no misexpression of LOG3/4 is seen at 8-cell stage, TMO5 and LHW may not exert their earliest function through cytokinin-mediated signalling. It will be interesting to see if misregulated factors identified specifically in 8-cell *tmo5 t5l* and *lhw* mutant embryos have a role in subsequent vascular tissue initiation.

Next, we generated a reference transcriptome for five early embryonic stages. During the earliest stages of Arabidopsis embryogenesis, all basic basal tissue types of the future plant are formed, making this dataset a powerful tool to shed light on the transcriptional regulation machinery underlying early tissue initiation during plant development. Our data are in accordance with previously published early embryonic datasets (Hofmann et al., 2019; Nodine & Bartel, 2012), and gene expression profiles of known early embryonic factors show expected expression patterns. Expression clustering analysis combined with a GO-enrichment test revealed that each cluster is involved in a unique set of cellular process. Genes that have gradually increasing expression towards later stages are involved in processes related to intercellular transport and plant cell wall regulation. Genes that are specifically upregulated in 16-cell stage embryos are involved in processes related to translation and ribosome structure. Genes that have a high expression in the earlier stages are involved in processes related to embryonic patterning and secondary metabolism. Factors involved in regulation and patterning during the earliest stages of embryogenesis

are largely unknown. Information gained from the cluster analysis can identify novel genes involved in transcriptional regulation of the earliest specification events in plant development.

## Methods

### *Plant material*

Plants used in all experiments were Columbia (Col-0) ecotype except for the *M0171::GAL4* line, which is in the C24 background. The *M0171::GAL4* (Rademacher et al., 2012), *UAS-bdl* (Weijers, 2006), *tmo5 t51l* and *lhw* (De Rybel et al., 2013b) have been previously described.

After seed sterilization, seedlings were plated on half-strength Murashige-Skoog (MS) plates containing 0.8% Dashin agar (Duchefa), an 1% sucrose. After two weeks of growth on plates, seedlings were transferred to soil and further grown at a constant temperature of 22°C under long-day conditions (16 hours light/8 hours dark). For *M0171-GAL4 - UAS-bdl* crossing experiments, the *M0171-GAL4* line was used as female parent, and F1 seeds were harvested 67 or 72 hours after pollination, for 8-cell or 16-cell embryos, respectively. *tmo5/tmo5l* true mutants were selected based on the short root phenotype before transferring to soil.

### *Embryo isolation*

Ovules were collected from ~60 siliques using vacuum extraction. Siliques were stuck to double-sided tape and sliced open using a needle. Open siliques were submerged in 1x Phosphate-Buffered Saline (PBS) buffer and ovules were collected using a vacuum pump through 50 µm filters. Collected ovules were then transferred to Isolation buffer (1x First Strand Buffer (FSB; Invitrogen), 1mM Dithiotreitol (DTT), 4% RNaseLater, MQ), and volume was reduced to ~20 µL. Embryo isolation was performed according to (Raissig, 2013) with the following adaptations. A Zeiss Confocor 1 inverted microscope (Carl Zeiss Microscopy GmbH, Jena, Germany) together with an Eppendorf Transferman 4r micromanipulator (Eppendorf AG) and VacuTip II microcapillaries (Eppendorf) were used to isolate about 40-50 washed embryos in 50 µl isolation buffer.

*RNA isolation and RNA-seq library preparation*

Isolated embryos were immediately incubated with 500 µl of TRIzol reagent (Ambion, CA, USA) for 30 min at 60°C, and samples were vortexed briefly (2×for two seconds each) to completely lyse cells. 100 µl of chloroform was added, and incubated at room temperature for three minutes after vigorous vortexing for 15 seconds. The samples were centrifuged at 12,000g for 15 min at 4 °C, and the aqueous phase (~350 µl) was transferred to a new LoBind tube. To precipitate the RNA, 250 µl of isopropanol and 1.5 µl of GlycoBlue (22.5 µg; Life Tech) was added followed by a -20 °C overnight incubation and centrifugation at >20,000 g for 30 min at 4 °C. After removal of the supernatant, the pellet was washed by adding 500 µl of 75% ethanol, vortexing briefly and then centrifuged at max speed for 15 min at 4 °C. This 75% ethanol wash step was repeated, and after removal of the 75% ethanol the pellet was air dried on ice for 10 min. Precipitated RNA was then resuspended with 11 µl of nuclease-free water and incubated at 60 °C for 10 minutes to fully resuspend.

Samples were DNaseI treated using the RNase-free DNase set (Qiagen), and cleaned up using the RNeasy Minelute kit (Qiagen). Samples were eluted in 12 µL RNase-free water and stored at -80 °C.

Smart-seq2 mRNA libraries were generated according to (Picelli et al., 2013) with the following adaptation. Final library preparation is done using the ThruPLEX DNA-seq kit (Takara Bio UASA). Control of quality and fragment length for both amplified cDNA and final libraries was done using High Sensitivity DNA chips and Bioanalyzer (Agilent)

*RNA-sequencing and quantification*

For differential expression analysis, quality assessment for raw RNA-seq reads was performed using FastQC ([www.bioinformatics.babraham.ac.uk/projects/fastqc](http://www.bioinformatics.babraham.ac.uk/projects/fastqc)). Illumina adapters at the ends of the (paired) reads were cleaned up using TrimGalore (v0.5.0; <https://github.com/FelixKrueger/TrimGalore>) with the parameters “--stringency 5 --paired --length 70 --clip\_R1 30 --clip\_R2 30”. The cleaned FASTQ reads were mapped onto the Arabidopsis genome (TAIR10) using HISAT2 (v2.1.0; Kim et al. 2015) with default parameters. Post-processing of SAM/BAM files was performed using SAMTOOLS (v1.9; Li et al. 2009). FeatureCounts (v1.6.2; Liao et al. 2014) was used to count the raw reads corresponding to each gene, with the parameters “-t ‘exon’ -g ‘gene\_id’ -Q 30 -p --primary”. DEseq2 (Love et al., 2014) was used to normalize the raw counts and perform

the differential expression analysis ( $\text{Padj} < 0.05$ ).

For PCA comparison analysis on embryo timeline dataset, we performed quality control, read filtering and base correction for the raw read data using the Fastp version 0.19.7 tool1 (Chen et al., 2018). Then, we used the high-quality read data to quantify the Arabidopsis genome TAIR11 representative gene model expression using Salmon version 0.13.0 in mapping-based mode with mapping validation2 (Patro et al., 2017). Read counts were used as input for differential expression analysis using the Bioconductor package edgeR version 3.24.3. A one-way analysis of variance (ANOVA)-like testing was performed using the glmQLFTest function in edgeR with an FDR cutoff of 0.05. The log-counts-per-million (logCPM) values were used for K-means clustering using the MeV version 4.8.13 (Howe et al., 2011). Gene ontology (GO) enrichment analysis was performed using the Bioconductor package clusterProfiler version 3.10.14 (Yu et al., 2012). For the principal component analysis (PCA), we also integrated the RNA-seq data came from (Hofmann et al., 2019; Nodine & Bartel, 2012). The logCPM values were used as input data and the built-in removeBatchEffect function provided by the Bioconductor package limma version 3.38.37 was used to remove the batch effect (Ritchie et al., 2015). After that, we used the built-in R function prcomp to perform the principal component analysis (PCA).

## Acknowledgements

This work was supported by a Netherlands Organization for Scientific Research (NWO) grant (ALW 824.14.009) to D.W.

## References

- Beeckman, T., De Rycke, R., Viane, R., & Inzé, D. (2006). Histological Study of Seed Coat Development in *Arabidopsis thaliana*. *Journal of Plant Research*. <https://doi.org/10.1007/pl00013924>
- Breuninger, H., Rikirsch, E., Hermann, M., Ueda, M., & Laux, T. (2008). Differential Expression of WOX Genes Mediates Apical-Basal Axis Formation in the *Arabidopsis* Embryo. *Developmental Cell*. <https://doi.org/10.1016/j.devcel.2008.03.008>
- Brown, R. C., Lemmon, B. E., Nguyen, H., & Olsen, O. A. (1999). Development of endosperm in *Arabidopsis thaliana*. *Sexual Plant Reproduction*. <https://doi.org/10.1007/s004970050169>
- Bryan, A. C., Obaidi, A., Wierzba, M., & Tax, F. E. (2012). XYLEM INTERMIXED WITH PHLOEM1, a leucine-rich repeat receptor-like kinase required for stem growth and vascular development in *Arabidopsis thaliana*. *Planta*. <https://doi.org/10.1007/s00425-011-1489-6>
- Campbell, L., & Turner, S. R. (2017). A Comprehensive Analysis of RALF Proteins in Green Plants Suggests There Are Two Distinct Functional Groups. *Frontiers in Plant Science*. <https://doi.org/10.3389/fpls.2017.00037>
- Chandler, J. W., Cole, M., Flier, A., Grewe, B., & Werr, W. (2007). The AP2 transcription factors DORNROSCHEN and DORNROSCHEN-LIKE redundantly control *Arabidopsis* embryo patterning via interaction with PHAVOLUTA. *Development*. <https://doi.org/10.1242/dev.001016>
- Chandler, J. W., & Werr, W. (2017). DORNROSCHEN, DORNROSCHEN-LIKE, and PUCHI redundantly control floral meristem identity and organ initiation in *Arabidopsis*. *Journal of Experimental Botany*. <https://doi.org/10.1093/jxb/erx208>
- Chen, S., Zhou, Y., Chen, Y., & Gu, J. (2018). Fastp: An ultra-fast all-in-one FASTQ preprocessor. *Bioinformatics*. <https://doi.org/10.1093/bioinformatics/bty560>
- Crawford, B. C. W., Sewell, J., Golembeski, G., Roshan, C., Long, J. A., & Yanofsky, M. F. (2015). Genetic control of distal stem cell fate within root and embryonic meristems. *Science*. <https://doi.org/10.1126/science.aaa0196>

- De Rybel, B., Adibi, M., Breda, A. S., Wendrich, J. R., Smit, M. E., Novák, O., ... Weijers, D. (2014). Plant development. Integration of growth and patterning during vascular tissue formation in Arabidopsis. *Science* (New York, N.Y.), 345(6197), 1255215. <https://doi.org/10.1126/science.1255215>
- De Rybel, B., Möller, B., Yoshida, S., Grabowicz, I., Barbier de Reuille, P., Boeren, S., ... Weijers, D. (2013a). A bHLH complex controls embryonic vascular tissue establishment and indeterminate growth in Arabidopsis. *Developmental Cell*, 24(4), 426–437. <https://doi.org/10.1016/j.devcel.2012.12.013>
- De Rybel, B., Möller, B., Yoshida, S., Grabowicz, I., Barbier de Reuille, P., Boeren, S., ... Weijers, D. (2013b). A bHLH Complex Controls Embryonic Vascular Tissue Establishment and Indeterminate Growth in Arabidopsis. *Developmental Cell*, 24(4), 426–437. <https://doi.org/10.1016/j.devcel.2012.12.013>
- Gehring, M., Missirlian, V., & Henikoff, S. (2011). Genomic analysis of parent-of-origin allelic expression in arabidopsis thaliana seeds. *PLoS ONE*. <https://doi.org/10.1371/journal.pone.0023687>
- Gooh, K., Ueda, M., Aruga, K., Park, J., Arata, H., Higashiyama, T., & Kurihara, D. (2015). Live-Cell Imaging and Optical Manipulation of Arabidopsis Early Embryogenesis. *Developmental Cell*. <https://doi.org/10.1016/j.devcel.2015.06.008>
- Haecker, A. (2004). Expression dynamics of WOX genes mark cell fate decisions during early embryonic patterning in Arabidopsis thaliana. *Development*. <https://doi.org/10.1242/dev.00963>
- Hofmann, F., Schon, M. A., & Nodine, M. D. (2019). The embryonic transcriptome of Arabidopsis thaliana. *Plant Reproduction*. <https://doi.org/10.1007/s00497-018-00357-2>
- Howe, E. A., Sinha, R., Schlauch, D., & Quackenbush, J. (2011). RNA-Seq analysis in MeV. *Bioinformatics*. <https://doi.org/10.1093/bioinformatics/btr490>
- Hsieh, T. F., Shin, J., Uzawa, R., Silva, P., Cohen, S., Bauer, M. J., ... Fischer, R. L. (2011). Regulation of imprinted gene expression in Arabidopsis endosperm. *Proceedings of the National Academy of Sciences of the United States of America*. <https://doi.org/10.1073/pnas.1019273108>
- Hu, T. X., Yu, M., & Zhao, J. (2011). Comparative transcriptional analysis reveals differential

gene expression between asymmetric and symmetric zygotic divisions in tobacco. *PLoS ONE*. <https://doi.org/10.1371/journal.pone.0027120>

Jürgens, G., & Mayer, U. (1994). “Arabidopsis,” in *A colour Atlas of Developing Embryos. Harcourt Health Sciences*.

Köszei, D., Johnston, A. J., Rutten, T., Czihal, A., Altschmied, L., Kumlehn, J., ... Bäumlein, H. (2011). Members of the RKD transcription factor family induce an egg cell-like gene expression program. *Plant Journal*. <https://doi.org/10.1111/j.1365-313X.2011.04592.x>

Ku, S. J., Park, J. Y., Ha, S. B., & Kim, J. (2009). Overexpression of IAA1 with domain II mutation impairs cell elongation and cell division in inflorescences and leaves of Arabidopsis. *Journal of Plant Physiology*. <https://doi.org/10.1016/j.jplph.2008.07.006>

Laux, T. (1997). Embryogenesis: A New Start in Life. *The plant cell online*. <https://doi.org/10.1105/tpc.9.7.989>

Laux, T. (2004). Genetic Regulation of Embryonic Pattern Formation. *The plant cell online*. <https://doi.org/10.1105/tpc.016014>

Lewis, D. R., Olex, A. L., Lundy, S. R., Turkett, W. H., Fetrow, J. S., & Muday, G. K. (2013). A Kinetic Analysis of the Auxin Transcriptome Reveals Cell Wall Remodeling Proteins That Modulate Lateral Root Development in Arabidopsis. *The Plant Cell*. <https://doi.org/10.1105/tpc.113.114868>

Long, Y., Smet, W., Cruz-Ramírez, A., Castelijns, B., de Jonge, W., Mähönen, A. P., ... Blilou, I. (2015). Arabidopsis BIRD Zinc Finger Proteins Jointly Stabilize Tissue Boundaries by Confining the Cell Fate Regulator SHORT-ROOT and Contributing to Fate Specification. *The Plant Cell*. <https://doi.org/10.1105/tpc.114.132407>

Mayer, U., Ruiz, R. A. T., Berleth, T., Miseéra, S., & Jürgens, G. (1991). Mutations affecting body organization in the Arabidopsis embryo. *Nature*. <https://doi.org/10.1038/353402a0>

Motose, H., Sugiyama, M., & Fukuda, H. (2004). A proteoglycan mediates inductive interaction during plant vascular development. *Nature*. <https://doi.org/10.1038/nature02613>

Nodine, M. D., & Bartel, D. P. (2010). MicroRNAs prevent precocious gene expression and enable pattern formation during plant embryogenesis. *Genes and Development*. <https://doi.org/10.1101/gad.1986710>

Nodine, M. D., & Bartel, D. P. (2012). Maternal and paternal genomes contribute equally to the transcriptome of early plant embryos. *Nature*, 482(7383), 94–97. <https://doi.org/10.1038/nature10756>

Ohashi-Ito, K., Saegusa, M., Iwamoto, K., Oda, Y., Katayama, H., Kojima, M., ... Fukuda, H. (2014). A bHLH complex activates vascular cell division via cytokinin action in root apical meristem. *Current Biology: CB*, 24(17), 2053–2058. <https://doi.org/10.1016/j.cub.2014.07.050>

Palovaara, J., de Zeeuw, T., & Weijers, D. (2016). Tissue and Organ Initiation in the Plant Embryo: A First Time for Everything. *Annual Review of Cell and Developmental Biology*, 32(1), annurev-cellbio-111315-124929. <https://doi.org/10.1146/annurev-cellbio-111315-124929>

Palovaara, J., Saiga, S., Wendrich, J. R., Van 't Wout Hofland, N., Van Schayck, J. P., Hater, F., ... Weijers, D. (2017). Transcriptome dynamics revealed by a gene expression atlas of the early Arabidopsis embryo. *Nature Plants*. <https://doi.org/10.1038/s41477-017-0035-3>

Patro, R., Duggal, G., Love, M. I., Irizarry, R. A., & Kingsford, C. (2017). Salmon provides fast and bias-aware quantification of transcript expression. *Nature Methods*. <https://doi.org/10.1038/nmeth.4197>

Peterman, T. K. (2004). Patellin1, a Novel Sec14-Like Protein, Localizes to the Cell Plate and Binds Phosphoinositides. *Plant physiology*. <https://doi.org/10.1104/pp.104.045369>

Picelli, S., Björklund, Å. K., Faridani, O. R., Sagasser, S., Winberg, G., & Sandberg, R. (2013). Smart-seq2 for sensitive full-length transcriptome profiling in single cells. *Nature Methods*. <https://doi.org/10.1038/nmeth.2639>

Picelli, S., Faridani, O. R., Björklund, Å. K., Winberg, G., Sagasser, S., & Sandberg, R. (2014). Full-length RNA-seq from single cells using Smart-seq2. *Nature Protocols*. <https://doi.org/10.1038/nprot.2014.006>

Piya, S., Shrestha, S. K., Binder, B., Stewart, C. N., & Hewezi, T. (2014). Protein-protein interaction and gene co-expression maps of ARFs and Aux/IAAs in Arabidopsis. *Frontiers in Plant Science*. <https://doi.org/10.3389/fpls.2014.00744>

Rademacher, E. H., Lokerse, A. S., Schlereth, A., Llavata-Peris, C. I., Bayer, M., Kientz, M., ... Weijers, D. (2012). Different Auxin Response Machineries Control Distinct Cell Fates in

the Early Plant Embryo. *Developmental Cell*. <https://doi.org/10.1016/j.devcel.2011.10.026>

Radoeva, T., Lokerse, A. S., Llavata-Peris, C. I., Wendrich, J. R., Xiang, D., Liao, C.-Y., ... Weijers, D. (2019). A Robust Auxin Response Network Controls Embryo and Suspensor Development through a Basic Helix Loop Helix Transcriptional Module. *The Plant Cell*. <https://doi.org/10.1105/tpc.18.00518>

Radoeva, T., Saiga, S., & Weijers, D. (2018). Cell-type-specific promoter identification using enhancer trap lines. In *Methods in Molecular Biology*. [https://doi.org/10.1007/978-1-4939-8657-6\\_8](https://doi.org/10.1007/978-1-4939-8657-6_8)

Raissig, M. T., Gagliardini, V., Jaenisch, J., Grossniklaus, U., & Baroux, C. (2013). Efficient and Rapid Isolation of Early-stage Embryos from *Arabidopsis thaliana* Seeds. *Journal of Visualized Experiments*. <https://doi.org/10.3791/50371>

Ritchie, M. E., Phipson, B., Wu, D., Hu, Y., Law, C. W., Shi, W., & Smyth, G. K. (2015). limma powers differential expression analyses for RNA-sequencing and microarray studies. *Nucleic Acids Research*. <https://doi.org/10.1093/nar/gkv007>

Robert, H. S., Grunewald, W., Sauer, M., Cannoot, B., Soriano, M., Swarup, R., ... Friml, J. (2015). Plant embryogenesis requires AUX/LAX-mediated auxin influx. *Development*. <https://doi.org/10.1242/dev.115832>

Schlereth, A., Möller, B., Liu, W., Kientz, M., Flipse, J., Rademacher, E. H., ... Weijers, D. (2010). MONOPTEROS controls embryonic root initiation by regulating a mobile transcription factor. *Nature*, 464(7290), 913–916. <https://doi.org/10.1038/nature08836>

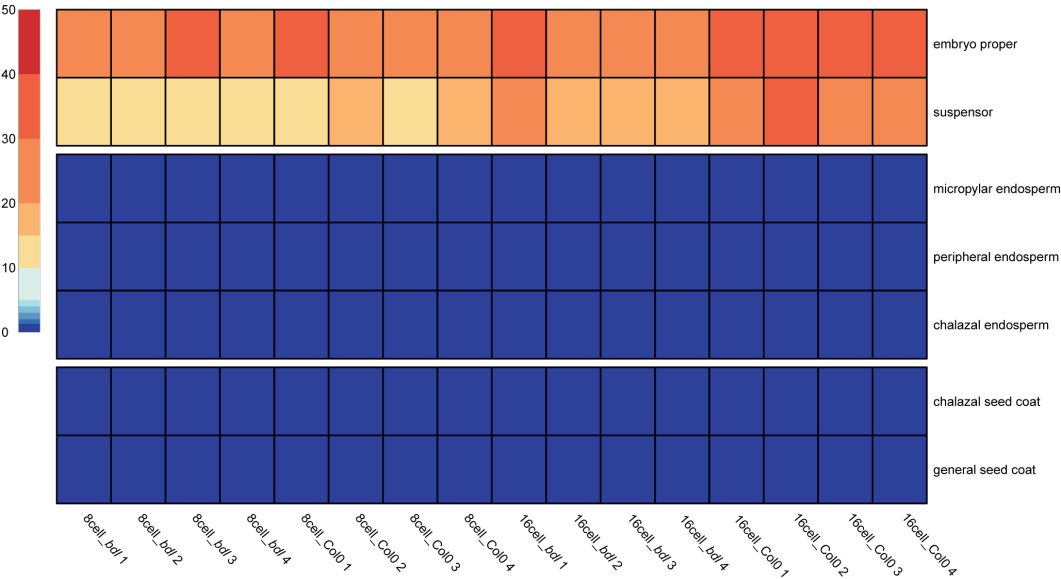
Schon, M. A., & Nodine, M. D. (2017). Widespread Contamination of *Arabidopsis* Embryo and Endosperm Transcriptome Data Sets. *The Plant Cell*. <https://doi.org/10.1105/tpc.16.00845>

Vera-Sirera, F., De Rybel, B., Úrbez, C., Kouklas, E., Pesquera, M., Álvarez-Mahecha, J. C., ... Blázquez, M. A. (2015). A bHLH-Based Feedback Loop Restricts Vascular Cell Proliferation in Plants. *Developmental Cell*. <https://doi.org/10.1016/j.devcel.2015.10.022>

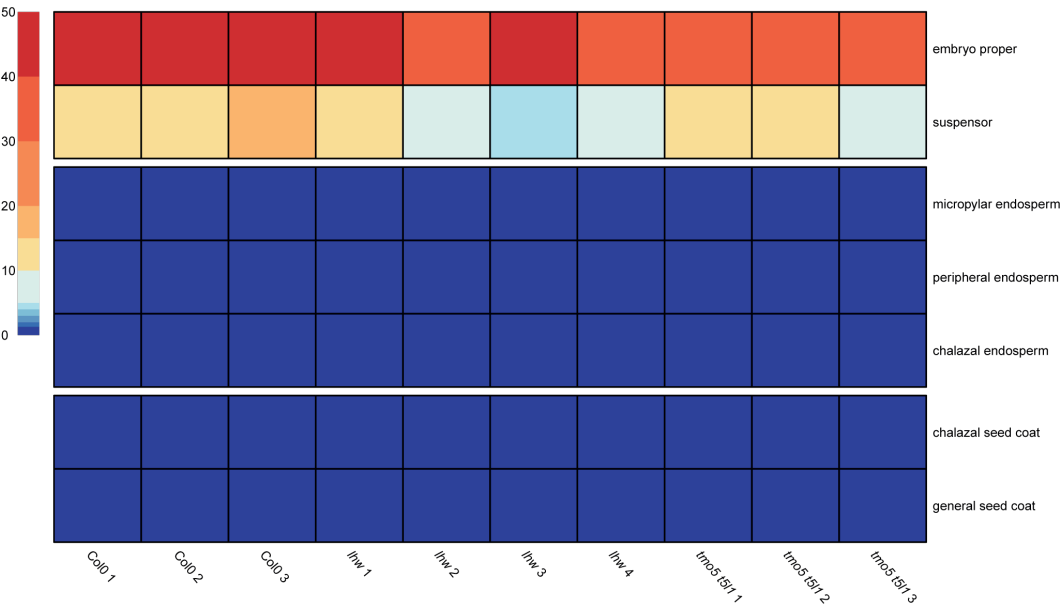
Vorwerk, S., Biernacki, S., Hillebrand, H., Janzik, I., Müller, A., Weiler, E. W., & Piotrowski, M. (2001). Enzymatic characterization of the recombinant *Arabidopsis thaliana* nitrilase subfamily encoded by the NIT2/NIT1/NIT3-gene cluster. *Planta*. <https://doi.org/10.1007/s004250000420>

- Weijers, D., Schlereth, A., Ehrismann, J. S., Schwank, G., Kientz, M., & Jürgens, G. (2006). Auxin triggers transient local signaling for cell specification in Arabidopsis embryogenesis. *Developmental Cell*. <https://doi.org/10.1016/j.devcel.2005.12.001>
- Welch, D., Hassan, H., Blilou, I., Immink, R., Heidstra, R., & Scheres, B. (2007). Arabidopsis JACKDAW and MAGPIE zinc finger proteins delimit asymmetric cell division and stabilize tissue boundaries by restricting SHORT-ROOT action. *Genes and Development*. <https://doi.org/10.1101/gad.440307>
- Xiang, D., Venglat, P., Tibiche, C., Yang, H., Risseuw, E., Cao, Y., ... Datla, R. (2011). Genome-Wide Analysis Reveals Gene Expression and Metabolic Network Dynamics during Embryo Development in Arabidopsis. *PLANT PHYSIOLOGY*. <https://doi.org/10.1104/pp.110.171702>
- Yoshida, S., Barbier de Reuille, P., Lane, B., Bassel, G. W., Prusinkiewicz, P., Smith, R. S., & Weijers, D. (2014). Genetic control of plant development by overriding a geometric division rule. *Developmental Cell*, 29(1), 75–87. <https://doi.org/10.1016/j.devcel.2014.02.002>
- Yu, G., Wang, L.-G., Han, Y., & He, Q.-Y. (2012). clusterProfiler: an R package for comparing biological themes among gene clusters. *Omics : A Journal of Integrative Biology*. <https://doi.org/10.1089/omi.2011.0118>

Supplementary materials



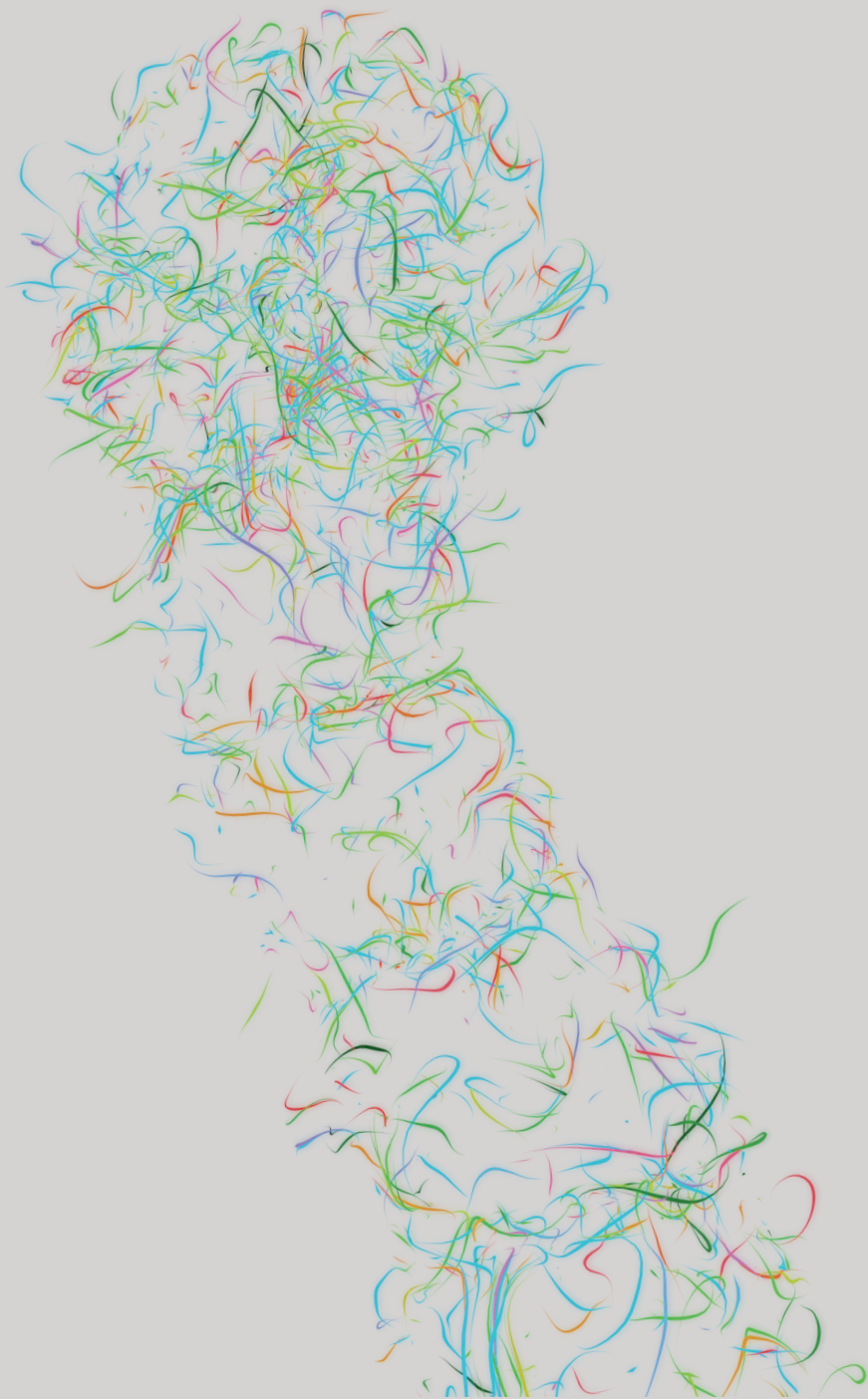
**Figure S1:** Heat map of tissue enrichment test results of 16 transcriptomes from 8-cell and 16-cell M0171>>ddl and wild-type embryos. Legend show tissue enrichment score values (-log10 p-value), rows represent tissue subregions. Tissue enrichment tests are performed like described in (Schon & Nodine, 2017).



**Figure S2:** Heat map of tissue enrichment test results of 16 transcriptomes from 8-cell wild-type, lhw and tmo5 t5l1 embryos. Legend show tissue enrichment score values (-log10 p-value), rows represent tissue subregions. Tissue enrichment tests are performed like described in (Schon & Nodine, 2017).

**Table S1:** RNA-sequencing details for three datasets (M0171>>*bdl* vs M0171>>*col0*, *tmo5 t5l1* vs *lhw* vs *col0*, embryo transcriptomic timeline). Details are given for sequencing technique, sequencing read type, number of clusters sequenced, and base quality in percentage of bases that has a quality (Q) score over 30)

Sample ID	Illumina sequencer	Sequencing read type	Clusters	Base quality (%>=30)
8cell M0171>> <i>col0</i> _1	NovaSeq 6000	paired-end 150bp	12,969,831	88.33
8cell M0171>> <i>col0</i> _2	NovaSeq 6000	paired-end 150bp	13,852,123	88.81
8cell M0171>> <i>col0</i> _3	NovaSeq 6000	paired-end 150bp	17,720,045	87.75
8cell M0171>> <i>col0</i> _4	NovaSeq 6000	paired-end 150bp	15,960,042	88.07
8cell M0171>> <i>bdl</i> _1	NovaSeq 6000	paired-end 150bp	18,690,528	88.4
8cell M0171>> <i>bdl</i> _2	NovaSeq 6000	paired-end 150bp	15,872,089	88.88
8cell M0171>> <i>bdl</i> _3	NovaSeq 6000	paired-end 150bp	15,683,241	87
8cell M0171>> <i>bdl</i> _4	NovaSeq 6000	paired-end 150bp	14,666,397	87.42
16cell M0171>> <i>col0</i> _1	NovaSeq 6000	paired-end 150bp	12,707,123	87.73
16cell M0171>> <i>col0</i> _2	NovaSeq 6000	paired-end 150bp	15,461,485	88.31
16cell M0171>> <i>col0</i> _3	NovaSeq 6000	paired-end 150bp	13,885,398	87.87
16cell M0171>> <i>col0</i> _4	NovaSeq 6000	paired-end 150bp	18,263,901	87.7
16cell M0171>> <i>bdl</i> _1	NovaSeq 6000	paired-end 150bp	18,569,085	88.52
16cell M0171>> <i>bdl</i> _2	NovaSeq 6000	paired-end 150bp	16,999,593	88.81
16cell M0171>> <i>bdl</i> _3	NovaSeq 6000	paired-end 150bp	15,674,852	86.77
16cell M0171>> <i>bdl</i> _4	NovaSeq 6000	paired-end 150bp	15,936,176	86.82
<i>col0</i> _1	HiSeq 4000	paired-end 150bp	22,738,106	76.47
<i>col0</i> _2	HiSeq 4000	paired-end 150bp	21,067,000	79.7
<i>col0</i> _3	HiSeq 4000	paired-end 150bp	19,468,068	80.98
<i>col0</i> _4	HiSeq 4000	paired-end 150bp	19,580,008	81.25
<i>tmo5 t5l1</i> _1	HiSeq 4000	paired-end 150bp	27,162,015	79.94
<i>tmo5 t5l1</i> _2	HiSeq 4000	paired-end 150bp	25,966,638	78.2
<i>tmo5 t5l1</i> _3	HiSeq 4000	paired-end 150bp	22,910,209	73.34
<i>tmo5 t5l1</i> _4	HiSeq 4000	paired-end 150bp	23,425,520	75.11
<i>lhw</i> _1	HiSeq 4000	paired-end 150bp	7,473,991	80.48
<i>lhw</i> _2	HiSeq 4000	paired-end 150bp	33,091,045	78.43
<i>lhw</i> _3	HiSeq 4000	paired-end 150bp	16,353,911	81.99
<i>lhw</i> _4	HiSeq 4000	paired-end 150bp	22,170,263	75.62
2cell_1	NovaSeq 6000	paired-end 150bp	17,136,937	79.51
2cell_2	NovaSeq 6000	paired-end 150bp	12,536,341	80.39
2cell_3	NovaSeq 6000	paired-end 150bp	20,540,356	78.79
2cell_4	NovaSeq 6000	paired-end 150bp	21,512,315	79.84
4cell_1	NovaSeq 6000	paired-end 150bp	21,102,615	79.09
4cell_2	NovaSeq 6000	paired-end 150bp	18,453,870	80.25
4cell_3	NovaSeq 6000	paired-end 150bp	21,187,619	79.62
4cell_4	NovaSeq 6000	paired-end 150bp	18,580,708	79.86
8cell_1	NovaSeq 6000	paired-end 150bp	13,183,022	79.94
8cell_2	NovaSeq 6000	paired-end 150bp	20,609,391	79.32
8cell_3	NovaSeq 6000	paired-end 150bp	17,860,444	79.6
8cell_4	NovaSeq 6000	paired-end 150bp	19,720,759	79.33
16cell_1	BGISeq 500	single-end 50bp	20,994,339	80.1
16cell_2	BGISeq 500	single-end 50bp	24,463,992	79.75
16cell_3	BGISeq 500	single-end 50bp	34,784,718	79.68
Early Globular_1	BGISeq 500	single-end 50bp	18,914,483	80.21
Early Globular_2	BGISeq 500	single-end 50bp	20,225,549	79.65
Early Globular_3	BGISeq 500	single-end 50bp	28,685,556	79.33



# Chapter 6

## **IQD-family proteins connect auxin signalling to microtubule-dependent cell division control**

Thijs de Zeeuw<sup>1</sup>, Soeren Strauss<sup>2</sup>, Mark Roosjen<sup>1</sup>, Sumanth Mutte<sup>1</sup>, Zhaodong Hao<sup>1</sup>, Jos Wendrich<sup>1,3</sup>, Richard Smith<sup>2</sup>, Dolf Weijers<sup>1\*</sup>

1. Laboratory of Biochemistry, Wageningen University, Stippeneng 4, 6708 WE Wageningen, the Netherlands

2. Laboratory of Computational modelling of morphogenesis and biomechanisms, Max Planck Institute, Carl-von-Linne-Weg 10, D-50829, Cologne, Germany

3. Present address: VIB, Technologiepark 71, 9052, Ghent, Belgium



## Abstract

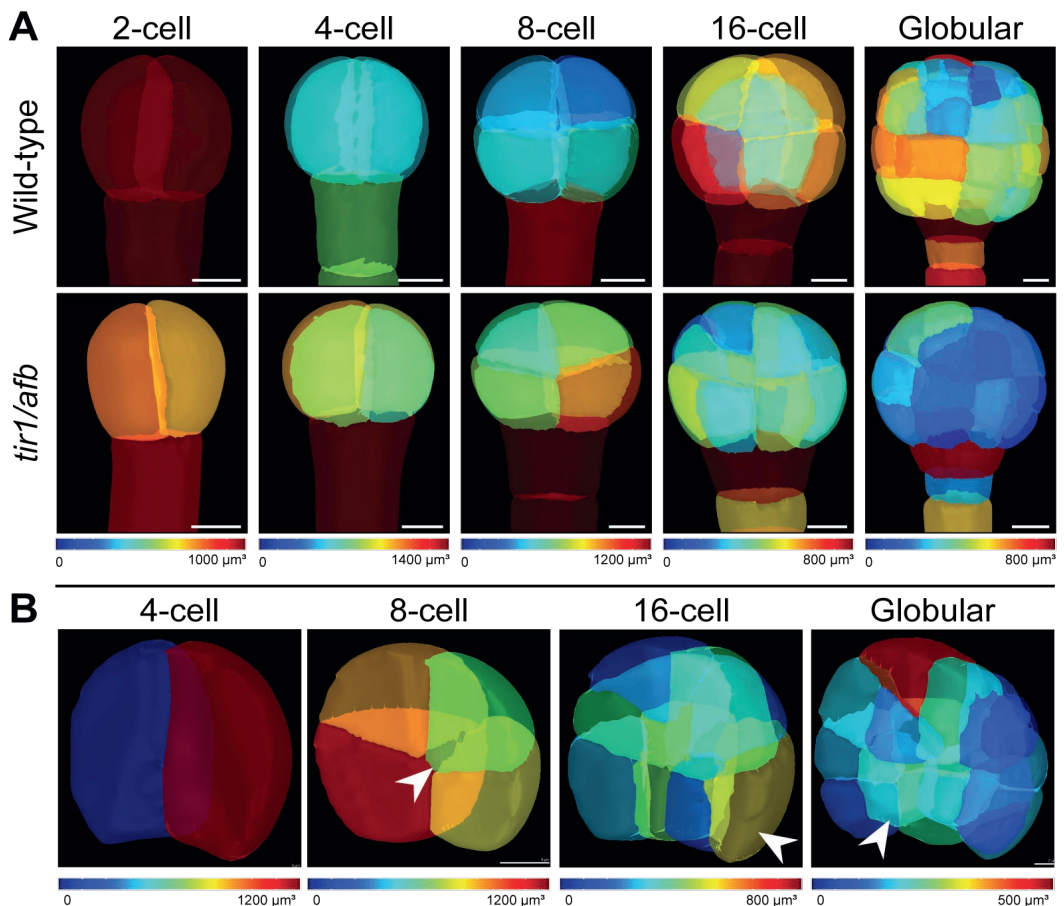
In contrast to animal cells, plant cells are unable to migrate because of their enclosure in pectocellulosic plant cell walls. Therefore, control of cell division orientation is crucial for correct plant development and ultimately plant shape. Most cell divisions in the *Arabidopsis thaliana* embryo divide according “shortest-wall” principles explained by simple geometric rules, except for formative asymmetric divisions. In the auxin-insensitive *bdl*-mutant all formative asymmetric cell divisions switch to symmetric “shortest-wall” divisions, indicating that these divisions are regulated by auxin-signalling. However, since a role in division orientation was inferred from overexpressing a dominant response inhibitor, it is unclear if endogenous auxin regulates division orientation, nor is it known what factors mediate its role. Here, we show that a *tir1/afb* auxin receptor hexuple mutant shows division defects that are comparable to the *bdl*-mutant. We next implemented our previously developed early *Arabidopsis* transcriptome pipeline to compare auxin-insensitive mutant and wild-types 8-cell embryos, and identify factors involved in regulation of cell division orientation through cytoskeletal regulation downstream of auxin. We identify IQ-domain 6 as a possible target downstream of auxin-signalling involved in regulation of cell division plane orientation. Characterization of the IQD6-8 subclade suggests these proteins are involved in cell division orientation control through  $\text{Ca}^{2+}$ -dependent cytoskeleton regulation.

## Introduction

Because of their enclosure in rigid pecto-cellulose cell walls, plant cells are unable to migrate after division (Höfte & Voxeur, 2017). Therefore, control of cell division orientation is crucial for correct plant development and ultimately plant shape. A central question in plant biology is how division orientation is genetically controlled. Empirical rules have been formulated that can rationalise the role cell shape has in determining division plane. The most prominent geometric division rule, proposed by Errera, 1888 and de Wildeman, 1893, states that a cell will divide along the plane of least area that encloses a fixed cellular volume. This type of division was later defined as the “shortest wall” rule and is considered the default division orientation solely based on geometric principles. Experimental data supports this rule but also shows that division plane selection involves a competition between alternative division planes with local area minima, transforming this rule to a stochastic rule (Besson & Dumais, 2011, 2014). All symmetric division during early *Arabidopsis thaliana* embryogenesis can be explained using the geometric “shortest wall” rule, but all formative asymmetric divisions need additional regulation (Yoshida et al., 2014). Inhibition of auxin response in the embryo by expression of a non-degradable version of the AUXIN/INDOLE ACETIC ACID (AUX/IAA) protein BODENLOS/IAA12 (BDL; (Hamann et al., 2002)) under control of the *RPS5A* promoter (*RPS5A>>bdl*; (Yoshida et al., 2014); henceforth referred to as “*bdl*-mutant”) inhibits formative asymmetric divisions in *Arabidopsis* embryos (Yoshida et al., 2014), suggesting that auxin is involved in regulation of division plane orientation during formative asymmetric divisions. Auxin exerts a multitude of cellular outputs through transcriptional regulation of hundreds to thousands of target genes (Paponov et al., 2008). When present, auxin functions as a molecular glue increasing the affinity of SKP1-CULLIN-F-BOX (SCF-TIR1/AFB; (Ruegger et al., 1998)) ubiquitin ligase complexes to Aux/IAA transcriptional co-repressors like BDL (Hamann et al., 2002), resulting in their degradation through the 26S proteasome. Degradation of Aux/IAA proteins releases the AUXIN RESPONSE FACTORS (ARFs; (Tiwari et al., 2007)) transcription factors from inhibition, which can then exert their transcriptional function (reviewed in (Chapman & Estelle, 2009)). Previously, we showed that *bdl*-mutant embryos show defects in microtubule (MT) - and actin cytoskeletal structures (chapter 3 & 4 of this thesis), suggesting that downstream regulation of cell division plane orientation by auxin is regulated through control of the cytoskeleton.

Here, we apply our *Arabidopsis* embryo transcriptome analysis pipeline (chapter 5 of this thesis) to explore molecular regulation connecting auxin signalling to control

cytoskeleton organisation and regulation of division plane orientation during the transition from the 8-cell to the 16-cell embryonic stage. Transcriptional downregulation of the IQ67-domain (IQD) protein IQD6 in the *bdl*-mutant drew our attention. The 33-member IQD protein family has been characterized as a family of MT-Associated Proteins (MAPs) important in different aspects of plant development (Abel et al., 2005; Bürstenbinder et al., 2017b; Liang et al., 2018). Here we report MT-localization of IQD6 and its close relatives IQD7 and IQD8 in *Arabidopsis* embryos and roots, and demonstrate interaction with calmodulins and a variety of cytoskeletal components. Analysis of higher-order *iqd678* mutants shows that these proteins are involved in division plane orientation regulation in the *Arabidopsis* embryo and thus identify IQD proteins as mediators of auxin-dependent



**Figure 1:** 3D embryonic phenotype with volumetric measurements for wild-type and the auxin-insensitive *tir1/afb* mutant. **a** 3D comparison of wild-type and *tir1/afb*-mutant embryos from 2-cell to globular stage. **b** Detailed views of cells from 4-cell to globular stage embryos showing the variation in cell division orientation. Arrowheads indicate embryo quarters divided according to wild-type division patterns. Construction of meshes and volume measurements were performed on segmented modified Pseudo-Schiff propidium iodide (mPS-PI) stained embryonic cells using MorphoGraphX software (Barbier de Reuille et al., 2015). Mesh colour per cell corresponds to cellular volume indicated in the colour scale. Scale bars indicate 5  $\mu\text{m}$  distance.

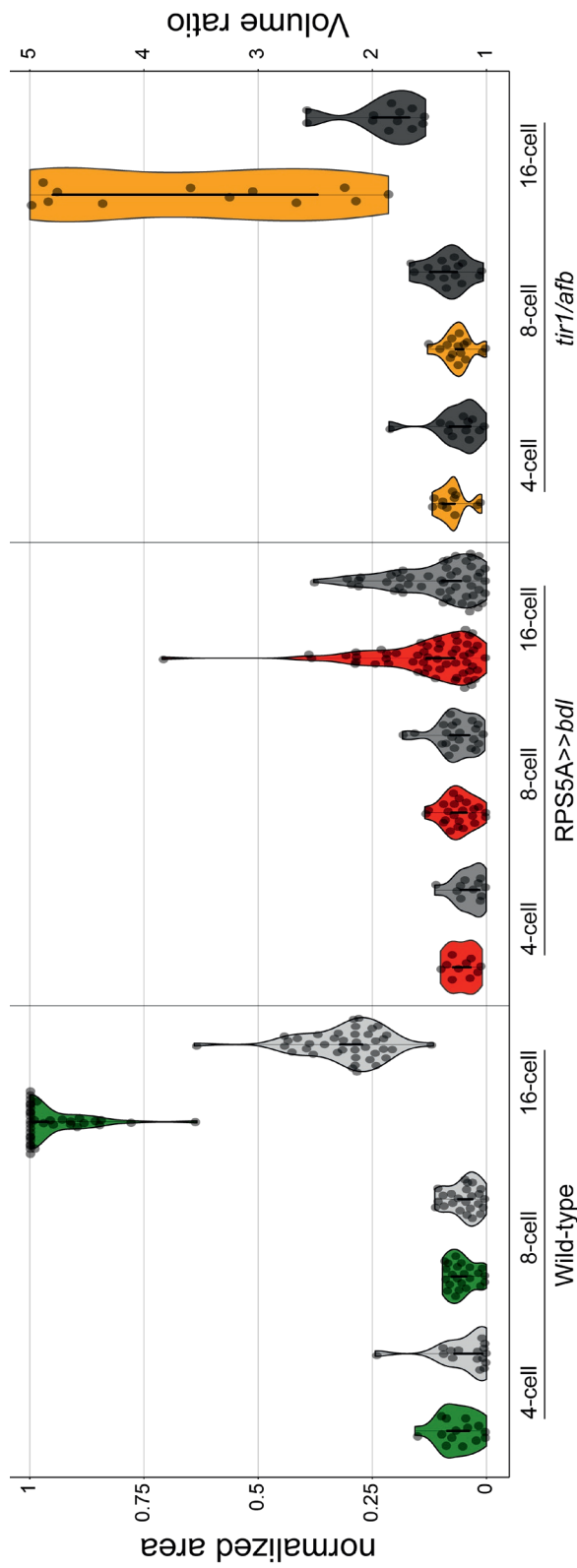
cell division control.

## Results

### *TIR1/AFB-dependent auxin response controls cell division orientation in the early embryo*

The *bdl* mutation that induces cell division defects in the early embryo prevents degradation by the TIR1/AFB-proteasome pathway (Rademacher et al., 2012). Thus, if endogenous auxin acts through these components to control division orientation, one would expect mutants in the TIR1/AFB family proteins to cause similar defects. The Arabidopsis genome encodes six TIR1/AFB proteins with functional redundancies between groups of different members of the family (Parry et al., 2009; Prigge et al., 2016). Since higher-order hexuple mutants (*tir1afb12345*) are infertile, a *tir1afb12345* with segregating *TIR1-mOrange2::AFB5-mCherry::AFB2-mCitrine* transgene was recently successfully created (hereafter referred to as *tir1/afb*-mutant) (Prigge et al., 2019). The hemizygous hexuple *tir1/afb*-mutant has 25% hexuple progeny, which results in early embryo division defects that superficially resemble defects in the *bdl*-mutant (Prigge, 2019). To accurately analyse this *tir1/afb* embryonic mutant division plane phenotype, we implemented a previously established fluorescent staining method combined with high-resolution confocal imaging and cell segmentation (Yoshida et al., 2014). Mutants show skewed division planes in the majority of cells at all early embryonic stages, that strongly resemble divisions observed in *bdl*-mutant embryos (Fig. 1a) (Yoshida et al., 2014). Even though the majority of cells in mutant embryos show the division plane defects resembling the *bdl*-mutant phenotype, we observed more variation in cell division angles and cell volume distribution in daughter cells within the same embryo, at different stages (Fig. 1b). As an illustration of this variation within the mutant embryos, a small number of cells shows division planes that resemble the wild-type, highly asymmetric division pattern (Fig. 1b; arrowheads).

To study the division defects in the *tir1/afb*-mutant in more detail, we implemented a 3D equivalent of the “shortest wall” rule by finding the division plane with minimum- and maximum surface area passing through the centroid of the cell, previously implemented for the *bdl*-mutant (Yoshida et al., 2014). We measured surface area of the true division plane taken during divisions leading to 4-, 8-, and 16-cell embryos, and normalized this against the surface area of the smallest (e.g. “shortest wall”)- and largest cell division surface area possible (Fig. 2). Additionally, we measured the volumes of daughter cells resulting



**Figure 2:** 3D cell division analysis comparing wild-type-, *bdl*-mutant (*RPS5A>>bdl*)-, and *tir1/afb*-mutant embryos. Violin plots representing distribution of cell wall areas as a fraction of the smallest (0 on the left y-axis) and largest (1 on the left y-axis) wall area within the volume of two daughter cells. Wild-type values are shown in green, *bdl*-mutant values are shown in red, *tir1/afb* values are shown in orange. The cell volume ratios resulting from these divisions are represented in gray (light to dark), and values are on the right y-axis. Individual measured cells are shown in the violin plots. At least 3 individual embryos were used per condition.

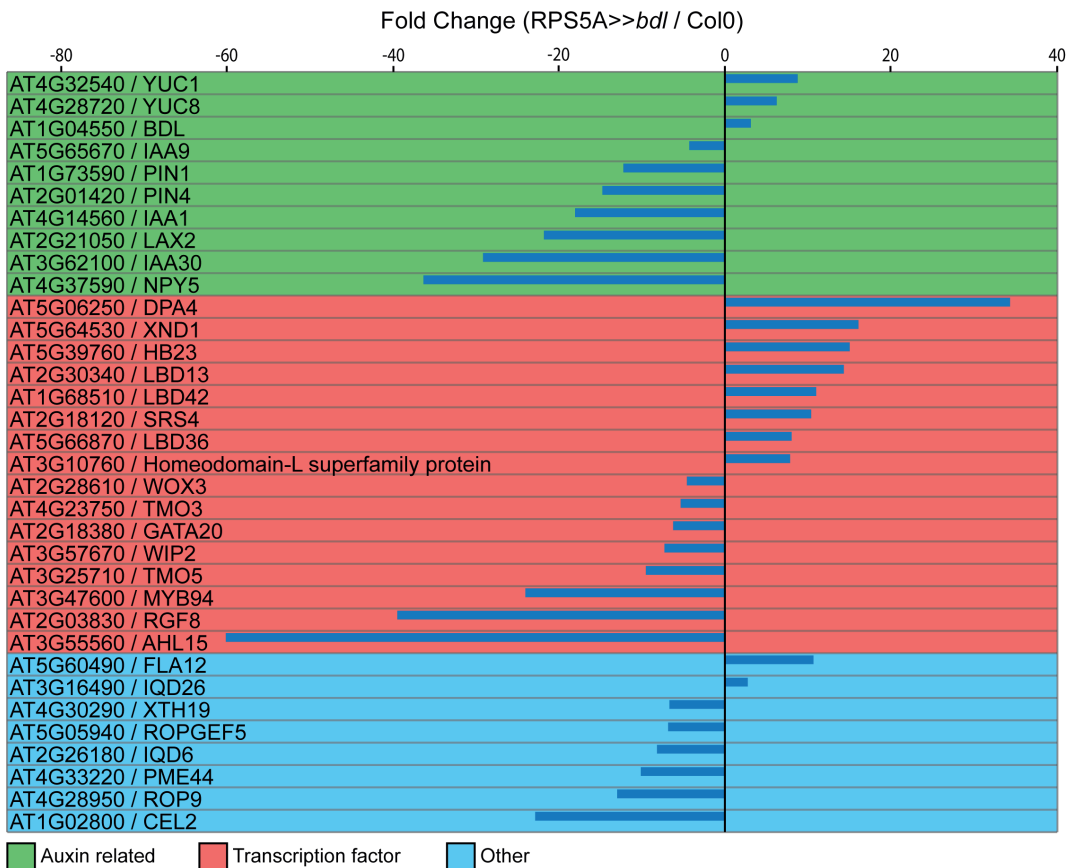
from the divisions to analyse volume distribution ratios for the divisions. As reported previously, the division leading to 4-cell and 8-cell embryos use minimal surface area in wild-type, and daughter cell volume ratios shows that these divisions are symmetric (Fig. 2). In contrast, the division leading to 16-cell embryos uses maximal surface area, and divisions are asymmetric (Fig. 2). Consistent with previous data (Yoshida et al., 2014), in the *bdl*-mutant background the division leading to 16-cell embryos shifts to a symmetric division using minimum surface area (Fig. 2). In the *tir1/afb*-mutant background, divisions leading to 4-cell and 8-cell embryos are symmetric and use minimal surface area (Fig. 2). The divisions leading to 16-cell embryos show a high variation in division plane surface area, with division plane area ranging from a normalized area of 0.21 to 1 (Fig. 2). These divisions reduce the volume distribution ratios, making the average division more symmetric (Fig. 2). These results match our observed cell division- and volume ratio variation in the 3D-imaging, and indicate that the *tir/afb*-mutant phenotype is not identical to the *bdl*-mutant phenotype, but does switch towards a division plane with a reduced division plane surface area. Hence, endogenous auxin response is required for cell division orientation control.

### *Cell division-associated factors are regulated downstream of auxin in Arabidopsis embryos*

To unravel the mechanisms underlying the molecular control of asymmetric cell divisions in the Arabidopsis embryo we performed a transcriptomic analysis, comparing 8-cell WT- and *bdl*-mutant embryos. Given that BDL is a transcriptional inhibitor, one would expect the genes that are causal to the misregulation of division orientation to be misregulated in *bdl* mutant embryos.

After statistical analysis, we retained a list of 849 down-regulated genes, and 911 up-regulated genes with a fold change  $<-2$  or  $>2$  ( $\text{Log}_2\text{FC} <-2/>2$ ), respectively, in the *bdl*-mutant. Among the 34 most highly misexpressed genes in the *bdl*-mutant, we identified a substantial number of genes related to auxin signalling (*IAA1*, *IAA9*, *IAA30*, *NAKED PINS IN YUC MUTANTS (NPY5)*), biosynthesis (*YUC1*, *YUC8*), and transport (*PIN1*, *PIN4*, *LAX2*) (Fig. 3). Regulation of these factors was expected, since previous studies show auxin-dependent regulation of *IAAs* (Hagen & Guilfoyle, 2002), *NPY5* (Li et al., 2011), *YUCs* (Suzuki et al., 2015; Takato et al., 2017), *PINs* (Vieten et al., 2005) and *LAXs* (Radoeva et al., 2019; Swarup et al., 2008).

The majority of highly misregulated genes are transcription factors, of which most are known to be key regulators in Arabidopsis development and patterning (Fig. 3). Upregulated transcription factors are involved in leaf shape and transcriptional repression (*DPA4*) (Engelhorn et al., 2012), vascular differentiation in various tissues (*XND1*, *SRS4*) (Kuusk et al., 2006; Zhao et al., 2008), stem cell elongation and pollen germination (*HB23*), lateral organ formation (*LBD13*, *LBD36*, *LBD42*), and transcriptional regulation (Homeodomain-L superfamily protein) (Korfhage et al., 2007; Smith & Long, 2010). Downregulated transcription factors are involved in lateral-, flower-, and Shoot Apical Meristem (SAM) development (*WOX3*, *GATA20*) (Shimizu et al., 2009; Zhao et al., 2004), MP-dependent embryo- and root stem cell development and maintenance (*WIP2*, *TMO3*, *TMO5*) (Crawford et al., 2015; Shimizu et al., 2009; Schlereth et al., 2010), cuticle formation (*MYB94*) (Cui et al., 2016), (lateral) root development (*RGF8*) (Meng et al.,



**Figure 3:** Misregulated genes in the auxin-insensitive *bdl*-mutant (RPS5A>>*bdl*) background. Log2 Fold-change values are given for expression levels of genes in the *bdl*-mutant relative to wild-type (RPS5A>>*col0*). Proteins highlighted in green are involved in auxin transport- and biosynthesis. Proteins highlighted in red are transcription factors. Proteins highlighted in blue are general factors not involved in either auxin regulated processes or transcriptional regulation.

2012), and hypocotyl growth (*AHL15*) (Zhao et al., 2013).

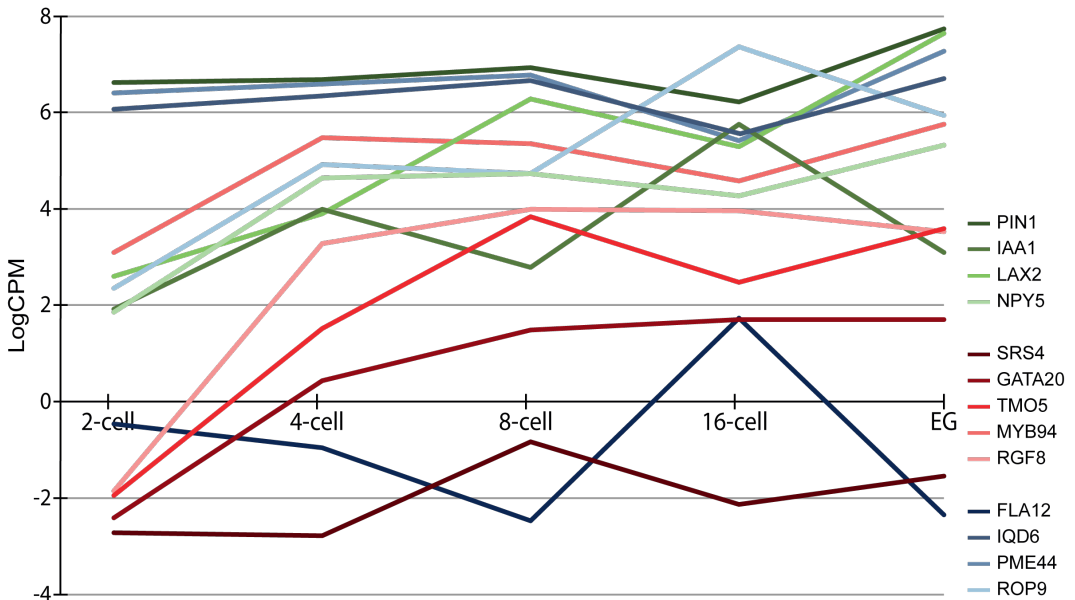
In an attempt to dissect the cell biological mechanisms underlying the aberrant division plane phenotype of the *bdl*-mutant, we focused on misexpressed non-transcription factor genes that have previously been linked to cell wall architecture and composition, cytoskeletal processes, and division plane regulation (Fig. 3). *FASCICLIN-LIKE ARABINOGLACTAN-PROTEIN 12* (*FLA12*) is upregulated in the *bdl*-mutant and is shown to be involved in cell wall architecture and composition, and *FLA12* overexpression (OX) lines show acceleration of xylem development (Endo et al., 2018). The Xyloglucan Endotransglucosylase/hydrolase *XTH19* was downregulated in the *bdl*-mutant and is involved in cell growth and cell wall mechanisms (Miedes et al., 2013; Vissenberg et al., 2005). *PECTIN METHYLESTERASE 44* (*PME44*) was downregulated in the *bdl*-mutant and is crucial for demethylesterification of pectins in the plant cell wall (Müller et al., 2013). *CELLULASE2* (*CEL2*) is downregulated in the *bdl*-mutant and is closely related to the endo-1,4- $\beta$ -glucanase *KORRIGAN*, which localizes to the cell plate and is essential for correct cytokines (Sato et al., 2001). *RHO-RELATED PROTEIN FROM PLANTS 9* (*ROP9*) and *ROP GUANINE NUCLEOTIDE EXCHANGE FACTOR 5* (*ROPGEF5*) are both downregulated in the *bdl*-mutant. ROPGEFs are upstream catalysts of GDP-bound inactive to GTP-bound active conformation of ROPs (Berken et al., 2005; Shichrur & Yalovsky, 2006), which subsequently promote signal diversification by binding a range of effectors leading to a plethora of responses, among them the regulation of cell shape and polar growth, hormone signal transduction, secondary cell-wall formation (Berken, 2006; Nibau et al., 2006; Yang, 2008; Yang & Fu, 2007). *IQ-domain 26* (*IQD26*) and *IQD6* are both misregulated in the *bdl*-mutant. IQD proteins interact with  $\text{Ca}^{2+}$ -Calmodulin (CaM) signalling modules to mediate  $\text{Ca}^{2+}$ -dependent regulation of MT organization and dynamics (Bürstenbinder et al., 2017a, 2017b; Wendrich et al., 2018).

To further characterize candidates for regulation of division plane orientation, we used our previously generated embryonic transcriptomic dataset (chapter 4 of this thesis) to analyse the expression levels of the most highly differentially regulated genes over the different WT embryonic stages, when statistically possible (FDR<0.05) (Fig. 4). As expected, most genes that were heavily downregulated in the *bdl*-mutant show a high expression during early embryonic stages, and vice versa, with exception of *GATA20* which is lowly expressed and downregulated in the mutant background. With a few exceptions, most genes showed a relatively constant expression over the different embryonic stages. *IAA1*, *FLA12* and *ROP9* were upregulated in 16-cell stage embryos. *LAX2* expression

gradually increased over the subsequent stages with high expression at 8-cell stage, and *TMO5* expression increased toward 8-cell stage.

To address if, like the division defects, the transcriptional effects in *bdl*-mutant embryos are reflecting endogenous auxin action, we generated transcriptomic profiles of 8-cell *tir1/afb*-mutant embryos. Hexuple mutant embryos were isolated from a line that segregates a *TIR1-mOrange2::AFB5-mCherry::AFB2-mCitrine* transgene that dominantly complements the mutant phenotype (Prigge et al., 2019). Unfortunately, we did not succeed in separation of non-fluorescent *tir1/afb* sextuple embryos from complemented fluorescent embryos. Therefore, we instead collected all segregating embryo, where we expect 25% of the embryo population to be hexuple mutants, diluting the transcriptional effects, yet allowing to see the largest changes in mutant embryos. After statistical analysis, we retained a list of 115 down-regulated genes, and 1175 up-regulated genes with a fold change Log2FC of  $<-1$  or  $>1$ , respectively, in the *tir1/afb*-mutant compared to WT. The large group of 1175 upregulated genes could be secondary responses resulting altered development starting directly after fertilization, and perhaps even before.

Comparison of differentially expressed genes in the *tir1/afb* hexuple mutant and the *bdl*-mutant identified a group of 37 commonly upregulated genes with some known regulators like CUC1/2, IQD3, IQD14, IQD28 and GATA7 (Fig. 5). In contrast, LOG4

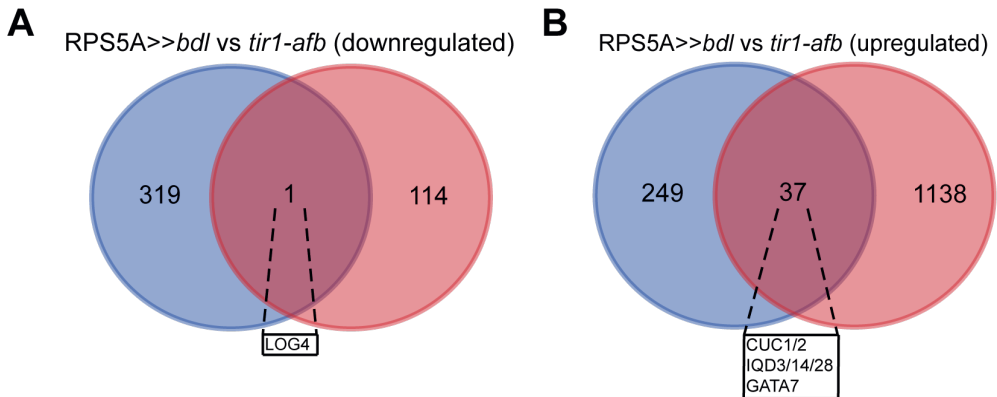


**Figure 4:** Expression levels of genes misregulated in *RPS5A>>bdl* embryos during the first stages of wild-type embryogenesis. The early Arabidopsis embryo reference dataset generated in chapter 4 of this thesis was used to obtain expression levels. The log-counts-per-million (logCPM) values after mapping were used.

was the only factor downregulated in both the *bdl*-mutant and the *tir1/afb*-mutant (Fig. 5). The small overlap in misexpressed genes between the two auxin-defective mutants is surprising, but could in part be explained by the large wild-type embryo population (75%) due to segregation of the *tir1/afb* mutation, as well as by the fact that upregulation is easier to detect than downregulation. Nonetheless, there is a small but significant overlap in upregulated genes, suggesting that *tir1/afb* and *bdl*-mutants in part affect cell division through common components.

### IQ-domain proteins are misregulated in auxin-signalling deficient datasets

The IQ67-domain gene family, with multiple misregulated members in the *bdl*-mutant background (Fig. 6), drew our attention based on previously reported functions in cytoskeletal network control (Abel et al., 2013; Bürstenbinder et al., 2017b; Wendrich et al., 2018). Previously, it was shown that 13 of 33 IQD family members were misregulated in seedlings (Schlereth et al., 2010) or embryos (Möller et al., 2017) in which auxin response was inhibited (Wendrich et al., 2018). *IQD6* and *IQD18* are downregulated in 8-cell *bdl*-mutant embryos (Fig. 6), and are of specific interest since IQD18 and several closely related members (IQD15-17) were suggested to be involved in Arabidopsis embryogenesis (Wendrich et al., 2018). *IQD6* is dramatically downregulated in the *bdl*-mutant, and expression is high in all early wild-type Arabidopsis embryonic stages (Fig. 4). Taken together, the over-representation of *IQD* genes in different auxin-deficient datasets suggests a role for these proteins downstream of auxin signalling during different

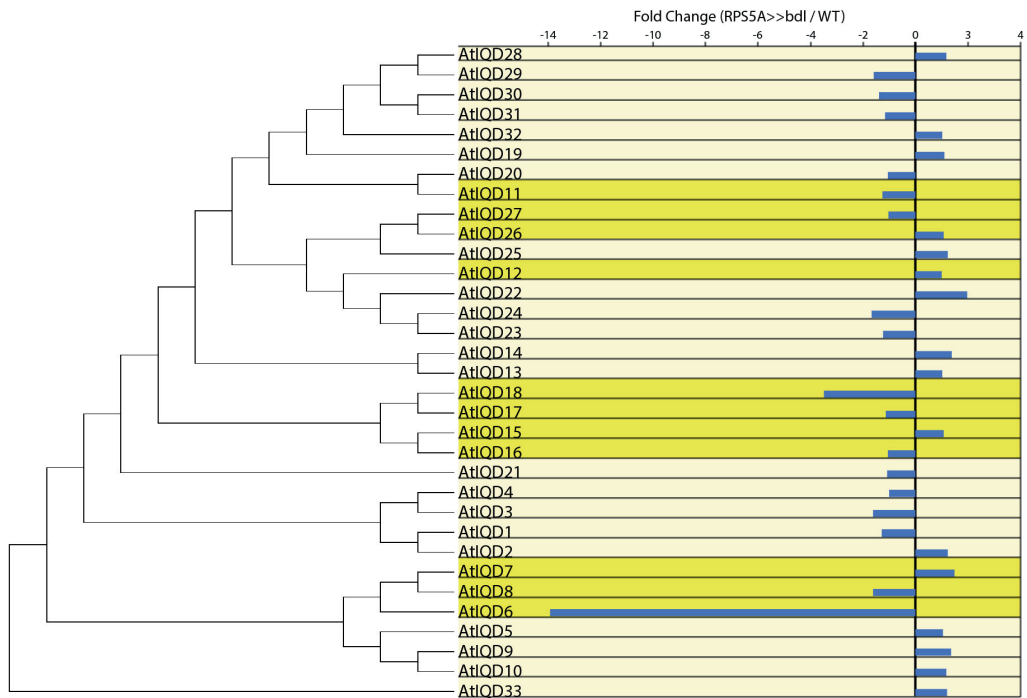


**Figure 5:** Comparison of misregulated genes in 8-cell Arabidopsis embryos of the auxin-insensitive *bdl*-mutant (RPS5A>>*bdl*) and *tir1/afb* mutant. Venn-diagrams indicate the number of overlapping down-regulated- and upregulated genes in both backgrounds. Text-boxes show genes with known functions in cell division and pattern formation.

phases of Arabidopsis development, with a potentially prominent role for IQD6 during embryogenesis. To further elucidate the function of IQD6, we set out to characterize IQD6 together with the closely related subclade members IQD7 and IQD8 in early Arabidopsis embryos.

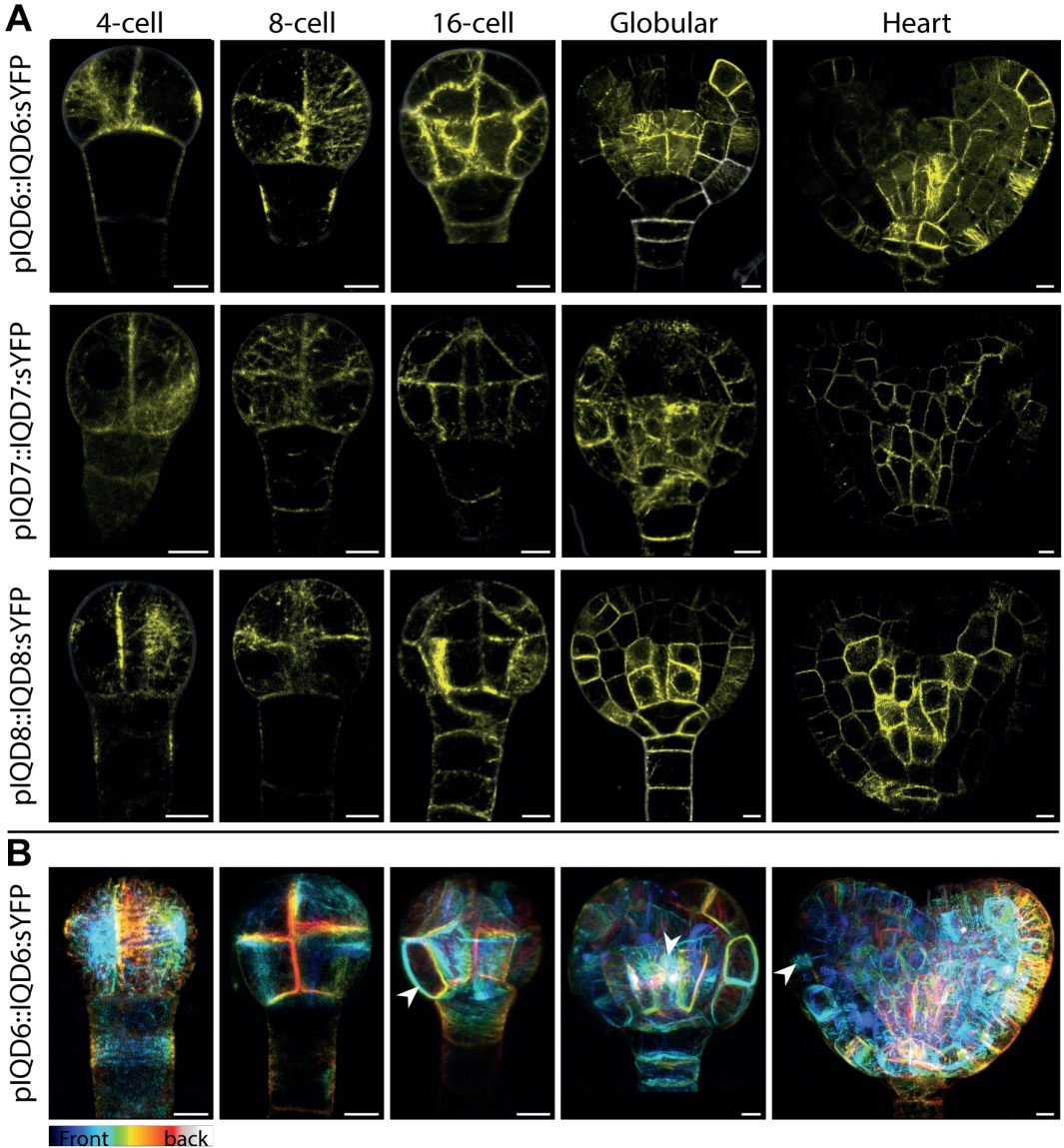
### *IQD proteins localize to microtubule arrays*

IQD proteins have been shown to reside both on cortical MT (CMTs) and in the nucleus, suggesting functions in different cellular locations (Abel et al., 2013; Bürstenbinder et al., 2013; Wendrich et al., 2018). However, it remains unclear if all members have a similar localization and function. We determined the subcellular localization of IQD6, -7, and -8 in stably transformed lines (*pIQDX::IQDX::sYFP*), focusing on the embryo and the post-embryonic root. All three IQD proteins were observed in filamentous structures near cell membranes in all early embryonic stages (Fig. 7). 3D projections also clearly showed protein localization in nuclear spindle, phragmoplast and preprophase band (PPB) (Fig.7;



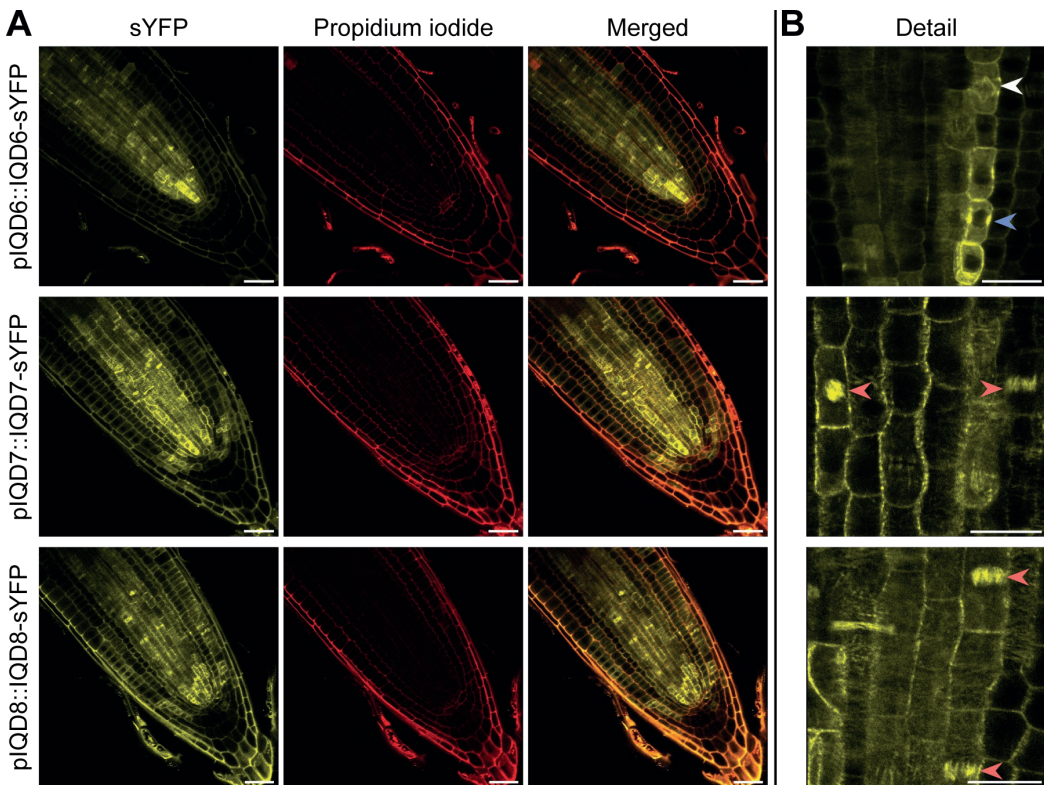
**Figure 6:** Phylogenetic tree of all Arabidopsis IQD proteins, rooted to IQD33, combined with their misexpression in 8-cell *bdl*-mutant (*RPS5A>>bdl*) embryos. Log2 Fold-change values are given for expression levels of genes in the *bdl*-mutant relative to wild-type (*RPS5A>>col0*). Yellow boxes indicate subclades previously shown to be misregulated in auxin-related datasets (Möller, 2012; Schlereth et al., 2010; Wendrich, 2016; Wendrich et al., 2018).

arrowheads). These structures strongly resemble the structure also observed for (cortical) MTs in the embryo (Chapter 3 of this thesis; (Liao & Weijers, 2018), suggesting that these three IQD-proteins are MT-localized in the Arabidopsis embryo. Nuclear spindle, phragmoplast and PPB localisation were not observed for all previously studied IQD



**Figure 7:** IQD subcellular protein localization during the first stages of Arabidopsis embryogenesis. Colour scale indicates depth of individual images within the stack from front to back. Scale bars indicate 5  $\mu$ m distance. **a** IQD6-, 7-, and 8 are visualized using a *pIQDX::IQDX:sYFP* reporter line merged with membrane visualisation using SCRI Renaissance Stain 2200 (SR2200), showing strand-like structures in 4-cell- to heart stage embryos resembling microtubular structures. **b** Depth colour-coded IQD6-sYFP stacks merged with R2200 membrane stacks show protein localization in 3D. Arrowheads indicate observed localization of protein in pre-prophase bands (PPB), spindles and phragmoplasts.

protein subclades (Wendrich et al., 2018), suggesting a difference in function for these different IQD-family subclades. In contrast to previously reported localization of IQD6-8 proteins upon transient overexpression (Bürstenbinder et al., 2017b), these proteins do not localize to nuclei in embryos and post-embryonic roots when expressed at endogenous levels (Fig. 8). IQD6 localises in all cells of the young embryo, which changes to a more prominent localization in vascular cells of globular and heart stage embryos (Fig. 7) and exclusive localization in vascular cells in roots (Fig. 8). IQD7, and IQD8 both localize to all cells of the young embryo and later remain localized more broadly than IQD6, but most dominantly in the vascular cells in globular and heart stage embryos and in roots (Fig. 8). In roots, all three proteins are also observed in nuclear spindles, phragmoplasts and PPBs (Fig. 8; coloured arrowheads).

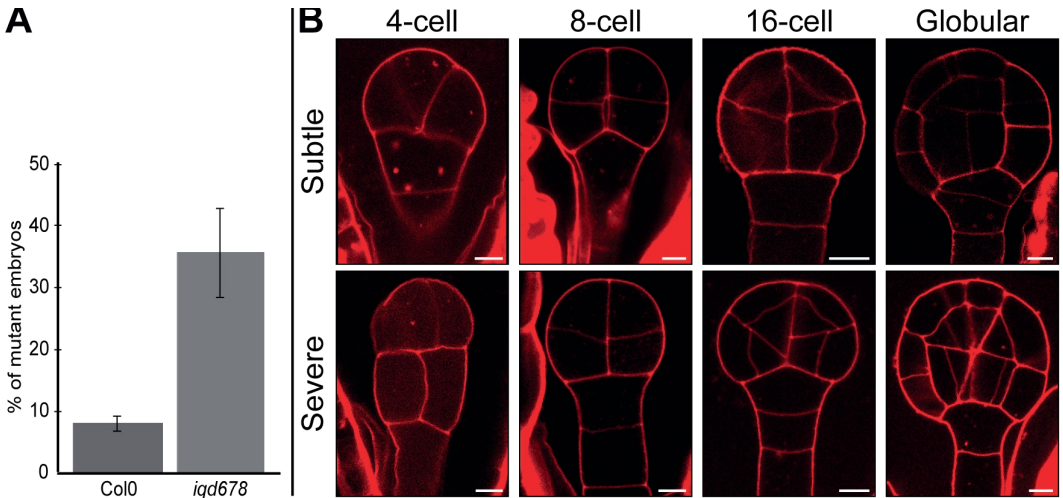


**Figure 8:** IQD subcellular protein localization in 5-day old Arabidopsis roots. **a** IQD6-, 7-, and 8 are visualized using a *pIQDX::IQDX:sYFP* reporter line merged with membrane visualisation using Propidium Iodide (PI) staining. Scale bars indicate 30  $\mu\text{m}$  distance. **b** Details of roots with arrowheads indicate observed localization of protein in pre-prophase bands (PPB; blue), spindles (white) and phragmoplasts (red). Scale bars indicate 15  $\mu\text{m}$  distance.

## *IQD6-8* *clade proteins are involved in cell division plane orientation regulation*

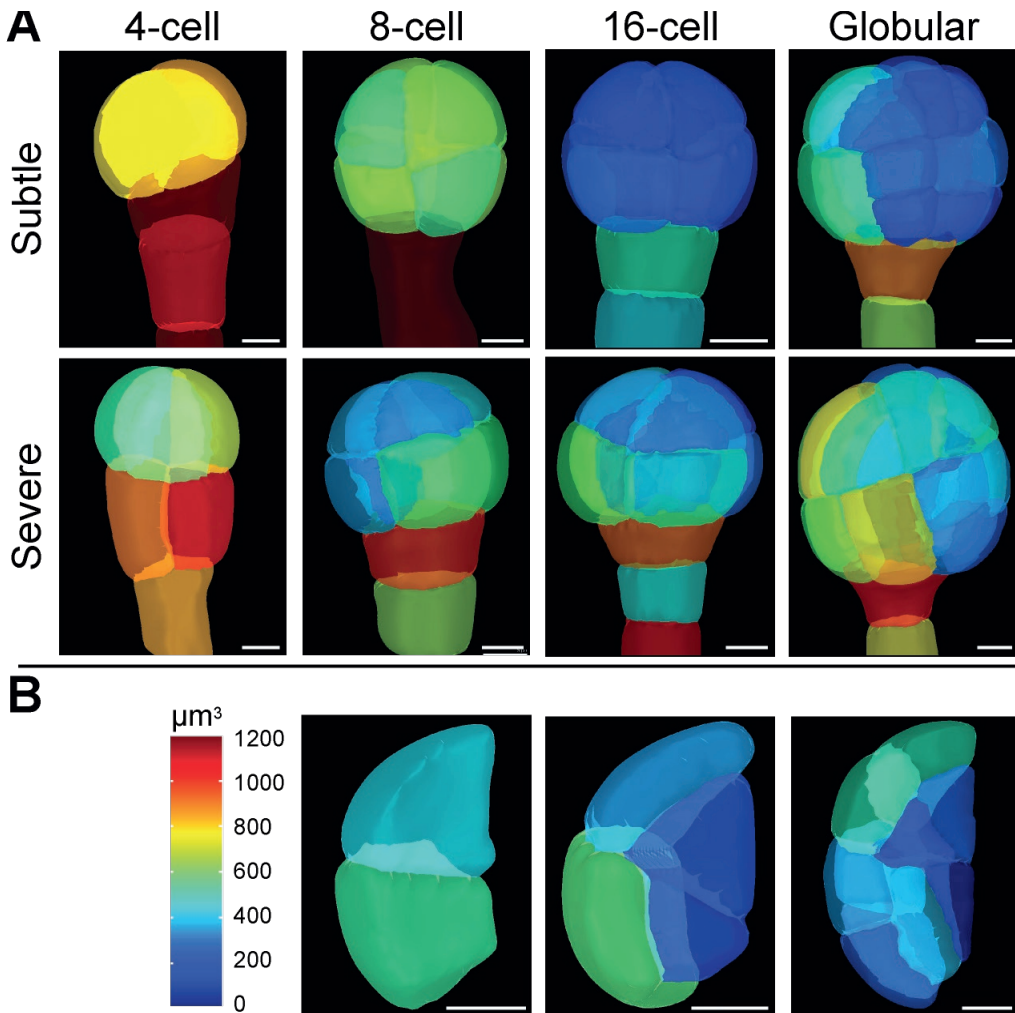
To investigate the possible involvement of IQD6, -7 and -8 in division plane orientation during *Arabidopsis* embryogenesis, we analysed an *iqd678* triple mutant. In 35% of the analysed embryos (Fig. 9a), the mutant shows a shift in division plane orientation during different stages of early embryogenesis. These defects are qualitatively distinct, and can either be subtle or severe (Fig. 9b). Because the subtle changes in division plane orientations are difficult to observe using 2D-imaging techniques, we analysed the early embryonic phenotype using 3D-imaging and cell segmentation (Fig. 10). From our analysis it is clear that there is variation in cell division angles within the same embryo (Fig. 10a). Detailed analysis shows that even when cell division planes are heavily skewed in division leading to 8 cell embryos, the divisions leading to 16-cell embryos can still be asymmetric and form the inner- and outer cell layers (Fig. 10b). This explains why overall, adult mutant plants are viable without a distinguishable phenotype, with all major tissues formed. Roots do show oblique divisions in the cortex cell layer and occasionally in the endodermis (Fig. 11), but general growth is not strongly impaired.

To analyse the division plane orientation defect in detail, we repeated the 3D cell surface area- and daughter cell volume ratio analysis done previously for *bd1*-mutants and *tir1/afb*-mutants (Fig. 12). In the *iqd678*-mutant background, divisions leading to 8-cell embryos are symmetric and use minimal surface area, similar to wild-type embryos (Fig.



**Figure 9:** 2D embryonic phenotype for the *iqd678* mutant. **a** Quantification of skewed division planes in early embryos. Quantification is based on visual inspection of at least 250 individual chloral-hydrate cleared embryos. **b** Visualization of skewed division plane phenotype using a modified Pseudo-Schiff propidium iodide (mPS-PI) membrane staining in 4-cell to globular embryos. embryos can show either a subtle (hard to observe in 2D) or severe phenotype.

12). In contrast, the divisions leading to 16-cell embryos show a high variety in division plane surface area, with division plane area ranging from a normalized area of 0.32 to 1 (Fig. 12). The high variation in divisions also translates to a high variation in volume distribution ratios, ranging from wild-type-like asymmetric divisions to highly symmetric divisions with volume ratios smaller than division in the *bdl*-mutant (Fig. 12). These results match our observed cell division variation in the 3D-imaging, and indicate that IQD6-8 proteins are involved in cell division placement downstream of auxin response. However,

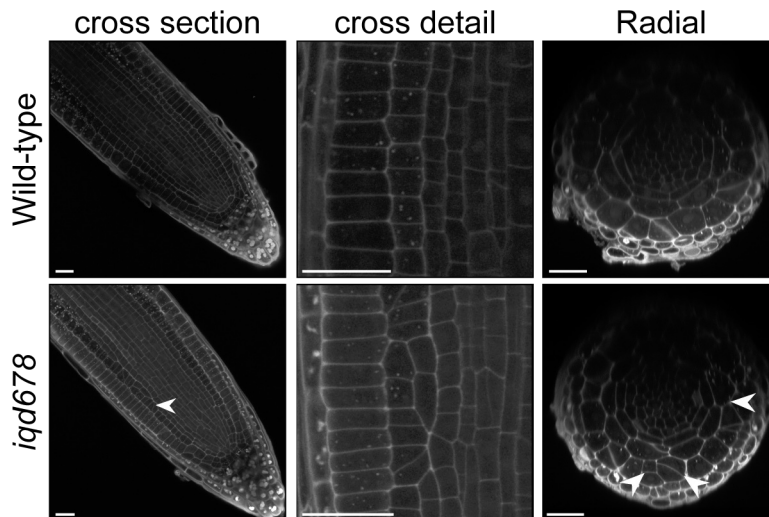


**Figure 10:** 3D embryonic phenotype with volumetric measurements for the *iqd678* mutant. Construction of meshes and volume measurements were performed on segmented modified Pseudo-Schiff propidium iodide (mPS-PI) stained embryonic cells using MorphoGraphX software (Barbier de Reuille et al., 2015). Mesh colour per cell corresponds to cellular volume (in  $\mu\text{m}^3$ ) indicated in the colour scale. Scale bars indicate 5  $\mu\text{m}$  distance. **a** Visualization of skewed division plane phenotype 4-cell to globular embryos. embryos can show either a subtle or severe phenotype. **b** Detailed views of cells form 8-cell to globular stage embryos shows the skewed division plane phenotype.

as the *iqd678*-mutant has a weaker division plane area ratio phenotype, and a more variable daughter cell volume ratio, other components must also contribute.

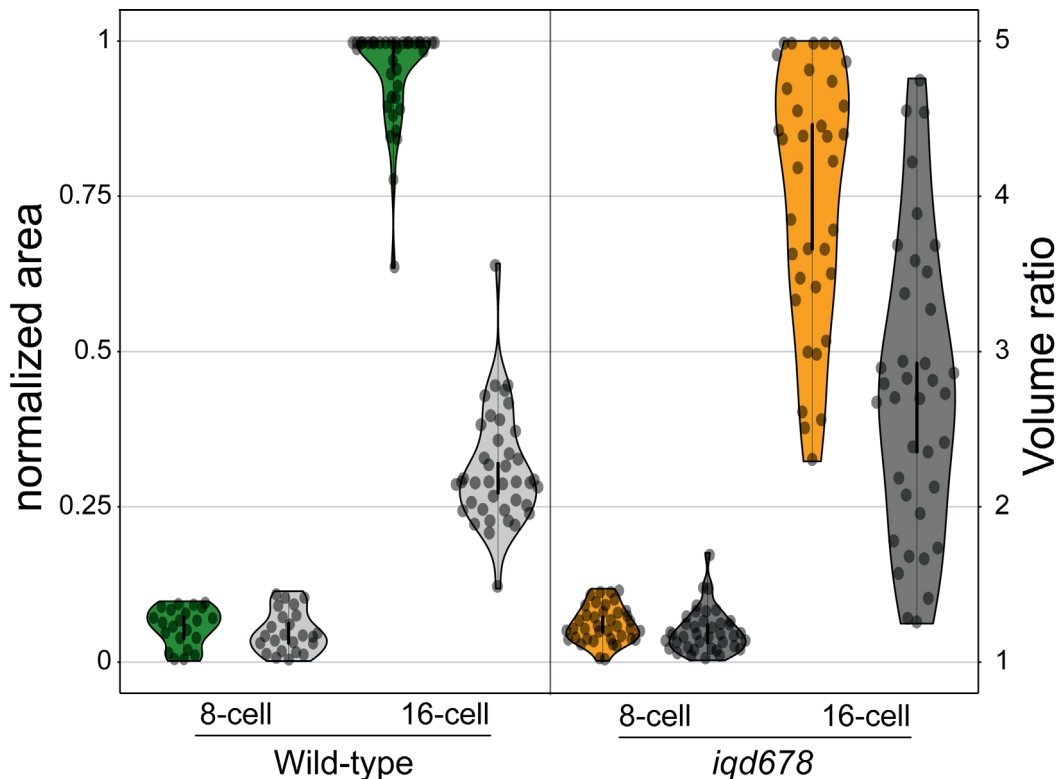
### *IQD6 interacts with Calmodulins and Tubulins in vivo*

To understand potential mechanisms of action of this IQD protein subclade in cell division orientation control, we studied protein interactions using an unbiased IP-MS/MS approach. Since IQD18-interacting proteins were previously determined using the same approach (Wendrich et al., 2018), IQD6-interacting proteins were also compared to IQD18-interacting proteins to identify differences in interaction partners and function between distinctly localized IQD proteins. Since IQD proteins are not highly expressed, and because cell division is a general process shared across cells and organs of the plant, we decided to generate stable transgenic cell cultures expressing either *pIQD6::IQD6:sYFP* or *pIQD18::IQD18:sYFP*. In these cultures, localization of both proteins reflected the patterns observed in embryos and roots (Fig. S1), and we therefore reasoned that these would report on the protein associations acting in cell division control. In both cases, both the IQD6 or -18 protein was among the most abundant protein groups in the sample upon immunoprecipitation, validating the quality of the performed IP-MS/MS. The previously generated IP-MS/MS IQD18 dataset (Wendrich et al., 2018) was analysed using the same statistical criteria as the cell culture data, and was used to validate the generated dataset, and compare interactors for IQD18 in cell cultures and roots.



**Figure 11:** phenotype for the *iqd678* mutant in 5-day old seedling roots. Roots are visualized using a modified Pseudo-Schiff propidium iodide (mPS-PI) stain. Arrowhead and cross section detail show division defects in cortex and endodermis cell layers in *iqd678* roots. Division defects are radially shown in the same region. Arrowheads indicate oblique divisions in cortex and endodermis cell layers. Scale bars indicate 20  $\mu$ m distance

IQD18 associates with tubulins, calmodulin-like proteins, protein kinases and the auxin transport protein BIG (Gil et al., 2001) both in roots and cell cultures (Fig. 13a). These interactions support the previously shown MT association and involvement in  $\text{Ca}^{2+}$ -signalling of IQD proteins (Abel et al., 2013; Bürstenbinder et al., 2013; Wendrich et al., 2018). Possible heterodimerization with IQD14- and 17, and interactions with actin and SPIRAL2 (SPR2) are not found in cell culture samples, meaning that these interactions are either root-specific, or are lost due to the artificial nature of the cell culture system. Since all interaction partners that are found exclusively in roots were previously linked to MTs (Abel et al., 2005; Wendrich et al., 2018), the interaction could also be influenced by the stability of the CMTs. To test this, IP-MS/MS experiments on IQD18 cell cultures were repeated after stabilizing MTs by adding 10  $\mu\text{M}$  Paclitaxel (taxol) to cell cultures prior to harvesting of material for IP. In MT-stabilized cell cultures IQD18 additionally interacts with actin, actin depolymerization factors (ADF) and the MT-associated SPIRAL1 (SPR1) (Fig. 13b).

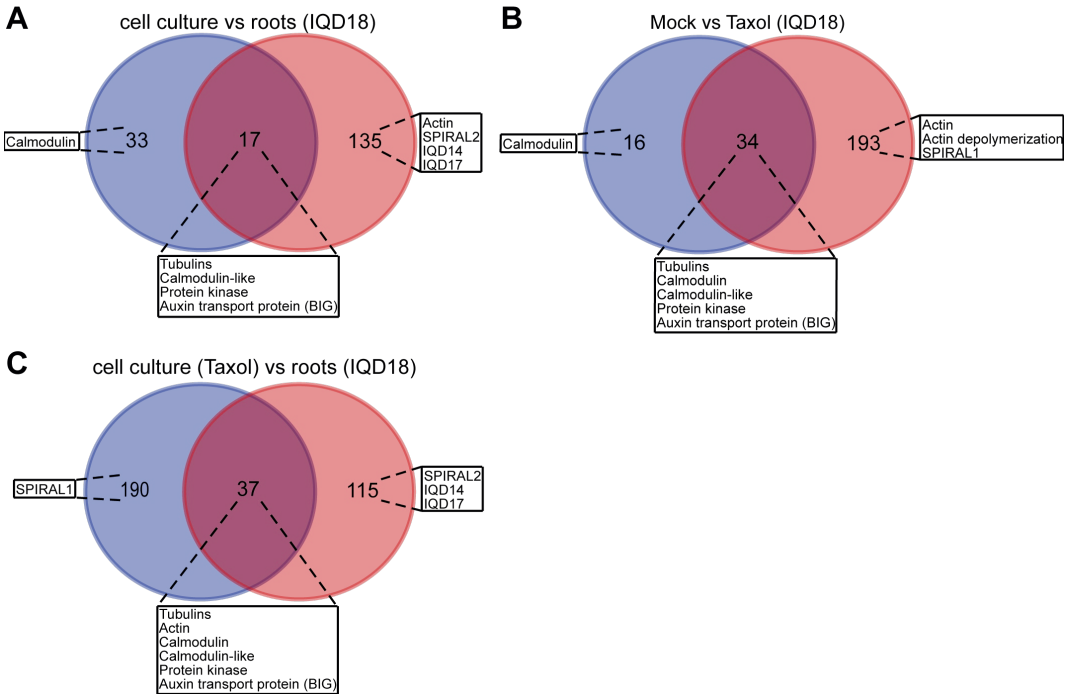


**Figure 12:** 3D cell division analysis comparing wild-type and *iqd678*-mutant embryos. Violin plots representing distribution of cell wall areas as a fraction of the smallest (0 on the left y-axis) and largest (1 on the left y-axis) wall area within the volume of two daughter cells. Wild-type values are shown in green, *iqd678*-mutant values are shown in orange. The cell volume ratios resulting from these divisions are represented in gray (light to dark), and values are on the right y-axis. Individual measured cells are shown in the violin plots. At least 5 individual embryos were used per condition.

SPR1 may be a cell culture specific interactor, since it was not identified in Arabidopsis roots and siliques (Fig. 13c; (Wendrich et al., 2018). Since the IP-MS/MS performed on taxol-treated IQD18 cell cultures identified more (transient) interactions, further analysis was done on this data.

The different subcellular localization observed between IQD6-8 and IQD15-18 in both the embryo and root may suggest a difference in function. To identify differences in interaction partners and cellular function, we performed a comparative IP-MS/MS analysis on IQD6- and 18 cell cultures treated with taxol. Both proteins interact with tubulins, actin, SPR1, calmodulins, calmodulin-like proteins and BIG (Fig. 14). IQD18 putatively specifically interacts with protein kinases and ANGUSTIFOLIA (AN). IQD6 putatively specifically interacts with the calcium-binding protein CML14 (Fig. 14). IQD6 interaction with different tubulins, actin and SPR1 together with Calmodulin suggests a role for IQD6 connecting  $Ca^{2+}$  signalling with regulation of cytoskeletal structures.

IQD18 has been shown previously to be involved in  $Ca^{2+}$ -signalling, with specific interaction partners in response to calcium chelation using EGTA treatments (Wendrich et al., 2018). A variety of IQD proteins have calcium-dependent binding-properties and

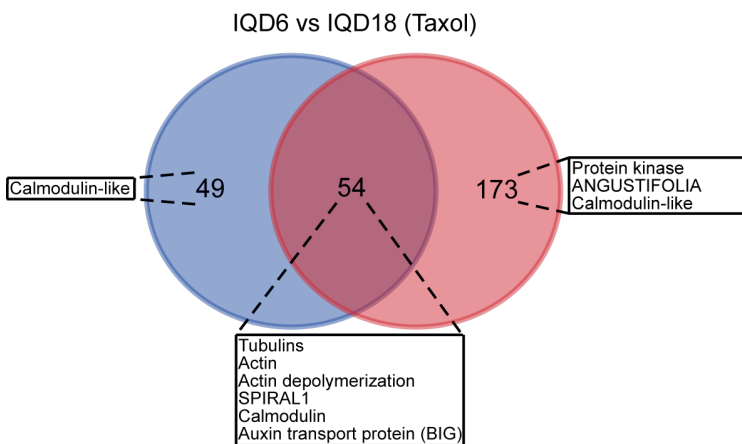


**Figure 13:** Venn-diagrams showing overlapping and unique protein groups interacting with IQD18 identified through IP-MS/MS on: **a** Arabidopsis roots (J. R. Wendrich, 2016) and cell cultures, **b** mock- and Pacitaxol (taxol) treated cell cultures, **c** taxol-treated cell cultures and roots.

interaction-partners (Bürstenbinder et al., 2013; Wendrich et al., 2018), and calcium chelation causes a dramatic change in IQD protein localization in Arabidopsis roots (Wendrich et al., 2018). We therefore performed IP-MS/MS on calcium- and EGTA-treated Arabidopsis cell culture samples to identify calcium-dependent interaction partners for IQD6 and IQD18. Similar to EGTA-treated root samples (Wendrich et al., 2018), IQD18 showed more prominent binding to Calmodulins and the Calmodulin-binding protein CML14 when treated with EGTA (Fig. 15a). EGTA-treated IQD18 samples lost the interaction with the Auxin transport protein BIG, suggesting calcium may inhibit binding of IQD18 to this specific interactor (Fig. 15a). In  $\text{Ca}^{2+}$ -treated cell culture, IQD6 interacts specifically with the Actin Depolymerization Factor 4 (ADF4), and loses its interaction to actin itself (Fig. 15b). In contrast to IQD18,  $\text{Ca}^{2+}$ -signalling seems to affect IQD6 interaction with actin and actin-related factors, which could suggest a different mechanism for these IQD proteins to affect actin-cytoskeletal structures through  $\text{Ca}^{2+}$  signalling.

## Discussion

In this study, we identified factors involved in the regulation of cell division orientation in Arabidopsis plants downstream of auxin signalling. We first asked if the defects in cell division orientation in embryos in which the dominant auxin response inhibitor *bdl* was expressed (Yoshida et al., 2014) did indeed reflect a role of endogenous auxin in division orientation. To this end we analysed a hexuple mutant in all TIR1/AFB auxin receptors. This mutant was reported to have superficially similar division defects in the embryo (Prigge et al., 2019). Analysing the *tir1/afb*-mutant in detail, we showed that indeed, several cell divisions resemble those observed in the *bdl*-mutant. However, this mutant

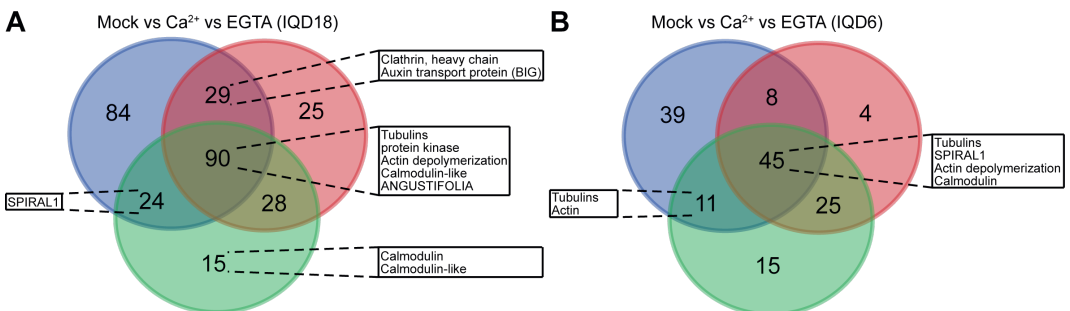


**Figure 14:** Venn-diagram showing overlapping and unique protein groups interacting with IQD6- and 18 identified through IP-MS/MS performed on Pacitaxol (taxol)-treated Arabidopsis cell cultures.

has a large variation in cell division angles and cell volume distribution in daughter cells. This variation in cell division angles is reflected in the large variation we observed when analysing cell division surface area. Interestingly, cell division area in a fraction of cells leading to 16-cell embryos does shift towards a minimal surface area and do resemble *bdl*-mutant divisions. This shows that the *tir1/afb* mutations do influence cell division regulation, but the phenotype is not completely penetrant in every embryonic cell. It is possible, even likely, that not all mutations are full knockouts, which may account for incomplete penetrance. Alternatively, *bdl* misexpression has effects that exceed the loss of auxin-dependent Aux/IAA protein degradation. Aux/IAA's inhibit ARFs, and the degree to which they can do so depends on their abundance. Removing TIR1/AFB proteins will eliminate Aux/IAA degradation, and lead to accumulation that is dictated by the Aux/IAA gene expression levels. It is likely that the RPS5A-driven *bdl* expression will lead to higher protein accumulation levels. The prediction from this hypothesis is that removal of all the *bdl*-targeted ARF proteins will in fact lead to *bdl*-like defects, which remains to be seen. It is also possible that *bdl* affects cells in other, ARF-independent ways, for example by titrating TPL/TPR proteins or other partners, thus causing dominant-negative effects. Future analysis of true null mutant *tir1/afb*-mutants, as well as *arf* loss of function mutants, should help clarify this issue.

In any event, from our data we conclude that endogenous auxin-signalling is indeed involved in regulation of cell division plane orientation, but the difference in cell division phenotype between the different mutants suggests the involvement of different factors or alternative downstream mechanisms.

Using our previously optimized embryonic transcriptome analysis pipeline (Chapter 4 of this thesis), we identified factors potentially involved in the observed cell division defects downstream of auxin signalling using both the *bdl*-mutant and the *tir1/afb*-mutant.



**Figure 15:** Venn-diagrams showing overlapping and unique protein groups identified through IP-MS/MS performed on mock-, calcium-, or EGTA treated Arabidopsis cell cultures for: a IQD18 and b IQD6

A surprisingly large group of genes was upregulated in the *tir1/afb*-mutant background, which may be an indirect consequence of altered embryo development from early stages onward. In addition, it should be kept in mind that this hexuple mutant carries 7 T-DNA insertions (6 *tir1/afb* mutations and a complementing transgene). T-DNA insertion mutants can often have second-site mutations, rearrangements, or epigenetic trans-effects on gene expression (Gao & Zhao, 2013; Nacry et al., 1998; Tax & Vernon, 2001). It is therefore possible that some of the transcriptional effects are unrelated to the *tir1/afb* mutant.

Nonetheless, a fraction of genes upregulated in the *tir1/afb*-mutant overlaps with genes upregulated in the *bdl*-mutant background. A large group of genes is downregulated in the *bdl*-mutant background, possibly showing factors that are directly regulated downstream of auxin. Surprisingly, very limited overlap of transcriptionally downregulated factors was found between in the *bdl*- and *tir1/afb*-mutant backgrounds, and in general there is a limited number of genes downregulated in the *tir1/afb*-mutant background compared to the *bdl*-mutant background. This difference in transcriptomic profile could be caused by the small number of mutant embryos (25%) in the analysed population of embryos, due to segregation of the dominant transgene complementing the *tir1/afb* mutation. As an example: When a gene with a gene count value of 4 would be 10-fold upregulated in the *bdl*-mutant, this would result in a gene count value of 40. In the *tir1/afb*-mutant this would result in a gene count value of 10, meaning a 2.5 times fold-change. When a gene with a gene count value of 4 would be 10-fold downregulated in the *bdl*-mutant, this would result in a gene count value of 0.4. In the *tir1/afb*-mutant this would result in a gene count value of 3.1, resulting in a 1.3 times fold-change. This means fold-changes of downregulated genes should be <10 in the *bdl*-mutant to detect them as downregulated genes in the *tir1/afb*-mutant. This example also shows that upregulated genes are easier to detect in our *tir1/afb*-mutant dataset, partly explaining the bigger overlap of detected upregulated genes in the two mutant backgrounds. Alternatively, the difference in transcriptomic profile in the two mutant backgrounds could indicate a difference in downstream molecular regulation in the mutants.

Previously, we hypothesized that plant cell division control is controlled by cytoskeletal-dependent control downstream of auxin signalling (Chapter 3 of this thesis). Exploiting the *bdl*-mutant transcriptomic dataset, we identified factors that may connect auxin signalling with cytoskeletal regulation and cell division control. The IQ-domain protein IQD6 is strongly downregulated in the *bdl*-mutant background and caught our attention based on previously reported involvement in calcium-dependent cytoskeletal

control for this protein family (Abel et al., 2013; Bürstenbinder et al., 2017b; Liang et al., 2018). IQD6 forms a subclade together with IQD7- and IQD8. We show that all three IQD proteins in this sub-clade localize to the CMA and specialized microtubular structures (PPB, spindle and phragmoplast) in the early embryo and post-embryonic roots. IQD6 is localized in all early embryonic cells, with more predominant localization in vascular cells of older embryos and the post-embryonic root. Similarly, IQD7- and IQD8 localize in all early embryonic cells, but remain more broadly localized in older embryos and the post-embryonic roots. As previously suggested for other subclades of the IQD-protein family (Wendrich et al., 2018), the localisation of these three IQD-proteins on multiple microtubular structures suggests that these proteins might be involved in the regulation of microtubules.

Given the phylogenetic patterns of this IQD family subclade, and the similar localization pattern of IQD6-, -7 and -8 proteins in the Arabidopsis embryo, it is likely that these proteins act redundantly. Therefore, to study the function of the IQD6-8 subclade we analysed the phenotype of the *iqd678* mutant in both embryos and roots. The mutant shows clear defects in cell division orientation in both embryos and roots, indicating that the IQD6-8 protein subclade is involved in cell division orientation regulation. Analysing the *iqd678*-mutant in detail, we showed that this mutant has a large variability in cell division plane orientation with either subtle or severe phenotypic consequences, and measurements of division plane surface area and volume ratios confirm the high variability in cell division. Interestingly, even though cell division planes can be heavily skewed in mutant embryos at all stages, divisions following on those divisions which are essential for embryonic patterning are predominantly correctly placed. Correct patterning is confirmed by the viability of adult plants without a distinguishable phenotype. Since patterning events are disturbed in the *bd1*-mutant, this phenotype indicates that if this IQD-subclade is involved in cell division regulation downstream of auxin signalling, additional factors have to be involved. Interestingly, cell division orientation for divisions forming 4-cell and 8-cell embryos are more variable in the *iqd678*-mutant, but they do divide using minimal surface area. Since it was suggested previously that based on geometry, plant cell division plane determination is a stochastic process with a multitude of possible division planes (Besson & Dumais, 2014), it is possible that this IQD-subclade is involved in control of stochasticity of cell divisions, but not in regulation of formative asymmetric divisions during development.

Our IP-MS/MS performed on an Arabidopsis cell culture system confirms the

possible role for IQD6 in cytoskeletal orientation regulation, as it interacts with actins, tubulins, and the plant-specific microtubule-localized SPR1 protein, which is involved in microtubule reorientation through katanin-mediated severing of microtubules and directed cell expansion (Nakajima et al., 2004; Sedbrook et al., 2004). Interaction of both IQD6 and IQD18 with calmodulins, calmodulin-like proteins, and the calmodulin-binding related BIG protein (Gil et al., 2001; Luschnig, 2001) suggests a role for IQD proteins in calcium-dependent intracellular signalling and transport. Further analysis of calcium- and EGTA-treated cell cultures revealed that IQD6 interactions with actin and actin-related factors are calcium-dependent, where IQD18 interactions with calmodulins and calmodulin-like proteins seems to be calcium-dependent. Our characterization of the IQD6-8 subclade suggest a function for these proteins connecting  $\text{Ca}^{2+}$ -dependent control of the actin cytoskeleton to cell division plane regulation.

In conclusion, using two independent auxin-insensitive mutants, we showed that endogenous auxin response is required for cell division orientation control in the Arabidopsis embryo. Additionally, we identified a subclass of IQD proteins regulated downstream of BDL-mediated auxin-signalling in early Arabidopsis embryos. Functional characterization suggests a role for these proteins in regulation of cell division orientation through  $\text{Ca}^{2+}$ -mediated regulation of cytoskeletal structures.

## Methods

### *Plant material*

Plants used in all experiments were Columbia (Col-0) ecotype. *pRPS5A::GAL4:VP16* driver line (Weijers et al., 2003) plants were used for crossing with Col-0 plant or *UAS-bdl* plants (Weijers et al., 2006). *RPS5A::GAL4:VP16* plants were used as female parent. The *tir1/afb* hexuple mutant (*tir1afb12345* with segregating *TIR1-mOrange2::AFB5-mCherry::AFB2-mCitrine* transgene) is previously described in Prigge et al., 2019. *iqd678* mutant plants were kindly provided by dr. Katharina Bürstenbinder.

After seed sterilization, seedlings were plated on half-strength Murashige-Skoog (MS) plates containing 0.8% Dashin agar (Duchefa), an 1% sucrose. After two weeks of growth on plates, seedlings were transferred to soil and further grown at a constant temperature of 22°C under long-day conditions (16 hours light/8 hours dark).

For *Arabidopsis* cell cultures, wild type *Arabidopsis Landsberg erecta* and transgenic PSB-D cell suspension cultures were maintained weekly in MSMO medium (4.43 g/liter MSMO (Sigma-Aldrich), 30 g/liter sucrose, 0.5 mg/liter  $\alpha$ -naphthaleneacetic acid, 0.05 mg/liter kinetin, pH 5.7, adjusted with 0.1 M KOH) in the dark at 25°C gently shaking at 130rpm. Cells were sub cultured every 7 days in a 1:10 dilution.

Transformations were conducted without callus selection essentially as described by (<https://doi.org/10.1074/mcp.M700078-MCP200>) In brief, *Agrobacterium* and PSB-D cells were co-cultivated in a 6 well plate in MSMO medium supplemented with 200  $\mu$ M 4'-Hydroxy-3',5'-dimethoxyacetophenone (Sigma-Aldrich). After two days, PSB-D cells were washed twice in MSMO medium containing 25  $\mu$ g/ml kanamycin, 500  $\mu$ g/ml carbenicillin, and 500  $\mu$ g/ml vancomycin (MSMO-KVC) for 10 minutes at 800 rpm. Cells were subsequently weekly maintained in MSMO-KVC. After two weeks cells were weekly maintained in MSMO containing only 25  $\mu$ g/ml kanamycin. *Agrobacterium* clearance was confirmed on a RGTK plate.

### *Cloning and transformation*

Whole genomic fusions were prepared by cloning up to 3kb of promoter including downstream genomic region up to the stop codon into the pPLV117, containing a super Yellow Fluorescent Protein (sYFP) downstream of the LIC-site, using Ligation Independent Cloning (LIC; (LIC; (Aslanidis & de Jong, 1990; De Rybel et al., 2011; Wendrich, 2016)). All oligonucleotides used in this study are listed in Table S1. All constructs were confirmed by sequencing and transformed into *Arabidopsis* using floral dipping (Clough & Bent, 1998). Representative pictures from at least three independent transgenic lines are shown.

### *IP-MS on IQD cell cultures*

For affinity purifications 50 ml of 3-day old transgenic PSB-D cell suspension cultures were used. For  $\text{CaCl}_2$ , EGTA and paclitaxel (taxol) treatments, cells were sedimented to remove part of the medium and add the treatment media. The volume was returned to 50 mL after addition of treatments, and incubated for 5 minutes. Final concentrations for treatments were 10 mM  $\text{CaCl}_2$ , 10mM EGTA, and 10  $\mu$ M taxol. Cells were harvested on a 100 $\mu$ m nylon mesh, directly frozen in liquid nitrogen and grinded to a fine powder. For

protein extraction, grinded cells were suspended in 2 volumes lysis buffer (50mM Tris pH8, 150mM NaCl, 2mM MgCl<sub>2</sub>, 0.2 mM EDTA, 0.2%NP40, 20% Glycerol, 1mM DTT and 1xCPI) and sonicated in a Biorupter (Diagenode) at 4°C for three cycles (15s ON, 60s OFF). After sonication, lysate was spun down for 30 minutes at 14.000xg at 4°C. Supernatant was collected and protein concentration measured by the Bradford assay (Bio-rad).

Affinity purifications were conducted in technical triplicate. For each reaction 50µl GFP-TRAP agarose beads (Chromotek) were equilibrated by washing beads three times in lysis buffer for 2min at 2000xg at 4°C. For each replicate 10mg of whole cell lysate was used and incubated with beads at 4°C while rotating head over tail. After 90 minutes beads were sedimented by centrifugation for 2min at 2000xg at 4°C, washed twice in lysis buffer, twice in lysis buffer without NP40 and trice in 50mM Ammonium Bicarbonate (ABC).

#### *Sample preparation for mass spectrometry*

After last wash, bead precipitated proteins were alkylated in 50mM ABC supplemented with 50mM Acrylamide (Sigma-Aldrich) and incubated in the dark at 25°C for 30 minutes. After alkylation, on-bead trypsin digestion was performed by using 0.35µg trypsin (Roche) and incubated overnight at 25°C. After overnight digestion peptides were desalted and concentrated by C18 Stagetips as described previously (<https://doi.org/10.1038/nprot.2007.261>) with the modification that extra 1mg C18 Lichoprep beads were added. After C18 desalting peptides were vacuum dried and resuspended in 50µl 0.1% formic acid.

#### *LC-MS/MS and data analysis*

Peptides were applied to online nano LC-MS/MS mass spectrometer (Thermo Scientific) using a 60-minute acetonitrile gradient from 5-50%. Spectra were recorded on a LTQ-XL mass spectrometer (Thermo Scientific) and analysed according to ([https://doi.org/10.1007/978-1-4939-6469-7\\_14](https://doi.org/10.1007/978-1-4939-6469-7_14)). Maxquant output Proteingroups.txt was filtered in Perseus (v1.6.2.3.).

*Embryo isolation*

Ovules were collected from ~60 siliques using vacuum extraction. Siliques were stuck to double-sided tape and sliced open using a needle. Open siliques were submerged in 1x Phosphate-Buffered Saline (PBS) buffer and ovules were collected using a vacuum pump through 50  $\mu\text{m}$  filters. Collected ovules were then transferred to Isolation buffer (1x First Strand Buffer (FSB; Invitrogen), 1mM Dithiotreitol (DTT), 4% RNaseLater, MQ), and volume was reduced to ~20  $\mu\text{L}$ . Embryo isolation was performed according to (Raissig et al., 2013) with the following adaptations. A Zeiss Confocor 1 inverted microscope (Carl Zeiss Microscopy GmbH, Jena, Germany) together with an Eppendorf Transferrman 4r micromanipulator (Eppendorf AG) and VacuTip II microcapillaries (Eppendorf) were used to isolate about 40-50 washed embryos in 50  $\mu\text{L}$  isolation buffer.

*RNA isolation and RNA-seq library preparation*

Isolated embryos were immediately incubated with 500  $\mu\text{L}$  of TRIzol reagent (Ambion, CA, USA) for 30 min at 60°C, and samples were vortexed briefly (2× for two seconds each) to completely lyse cells. 100  $\mu\text{L}$  of chloroform was added, and incubated at room temperature for three minutes after vigorous vortexing for 15 seconds. The samples were centrifuged at 12,000g for 15 min at 4 °C, and the aqueous phase (~350  $\mu\text{L}$ ) was transferred to a new LoBind tube. To precipitate the RNA, 250  $\mu\text{L}$  of isopropanol and 1.5  $\mu\text{L}$  of GlycoBlue (22.5  $\mu\text{g}$ ; Life Tech) was added followed by a -20 °C overnight incubation and centrifugation at >20,000 g for 30 min at 4 °C. After removal of the supernatant, the pellet was washed by adding 500  $\mu\text{L}$  of 75% ethanol, vortexing briefly and then centrifuged at max speed for 15 min at 4 °C. This 75% ethanol wash step was repeated, and after removal of the 75% ethanol the pellet was air dried on ice for 10 min. Precipitated RNA was then resuspended with 11  $\mu\text{L}$  of nuclease-free water and incubated at 60 °C for 10 minutes to fully resuspend.

Samples were DNaseI treated using the RNase-free DNase set (Qiagen), and cleaned up using the RNeasy Minelute kit (Qiagen). Samples were eluted in 12  $\mu\text{L}$  RNase-free water and stored at -80 °C.

Smart-seq2 mRNA libraries were generated according to (Picelli et al., 2013) with the following adaptation. Final library preparation is done using the ThruPLEX DNA-seq kit (Takara Bio UASA). Control of quality and fragment length for both amplified cDNA and final libraries was done using High Sensitivity DNA chips and Bioanalyzer (Agilent)

*Microarray and quantification*

RNA was amplified using the Ovation Pico WTA System V2 (NuGEN, CA, USA), labelled with the ENCORE Biotin Module (NuGEN) and hybridized to Arabidopsis Gene 1.1 ST 24-array plates (atlas) or single array strips (nuclear vs. cellular RNA) (Affymetrix, CA, USA) according to the manufacturers protocol. Microarray analysis was performed using the MADMAX pipeline (Lin et al., 2017) and a custom CDF file (MBNI CustomCDF version 19.0.0) (Dai et al., 2005). Here, all expression values were (quantile) normalised by the Robust multi-array average algorithm (RMA) (Irizarry et al., 2012) using the median polish (nuclear vs. cellular RNA) or M-estimator (atlas) algorithm for probes to probe set summarisation. Probe sets were redefined using current genome information (Dai et al., 2005) and re-organized according to TAIR10 gene definitions. Linear models and an intensity-based moderated t statistic approach (Phipson et al., 2016; Sartor et al., 2006) were used to identify differentially expressed genes (probe sets). P-values were corrected for multiple testing using an optimized false discovery rate (FDR) approach (Storey & Tibshirani, 2003).

*RNA-sequencing and quantification*

For differential expression analysis, quality assessment for raw RNA-seq reads was performed using FastQC ([www.bioinformatics.babraham.ac.uk/projects/fastqc](http://www.bioinformatics.babraham.ac.uk/projects/fastqc)). Illumina adapters at the ends of the (paired) reads were cleaned up using TrimGalore (v0.5.0; <https://github.com/FelixKrueger/TrimGalore>) with the parameters “--stringency 5 --paired --length 70 --clip\_R1 30 --clip\_R2 30”. The cleaned FASTQ reads were mapped onto the Arabidopsis genome (TAIR10) using HISAT2 (v2.1.0; (Kim et al., 2015)) with default parameters. Post-processing of SAM/BAM files was performed using SAMTOOLS (v1.9; (Li et al., 2009)). FeatureCounts (v1.6.2; (Liao et al., 2014)) was used to count the raw reads corresponding to each gene, with the parameters “-t ‘exon’ -g ‘gene\_id’ -Q 30 -p --primary”. DESeq2 (Love et al., 2014) was used to normalize the raw counts and perform the differential expression analysis ( $\text{Padj} < 0.05$ ).

*Microscopic imaging and fluorescent staining*

Images were acquired in 8-bit format using a Leica TCS SP5II confocal laser scanning

microscope with a  $63 \times \text{NA} = 1.20$  water-immersion objective with pinhole set to 1.0 Airy unit. mGFP was excited by an argon-ion laser and SCRI Renaissance Stain 2200 (SR2200) (Renaissance Chemicals, <http://www.renchem.co.uk>) was excited using a diode laser, and their emissions were detected sequentially with a Leica HyD in photon counting mode. Excitation and detection of fluorophores were configured as follows: mYFP was excited at 515 nm and detected at 540–600 nm; Renaissance 2200 was excited at 405 nm and detected at 430–470 nm.

Embryos were stained by the modified Pseudo-Schiff propidium iodide (mPS-PI) staining method described in (Yoshida et al., 2014) with the following modification: An extra treatment with 1% SDS and 0.2 M NaOH for 10 minutes at 37 °C was added after fixation. The stained ovules/embryos were mounted in a drop of chloral hydrate in a well generated by SecureSealtm round imaging spacers (20mm, Thermofisher) and observed by confocal microscopy taking z-stack images. A series of 2D confocal images were recorded at 0.1  $\mu\text{m}$  intervals using a Leica TCS SP5II confocal laser scanning microscope with a  $63 \times \text{NA} = 1.20$  water-immersion objective with pinhole set to 1.0 Airy unit. PI was excited using a diode laser with excitation at 561 nm and detection at 600–700 nm.

Roots were stained using a simplified mPS-PI protocol. After fixation, 5-day old seedlings were rinsed and incubated in 1% periodic acid for 40 minutes at room temperature. The tissue was rinsed again and incubated in Schiff's reagent with a final volume of 300  $\mu\text{M}$  PI for 1 hour at room temperature. Seedlings were mounted in chloral hydrate solution under coverslips spaced by small coverslips to maintain shape.

## 6

### *Shortest division plane estimation and comparison to actual division plane*

To compute the relative division plane area, we used the following pipeline in MorphoGraphX. First the daughter cells of recently divided cells in segmented meshes were merged. Then the areas of the shortest ( $A_{\text{min}}$ ) and longest division plane ( $A_{\text{max}}$ ) in merged cells were determined by sampling of >5000 division directions uniformly spread on the cell volume, going through the centroid of the cell.

Then the actual division plane was approximated as a flat wall by computing the principal components of the voxels that were located at the shared border of the two daughter cells. After we simulated a division using this flat wall to determine the surface area of the real division wall ( $A$ ). Finally, we computed  $\hat{A} = (A - A_{\text{min}}) / (A_{\text{max}} - A_{\text{min}})$ .

Where  $\hat{A}$  is the normalized cell wall area,  $A_{\min}$  the area of the shortest sampled division plane,  $A_{\max}$  the largest sampled division plane, and  $A$  the area of the real cell wall.

## Acknowledgements

The authors would like to thank Dr. Katharina Burstenbinder for kindly providing the *iqd678* triple mutant lines, and Dr. Michael Prigge and Mark Estelle for kindly providing us the *tir1/afb* hexuple mutant lines. This work was supported by a Netherlands Organization for Scientific Research (NWO) grant (ALW 824.14.009) to D.W.

## References

- Abel, S., Bürstenbinder, K., & Müller, J. (2013). The emerging function of IQD proteins as scaffolds in cellular signaling and trafficking. *Plant Signaling and Behavior*. <https://doi.org/10.4161/psb.24369>
- Abel, S., Savchenko, T., & Levy, M. (2005). Genome-wide comparative analysis of the IQD gene families in *Arabidopsis thaliana* and *Oryza sativa*. *BMC Evolutionary Biology*. <https://doi.org/10.1186/1471-2148-5-72>
- Aslanidis, C., & de Jong, P. J. (1990). Ligation-independent cloning of PCR products (LIC-PCR). *Nucleic Acids Research*. <https://doi.org/10.1093/nar/18.20.6069>
- Barbier de Reuille, P., Routier-Kierzkowska, A.-L., Kierzkowski, D., Bassel, G. W., Schüpbach, T., Tauriello, G., ... Smith, R. S. (2015). MorphoGraphX: A platform for quantifying morphogenesis in 4D. *ELife*, 4, 05864. <https://doi.org/10.7554/eLife.05864>
- Berken, A. (2006). ROPs in the spotlight of plant signal transduction. *Cellular and Molecular Life Sciences*. <https://doi.org/10.1007/s00018-006-6197-1>
- Berken, Antje, Thomas, C., & Wittinghofer, A. (2005). A new family of RhoGEFs activates the Rop molecular switch in plants. *Nature*. <https://doi.org/10.1038/nature03883>
- Besson, S., & Dumais, J. (2011). Universal rule for the symmetric division of plant cells. *Proceedings of the National Academy of Sciences of the United States of America*, 108(15), 6294–6299. <https://doi.org/10.1073/pnas.1011866108>
- Besson, S., & Dumais, J. (2014). Stochasticity in the symmetric division of plant cells: When the exceptions are the rule. *Frontiers in Plant Science*. <https://doi.org/10.3389/fpls.2014.00538>
- Bürstenbinder, K., Mitra, D., & Quegwer, J. (2017). Functions of IQD proteins as hubs in cellular calcium and auxin signaling: A toolbox for shape formation and tissue-specification in plants? *Plant Signaling and Behavior*. <https://doi.org/10.1080/15592324.2017.1331198>
- Bürstenbinder, K., Möller, B., Plötner, R., Stamm, G., Hause, G., Mitra, D., & Abel, S. (2017). The IQD Family of Calmodulin-Binding Proteins Links Calcium Signaling to Microtubules, Membrane Subdomains, and the Nucleus. *Plant Physiology*. <https://doi.org/10.1104/pp.16.01743>

- Bürstenbinder, K., Savchenko, T., Müller, J., Adamson, A. W., Stamm, G., Kwong, R., ... Abel, S. (2013). Arabidopsis calmodulin-binding protein iq67-domain 1 localizes to microtubules and interacts with kinesin light chain-related protein-1. *Journal of Biological Chemistry*. <https://doi.org/10.1074/jbc.M112.396200>
- Chapman, E. J., & Estelle, M. (2009). Mechanism of Auxin-Regulated Gene Expression in Plants. *Annual Review of Genetics*. <https://doi.org/10.1146/annurev-genet-102108-134148>
- Clough, S. J., & Bent, A. F. (1998). Floral dip: A simplified method for *Agrobacterium*-mediated transformation of *Arabidopsis thaliana*. *Plant Journal*. <https://doi.org/10.1046/j.1365-3113X.1998.00343.x>
- Crawford, B. C. W., Sewell, J., Golembeski, G., Roshan, C., Long, J. A., & Yanofsky, M. F. (2015). Genetic control of distal stem cell fate within root and embryonic meristems. *Science*. <https://doi.org/10.1126/science.aaa0196>
- Cui, F., Brosché, M., Lehtonen, M. T. T., Amiryousefi, A., Xu, E., Punkkinen, M., ... Overmyer, K. (2016). Dissecting Absciscic Acid Signaling Pathways Involved in Cuticle Formation. *Molecular Plant*. <https://doi.org/10.1016/j.molp.2016.04.001>
- Dai, M., Wang, P., Boyd, A. D., Kostov, G., Athey, B., Jones, E. G., ... Meng, F. (2005). Evolving gene/transcript definitions significantly alter the interpretation of GeneChip data. *Nucleic Acids Research*. <https://doi.org/10.1093/nar/gni179>
- De Rybel, B., van den Berg, W., Lokerse, A. S., Liao, C.-Y., van Mourik, H., Möller, B., ... Weijers, D. (2011). A Versatile Set of Ligation-Independent Cloning Vectors for Functional Studies in Plants. *Plant Physiology*. <https://doi.org/10.1104/pp.111.177337>
- de Wildeman, E. (1893). Études sur l'attache des cloisons cellulaires. *Mémoires Couronnés et Mémoires Des Savants Étrangers*, 53, 1–84.
- Endo, S., Iwamoto, K., & Fukuda, H. (2018). Overexpression and cosuppression of xylem-related genes in an early xylem differentiation stage-specific manner by the AtTED4 promoter. *Plant Biotechnology Journal*. <https://doi.org/10.1111/pbi.12784>
- Engelhorn, J., Reimer, J. J., Leuz, I., Gobel, U., Huettel, B., Farrona, S., & Turck, F. (2012). DEVELOPMENT-RELATED PcG TARGET IN THE APEX 4 controls leaf margin architecture in *Arabidopsis thaliana*. *Development*. <https://doi.org/10.1242/dev.078618>

Errera, L. (1888). Über Zellformen und Siefenblasen. *Bot. Centralbl.*, 34, 395–399.

Gao, Y., & Zhao, Y. (2013). Epigenetic suppression of T-DNA insertion mutants in arabidopsis. *Molecular Plant*. <https://doi.org/10.1093/mp/sss093>

Gil, P., Dewey, E., Friml, J., Zhao, Y., Snowden, K. C., Putterill, J., ... Chory, J. (2001). BIG: A calossin-like protein required for polar auxin transport in Arabidopsis. *Genes and Development*. <https://doi.org/10.1101/gad.905201>

Hagen, G., & Guilfoyle, T. (2002). Auxin-responsive gene expression: Genes, promoters and regulatory factors. *Plant Molecular Biology*. <https://doi.org/10.1023/A:1015207114117>

Hamann, T., Benkova, E., Bäurle, I., Kientz, M., & Jürgens, G. (2002). The Arabidopsis BODENLOS gene encodes an auxin response protein inhibiting MONOPTEROS-mediated embryo patterning. *Genes and Development*. <https://doi.org/10.1101/gad.229402>

Höfte, H., & Voxeur, A. (2017). Plant cell walls. *Current Biology*. <https://doi.org/10.1016/j.cub.2017.05.025>

Irizarry, R. A., Hobbs, B., Collin, F., Beazer-Barclay, Y. D., Antonellis, K. J., Scherf, U., & Speed, T. P. (2012). Exploration, normalization, and summaries of high density oligonucleotide array probe level data. *In Selected Works of Terry Speed*. [https://doi.org/10.1007/978-1-4614-1347-9\\_15](https://doi.org/10.1007/978-1-4614-1347-9_15)

Kim, D., Langmead, B., & Salzberg, S. L. (2015). HISAT: A fast spliced aligner with low memory requirements. *Nature Methods*. <https://doi.org/10.1038/nmeth.3317>

Korfhage, U., Trezzini, G. F., Meier, I., Hahlbrock, K., & Somssich, I. E. (2007). Plant Homeodomain Protein Involved in Transcriptional Regulation of a Pathogen Defense-Related Gene. *The Plant Cell*. <https://doi.org/10.2307/3869873>

Kuusk, S., Sohlberg, J. J., Magnus Eklund, D., & Sundberg, E. (2006). Functionally redundant SHI family genes regulate Arabidopsis gynoecium development in a dose-dependent manner. *Plant Journal*. <https://doi.org/10.1111/j.1365-313X.2006.02774.x>

Li, H., Handsaker, B., Wysoker, A., Fennell, T., Ruan, J., Homer, N., ... Durbin, R. (2009). The Sequence Alignment/Map format and SAMtools. *Bioinformatics*. <https://doi.org/10.1093/bioinformatics/btp352>

Li, Y., Dai, X., Cheng, Y., & Zhao, Y. (2011). NPY genes play an essential role in root

gravitropic responses in Arabidopsis. *Molecular Plant*. <https://doi.org/10.1093/mp/ssq052>

Liang, H., Zhang, Y., Martinez, P., Rasmussen, C. G., Xu, T., & Yang, Z. (2018). The Microtubule-Associated Protein IQ67 DOMAIN5 Modulates Microtubule Dynamics and Pavement Cell Shape. *Plant Physiology*. <https://doi.org/10.1104/pp.18.00558>

Liao, C. Y., & Weijers, D. (2018). A toolkit for studying cellular reorganization during early embryogenesis in Arabidopsis thaliana. *Plant Journal*. <https://doi.org/10.1111/tpj.13841>

Liao, Y., Smyth, G. K., & Shi, W. (2014). FeatureCounts: An efficient general purpose program for assigning sequence reads to genomic features. *Bioinformatics*. <https://doi.org/10.1093/bioinformatics/btt656>

Lin, K., Kools, H., de Groot, P. J., Gavai, A. K., Basnet, R. K., Cheng, F., ... Leunissen, J. A. M. (2017). MADMAX – Management and analysis database for multiple -omics experiments. *Journal of Integrative Bioinformatics*. <https://doi.org/10.1515/jib-2011-160>

Love, M. I., Huber, W., & Anders, S. (2014). Moderated estimation of fold change and dispersion for RNA-seq data with DESeq2. *Genome Biology*. <https://doi.org/10.1186/s13059-014-0550-8>

Luschnig, C. (2001). Auxin transport: Why plants like to think BIG. *Current Biology*. [https://doi.org/10.1016/S0960-9822\(01\)00497-3](https://doi.org/10.1016/S0960-9822(01)00497-3)

Meng, L., Buchanan, B. B., Feldman, L. J., & Luan, S. (2012). CLE-like (CLEL) peptides control the pattern of root growth and lateral root development in Arabidopsis. *Proceedings of the National Academy of Sciences*. <https://doi.org/10.1073/pnas.1119864109>

Miedes, E., Suslov, D., Vandenbussche, F., Kenobi, K., Ivakov, A., Van Der Straeten, D., ... Vissenberg, K. (2013). Xyloglucan endotransglucosylase/hydrolase (XTH) overexpression affects growth and cell wall mechanics in etiolated Arabidopsis hypocotyls. *Journal of Experimental Botany*. <https://doi.org/10.1093/jxb/ert107>

Möller, B. K. (2012). Identification of novel MONOPTEROS target genes in embryonic root initiation. *Wageningen University*.

Möller, Barbara K., Ten Hove, C. A., Xiang, D., Williams, N., López, L. G., Yoshida, S., ... Weijers, D. (2017). Auxin response cell-autonomously controls ground tissue initiation in the early Arabidopsis embryo. *Proceedings of the National Academy of Sciences of the*

*United States of America*. <https://doi.org/10.1073/pnas.1616493114>

Müller, K., Levesque-Tremblay, G., Bartels, S., Weitbrecht, K., Wormit, A., Usadel, B., ... Kermode, A. R. (2013). Demethylesterification of cell wall pectins in *Arabidopsis* plays a role in seed germination. *Plant Physiology*. <https://doi.org/10.1104/pp.112.205724>

Nacry, P., Camilleri, C., Courtial, B., Caboche, M., & Bouchez, D. (1998). Major chromosomal rearrangements induced by T-DNA transformation in *Arabidopsis*. *Genetics*.

Nakajima, K., Furutani, I., Tachimoto, H., Matsubara, H., & Hashimoto, T. (2004). SPIRAL1 Encodes a Plant-Specific Microtubule-Localized Protein Required for Directional Control of Rapidly Expanding *Arabidopsis* Cells. *The Plant Cell*. <https://doi.org/10.1105/tpc.017830>

Nibau, C., Wu, H. ming, & Cheung, A. Y. (2006). RAC/ROP GTPases: “hubs” for signal integration and diversification in plants. *Trends in Plant Science*, 11(6), 309–315. <https://doi.org/10.1016/j.tplants.2006.04.003>

Paponov, I. A., Paponov, M., Teale, W., Menges, M., Chakrabortee, S., Murray, J. A. H., & Palme, K. (2008). Comprehensive transcriptome analysis of auxin responses in *Arabidopsis*. *Molecular Plant*. <https://doi.org/10.1093/mp/ssm021>

Parry, G., Calderon-Villalobos, L. I., Prigge, M., Peret, B., Dharmasiri, S., Itoh, H., ... Estelle, M. (2009). Complex regulation of the TIR1/AFB family of auxin receptors. *Proceedings of the National Academy of Sciences*. <https://doi.org/10.1073/pnas.0911967106>

Phipson, B., Lee, S., Majewski, I. J., Alexander, W. S., & Smyth, G. K. (2016). Robust hyperparameter estimation protects against hypervariable genes and improves power to detect differential expression. *Annals of Applied Statistics*. <https://doi.org/10.1214/16-AOAS920>

Picelli, S., Björklund, Å. K., Faridani, O. R., Sagasser, S., Winberg, G., & Sandberg, R. (2013). Smart-seq2 for sensitive full-length transcriptome profiling in single cells. *Nature Methods*. <https://doi.org/10.1038/nmeth.2639>

Prigge, M. J., Greenham, K., Zhang, Y., Santner, A., Castillejo, C., Mutka, A. M., ... Estelle, M. (2016). The *Arabidopsis* Auxin Receptor F-Box Proteins AFB4 and AFB5 Are Required for Response to the Synthetic Auxin Picloram. *Genetics*. <https://doi.org/10.1534/g3.115.025585>

- Prigge, M. J., Kadakia, N., Greenham, K., & Estelle, M. (2019). Members of the Arabidopsis auxin receptor gene family are essential early in embryogenesis and have broadly overlapping functions. *BioRxiv*. <https://doi.org/10.1101/529248>
- Rademacher, E. H., Lokerse, A. S., Schlereth, A., Llavata-Peris, C. I., Bayer, M., Kientz, M., ... Weijers, D. (2012). Different Auxin Response Machineries Control Distinct Cell Fates in the Early Plant Embryo. *Developmental Cell*. <https://doi.org/10.1016/j.devcel.2011.10.026>
- Radoeva, T., Lokerse, A. S., Llavata-Peris, C. I., Wendrich, J. R., Xiang, D., Liao, C.-Y., ... Weijers, D. (2019). A Robust Auxin Response Network Controls Embryo and Suspensor Development through a Basic Helix Loop Helix Transcriptional Module. *The Plant Cell*. <https://doi.org/10.1105/tpc.18.00518>
- Raissig, M. T., Gagliardini, V., Jaenisch, J., Grossniklaus, U., & Baroux, C. (2013). Efficient and Rapid Isolation of Early-stage Embryos from Arabidopsis thaliana Seeds. *Journal of Visualized Experiments*. <https://doi.org/10.3791/50371>
- Ruegger, M., Dewey, E., Gray, W. M., Hobbie, L., Turner, J., & Estelle, M. (1998). The TIR1 protein of Arabidopsis functions in auxin response and is related to human SKP2 and yeast Grr1p. *Genes and Development*. <https://doi.org/10.1101/gad.12.2.198>
- Sartor, M. A., Tomlinson, C. R., Wesselkamper, S. C., Sivaganesan, S., Leikauf, G. D., & Medvedovic, M. (2006). Intensity-based hierarchical Bayes method improves testing for differentially expressed genes in microarray experiments. *BMC Bioinformatics*. <https://doi.org/10.1186/1471-2105-7-538>
- Sato, S., Kato, T., Kakegawa, K., Ishii, T., Liu, Y. G., Awano, T., ... Shibata, D. (2001). Role of the putative membrane-bound endo-1,4- $\beta$ -glucanase KORRIGAN in cell elongation and cellulose synthesis in Arabidopsis thaliana. *Plant and Cell Physiology*. <https://doi.org/10.1093/pcp/pce045>
- Schlereth, A., Möller, B., Liu, W., Kientz, M., Flipse, J., Rademacher, E. H., ... Weijers, D. (2010). MONOPTEROS controls embryonic root initiation by regulating a mobile transcription factor. *Nature*, 464(7290), 913–916. <https://doi.org/10.1038/nature08836>
- Sedbrook, J. C., Ehrhardt, D. W., Fisher, S. E., Scheible, W.-R., & Somerville, C. R. (2004). The Arabidopsis SKU6 / SPIRAL1 Gene Encodes a Plus End–Localized Microtubule-Interacting Protein Involved in Directional Cell Expansion . *The Plant Cell*. <https://doi.org/10.1105/tpc.100000>

org/10.1105/tpc.020644

Shichrur, K., & Yalovsky, S. (2006). Turning ON the switch--RhoGEFs in plants. *Trends in Plant Science*, 11(2), 57–59. <https://doi.org/10.1016/j.tplants.2005.12.001>

Shimizu, R., Ji, J., Kelsey, E., Ohtsu, K., Schnable, P. S., & Scanlon, M. J. (2009). Tissue Specificity and Evolution of Meristematic WOX3 Function. *Plant Physiology*. <https://doi.org/10.1104/pp.108.130765>

Smith, Z. R., & Long, J. A. (2010). Control of Arabidopsis apical-basal embryo polarity by antagonistic transcription factors. *Nature*, 464(7287), 423–426. <https://doi.org/10.1038/nature08843>

Storey, J. D., & Tibshirani, R. (2003). Statistical significance for genomewide studies. *Proceedings of the National Academy of Sciences*. <https://doi.org/10.1073/pnas.1530509100>

Suzuki, M., Yamazaki, C., Mitsui, M., Kakei, Y., Mitani, Y., Nakamura, A., ... Shimada, Y. (2015). Transcriptional feedback regulation of YUCCA genes in response to auxin levels in Arabidopsis. *Plant Cell Reports*. <https://doi.org/10.1007/s00299-015-1791-z>

Swarup, K., Benková, E., Swarup, R., Casimiro, I., Péret, B., Yang, Y., ... Bennett, M. J. (2008). The auxin influx carrier LAX3 promotes lateral root emergence. *Nature Cell Biology*. <https://doi.org/10.1038/ncb1754>

Takato, S., Kakei, Y., Mitsui, M., Ishida, Y., Suzuki, M., Yamazaki, C., ... Shimada, Y. (2017). Auxin signaling through SCF TIR1/AFBs mediates feedback regulation of IAA biosynthesis. *Bioscience, Biotechnology and Biochemistry*. <https://doi.org/10.1080/09168451.2017.1313694>

Tax, F. E., & Vernon, D. M. (2001). T-DNA-associated duplication/translocations in Arabidopsis. Implications for mutant analysis and functional genomics. *Plant Physiology*. <https://doi.org/10.1104/pp.126.4.1527>

Tiwari, S. B., Wang, X.-J., Hagen, G., & Guilfoyle, T. J. (2007). AUX/IAA Proteins Are Active Repressors, and Their Stability and Activity Are Modulated by Auxin. *The Plant Cell*. <https://doi.org/10.2307/3871536>

Vieten, A., Vanneste, S., Wisniewska, J., Benkova, E., Benjamins, R., Beeckman, T., ... Friml, J. (2005). Functional redundancy of PIN proteins is accompanied by auxin-

dependent cross-regulation of PIN expression. *Development*. <https://doi.org/10.1242/dev.02027>

Vissenberg, K., Oyama, M., Osato, Y., Yokoyama, R., Verbelen, J. P., & Nishitani, K. (2005). Differential expression of AtXTH17, AtXTH18, AtXTH19 and AtXTH20 genes in Arabidopsis roots. Physiological roles in specification in cell wall construction. *Plant and Cell Physiology*. <https://doi.org/10.1093/pcp/pci013>

Weijers, D., Schlereth, A., Ehrismann, J. S., Schwank, G., Kientz, M., & Jürgens, G. (2006). Auxin triggers transient local signaling for cell specification in Arabidopsis embryogenesis. *Developmental Cell*. <https://doi.org/10.1016/j.devcel.2005.12.001>

Weijers, D., Van Hamburg, J. P., Van Rijn, E., Hooykaas, P. J. J., & Offringa, R. (2003). Diphtheria Toxin-Mediated Cell Ablation Reveals Interregional Communication during Arabidopsis Seed Development. *Plant Physiology*. <https://doi.org/10.1104/pp.103.030692>

Wendrich, J. R. (2016). Stem cell organization in Arabidopsis: from embryos to root. *Wageningen University*.

Wendrich, J., Yang, B.-J., Mijnhout, P., Xue, H.-W., Rybel, B. De, & Weijers, D. (2018). IQD proteins integrate auxin and calcium signaling to regulate microtubule dynamics during Arabidopsis development. *BioRxiv*. <https://doi.org/10.1101/275560>

Yang, Z. (2008). Cell Polarity Signaling in Arabidopsis. *Cell*, 24, 551–575. <https://doi.org/10.1146/annurev.cellbio.23.090506.123233>. *Cell*

Yang, Z., & Fu, Y. (2007). ROP/RAC GTPase signaling. *Current Opinion in Plant Biology*. <https://doi.org/10.1016/j.pbi.2007.07.005>

Yoshida, S., Barbier de Reuille, P., Lane, B., Bassel, G. W., Prusinkiewicz, P., Smith, R. S., & Weijers, D. (2014). Genetic control of plant development by overriding a geometric division rule. *Developmental Cell*, 29(1), 75–87. <https://doi.org/10.1016/j.devcel.2014.02.002>

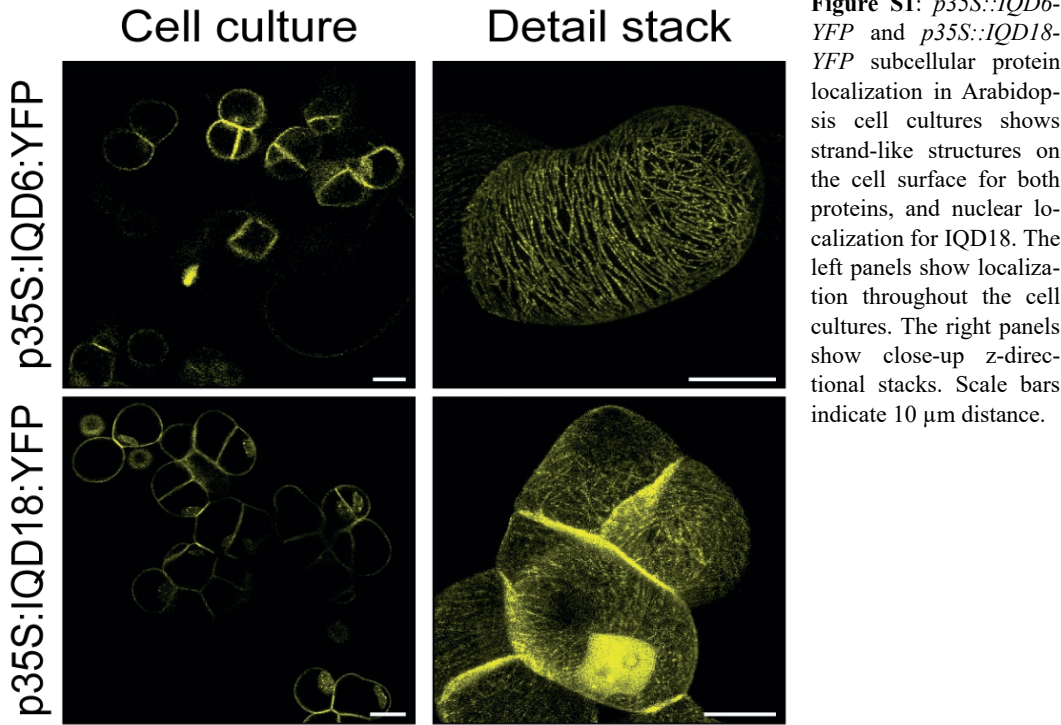
Zhao, C., Avci, U., Grant, E. H., Haigler, C. H., & Beers, E. P. (2008). XND1, a member of the NAC domain family in Arabidopsis thaliana, negatively regulates lignocellulose synthesis and programmed cell death in xylem. *Plant Journal*. <https://doi.org/10.1111/j.1365-3113X.2007.03350.x>

Zhao, J., Favero, D. S., Peng, H., & Neff, M. M. (2013). Arabidopsis thaliana AHL

family modulates hypocotyl growth redundantly by interacting with each other via the PPC/DUF296 domain. *Proceedings of the National Academy of Sciences*. <https://doi.org/10.1073/pnas.1219277110>

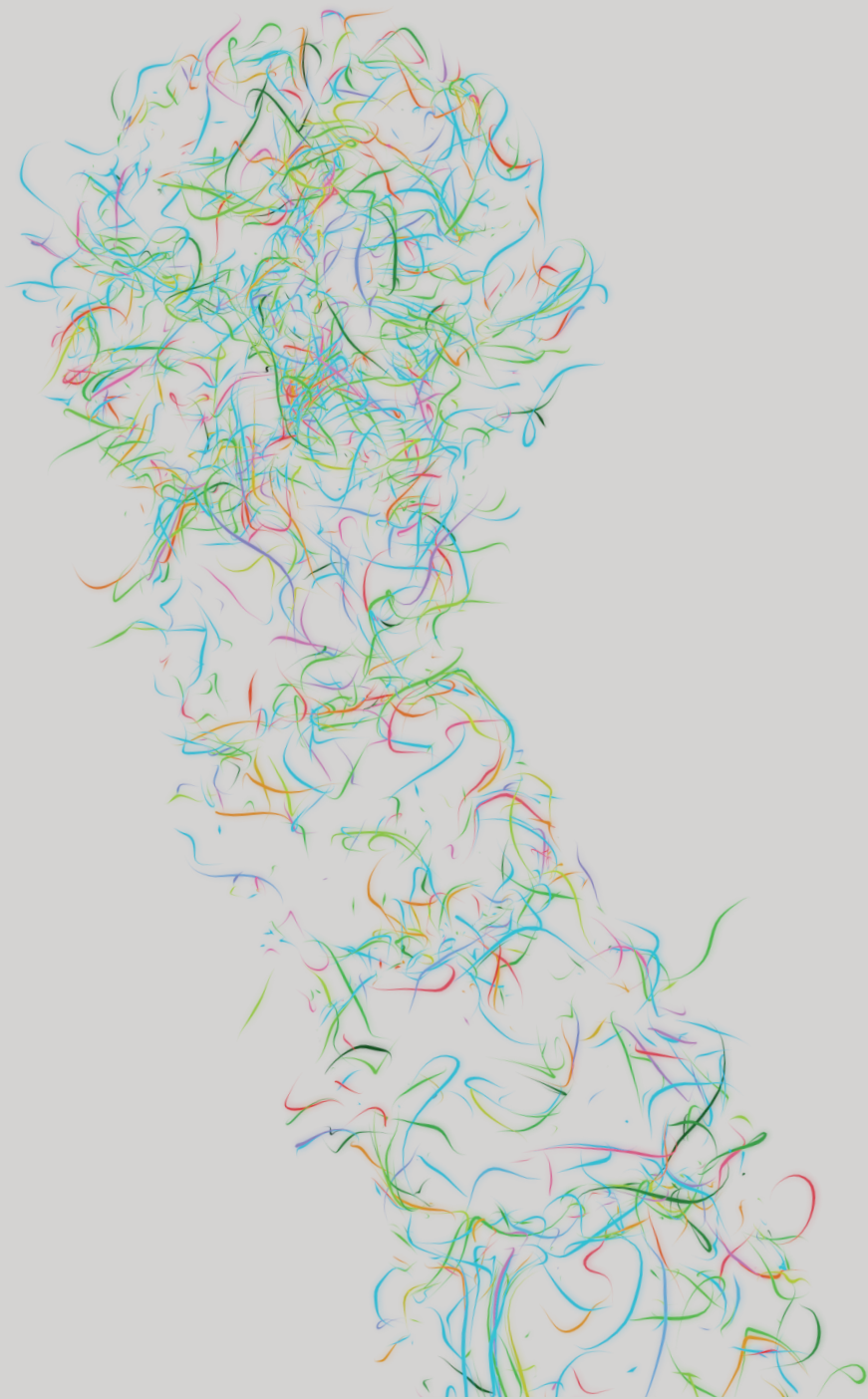
Zhao, Y., Medrano, L., Ohashi, K., Fletcher, J. C., Yu, H., Sakai, H., & Meyerowitz, E. M. (2004). HANABA TARANU Is a GATA Transcription Factor That Regulates Shoot Apical Meristem and Flower Development in Arabidopsis. *The Plant Cell*. <https://doi.org/10.1105/tpc.104.024869>

Supplementary materials



**Table S1:** Oligonucleotides used for Ligation-independent Cloning (LIC) of translational IQD-protein fusions in this study.

Gene	Sense/ Antisense	Sequence
IQD6 / AT2G26180	Sense	5'-TAGTTGGAATGGGTTCCCAACAAAAAAGTGCAACAGAC-3'
IQD6 / AT2G26180	Antisense	5'-TTATGGAGTTGGGTTCCACCTCTCGGCTTCTCGAATCGAGTA-3'
IQD7 / AT1G17480	Sense	5'-TAGTTGGAATGGGTTTGCAAAACCCGACACTAAA-3'
IQD7 / AT1G17480	Antisense	5'-TTATGGAGTTGGGTTCCGCTTCGCTGGCTCTTGG-3'
IQD8 / AT1G17480	Sense	5'-TAGTTGGAATGGGTTCAAAGGAAGGAATAATGGAGTCTG-3'
IQD8 / AT1G17480	Antisense	5'-TTATGGAGTTGGGTTCCGCTCTCTGGCTCTTTGC-3'



# Chapter 7

## General discussion

Thijs de Zeeuw



Land plants can grow to tremendous body sizes, yet even the most complex plant architectures are the result of iterations of the same developmental processes: organ initiation, growth, and pattern formation. A central question in plant biology is how these processes are regulated and coordinated to allow for the formation of ordered, three-dimensional structures. All elementary plant developmental processes first occur in early embryogenesis, during which, from a fertilized egg cell, precursors for all major tissues and stem cells are initiated, followed by tissue growth and patterning (Johri et al., 1992; Jürgens & Mayer, 1994). In contrast to animal cells, plant cells are unable to migrate because of their enclosure in pecto-cellulosic plant cell walls. Therefore, control of cell division orientation is crucial for correct plant development and ultimately plant shape. Plant cell division simulations and abstractions are mainly based on classical rules proposed in the 18th century by mathematicians, stating that a cell will divide along the plane of least area that encloses a fixed cellular volume (de Wildeman, 1893; Errera, 1888). This type of division was later defined as the “shortest wall” rule (Besson & Dumais, 2014) and is considered the default division orientation solely based on geometric principles. All symmetric division during early *Arabidopsis thaliana* embryogenesis can be explained using the geometric “shortest wall” rule, but all formative asymmetric divisions need additional regulation (Yoshida et al., 2014). Inhibition of auxin response in the embryo by expression of a nondegradable version of the AUX/IAA protein BODENLOS/IAA12 (BDL) under control of the *RPS5A* promoter (*RPS5A>>bdl*; *bdl*-mutant) inhibits formative asymmetric divisions in *Arabidopsis* embryos (Yoshida et al., 2014), indicating that auxin signalling is involved in the genetic regulation underlying formative divisions. A major unanswered question is how cell division orientation is regulated downstream of auxin-signalling, and which molecular and cell-biological factors are responsible for this regulation. In this thesis, combining modelling strategies with high-resolution microscopic visualization, transcriptomic analysis and computational tools, we identify factors involved in regulation of cell division orientation downstream of auxin-signalling.

## **Symmetric non-formative divisions in *Arabidopsis* embryos can be explained by cortical microtubule organisation**

In **Chapter 3**, using realistic cell shapes for modelling, we created a cortical Microtubule (CMT) model to explain cell division patterns in the *Arabidopsis thaliana* embryos, combining MT dynamics with geometrical division rules. Combining this modelling

strategy with high-resolution imaging of an embryo specific Green Fluorescent Protein (GFP)-tagged TUA6 protein to visualize MTs in Arabidopsis embryos enabled us to predict MT organisation in the embryo, and the modelled CMA orientation predicts division plane position in plant embryos.

From this work, we argue that it is plausible that a minimal set of rules based on cell geometry and simple MT-MT interactions- and dynamics is sufficient to predict most divisions during Arabidopsis embryogenesis. As in previous cell division studies (Von Wangenheim et al., 2016; Yoshida et al., 2014), our results show that cell division regulatory mechanism for most proliferative divisions in plants follow a “default” division, requiring minimal regulation. Only essential formative divisions require regulatory input, in this case through auxin-mediated MT regulation. We illustrate that minimal MT regulation through a combination of mechanisms can be sufficient to trigger the formative divisions during embryogenesis. The MT-regulation we propose to be involved in cell division orientation regulation is based on observed reduction of microtubule stability in auxin-insensitive mutants and plausible consequences of known molecular processes. Enhanced MT stability on newly formed division faces could be transiently established by auxin-mediated localization of MT-associated proteins (MAPs). Although not shown in plants, within cultured neuron cells, different MT populations may exhibit a wide range of stabilities within the same cell (Witte et al., 2008), and *in vitro* studies show that MAPs are able to bind to MT polymers to locally stabilize MT regions (Job et al., 1985). Edge-catastrophe could be reduced by the activity of MAPs that stabilize bending MTs. CLASP is one plant protein suggested to localize to cell edges to reduce edge-induced MT depolymerization (Ambrose et al., 2011; Pietra et al., 2013), but it’s function remains to be elucidated. Our results show that implementing an edge-catastrophe reduction can correctly predict wild-type division planes only when it is strictly spatially controlled. This special restriction should be reflected in the localization of MAPs when they are involved in cell division orientation control. Future molecular- and cell biological research should aim for the identification of factors involved in local MT stabilization and edge-catastrophe reducing factors, and the spatial regulation of these factors in plant cells. This study further shows that MT-dynamics are the main determinant for the function of MTs in cell division control, making live-imaging of the MT-network crucial to follow (local) changes in MT-dynamics. Live-imaging of MTs in the embryo is however challenging, since signal emission is hindered by the seed coat cell layers, causing weak signals and high amounts of noise due to signal scattering. To gain the high resolution necessary to observe MTs in

detail, future attempts should focus on imaging using two-photon excitation systems (Gooh et al., 2015; Kimata et al., 2019), and possibly novel embryo culturing systems to allow embryonic development without surrounding seed coat cell layers.

While it is clear that MTs play a role in cell division orientation regulation, the mechanism by which this regulation occurs is unknown. Directional cues for cell division orientation have previously been hypothesized to be provided by cell polarity (Lukowitz et al., 2004; Ueda et al., 2011; Wang et al., 2007; Yoshida et al., 2014, 2019). The involvement of cell polarity in CMT array regulation is further suggested by the necessity of a polar factor regulating MT-stability at cell edges in our model. Although mechanisms regulating cell polarity are largely unknown, identified polarly localized proteins like SOSEKI (SOK) (Yoshida, 2019), Rab-A5c (Kirchhelle et al., 2019), and CLASP (Ambrose et al., 2011) have been shown to react to the CMT array and mechanical stresses (Kirchhelle et al., 2019; Wodarz, 2002), and mutants for polarly localized proteins shown defects in cell division patterns (Ambrose et al., 2011; Kirchhelle et al., 2019; Yoshida et al., 2019). To further unravel the possible involvement of the CMT array in cell polarity mechanisms, and the role of cell polarity in cell division regulation, more factors involved in cell polarity regulation should be identified. Research focusing on cell polarity is hindered by lethality of mutants for key factors involved in the process. Combining high-throughput mutant screening with different polarity markers like NIP5 and BOR1 (Liao & Weijers, 2018) in early Arabidopsis embryos could possibly enable identification of factors connecting polarity-dependent CMT regulation to cell division orientation control downstream of auxin-signalling.

## Auxin response inhibition alters actin filament organisation and cell shape

A multitude of cellular structures and processes can contribute to the regulation of cell division orientation in plant cells. In **Chapter 4**, we visualized actin filament organisation, cell shape and nuclear position to determine their role in regulation of cell division orientation. The actin cytoskeleton has previously been shown to regulate cell shape in a variety of cells during plant development (Harries et al., 2005; Vidali et al., 2009; Wu & Bezanilla, 2018), and loss of function mutants of many actin-binding proteins exhibit severe defects in cell shape (Ringli et al., 2002; Vidali et al., 2010, 2009). Since cell division orientation is predominately based on cell geometry (Besson & Dumais, 2014; Chakraborty et al., 2018; Yoshida et al., 2014), it is likely that local cell shape changes can result in a change

of division plane orientation. Additionally, our visualization of F-actin filaments in the Arabidopsis embryo, together with previous research in Arabidopsis embryos and *Nicotiana benthamiana* BY-2 cells, shows that thick F-actin bundles form peri-nuclear arches around embryonic nuclei (Liao & Weijers, 2018; Yu et al., 2006). These peri-nuclear F-actin rings possibly regulate or stabilize nuclear position, as actin was shown to be involved in nuclear movement in several cell types (Elsner et al., 2012; Kimata et al., 2019; Ramakrishna et al., 2019; Von Wangenheim et al., 2016). Analysing the F-actin cytoskeleton in detail in the *bdl*-mutant, we show that F-actin stability and peri-nuclear arches are affected downstream of auxin-signalling. Analysis of *bdl*-mutant embryonic cell morphology reveals that these cells are primarily elongated in the longitudinal direction. These finding possibly connect F-actin regulation with cell morphological changes downstream of auxin-signalling. Although cell morphology is a main determinant for cell division orientation (Besson & Dumais, 2014; Yoshida et al., 2014), we confirm in **Chapter 4** of this thesis that the formative division in the embryo cannot be regulated solely by regulation of cell morphology. This suggests that the observed cell morphological differences are not sufficient to fully explain division pattern in Arabidopsis embryos.

Analysis of nuclear position relative to the cell membrane reveals that nuclear position is highly variable in both 4-cell and 8-cell wild-type- and *bdl*-mutant embryos. Although nuclear size (Elsner et al., 2012) and position (Iwabuchi et al., 2019; Kimata et al., 2019; Von Wangenheim et al., 2016) has previously been shown to be essential for correct cell division position in elongated and highly vacuolated cells, the high variability in nuclear position in the small embryonic cells argues against the involvement of nuclear position as a determining factor for the invariant embryonic division pattern. Alternatively, nuclear position is specific for regulation of cell division position in particular developmental stages and cell types, like previously suggested for polar vacuole distribution (Kimata et al., 2019).

In **Chapter 4**, using the *bdl*-mutant as a cell-biological tool, we gained insight in the role of different factors on cell division orientation control and pattern formation in the embryo downstream of auxin-signalling. As previously discussed, additional factors like cell polarity can contribute to processes like CMT stability regulation, but also actin organisation and cell shape (Li et al., 2003; Yang, 2008). Disruption of polarity is associated with incorrect divisions and in many cases lethality (Lukowitz et al., 2004; Ueda et al., 2011; Wang et al., 2007), but downstream cellular mechanisms are unknown. It is possible that the formative divisions during embryogenesis that deviate from geometrically-defined

division are the first divisions that require an established polarity (Yoshida et al., 2014). Visualizing polarity markers like NIP5 and BOR1 (Liao & Weijers, 2018) in the *bdl*-mutant background should allow to identify changes or defects in polarity in 8-cell embryos. Connecting possible defects in early-embryonic polarity with different cellular processes like CMT array dynamics, actin dynamics and cell shape will further elucidate the pathway regulating cell division orientation downstream of auxin-signalling.

## A reference transcriptome for early Arabidopsis embryogenesis

Our combined results in chapter 3- and 4 suggest a role for plant cytoskeletal structures in regulation of cell division orientation. In an attempt to dissect the mechanisms underlying regulation of the cytoskeleton and cell morphology downstream of auxin-signalling, in **Chapter 5** we developed and optimized a pipeline for high-quality transcriptomic analysis of Arabidopsis embryos. Validation of our pipeline using several mutants with either strong- or mild transcriptomic profile changes showed that our method is sensitive enough to detect substantial groups of misexpressed genes involved in different developmental processes.

Key developmental processes are initiated in the early Arabidopsis embryo through a tightly coordinated interplay of oriented cell division, cell-cell communication and genetic regulation (Johri et al., 1992; Jürgens & Mayer, 1994). To generate a resource for exploring the genetic regulation underlying tissue initiation during embryogenesis, we created an early Arabidopsis embryo temporal reference transcriptome containing transcriptome profiles for 2-cell to globular-stage embryos. This data shows that key tissue specification events might occur earlier in development than previously known. Key factors in vascular tissue initiation like TMO5 and LHW are expressed in early-stage embryos well before vascular tissue initiation. Future research should show if early expression of these genes is biologically relevant, but this finding shows that with our approach we are able to detect novel expression patterns for genes essential in embryonic development.

Using gene expression cluster analysis and GO-enrichment studies we demonstrate that the reference transcriptome dataset contains clusters of genes with unique expression patterns correlating to specific cellular processes. By identifying genes with known key functions in initiation of different cell types in the gene expression clusters, this dataset can help identifying novel genes involved in the same processes. Overall, this reference dataset will be a powerful tool for future embryonic developmental biology.

## Auxin-signalling is involved in cell division control and radial patterning

In **Chapter 6**, we analyse downstream embryonic effects of auxin-insensitivity using the *bdl*- and *tir1/afb*-mutants. Combining high-resolution imaging with computational tools to analyse the embryonic division phenotype qualitatively and quantitatively, we show that the *tir1/afb*-mutant division defect is not identical to the *bdl*-mutant phenotype (Yoshida et al., 2014). Where the *bdl*-mutant is characterized by a complete lack of embryonic formative asymmetric division, the *tir1/afb*-mutant shows a large variety in division plane orientation and surface area during formative divisions. Within the same *tir1/afb* embryo, during formative asymmetric divisions, cells either divide according wild-type patterns, or divisions can shift towards a more symmetric division using minimal surface area. This shows that auxin-insensitivity through mutation of the TIR1/AFB complex does influence formative asymmetric cell divisions, but the division phenotype is not completely penetrant in all embryonic cells. This might indicate that auxin-signalling is not completely absent in the *tir1/afb*-mutant background. Alternatively, BDL protein levels are significantly higher in the *bdl*-mutant compared to the *tir1/afb*-mutant, this excess of BDL protein could regulate additional factors necessary for the robust division pattern observed in the *bdl*-mutant background.

To test this, we exploited our optimized Arabidopsis embryo transcriptome pipeline to analyse and compare the transcriptomic profiles of 8-cell *bdl*- and *tir1/afb* mutant embryos. We identified a large group of upregulated genes in the *tir1/afb*-mutant, which probably represents secondary molecular responses to regulation by the big TIR1/AFB protein complex. Since the TIR1/AFB protein complex and BDL are known to function in the same regulatory pathway, it is surprising that we found very limited overlap between directly downregulated factors in the two mutants. Partly, this can be explained by the small number of homozygous mutant embryos in the dataset for the segregating *tir1/afb*-mutant, causing very limited overlap of transcriptionally downregulated factors between the mutants. Alternatively, this might indicate that regulation downstream of BDL is stronger- or different from molecular regulation downstream of the TIR1/AFB complex, which would explain the difference in cell division phenotype in the mutants.

Using the *bdl*-mutant dataset, we identified a large group of heavily misregulated genes in 8-cell *bdl*-mutant embryos. The majority of misregulated genes are transcription factors (TFs), of which many are known to be involved in transcriptional regulation and pattern formation in different plant tissues. Most of the identified transcription factors do

not have a known function in embryonic cells, and it will be interesting to see if the heavily misregulated TFs have similar or specific functions in early embryonic pattern formation. Additionally, we identified a large group of non-transcription factor genes misregulated in the *bdl*-mutant with known functions in cell wall architecture and cytoskeletal regulation. As previously discussed, cell shape is a possible factor influencing cell division regulation downstream of auxin-signalling. Transcriptional regulation of cell wall related genes like *FASCICLIN-LIKE ARABINOGALACTAN-PROTEIN 12 (FLA12)*, Xyloglucan Endotransglucosylase/hydrolase *XTH19*, *PECTIN METHYLESTERASE 44 (PME44)*, and *CELLULASE2 (CEL2)*, which can cause changes in cell wall architecture (Miedes et al., 2013; Pelloux et al., 2007; Sato et al., 2001; Vissenberg et al., 2005) and tissue morphology (Wells et al., 2013), may contribute to regulating cell shape in the embryo. We have shown that the plant cytoskeleton is affected downstream of auxin-signalling, and could possibly play a role in cell division regulation. The actin cytoskeleton is known to be regulated by Rho-of-plant (ROP) GTPases like *RHO-RELATED PROTEIN FROM PLANTS 9 (ROP9)* through binding a variety of effectors, including protein kinases and actin-binding proteins (Fu et al., 2001; Zhao & Manser, 2005). Downregulation of both *ROP9* and an activator of ROPs *ROP GUANINE NUCLEOTIDE EXCHANGE FACTOR 5 (ROPGEF5)* in the *bdl*-mutant could affect cellular or sub-cellular assembly or disassembly of filamentous actin, which in turn can affect cell shape and cell division plane regulation (Yanagisawa et al., 2015). Auxin-dependent MT-cytoskeleton regulation has been hypothesized to depend on the calmodulin binding IQ-domain protein family (Wendrich et al., 2018). Heavy downregulation of *IQ-domain 6 (IQD6)* in the *bdl*-mutant captured our attention because this gene would directly connect auxin signalling with cytoskeletal control and regulation of cell division control.

## **IQD6-8 proteins link auxin signalling to Ca<sup>2+</sup>-dependent cell division control**

The IQD6 protein was previously reported to be involved in calcium-dependent control of plant cytoskeleton organisation (Bürstenbinder et al., 2017, 2013; Wendrich et al., 2018). We characterized the closely related IQD6-8 subclade to elucidate their function in cell division control and plant embryonic development. Localization of all members of this subclade on MTs and specialized MT-structures (spindle, preprophase band [PPB], and phragmoplast) in both embryos and roots indicates a role for these proteins in cytoskeleton regulation. Most other IQD proteins have been reported to localize to cortical MTs and

nuclei (Abel et al., 2005; Bürstenbinder et al., 2013; Wendrich et al., 2018), but localization to specialized MT-structures is less common. This localization might suggest a specialized function in plant cell division control for this subclade within the IQD protein family. Like other microtubule associated proteins (MAPs), the IQD6-8 subclade could function in organisation of spindle microtubules (Ambrose et al., 2007) through MT-stability regulation, limiting of phragmoplast array dimensions during mitosis (Raemaekers et al., 2003) to ensure invariant division patterns, or the integration of antiparallel microtubules in the phragmoplast during cytokinesis (Lee et al., 2007) to regulate cell plate formation.

Detailed analysis of *iqd678*-mutant shows clear defects in cell division orientation in both embryos and roots, indicating that the IQD6-8 protein subclade is involved in cell division orientation regulation. In embryos, the *iqd678*-mutant has a large variability in cell division plane orientation with either subtle or severe phenotypic consequences, confirmed both by cell division plane area and volume ratio measurements.

An IP-MS/MS experiment, identifying IQD6 partner proteins, confirms previously shown protein-protein interactions of IQD proteins with calmodulins and multiple factors associated with the cytoskeleton. Additionally, we showed  $\text{Ca}^{2+}$ -dependent interactions with actin and actin-depolymerization factors, suggesting that a role for IQD6 in cell division orientation control is possibly mediated through  $\text{Ca}^{2+}$ -dependent control of the cytoskeleton.

## Cell division orientation and formative cell divisions are separately regulated

Interestingly, although division plane orientation can be heavily skewed in *iqd678*-mutant early embryos, cell divisions crucial for radial patterning forming the 16-cell embryo are mostly placed correctly, creating inner and outer cell layers. The ability of this mutant to correctly regulate patterning events and overall development is illustrated by the viability of adult plants without a distinguishable phenotype. Combined, these results show that the IQD6-8 subclade is involved in cell division control, and possibly they contribute to the auxin-dependent division plane phenotype. However, the *iqd678*-mutant phenotype illustrates that if the IQD6-8 protein subclade is involved in auxin-signalling dependent cell division control, additional factors are required.

There is a clear difference in embryonic division phenotype between the *iqd678*-mutant with skewed division planes but correct formative divisions, and the lethal auxin

insensitive *tirl/afb*- and *bdl*-mutants with cell division- and patterning defects. This difference suggests that the IQD6-8 subclade might merely be involved in regulation of the division plane orientation robustness, possibly by harnessing the stochastic nature of geometry-based cell division plane orientation (Besson & Dumais, 2014) by regulation of metaphase spindle and phragmoplast (Kosetsu et al., 2017) through  $\text{Ca}^{2+}$ -signalling. Besides this mechanism, a separate auxin-regulated mechanism must exist, which is necessary for cellular changes underlying correct formative cell division.

## Outlook

In this thesis, we developed, optimized, and implemented early Arabidopsis imaging toolkits, transcriptional analysis pipelines, and computational methods to dissect the mechanisms underlying cell division regulation in Arabidopsis embryos. These efforts allowed us to identify a factor involved in cell division control and cell geometry. Our work shows that cell division regulation is a complex system, influenced by a multitude of developmental process like cell geometry, cell polarity, cytoskeleton dynamics, nuclear position and molecular regulation.

## References

- Abel, S., Bürstenbinder, K., & Müller, J. (2013). The emerging function of IQD proteins as scaffolds in cellular signaling and trafficking. *Plant Signaling and Behavior*. <https://doi.org/10.4161/psb.24369>
- Abel, S., Savchenko, T., & Levy, M. (2005). Genome-wide comparative analysis of the IQD gene families in *Arabidopsis thaliana* and *Oryza sativa*. *BMC Evolutionary Biology*. <https://doi.org/10.1186/1471-2148-5-72>
- Ambrose, C., Allard, J. F., Cytrynbaum, E. N., & Wasteneys, G. O. (2011). A CLASP-modulated cell edge barrier mechanism drives cell-wide cortical microtubule organization in *Arabidopsis*. *Nature Communications*. <https://doi.org/10.1038/ncomms1444>
- Besson, S., & Dumais, J. (2014). Stochasticity in the symmetric division of plant cells: When the exceptions are the rule. *Frontiers in Plant Science*. <https://doi.org/10.3389/fpls.2014.00538>
- Bürstenbinder, K., Mitra, D., & Quegwer, J. (2017). Functions of IQD proteins as hubs in cellular calcium and auxin signaling: A toolbox for shape formation and tissue-specification in plants? *Plant Signaling and Behavior*. <https://doi.org/10.1080/15592324.2017.1331198>
- Bürstenbinder, K., Savchenko, T., Müller, J., Adamson, A. W., Stamm, G., Kwong, R., ... Abel, S. (2013). *Arabidopsis* calmodulin-binding protein iq67-domain 1 localizes to microtubules and interacts with kinesin light chain-related protein-1. *Journal of Biological Chemistry*. <https://doi.org/10.1074/jbc.M112.396200>
- Chakraborty, B., Willemsen, V., de Zeeuw, T., Liao, C. Y., Weijers, D., Mulder, B., & Scheres, B. (2018). A Plausible Microtubule-Based Mechanism for Cell Division Orientation in Plant Embryogenesis. *Current Biology*. <https://doi.org/10.1016/j.cub.2018.07.025>
- Elsner, J., Michalski, M., & Kwiatkowska, D. (2012). Spatiotemporal variation of leaf epidermal cell growth: A quantitative analysis of *Arabidopsis thaliana* wild-type and triple cyclinD3 mutant plants. *Annals of Botany*. <https://doi.org/10.1093/aob/mcs005>
- Gooh, K., Ueda, M., Aruga, K., Park, J., Arata, H., Higashiyama, T., & Kurihara, D. (2015). Live-Cell Imaging and Optical Manipulation of *Arabidopsis* Early Embryogenesis. *Developmental Cell*. <https://doi.org/10.1016/j.devcel.2015.06.008>

- Harries, P. A., Pan, A., & Quatrano, R. S. (2005). Actin-related protein2/3 complex component ARPC1 is required for proper cell morphogenesis and polarized cell growth in *Physcomitrella patens*. *Plant Cell*. <https://doi.org/10.1105/tpc.105.033266>
- Iwabuchi, K., Ohnishi, H., Tamura, K., Fukao, Y., Furuya, T., Hattori, K., ... Hara-Nishimura, I. (2019). ANGUSTIFOLIA Regulates Actin Filament Alignment for Nuclear Positioning in Leaves. *Plant Physiology*. <https://doi.org/10.1104/pp.18.01150>
- Job, D., Pabion, M., & Margolis, R. L. (1985). Generation of microtubule stability subclasses by microtubule-associated proteins: Implications for the microtubule “dynamic instability” model. *Journal of Cell Biology*. <https://doi.org/10.1083/jcb.101.5.1680>
- Johri, B. M., Ambegaokar, K. B., & Srivastava, P. S. (1992). Comparative Embryology of Angiosperms. In *Comparative Embryology of Angiosperms*. <https://doi.org/10.1007/978-3-642-76395-3>
- Jürgens, G., & Mayer, U. (1994). “Arabidopsis,” in A colour Atlas of Developing Embryos. *Harcourt Health Sciences*.
- Kimata, Y., Kato, T., Higaki, T., Kurihara, D., Yamada, T., Segami, S., ... Ueda, M. (2019). Polar vacuolar distribution is essential for accurate asymmetric division of Arabidopsis zygotes. *Proceedings of the National Academy of Sciences of the United States of America*. <https://doi.org/10.1073/pnas.1814160116>
- Kirchhelle, C., Garcia-Gonzalez, D., Irani, N. G., Jérusalem, A., & Moore, I. (2019). Two mechanisms regulate directional cell growth in Arabidopsis lateral roots. *ELife*. <https://doi.org/10.7554/elife.47988>
- Kosetsu, K., Murata, T., Yamada, M., Nishina, M., Boruc, J., Hasebe, M., ... Goshima, G. (2017). Cytoplasmic MTOCs control spindle orientation for asymmetric cell division in plants. *Proceedings of the National Academy of Sciences of the United States of America*. <https://doi.org/10.1073/pnas.1713925114>
- Li, S., Blanchoin, L., Yang, Z., & Lord, E. M. (2003). The putative arabidopsis Arp2/3 complex controls leaf cell morphogenesis. *Plant Physiology*. <https://doi.org/10.1104/pp.103.028563>
- Liao, C. Y., & Weijers, D. (2018). A toolkit for studying cellular reorganization during early embryogenesis in Arabidopsis thaliana. *Plant Journal*. <https://doi.org/10.1111/tpj.13841>

Lukowitz, W., Roeder, A., Parmenter, D., & Somerville, C. (2004). A MAPKK Kinase Gene Regulates Extra-Embryonic Cell Fate in Arabidopsis. *Cell*. [https://doi.org/10.1016/S0092-8674\(03\)01067-5](https://doi.org/10.1016/S0092-8674(03)01067-5)

Pietra, S., Gustavsson, A., Kiefer, C., Kalmbach, L., Hörstedt, P., Ikeda, Y., ... Grebe, M. (2013). Arabidopsis SABRE and CLASP interact to stabilize cell division plane orientation and planar polarity. *Nature Communications*. <https://doi.org/10.1038/ncomms3779>

Ramakrishna, P., Duarte, P. R., Rance, G. A., Schubert, M., Vordermaier, V., Vu, L. D., ... De Smet, I. (2019). EXPANSIN A1-mediated radial swelling of pericycle cells positions anticlinal cell divisions during lateral root initiation. *Proceedings of the National Academy of Sciences of the United States of America*. <https://doi.org/10.1073/pnas.1820882116>

Ringli, C., Baumberger, N., Diet, A., Frey, B., & Keller, B. (2002). ACTIN2 is essential for bulge site selection and tip growth during root hair development of arabidopsis. *Plant Physiology*. <https://doi.org/10.1104/pp.005777>

Ueda, M., Zhang, Z., & Laux, T. (2011). Transcriptional Activation of Arabidopsis Axis Patterning Genes WOX8/9 Links Zygote Polarity to Embryo Development. *Developmental Cell*. <https://doi.org/10.1016/j.devcel.2011.01.009>

Vidali, L., Burkart, G. M., Augustine, R. C., Kerdavid, E., Tüzel, E., & Bezanilla, M. (2010). Myosin XI is essential for tip growth in *Physcomitrella patens*. *Plant Cell*. <https://doi.org/10.1105/tpc.109.073288>

Vidali, L., Van Gisbergen, P. A. C., Guérin, C., Franco, P., Li, M., Burkart, G. M., ... Bezanilla, M. (2009). Rapid formin-mediated actin-filament elongation is essential for polarized plant cell growth. *Proceedings of the National Academy of Sciences of the United States of America*. <https://doi.org/10.1073/pnas.0901170106>

Von Wangenheim, D., Fangerau, J., Schmitz, A., Smith, R. S., Leitte, H., Stelzer, E. H. K., & Maizel, A. (2016). Rules and self-organizing properties of post-embryonic plant organ cell division patterns. *Current Biology*. <https://doi.org/10.1016/j.cub.2015.12.047>

Wang, H., Ngwenyama, N., Liu, Y., Walker, J. C., & Zhang, S. (2007). Stomatal development and patterning are regulated by environmentally responsive mitogen-activated protein kinases in Arabidopsis. *Plant Cell*. <https://doi.org/10.1105/tpc.106.048298>

Wendrich, J., Yang, B.-J., Mijnhout, P., Xue, H.-W., Rybel, B. De, & Weijers, D. (2018).

- IQD proteins integrate auxin and calcium signaling to regulate microtubule dynamics during Arabidopsis development. *BioRxiv*. <https://doi.org/10.1101/275560>
- Witte, H., Neukirchen, D., & Bradke, F. (2008). Microtubule stabilization specifies initial neuronal polarization. *Journal of Cell Biology*. <https://doi.org/10.1083/jcb.200707042>
- Wodarz, A. (2002). Establishing cell polarity in development. *Nature Cell Biology*. <https://doi.org/10.1038/ncb0202-e39>
- Wu, S. Z., & Bezanilla, M. (2018). Actin and microtubule cross talk mediates persistent polarized growth. *The Journal of Cell Biology*. <https://doi.org/10.1083/jcb.201802039>
- Yang, Z. (2008). Cell Polarity Signaling in Arabidopsis. *Cell*, 24, 551–575. <https://doi.org/10.1146/annurev.cellbio.23.090506.123233>.Cell
- Yoshida, S., Barbier de Reuille, P., Lane, B., Bassel, G. W., Prusinkiewicz, P., Smith, R. S., & Weijers, D. (2014). Genetic control of plant development by overriding a geometric division rule. *Developmental Cell*, 29(1), 75–87. <https://doi.org/10.1016/j.devcel.2014.02.002>
- Yoshida, S., van der Schuren, A., van Dop, M., van Galen, L., Saiga, S., Adibi, M., ... Weijers, D. (2019). A SOSEKI-based coordinate system interprets global polarity cues in Arabidopsis. *Nature Plants*. <https://doi.org/10.1038/s41477-019-0363-6>
- Yu, M., Yuan, M., & Ren, H. (2006). Visualization of actin cytoskeletal dynamics during the cell cycle in tobacco (*Nicotiana tabacum* L. cv Bright Yellow) cells. *Biology of the Cell*. <https://doi.org/10.1042/bc20050074>

---

## Summary

Land plants can grow to exceptional body sizes, with the most complex specialized structures. Directional cell division has a fundamental role throughout the tremendous plant growth processes, yet its molecular regulation is still largely unknown. **Chapter 1** of this thesis discusses mechanisms and sub-cellular structures known to be involved in plant cell division orientation control, and explores tools used for dissection of this complex mechanism.

Dissecting the complex plant cell division control mechanisms requires a simple and highly predictable *in vivo* model system. The highly predictable a relatively simple development of the Arabidopsis embryo makes it suitable for studying plant cell division regulation. In **Chapter 2**, we explore the cellular basis -, cell division patterns -, and regulatory pathways underlying early plant embryogenesis. We describe previous research showing that most cell divisions in the Arabidopsis embryo divide according a geometry-based “shortest-wall” principle, except for formative, asymmetric divisions. When auxin-signalling is disabled by overexpression of the dominant negative response inhibitor BODENLOS (BDL; *bdl*-mutant) all divisions in the embryo switch to “shortest-wall” divisions, suggesting auxin-signalling based control of oriented cell divisions.

Since the microtubule (MT) cytoskeleton is a possible factor regulating cell division orientation downstream of auxin, dissecting its dynamics and regulatory mechanisms is crucial to understand cell division regulation. Combining high-resolution imaging of cell walls and MTs with a modelling strategy for MT organisation, in **Chapter 3**, we show that the cortical MT array is crucial for division plane orientation control in de Arabidopsis embryo. In our model, MT-dynamics are confined by cell shape -, MT stability at cell edges -, and local MT stability by auxin. Additionally, comparison of cell-biology in wild-type - and *bdl*-mutant embryos in **Chapter 4** reveals that F-actin organisation and cell expansion are affected in the mutant. These results suggest a function for the cytoskeleton and cell shape regulation in plant cell division orientation control downstream of BDL-mediated auxin-signalling.

Transcripts of factors regulating cytoskeletal structures and cell shape downstream of auxin should be differentially expressed in the *bdl*-mutant background. To allow for the identification of these factors, in **Chapter 5**, we establish and optimize a pipeline to generate high-quality embryo transcriptomes for the earliest embryonic stages. As a proof of concept, we use this pipeline to generate a reference transcriptome for early Arabidopsis

embryogenesis which can be used as a tool in future developmental embryonic research.

Since the role of auxin-signalling in cell division control is inferred from overexpression of a dominant response inhibitor, it is not clear if endogenous auxin truly regulates division orientation. In **Chapter 6**, we show that the segregating *tirl/afb* hexuple – and *bdl*-mutant embryos have similar division plane defects, suggesting that cell division regulation is regulated by auxin. However, we were not able to verify an overlap in transcriptomic regulation between the two auxin-insensitive mutants, possibly due to the small number of true mutants in the *tirl/afb*-mutant. Using the *bdl*-mutant transcriptome we identified IQ-domain 6 as a possible target of BDL-mediated auxin-signalling involved in cell division plane control. We show that the IQD6-8 protein family subclade localizes to MTs, and IQD6 binds cytoskeletal structures and calmodulins, in vivo. Loss of function of the IQD6-8 subclade results in skewed division planes in the embryo and roots, suggesting a role in cell division control, possible through  $\text{Ca}^{2+}$ -mediated cytoskeletal regulation.

Finally, in **Chapter 7**, we discuss future challenges in research focused on plant cell division orientation control, and the most important findings of this thesis are placed in a broader cell biological – and plant developmental framework.

---

## Samenvatting

Planten kunnen groeien tot ongekende grootte, met de meest complexe gespecialiseerde structuren. De richting van celdeling heeft een fundamentele rol in groei en vorming van planten, maar de moleculaire regulatie van die process is nog steeds grotendeels onbekend. In **hoofdstuk 1** worden mechanismen en cellulaire componenten besproken met een bekende rol in regulatie van plant celdelingsrichting, en dit hoofdstuk geeft een overzicht van mogelijke middelen om dit complexe systeem te ontrafelen.

Voor het ontrafelen van dit complexe systeem is een simpel en voorspelbaar *in vivo* celdeling model-systeem nodig. Het *Arabidopsis thaliana* embryo voldoet aan deze eisen door zijn relatief simpele ontwikkeling en voorspelbare celdelingspatroon. In **hoofdstuk 2** onderzoeken we welke cellulaire basis -, celdivisie patronen -, en moleculaire signaalroutes essentieel zijn voor vroege embryogenese. We beschrijven onderzoek wat laat zien dat de meeste cellen in het Arabidopsis embryo delen volgens een op cel-geometrie gebaseerde “kortste-wand” principe, maar dit geldt niet voor vormende assymetrische delingen. Wanneer auxine-signallering is uitgeschakeld door overexpressie van de dominant negatieve responsremmer BODENLOS (BDL; *bdl*-mutant) schakelen alle delingen naar een deling volgens het “korste-wand” principe, wat suggereert dat auxine-signallering een rol speelt in de regulatie van celdelingsrichting.

Omdat het microtubuli (MT) -cytoskelet een mogelijke factor is die celdeling reguleert, is het belangrijk om de dynamiek en regulerende mechanismen van deze subcellulaire structuur te begrijpen. In **hoofdstuk 3** combineren we hoge resolutie microscopie van celwanden en MT's met een modelleringstrategie voor MT-organisatie, en laten we zien dat corticale MT's cruciaal zijn voor regulatie van het delingsvlak in het Arabidopsis embryo. In ons model wordt MT-dynamiek beperkt door celvorm -, MT-stabiliteit in celranden -, en lokale regulatie van MT-stabiliteit door auxine. Vergelijking van celbiologie in wildtype - en *bdl*-mutant embryo's in **hoofdstuk 4** laat bovendien zien dat de organisatie van F-actine en cel-expansie worden beïnvloed in de mutant. Deze resultaten suggereren een functie voor de regulatie van het cytoskelet en celvorm bij de controle van de oriëntatie van celdelingen in planten onder invloed van BDL-gemedieerde auxine-signalering.

Factoren die cytoskeletstructuren en celvorm onder invloed van auxine reguleren, moeten differentieel tot expressie komen in *bdl*-mutant embryo's. Om misexpressie van deze factoren te kunnen identificeren, ontwikkelen en optimaliseren we in **hoofdstuk 5** een methode voor het genereren van hoogwaardige embryo-transcriptomen voor de vroegste

embryonale stadia. Om ons concept te testen gebruiken we deze methode om een referentie-transcriptoom te genereren voor vroege Arabidopsis embryogenese, die kan worden gebruikt als hulpmiddel bij toekomstig onderzoek naar ontwikkeling van het vroege embryo.

Omdat de rol van auxine-signalering bij de controle van de celdeling wordt afgeleid uit overexpressie van een dominante responsremmer, is het niet duidelijk of endogene auxine werkelijk de oriëntatie van de celdeling reguleert. In **hoofdstuk 6** laten we zien dat de segregerende auxine-insensitieve *tirl/afb* hexuple - en *bdl*-mutant embryo's vergelijkbare delingsvlak defecten hebben, wat suggereert dat oriëntatie van celdeling wordt gereguleerd door auxine. We konden echter geen overeenkomsten in transcriptionele regulatie tussen de twee auxine-ongevoelige mutanten verifiëren, mogelijk vanwege het kleine aantal echte mutanten in de *tirl/afb*-mutant dataset. Met behulp van het *bdl*-mutant transcriptoom identificeerden we het IQ-domein 6 eiwit als een doelwit van BDL-gemedieerde auxine-signalering, wat betrokken is bij de controle van het celdelingvlak. We laten zien dat de IQD6-8 eiwitten localiseren op MT's, en IQD6 bindt cytoskeletstructuren en calmodulines, *in vivo*. Verlies van functie van de IQD6-8 eiwitten resulteert in afwijkende delingsvlakken in het embryo en wortels, wat een rol suggereert in regulatie van celdeling, mogelijk via  $\text{Ca}^{2+}$ -gemedieerde regulatie van het cytoskelet.

Tenslotte bespreken we in **hoofdstuk 7** toekomstige uitdagingen in onderzoek gericht op de controle van de oriëntatie van celdeling in planten, en de belangrijkste bevindingen van dit proefschrift worden geplaatst in een breder celbiologisch - en plantenontwikkeling kader.

---

## Acknowledgements

I would like to thank everyone that has helped me both professionally and personally throughout my PhD. Completing a PhD is not something you can do on your own, so this thesis would not have been here without all your support.

First of all, I would like to thank my promoter and supervisor Dolf Weijers. Thank you Dolf for giving me the opportunity to start my PhD in the Biochemistry lab. As a supervisor, you are able to create an inspirational, critical, but also fun- and relaxed atmosphere. During the last 5 years, you have helped me deal with discoveries, setting my research strategy, frustrations, and big losses. Thank you for all the support. I really admire how you create an environment with a diversity of characters and personalities where everybody feels free to express themselves professionally and personally. I hope we will keep in touch in the future.

Next, I would like to thank all people that I have worked with in the department of Biochemistry for the pleasant and positive atmosphere in the lab. There are a few people within the group that I have started to see as mentors during me time at Biochemistry: Tanya, Kuan-Ju, Joakim, Prasad, and Liao. Each of you were always willing to answer questions and assist when needed, and you have taught me a lot both practically and theoretically. And, besides your obvious professional competences, you guys are also wonderful people. I want to thank Margo and Nicole for all the help both at work, in the bouldering gym, and at home. I am really happy we started our projects around the same time to have lots of fun and share our love for bouldering and boardgames. Special thanks to my paranymp Heidi for being helpful, fun, and for joining me to festivals, and I want to thank all the people that joined the Barcelona PhD trip including Maritza, Mattia, Dasha, Sacco. I am happy we could share this amazing trip with such fun people. I want to give special thanks to Sumanth, Zhaodong, and Mark for all the help with RNA-seq data analysis and IP-MS experiments presented in this thesis. Without their help I would not have been able to write this thesis.

I want to thank my fellow Zeeuw Wouter for sticking by my side during the full duration of my study. It was really nice to have some support both at University and at home when we both started the MSc- and PhD study. I will never forget all the crazy adventures we had in Breda, Wageningen, at Virgo parties, and off course my first time snowboarding. I hope we will keep in touch.

Every laboratory has a group of people that are essential to make it run smoothly. Willy, Cathy, Laura, Sacco, thank you for keeping the lab running, always answering questions, helping me through all the forms and bureaucracy, and taking care of all facilities and growth rooms.

During my PhD, I became specifically interested in different imaging techniques for plant cell imaging. I was really lucky to have a person like Jan-Willem in our group that could teach me all the theoretical- and practical knowledge, and take me on fun trips to learn more about new imaging techniques.

To Jos, Sebastien, Colette, Bert, Tom, Gudrun, and all other previous lab members: Thank you for all the help and fun. I wish you all the best, and I hope we will meet each other again soon.

During my PhD I had the opportunity to supervise multiple students during their thesis projects. Guiding them through their thesis was a meaningful and fulfilling experience for me. Wouter, Thijs, Elmar, Sander, thank you for the effort you put into your projects, and I wish you all the best in your future careers.

I want to thank Richard Smith for welcoming me into his lab to teach me how to use MorphoGraphX and for the discussions about my results. It was always interesting to discuss your view on biological processes from a different perspective. Furthermore, special thanks to Soeren Strauss, who helped me doing measurements using MorphoGraphX when it got more challenging. Writing some of the last chapter would definitely not have been possible without your help.

Ik wil al mijn gezellige huisgenoten bedanken die ik heb leren kennen tijdens mijn studie in Breda en Wageningen. Het voelt alsof ik er twee nieuwe families bij heb gekregen tijdens mijn tijd in het Klooster en huis het Zaad. Bart, Jochem & Liyanne, Niels, Boris, Elsje & Wesley: De perfecte familie om te hebben tijdens een HBO-studie. Altijd in voor een biertje, feesten, muziek maken, gamen, en nutteloze discussies. Maar het belangrijkste, vrienden voor het leven!

Stef, Hester, Loet & Anne, Tim & Ilse: De perfecte familie om te hebben tijdens je MSc-studie. Nog steeds in voor biertjes en feesten, maar ook met een knusse, rustige sfeer in huis waar goede verhalen- en muziek werden gedeeld. Tim & Ilse, jullie zijn altijd een grote steun geweest tijdens mijn PhD, ik ben blij dat we allemaal in Wageningen zijn blijven hangen om samen nog meer gezelligheid te delen.

---

Simon & Rosanne: bedankt voor alle ontspannen avonden en weekenden aan de Rijn of thuis met heerlijk eten, veel en lekker bier, en gezelligheid. Ik hoop dat jullie een beetje in de buurt blijven om dit voort te zetten.

Matthijs, Jonathan: Bedankt voor alle avonturen, het klimmen, en alle plezier in Wageningen. Matthijs, jij begreep dat ik een goede vriend nodig had op het moment dat ik het moeilijk had, om me af te leiden en te luisteren. Bedankt dat je er was!

Emanuel & Dorine, Jochem: Ik ben blij dat Wageningen zo'n sterke aantrekkingskracht heeft op Zeeuwen. Het is heerlijk om in de zomer na het werk te kunnen genieten van goed gezelschap, een biertje, en een muziekje aan de Rijn.

Als je in een andere deel van Nederland gaat studeren kom je erachter wie de echte jeugdvrienden zijn waar je veel om geeft. Damien, Patrick, Arnout, ik ben blij met jullie bezoeken aan Breda en Wageningen, laten we zorgen dat er nog veel volgen.

Mam, pap, natuurlijk heb ik uiteindelijk alles aan jullie te danken. Jullie zijn er altijd voor me geweest en jullie hebben mij de kans gegeven om me te ontwikkelen tot de persoon die ik nu ben. Mam, ik hou van je zorgzaamheid, openheid, doorzettingsvermogen en kracht. Pap, ik hou van je creativiteit, nieuwsgierigheid, positiviteit en (soms irritante) humor. Ik heb deze eigenschappen altijd proberen uit te dragen, en ze hebben me geholpen om alle geweldige mensen te ontmoeten die ik hiervoor heb genoemd. Lisa, mijn lieve zus. Het was geweldig om samen op te groeien. Ik ben enorm trots op jou doorzettingsvermogen en de manier waarop jij in het leven staat. Evelien was de grote zus waar ik altijd op kon bouwen en waarmee ik altijd kon lachen, praten, muziek luisteren en gewoon chillen. Tante, jij was, en bent een heel groot deel van mijn opvoeding. Ik had de luxe een soort derde ouder te hebben. Je zorgzaamheid lijkt eindeloos en ik zal alle leuke momenten met je nooit vergeten.

En de laatste, maar ook de belangrijkste persoon die ik wil bedanken, is Merel. Ik ben zo blij dat ik je als zo vroeg in mijn leven heb gevonden. Er zijn niet veel mensen die het geluk hebben dat ze op hun 18e al iemand vinden waar ze zich zo goed bij voelen en met wie alles lekker ongecompliceerd is. Daarbij heb je ook nog een gezellige familie te hebben, waar ik veel plezier en steun aan beleef. Omdat we al zo lang samen zijn heb ik het gevoel dat we ons samen tot een geweldig team ontwikkeld hebben, je bent altijd een geweldige steun voor me geweest. Ik geniet van elke dag samen met je, ik kijk uit naar al onze komende avonturen samen.



## Curriculum Vitae

Thijs de Zeeuw was born February 18th in Hoek, the Netherlands. In 2008 he completed his secondary education at SSG De Rede in Terneuzen and moved to Breda. There he pursued a BSc degree in biology and medical laboratory research. During his studies he became interested in plant development and plant breeding, largely because of a BSc-internship at the plant breeding company Nickerson-Zwaan. He moved to Wageningen to study Plant Biotechnology and in 2015 completed his MSc degree, specializing in molecular biology and plant genomics. During his MSc he focused on plant development and plant cell biology, and completed two theses on arbuscular mycorrhizae and lateral root development. In the first thesis project he worked with dr. ir. Erik Limpens and prof. dr. Ton Bisseling at the laboratory of Molecular Biology at Wageningen University, studying effectors mediating interaction and infiltration of plant roots with arbuscular mycorrhizae. During the second thesis he worked with dr. Barbara Möller and prof. dr. Tom Beeckman at the VIB in Gent, studying the role of the zinc finger transcription factor GATA23 in lateral root formation. In 2014, Thijs started a PhD project with prof. dr. Dolf Weijers at the laboratory of Biochemistry at Wageningen University working studying the molecular and cell-biological mechanisms controlling plant cell division orientation in *Arabidopsis thaliana*, resulting in this thesis. Next, Thijs wants to stay connected to academic research by taking up a technician position in a laboratory focussing on plant development-, cell biology-, and plant physiology.



---

## Publications

Chakraborty, B., Willemsen, V., **de Zeeuw, T.**, Liao, C. Y., Weijers, D., Mulder, B., & Scheres, B. (2018). A Plausible Microtubule-Based Mechanism for Cell Division Orientation in Plant Embryogenesis. *Current Biology*. <https://doi.org/10.1016/j.cub.2018.07.025>

Zeng, T., Holmer, R., Hontelez, J., te Lintel-Hekkert, B., Marufu, L., **de Zeeuw, T.**, Fangyuan, W., Schijlen, E., Bisseling, T., Limpens, E. (2018). Host- and stage-dependent secretome of the arbuscular mycorrhizal fungus *Rhizophagus irregularis*. *Plant Journal*. <https://doi.org/10.1111/tpj.13908>

Palovaara, J., **de Zeeuw, T.**, & Weijers, D. (2016). Tissue and Organ Initiation in the Plant Embryo: A First Time for Everything. *Annual Review of Cell and Developmental Biology*, 32(1), annurev-cellbio-111315-124929. <https://doi.org/10.1146/annurev-cell-bio-111315-124929>

**De Zeeuw, T.**, & Weijers, D. (2016). Plant organogenesis: Rules of order. *Current Biology*, 26(4), R157–R159.

The Graduate School

**EXPERIMENTAL  
PLANT  
SCIENCES**



Issued to: Thijs de Zeeuw  
Date: 19 February 2020  
Group: Biochemistry  
University: Wageningen University & Research

1) Start-Up Phase	<i>date</i>	<i>cp</i>
<p>► <b>First presentation of your project</b>  Hormonal disobedience in plant cell division control, Haigerloch 2015</p>	12 May 2015	1.5
<p>► <b>Writing or rewriting a project proposal</b></p>		
<p>► <b>Writing a review or book chapter</b>  Palovaara J*, de Zeeuw T* &amp; Weijers D. (2016) Tissue and organ initiation in the plant embryo: A first time for everything. <i>Annu Rev Cell Dev Biol</i>. DOI:10.1146/annurev-cellbio-111315-124929</p>	Aug 2016	3.0
► <b>MSc courses</b>		

Subtotal Start-Up Phase

45

2) Scientific Exposure	date	cp
► <b>EPS PhD student days</b>		
EPS PhD student day 2017 (Get2Gether, Soest)	9-10 Feb 2017	0.6
EPS PhD student day 2018 (Get2Gether, Soest)	15-16 Feb 2018	0.6
► <b>EPS theme symposia</b>		
EPS Theme 1 symposium 2015, Leiden	8 Jan 2015	0.3
EPS Theme 1 symposium 2016, Wageningen	21 Jan 2016	0.3
EPS Theme 1 symposium 2018, Wageningen	30 Jan 2018	0.3
► <b>Lunteren Days and other national platforms</b>		
Annual meeting Experimental Plant Sciences 2015	13-14 Apr 2015	0.6
Annual meeting Experimental Plant Sciences 2016	11-12 Apr 2016	0.6
Annual meeting Experimental Plant Sciences 2017	10-11 Apr 2017	0.6
► <b>Seminars (series), workshops and symposia</b>		
Thursday Seminar Biochemistry: prof. Tony Bacic (University of Melbourne, Australia)	27 Mar 2015	0.1
Thursday Seminar Biochemistry: prof. Alain Goossens (VIB Ghent, Belgium)	8 Dec 2015	0.1
Thursday Seminar Biochemistry: dr Francois Parcy (CEA Sciences, France)	15 Oct 2015	0.1
Thursday Seminar Biochemistry: prof. Mark Estelle (UC San Diego, USA)	7 Apr 2016	0.1
Invited Speaker Biochemistry: dr. Helene Robert-Boisivon (CEITEC, Czech Republic)	3 Jun 2016	0.1
Invited Speaker Biochemistry: prof. Chun-Ming Liu (Institute of Crop Science, CAAS, China)	20 Jun 2016	0.1
Thursday Seminar Biochemistry: prof. Lars Ostergaard (John Innes Centre, UK)	21 Dec 2016	0.1
Farewell Symposium EPS Ton Bisseling: The underground labyrinth: roots, friends and foes	8 Feb 2017	0.2
Thursday Seminar Biochemistry: prof. Gerd Jurgens (Max Planck Tübingen Germany)	11 May 2017	0.1
Thursday Seminar Biochemistry: dr Katharina Burstenbinder (Leibniz Institute for Plant Biochem, Germany)	1 Jun 2017	0.1
Thursday Seminar Biochemistry: dr. Arnold Boersma (RUG, NL)	19 Jul 2017	0.1
Seminar on Integrative Bioinformatics	12 Sep 2017	0.1
Symposium Plant Developmental Systems Biology	4 Oct 2017	0.3
Symposium Future of Biochemistry	26 Oct 2017	0.2
Thursday Seminar Biochemistry: prof. Richard Notebaart (WUR, NL)	2 Nov 2017	0.1
Invited speaker Biochemistry: dr. Mark Hink (University of Amsterdam, Netherlands)	14 Feb 2018	0.1
Invited speaker Biochemistry: dr. Dominik Wöll (Aachen University, Germany)	14 Feb 2018	0.1
Invited speaker Biochemistry: prof. Charles Delwiche (University of Maryland, USA)	18 Jun 2018	0.1
Invited speaker Biochemistry: prof. Victoria Mironova (Novosibirsk State University, Russia)	27 Jun 2018	0.1
Invited speaker Biochemistry: prof. Lucia Strader (Washington University, USA)	10 Sep 2018	0.1
Molecular Life Science Seminar: prof. Ludwik Leibler (ESPCI ParisTech, France)	22 Nov 2018	0.1
Invited speaker Biochemistry: prof. Alexis Maizel (COS Heidelberg, Germany)	17 Dec 2018	0.1
Invited speaker Biochemistry: prof. Jiri Friml (IST, Austria)	18 Dec 2018	0.1
Molecular Life Science Seminar: prof. Wolf Frommer (universitat Dusseldorf, Germany)	17 Jan 2019	0.1
Invited speaker Biochemistry: Dr. Minako Ueda (University of Nagoya, Japan)	4 Sep 2019	0.1
TWO seminars: prof. Miguel Blazquez (University of Valencia, Spain)	8 Oct 2019	0.1
TWO seminars: Dr. Jill Harrison (University of Bristol, UK)	8 Oct 2019	0.1
► <b>Seminar plus</b>		
► <b>International symposia and congresses</b>		
Embryo development meeting 2015, Haigerloch, Germany	11-13 May 2015	0.7
FASEB Mechanisms in plant development, Nagoya, Japan	27-28 Aug 2015	0.6
Embryo development meeting 2018, Haigerloch, Germany	7-9 May 2015	0.7
Asymmetric cell division workshop, Nottingham, UK	21 Sep 2016	0.3
International Plant Molecular Biology (IPMB), Montpellier, France	6-10 Aug 2018	1.2
► <b>Presentations</b>		
Poster: FASEB Mechanisms in plant development, Nagoya, Japan	4 Aug 2015	1.0
Talk: Application of novel microscopic imaging techniques, Göttingen, Germany	27 Jan 2016	1.0
Talk: Asymmetric cell division meeting, Nottingham, UK	21 Sep 2016	1.0
Talk: PhD trip Biochemistry to ICFO institute, Barcelona, Spain	17 May 2017	1.0
Talk: Embryo development meeting 2018, Haigerloch, Germany	8 May 2018	1.0
► <b>IAB interview</b>		
► <b>Excursions</b>		

Excursion novel imaging techniques in Biophysics lab, prof. Jörg Enderlein, Gottingen Germany	27-28 Jan 2016	0.6
PhD trip Biochemistry to Agrasys, ICFO, CRAG and Synchrotron, Barcelona Spain	15-21 May 2017	1.2
PhD trip Biochemistry to Molecular Genetics lab, prof. Rita Gross-Hardt, Bremen Germany	1-3 Dec 2018	0.3
<i>Subtotal Scientific Exposure</i>		17.6

<b>3) In-Depth Studies</b>	<u>date</u>	<u>cp</u>
▶ <b>Advanced scientific courses &amp; workshops</b>		
Course: Morphographx, 3D segmentation and division plane determination, Cologne, Germany	5-8 Jan 2015	1.2
Workshop: Arabidopsis ovule culturing and live imaging, Nagoya, Japan	31 Aug-1 Sep 2015	0.6
Course: Transcription Factors and Transcriptional Regulation, Wageningen	10-12 Dec 2018	1.0
▶ <b>Journal club</b>		
Journal club Prof. dr. Dolf Weijers lab	2015-2019	3.0
▶ <b>Individual research training</b>		
<i>Subtotal In-Depth Studies</i>		5.8

<b>4) Personal Development</b>	<u>date</u>	<u>cp</u>
▶ <b>General skill training courses</b>		
Workshop: WGS Workshop Carousel, Wageningen	17 Apr 2015	0.2
Course: Project and Time Management, Wageningen	Nov-Dec 2015	1.5
Course: Scientific Artwork with Photoshop and Illustrator, Wageningen	2-3 Oct 2017	0.6
Course: Adobe InDesign Essential Training, Wageningen	9-10 Oct 2017	0.6
Course: Career assessment, Wageningen	11 June 2018	0.3
▶ <b>Organisation of meetings, PhD courses or outreach activities</b>		
▶ <b>Membership of EPS PhD Council</b>		
<i>Subtotal Personal Development</i>		3.2

<b>TOTAL NUMBER OF CREDIT POINTS*</b>	<b>31.1</b>
Herewith the Graduate School declares that the PhD candidate has complied with the educational requirements set by the Educational Committee of EPS with a minimum total of 30 ECTS credits.	
* A credit represents a normative study load of 28 hours of study.	

The research presented in this thesis was performed at the Laboratory of Biochemistry, Wageningen University & Research, and was financially supported by a grant from the Netherlands Organization for Scientific Research (NWO; ALW 824.14.009).

Financial support from the Laboratory of Biochemistry for printing this thesis is gratefully acknowledged.

Cover design and artwork by Boris Steeman

Layout design by Tatyana Radoeva and Thijs de Zeeuw

Printed by proefschriftenmaken



